AD-A193 427 NONLINEAR STOCHASTIC INTERACTION IN AEROELASTIC STRUCTURES(U) TEXAS TECH UNIV LUBBOCK DEPT OF MECHANICAL ENGINEERING R A IBRAHIM 29 JAN 88 1/2

UNCLASSIFIED AFOSR-TR-88-0368 AFOSR-85-[illegible] F/G 20/4 NL

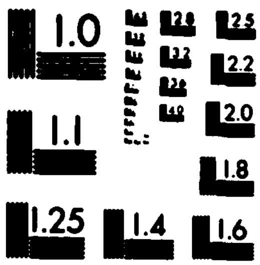

MICROCOPY RESOLUTION TEST CHART
NATIONAL BUREAU OF STANDARDS 1963 A

DTIC FILE COPY

AFOSR-TR- 88-0368

Final Report

NONLINEAR STOCHASTIC INTERACTION IN AEROELASTIC STRUCTURES

AD-A193 427

January 29, 1988

Approved for public release; distribution unlimited.

Prepared for

Air Force Office of Scientific Research
Grant No. AFOSR-86-0008
Program Director: Dr. A. K. Amos

Prepared by

Raouf A. Ibrahim*
Department of Mechanical Engineering
Texas Tech University
Lubbock, Texas 7940

* Currently: Wayne State University
Department of Mechanical Engineering
Detroit, Michigan 48202

88 3 31 017

Final Report

NONLINEAR STOCHASTIC INTERACTION IN AEROELASTIC STRUCTURES

January 29, 1988

Prepared for

Air Force Office of Scientific Research
Grant No. AFOSR-85-0008
Program Director: Dr. A. K. Amos

Prepared by

Raouf A. Ibrahim*
Department of Mechanical Engineering
Texas Tech University
Lubbock, Texas 7940

* Currently: Wayne State University
Department of Mechanical Engineering
Detroit, Michigan 48202

UNCLASSIFIED

SECURITY CLASSIFICATION OF THIS PAGE

REPORT DOCUMENTATION PAGE

1a. REPORT SECURITY CLASSIFICATION: Unclassified

1b. RESTRICTIVE MARKINGS:

2a. SECURITY CLASSIFICATION AUTHORITY:

2b. DECLASSIFICATION/DOWNGRADING SCHEDULE:

3. DISTRIBUTION/AVAILABILITY OF REPORT: Unlimited

4. PERFORMING ORGANIZATION REPORT NUMBER(S):

5. MONITORING ORGANIZATION REPORT NUMBER(S): AFOSR-TR- 88-0368

6a. NAME OF PERFORMING ORGANIZATION: Dept. of Mechanical Engineering, Texas Tech University

6b. OFFICE SYMBOL (If applicable):

7a. NAME OF MONITORING ORGANIZATION: AFOSR

6c. ADDRESS (City, State and ZIP Code): P. O. Box 4289, Lubbock, TX79409

7b. ADDRESS (City, State and ZIP Code): Same as 8C

8a. NAME OF FUNDING/SPONSORING ORGANIZATION: AFOSR

8b. OFFICE SYMBOL (If applicable): NA

9. PROCUREMENT INSTRUMENT IDENTIFICATION NUMBER: Grant No. AFOSR-85-0008

8c. ADDRESS (City, State and ZIP Code): Bolling Air Force Base, Washington, DC 20332 Bldg 410

10. SOURCE OF FUNDING NOS.

PROGRAM ELEMENT NO.	PROJECT NO.	TASK NO.	WORK UNIT NO.
61102F	2302	~~2302~~/B1	

11. TITLE (Include Security Classification): Nonlinear Stochastic Interaction in Aeroelastic Structures

12. PERSONAL AUTHOR(S): Ibrahim, Raouf A.

13a. TYPE OF REPORT: Final

13b. TIME COVERED: FROM 84/11/1 TO 87/12/31

14. DATE OF REPORT (Yr., Mo., Day): 88/1/29

15. PAGE COUNT: 112

16. SUPPLEMENTARY NOTATION:

17. COSATI CODES

FIELD	GROUP	SUB. GR.

18. SUBJECT TERMS (Continue on reverse if necessary and identify by block number): Random Vibration, Internal Resonance, Parametric Vibration, Parameter Uncertainties, Experimental Vibration.

19. ABSTRACT (Continue on reverse if necessary and identify by block number)

The linear and nonlinear modal interactions in aeroelastic structures under wide band random excitation are examined analytically and experimentally. The analytical investigation deals with the random response characteristics of two- and three-degree-of-freedom nonlinear models in the neighborhood of internal resonance conditions. These conditions take the form of linear relationships between the normal mode frequencies and are established from the linear modal analysis of each model. The Fokker-Planck equation approach is used to derive a general differential equation for the response joint moments. In view of the models nonlinearity the differential equation is found to constitute a set of infinite coupled first order differential equations. These equations are closed by using two different truncation schemes which are based on the properties of response joint cumulants. These two schemes are known as Gaussian and non-Gaussian closures. The analytical manipulations are performed by using the computer algebraic software MACSYMA, while the response statistical moments ar~ determined by numerical integration by using the IMSL software DVERK. The Gaussian closure solution gives a quasi-stationary response in the form of fluctuations between two limits. However, the non-Gaussian closure results in Contd.

20. DISTRIBUTION/AVAILABILITY OF ABSTRACT: UNCLASSIFIED/UNLIMITED ☒ SAME AS RPT. ☐ DTIC USERS ☐

21. ABSTRACT SECURITY CLASSIFICATION: Unclassified

22a. NAME OF RESPONSIBLE INDIVIDUAL: Dr. Hknp Nhl

22b. TELEPHONE NUMBER (Include Area Code): (202) 767-4937

22c. OFFICE SYMBOL: NA

DD FORM 1473, 83 APR EDITION OF 1 JAN 73 IS OBSOLETE. Unclassified

SECURITY CLASSIFICATION OF THIS PAGE

a strict stationary response. The general trend of the nonlinear interaction takes the form of energy exchange between the interacted modes when the system is internally tuned. In the case of three-mode interactions complex response characteristics are predicted in the form of multiple solutions and jump phenomenon in a stochastic sense.

The experimental investigation is carried out on a two-degree-of-freedom model whose analytical solution is known. When the first normal mode is externally excited by a band-limited random excitation the system mean square response is found to be linearly proportional to the excitation spectral density up to a certain level above which the two normal modes exhibit discontinuity mainly governed by the internal detuning and the system damping ratios. These response characteristics are changed when the second normal mode is externally excited. Under lower levels of excitation spectral density the response is dominated by the second normal mode. When the excitation level increases the first normal mode attends and interacts nonlinearly with the second mode in a form of energy exchange.

These *investigations do not take into account the interaction between the* aerodynamic forces on one hand and the elastic and inertia forces on the other hand. The interaction with random aerodynamic forces establishes the system nonlinear flutter and constitutes the second phase of this research project. A new proposal for the second phase has been submitted to AFOSR for another three years support.

Table of Contents

ABSTRACT

The linear and nonlinear modal interactions in aeroelastic structures under wide band random excitation are examined analytically and experimentally. The analytical investigation deals with the random response characteristics of two- and three-degree-of-freedom nonlinear models in the neighborhood of internal resonance conditions. These conditions take the form of linear relationships between the normal mode frequencies and are established from the linear modal analysis of each model. The Fokker-Planck equation approach is used to derive a general differential equation for the response joint moments. In view of the models nonlinearity the differential equation is found to constitute a set of infinite coupled first order differential equations. These equations are closed by using two different truncation schemes which are based on the properties of response joint cumulants. These two schemes are known as Gaussian and non-Gaussian closures. The analytical manipulations are performed by using the computer algebraic software MACSYMA, while the response statistical moments are determined by numerical integration by using the IMSL software DVERK. The Gaussian closure solution gives a quasi-stationary response in the form of fluctuations between two limits. However, the non-Gaussian closure results in a strict stationary response. The general trend of the nonlinear interaction takes the form of energy exchange between the interacted modes when the system is internally tuned. In the case of three-mode interactions complex response characteristics are predicted in the form of multiple solutions and jump phenomenon in a stochastic sense.

The experimental investigation is carried out on a two-degree-of-freedom model whose analytical solution is known. When the first normal mode is externally excited by a band-limited random excitation the system mean square response is found to be linearly proportional to the excitation spectral density up to a certain level above which the two normal modes exhibit discontinuity mainly governed by the internal detuning and the system damping ratios. These response characteristics are changed when the second normal mode is externally excited. Under lower levels of excitation spectral density the response is dominated by the second normal mode. When the excitation level increases the first normal mode attends and interacts nonlinearly with the second mode in a form of energy exchange.

These investigations do not take into account the interaction between the aerodynamic forces on one hand and the elastic and inertia forces on the other hand. The interaction with random aerodynamic forces establishes the system nonlinear flutter and constitutes the second phase of this research project. A new proposal for the second phase has been submitted to AFOSR for another three years support.

SUMMARY OF MAIN RESULTS

I. Introduction

In an effort to understand the dynamic behavior of nonlinear aeroelatic structures under random excitations a research project combines analytical and experimental investigations has been supported by the Air Force Office of Scientific Research. Based on the original proposal (February 1983) and its amendment (July 1984) three main objectives are considered. These are:

1. To investigate the autoparametric interaction in aeroelastic structures subjected to wide band random excitation. *Autoparametric interaction* usually occurs if the normal mode frequencies of the structure are commensurate (i.e. the normal mode frequencies are governed by an algebraic relationship known as *internal resonance*.

2. To investigate the effects of damping and stiffness random fluctuations in the absence and in the presence of internal resonance.

3. To conduct an experimental investigation with the purpose of understanding complex response characteristics and verifying the validity of theoretical results. The experimental investigation is very valuable in demonstrating how the normal modes are interacting under random excitations.

This report provides a brief summary of the main results of this research project during three- year period. The complete results are published in technical papers and presented at ASME, AIAA, IMAC, and international meetings. Various aspects of the research project are well documented in two Ph.D. dissertations and two Masters theses. Reprints of the technical papers are attached.

II. ANALYTICAL INVESTIGATION

II.1 Two-Mode Interaction

The linear and nonlinear random modal interactions in two-degree-of-freedom aeroelastic structural model are examined by using the Fokker-Planck equation approach together with two truncation schemes known as Gaussian and non-Gaussian closures. A general differential equation describing the evolution of the response statistical moments is derived for any moment order. For the case of linear modal interaction this differential equation is found to be consistent (i.e. the number of unknowns is equal to the number of the generated equations). The stationary response is determined for various system parameters. It is found that the linear interaction results in a suppression of one mode when the uncoupled frequencies of the structure are close to each other. For the case of nonlinear modal interaction (known as autoparametric coupling) the differential equation of the response moments forms an infinite coupled set of first order differential equations which are closed by Gaussian and non-Gaussian closure schemes. The Gaussian closure is known to be less accurate since it does not take into account the effect of the response non-normality. The Gaussian closure scheme yields 14 coupled differential equations in the first and second order moments of the response coordinates, while the non-Gaussian closure leads to 69 differential equations in the first through fourth order moments. The two sets of differential equations are solved by numerical integration by using the IMSL (International Mathematical and Statistical Library) subroutine DVERK (Runge-Kutta-Verner fifth and sixth numerical integration method). Both solutions are presented in the time and internal frequency domains. The solutions exhibit common features such as energy exchange between the two normal modes in the neighborhood of internal tuning. The Gaussian solution gives a quasi-stationary response in the form of fluctuations between two limits. However, the non-Gaussian solution results in a strict stationary response. The influence of random fluctuations in the system damping on the response mean squares is found to be very small. The stiffness random variation, however, shows to have a pronounced effect on the response mean squares.

II.2 Three-Mode Interaction

The linear and autoparametric modal interactions in a three-degree-of-freedom structural model subjected to wide band random excitation are examined by using the same approach described in section II.1. For a structure with constant parameters the linear response is obtained in a closed form. When the structure stiffness matrix involves random components the linear equations of motion, in terms of principal coordinates, are coupled through parametric terms. The response is found to be governed by the condition of mean square stability. The boundary of stable-unstable responses is obtained as a function of the internal detuning parameter. The results of the linear system with constant coefficients are used as a reference to measure the deviation of the system response when the nonlinear inertia coupling is included. Four possible internal resonance conditions are derived. These are:

i. Combination internal resonance

$$\omega_3 = \omega_1 + \omega_2$$

ii. Principal internal resonance between the first and second modes

$$\omega_2 = 2\omega_1$$

iii. Principal internal resonance between the first and third modes

$$\omega_3 = 2\omega_1$$

iv. Principal internal resonance between the second and third modes

$$\omega_3 = 2\omega_2$$

In the neighborhhood of combination internal resonance the Gaussian closure results in 27 differential equations while the non-Gaussian closure yields 209 differential equations in the response joint moments. The Gaussian solution exhibits two normal mode interaction when the condition of combination resonance is slightly shifted. This unexpected result is scrutinized and it is found that the system possesses principal internal resonance between the second and third modes when the three modes are not exactly tuned according to condition (i). The non-Gaussian solution successfully predicts three-mode interaction in the neighborhood of combination internal resonance. The autoparametric interaction occurs among the three modes in such a manner that the mean square of the first two normal modes is always greater than the linear solution while it is less for the third mode. This means that the nonlinear interaction takes place between the first and second modes on one hand and the third mode on the other hand. A new feature of considerable interest is the contrast in the form of the mean square response curves above the exact internal detuning for a certain combination of system parameters and excitation level. This is indicated by multiple solutions over a finite portion of internal detuning. The well-known saturation phenomenon which usually occurs in deterministic systems with quadratic nonlinear coupling does not take place in the present case since the excitation is random and includes a wide range of frequencies which always excite the system normal modes.

For the case of principal internal resonances it is found that the response statistics are sensitive to small excitation levels when the third and second modes are internally tuned. However, the autoparametric interaction is found to be only sensitive to a relatively high excitation spectral density under conditions (ii) and (iii). The stochastic interaction of the three cases is characterized by irregular energy exchange between the interacted modes.

III. EXPERIMENTAL INVESTIGATION

A series of experimental tests are conducted on a two-degree-of-freedom elastic model. The model is subjected to a band-limited random excitation whose central frequency is very close to one of the two normal mode frequencies of the model. The band width is selected such that no other higher modes are excited. The model normal mode frequencies are adjusted to have the ratio 2:1. This ratio is equivalent to the condition of internal resonance of the analytical model. When the first normal mode is externally excited the system mean square response is found to be linearly proportional to the excitation spectral density up to a certain level above which the two normal modes exhibit discontinuity. The observed discontinuity is mainly governed by the internal detuning parameter and the system damping ratios. The results are completely different when the second normal mode is externally excited. For small levels of excitation spectral density the response is dominated by the second normal mode. Under higher excitation levels the first normal mode attends and interacts nonlinearly with the second mode.

The measured results reveal some deviations from the predicted results. The deviation is mainly attributed to the fact that the experimental excitation is band-limited random excitation while it is assumed wide band in theory. Experimentally it was not appropriate to apply wide band random excitation which will excite higher modes not considered in the mathematical model. Another source of the deviation occurs in the process of transformation into principal coordinates. In theory the transformation is performed based on conservative linear system and a diagonal linear damping is introduced after transformation.

IV. NEW RESEARCH DIRECTIONS

The work accomplished during this period did not include the interaction of aerodynamic forces with elastic and inertia forces. This interaction accurately models the stochastic nonlinear flutter which has not been examined in the open literature. Although the results obtained from this research project are new and essential in providing more understanding to the response of nonlinear dynamic systems to random excitations, it is very important to examine the effects of nonlinear interaction with aerodynamic forces. A new proposal for three years support has been submitted to the AFOSR. The new proposal will examine the nonlinear stochastic flutter in subsonic and supersonic flight regimes for two basic models: a cantilever wing and a flat panel. The effect of Mach number on the response mean squares in the neighborhood of internal resonance will be determined. The analysis will be performed by using the computer algebraic manipulation software MACSYMA on SUN 3/260 computer at the Nonlinear Vibration Labaratory of Wayne State University.

PUBLICATIONS ACKNOWLEDGING AFOSR GRANT

1. Ibrahim, R. A. and Heo, H., "Autoparametric Vibration of Coupled Beams under Random Support Motion," *ASME Journal of Vibration, Acoustics, Stress, and Reliability in Design* 108(4), pp. 421-426, 1986.

   Presented at the ASME Design and Vibration Conference, Cincinnati, September 1985. ASME Paper 85-DET-184.

2. Ibrahim, R. A., "Numerical Solution of Nonlinear Problems in Stochastic Dynamics," Presented at the 1st International Conference on Computational Mechanics, May 25-29, 1986. Proceedings of *Computational Mechanics '86*, edited by G. Yagawa and S. N. Atluri, Springer-Verlag, Tokyo, Vol. 2, Section XI, pp. 155-160, 1986.

3. Ibrahim, R. A. and Heo, H., "Stochastic Response of Nonlinear Structures with Parameter Random Fluctuations," *AIAA Journal* 25(2), pp. 331-338, 1987.

   Presented at the AIAA/ASME/ASCE/AHS 27th Structures, Structural Dynamics and Materials Conference, Part 2, Paper No. 86-0962, San Antonio, Texas, May 19-21, 1986.

4. Ibrahim, R. A. and Hedayati, Z., "Stochastic Modal Interaction in Nonlinear Aeroelastic Structures," *Journal of Probabilistic Engineering Mechanics* 1(4), pp. 182-191, 1986.

   Presented at the 5th International Modal Analysis Conference, Imperial College, London, April 6-9, 1987.

5. Ibrahim, R. A., "Structural Dynamics with Parameter Uncertainties," *ASME Applied Mechanics Reviews* 40(3), pp. 309-328, 1987.

6. Ibrahim, R. A. and Sullivan, D. G., "Experimental Investigation of Autoparametric Interaction of Structures under Random Excitation," Proc. AIAA/ASME/ASCE/AHS 28th Structures, Structural Dynamics and Materials Conference, Montrey, California, April 6-8, 1987.

7. Ibrahim, R. A. and Li, W., "Structural Modal Interaction with Combination Internal Resonance under Wide Band Random Excitation," *Journal of Sound and Vibration* 123(2), 1988.

8. Li, W. and Ibrahim, R. A., "Critical and Non-Critical Principal Internal Resonances in Aeroelastic Structures under Wide Band Random Excitation," in preparation.

Professional Personnel

A. Faculty

1. Raouf A. Ibrahim, Professor of Mechanical Engineering, Principal Investigator.

B. Graduate Students

1. Zhian Hedayati, M.S. Thesis: *Random Modal Interaction of a Nonlinear Aeroelastic Structure*. Date of Completion: August 1985.
2. Hun Heo, Ph.D. Dissertation: *Nonlinear Stochastic Flutter of Aeroelastic Structural Systems*. Date of Completion: December 1985.
3. Douglas G. Sullivan, M.S. Thesis: *Experimental Investigation of Random Response of Aeroelastic Structures*. Date of Completion: December 1986.
4. Wenlung Li, Ph.D. Dissertation: *Stochastic Autoparametric Interaction in Aeroelastic Structures under Wide Band Random Excitation*. Date of Completion: December 1987.
5. Peter Orono, Ph.D. Dissertation: *Stochastic Nonlinear Flutter of a Cantilever Wing Subjected to Subsonic and Supersonic Gas Flow*. Date of Completion: in progress.
6. Soundararajan Madaboosi, M.S. Thesis: *Stochastic Nonlinear Flutter of a Panel subjected to Supersonic Gas Flow*. Date of Completion: in progress.

APPENDIX

REPRINTS OF SIX PUBLICATIONS

Reprinted from October 1986, Vol. 108, Journal of Vibration, Stress, and Reliability in Design

R. A. Ibrahim
Professor,
Mem. ASME.

H. Heo
Graduate Student.

Texas Tech University,
Department of Mechanical Engineering,
Lubbock, TX 79409

Autoparametric Vibration of Coupled Beams Under Random Support Motion

The dynamic response of a two degree-of-freedom system with autoparametric coupling to a wide band random excitation is investigated. The analytical modeling includes quadratic nonlinearity, and a general first-order differential equation of the moments of any order is derived. It is found that the moment equations form an infinite hierarchy set which is closed via two different closure methods. These are the Gaussian closure and the non-Gaussian closure schemes. The Gaussian closure solution shows that the system does not reach a stationary response while the non-Gaussian closure solution gives a complete stationary steady-state response. In both cases, the response is obtained in the neighborhood of the autoparametric internal resonance condition for various system parameters.

Introduction

The paper deals with the autoparametric random response of a system of coupled beams to a random support motion. The system resembles an analytical model of aeroelastic structures such as aircraft wing with fuel storage. The study of random response of aeroelastic structures has frequently been considered within the framework of linear coupling between two or more degrees of freedom. It involves the combination of structural dynamics and the theory of stochastic processes. The linear modeling gives the response of the system in the neighborhood of the equilibrium position. However, complex response characteristics such as multiple solutions, jump phenomenon, internal resonance, and limit cycles can only be predicted if the inherent nonlinearities of the system are considered.

The flutter problem of two- and three-dimensional plates undergoing limit cycle oscillations in a high supersonic flow was examined by Dowell [1]. The nonlinear membrane forces induced by the plate motion resulted in bounded plate amplitude. In a series of investigations [2-4], Dżygadlo analyzed the coupled parametric and self-excited (flutter) vibrations of plates subjected to periodic varying in-plane forces. In supersonic gas flow, it was found that the instability region of the harmonic resonance shrinks and shifts toward higher excitation frequencies and amplitudes as the Mach number increases.

Eastep and McIntosh [5] investigated panels flutter under random excitation and linear aerodynamic loading. The limit cycle oscillation was determined by representing the modal amplitude by a Fourier series and applying the Galerkin averaging for temporal solution. The existence of a limit cycle was predicted by studying the stability state of small perturbations about the limt cycle solution. The excitation was represented by a random field. The panel motion was described by a coupled set of linear nonhomogeneous differential equations with harmonic coefficients. The study was extended to determine the response of the panel under nonlinear aerodynamic loading in the absence of any random component. Two mechanisms were considered. The first is the nonlinear interaction between in-plane panel stresses and transverse transformation. This interaction provides a stabilizing influence on the panel in that it acts to restrain further deformation. The second is the nonlinear aerodynmic loading which has a destabilizing effect.

Nonlinearities may enter the vibrating system through geometric or physical sources. The geometric nonlinearities are identified by large deformation. Physical nonlinearities arise from the nonlinear nature of the physical properties of the material itself. These nonlinearities appear in the equations of motion in three possible forms: elastic, inertia and damping nonlinearities. Elastic nonlinearity stems from nonlinear strain displacement relations which are inevitable. Inertial nonlinearity are derived, in a Lagrangian formulation, from the kinetic energy. A general and fairly comprehensive description of the role of nonlinear modal interaction under harmonic excitation was given by Ibrahim and Barr [6] and Barr [7]. It was indicated that nonlinear mode interaction may give rise to what are effectively parametric instability phenomena within the system. The parametric action is not due to the external loading but to the motion of the system itself and, hence, is described as "autoparametric." One of the main features of autoparametric coupling is that responses of one part of the system give rise to loading of another part through time-dependent coefficients in the corresponding equation of motion. With autoparametric coupling the system may experience instability of internal resonance. Internal resonance can exist between two or more normal modes depending on the degree of nonlinearity admitted into the equations of motion. Thus, with quadratic nonlinearities, two

Contributed by the Technical Committee on Vibration and Sound and presented at the Design Engineering Technical Conference, Cincinnatti, Ohio, September 10-13, 1985 of THE AMERICAN SOCIETY OF MECHANICAL ENGINEERS. Manuscript received at ASME Headquarters January 1, 1985. Paper No. 85-DET-18.

modes i and j having linear natural frequencies ω_i and ω_j are in internal resonance if $\omega_j = 2\omega_i$, or three modes i, j, and k can be in internal resonance if $\omega_k = |\omega_i \pm \omega_j|$. With cubic nonlinearity two modes i and j can have internal resonance of the type $\omega_j = (1/3)\omega_i$ or $\omega_j = (2/3)\omega_i$. Autoparametric interaction may arise in many aeroelastic configurations such as airplane wing with a store [8] or a Tee-tail plane in bending [9]. The deterministic response of systems with autoparametric interaction has been reviewed by Ibrahim [10, 11] and are well documented by Evan-Iwanowski [12] and Nayfeh and Mook [13].

The first treatment of the autoparametric random interaction is believed to be due to Ibrahim and Roberts [14]. The differential equations of the system response moments were found to be coupled with higher-order moment terms. In other words, the moment equations form a set of infinite hierarchy. The equations were closed by expressing third and fourth-order moments in terms of lower-order moments based on the assumption that the response process is "nearly" Gaussian. The steady-state squares responses were found to behave quasi-stationary in the time domain in the neighborhood of the internal resonance condition $\omega_2 = 0.5\omega_1$. It is known that the result of any linear operator, with constant coefficients, applied to a random Gaussian process results in a Gaussian process. However, if the operator is nonlinear, the resulting operation will not be Gaussian. Consequently, it is important to consider the effect of the non-normality of the response of systems involving nonlinearities. Schmidt [15] employed the Stratonovich stochastic averaging method to determine the response of a system with autoparametric interaction. Contrary to the results of Ibrahim and Roberts, Schmidt found that the system response possesses a stationary probability density function. The discrepancy of the two results motivated the authors to employ the non-Gaussian closure (used recently by Wu and Lin [16], Lin and Wu [17], and Ibrahim and Soundararajan [18]) to determine the response of an aeroelastic structure in the neighborhood of internal resonance. The method leads to a stationary response for all response moments considered in the analysis.

Theoretical Analysis

Figure 1 shows a schematic diagram of an airplane wing with fuel storage. The wing and the storage are modeled by equivalent two beams having stiffnesses k_1 and k_2, and end masses m_1 and m_2, respectively. Under random support acceleration $\ddot{\xi}(t)$ the wind end moves vertically (q_1) and, under the conditions of internal resonance, the mass m_2 moves laterally (q_2). The mathematical modeling can be derived via the Lagrangian formulation. Both the axial and lateral components of the velocity of the wing and the fuel storage are included in determining the kinetic energy and, by using the static deformation curve of the cantilever, these components are found to be in the ratio $6q_i/5l_i$, where l_i is the length of beam i. The equations of motion in terms of the generalized coordinates q_i are [9]

$$\begin{bmatrix} m_1 + m_2(1 + 2.25(l_2/l_2)^2) & 1.5m_2l_2/l_1 \\ 1.5m_2l_2/l_1 & m_2 \end{bmatrix} \begin{Bmatrix} \ddot{q}_1 \\ \ddot{q}_2 \end{Bmatrix}$$

$$+ \begin{bmatrix} k_1 & 0 \\ 0 & k_2 \end{bmatrix} \begin{Bmatrix} q_1 \\ q_2 \end{Bmatrix} = -\ddot{\xi}(t) \begin{Bmatrix} m_1 + m_2 \\ 0 \end{Bmatrix}$$

$$-\ddot{\xi}(t) \begin{bmatrix} 2.25m_2l_2/l_1^2 & 1.5m_2/l_1 \\ 1.5m_2/l_1 & 1.2m_2/l_2 \end{bmatrix} \begin{Bmatrix} q_1 \\ q_2 \end{Bmatrix} - m_2 \begin{Bmatrix} \psi_1 \\ \psi_2 \end{Bmatrix} \quad (1)$$

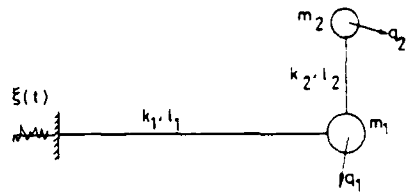

Fig. 1 Schematic diagram of coupled beams with autoparametric resonance

where

$$\psi_1 = 0.9\frac{l_2}{l_1^2} q_1\ddot{q}_1 + 0.45\frac{l_2}{l_1^2}\dot{q}_1^2 + \frac{1.2}{l_2}(q_2\ddot{q}_2 + \dot{q}_2^2)$$

$$+ \frac{0.3}{l_1} q_1\ddot{q}_2 + \frac{3}{l_1}(\ddot{q}_1 q_2 + \dot{q}_1\dot{q}_2)$$

$$\psi_2 = \frac{0.3}{l_1} q_1\ddot{q}_1 - \frac{1.2}{l_1}\dot{q}_1^2 + \frac{1.2}{l_2} q_2\ddot{q}_1$$

$$k_i = 3E_iI_i/l_i^3 \quad (2)$$

It is seen that the left-hand side of equations (1) represents the linear conservative part of the equations of motion. This part involves dynamic coupling. The first term on the right-hand side is the nonhomogeneous random excitation $\ddot{\xi}(t)$, the second term constitutes the parametric effect of the excitation, ψ_1 and ψ_2, in the third expression, include all quadratic nonlinearities. The linear eigenvalues and eigenvectors of system (1) are determined by setting the right-hand side to zero. The eigenvectors are used in establishing the linear transformation into the principal coordinates Y_i, i.e.

$$\{q\} = [R]\{Y\} \quad (3)$$

where $[R]$ is the modal matrix which is given in the Appendix.

Premultiplying equations (1) by $[R]^{-1}[m]^{-1}$, where $[m]$ is the mass matrix, and introducing transformation (3) gives

$$\begin{bmatrix} 1 & 0 \\ 0 & 1 \end{bmatrix} \begin{Bmatrix} Y_1'' \\ Y_2'' \end{Bmatrix} + \begin{bmatrix} 2\zeta_1 & 0 \\ 0 & 2\zeta_2 r \end{bmatrix} \begin{Bmatrix} Y_1' \\ Y_2' \end{Bmatrix}$$

$$+ \begin{bmatrix} 1 & 0 \\ 0 & r^2 \end{bmatrix} \begin{Bmatrix} Y_1 \\ Y_2 \end{Bmatrix}$$

$$= \xi''(\tau) \begin{Bmatrix} a_1 \\ b_1 \end{Bmatrix} + \epsilon \begin{Bmatrix} \bar{\psi}_1 \\ \bar{\psi}_2 \end{Bmatrix}$$

$$+ \epsilon\xi''(\tau) \begin{bmatrix} a_2 & a_3 \\ b_2 & b_3 \end{bmatrix} \begin{Bmatrix} Y_1 \\ Y_2 \end{Bmatrix} \quad (4)$$

where a linear viscous damping is incorporated, and $r = \omega_2/\omega_1$ is the ratio of the normal mode frequencies. The nondimensional principal coordinates Y_1 and Y_2 are related to the dimensional principal coordinates y_1 and y_2 through the relationship

$$\{Y_1, Y_2\} = \{y_1, y_2\}/q_1^0 \quad (5)$$

where q_1^0 is the response root mean square of the system when the length of the vertical beam shrinks to zero, i.e., the response of the wing beam with end mass ($m_1 + m_2$). A prime denotes differentiation with respect to the time parameter $\tau = \omega_1 t$. The nonlinear functions $\bar{\psi}_1$ and $\bar{\psi}_2$ are

$$\bar{\psi}_1 = a_4Y_1Y_1'' + a_5Y_1Y_2'' + a_6Y_2Y_1'' + a_7Y_2Y_2'' + a_8Y_1'^2$$
$$+ a_9Y_1'Y_2' + a_{10}Y_2'^2$$

$$
\begin{aligned}
\psi_2 &= b_4 Y_1 Y_1'' + b_5 Y_1 Y_2'' + b_6 Y_2 Y_1'' + b_7 Y_2 Y_2'' + b_8 Y_1'^2 \\
&\quad + b_9 Y_1' Y_2' + b_{10} Y_2'^2 \\
\epsilon &= q_1^0 / l_1
\end{aligned} \tag{6}
$$

The coefficient a_i and b_i depend on the system parameters.

Expressions (6) include all quadratic nonlinear terms which can be divided into two classes: nonlinear terms of the same mode and autoparametric terms such as $Y_1 Y_2''$. The autoparametric terms give rise to the internal resonance condition $r = \omega_2/\omega_1 = 0.5$.

The random acceleration $\xi''(\tau)$ is assumed to be Gaussian wide band random process with zero mean and a smooth spectral density $2D$ up to some frequency which is higher than any characteristic frequency of the system. If the acceleration terms are removed from the nonlinear part of equations (4) by successive elimination, equations (4) may be approximated by a set of Ito's equations and the response coordinates constitute a Markov process. Introducing the coordinate transformation

$$
\{Y_1, Y_2, Y_1', Y_2'\} = \{X_1, X_2, X_3, X_4\} \tag{7}
$$

equations (4) can be written by the following set of Ito's equations:

$$
\begin{aligned}
X_1' &= X_3 \\
X_2' &= X_4 \\
X_3' &= -X_1 - 2\zeta_1 X_3 - a_4 X_1^2 - (a_6 + r^2 a_5) X_1 X_2 - r^2 a_7 X_2^2 \\
&\quad - 2\zeta_1 a_4 X_1 X_3 - 2\zeta_2 r a_5 X_1 X_4 - 2\zeta_1 a_6 X_2 X_3 - 2\zeta_2 r a_7 X_2 X_4 \\
&\quad + a_8 X_3^2 + a_9 X_3 X_4 + a_{10} X_4^2 - (A_1 + A_2 X_1 + A_3 X_2 + A_4 X_1^2 \\
&\quad + A_5 X_1 X_2 + A_6 X_2^2) W(\tau) \\
X_4' &= -r^2 X_2 - 2\zeta_2 r X_4 - b_4 X_1^2 - (b_6 + r^2 b_5) X_1 X_2 \\
&\quad - r^2 b_7 X_2^2 - 2\zeta_1 b_4 X_1 X_3 - 2\zeta_2 r b_5 X_1 X_4 - 2\zeta_1 b_6 X_2 X_3 \\
&\quad - 2\zeta_2 r b_7 X_2 X_4 + b_8 X_3^2 + b_9 X_3 X_4 + b_{10} X_4^2 \\
&\quad - (B_1 + B_2 X_1 + B_3 X_2 + B_4 X_1^2 + B_5 X_1 X_2 + B_6 X_2^2) W(\tau)
\end{aligned} \tag{8}
$$

where the coefficients A_i and B_i depend on a_i and b_i.

In equations (8), the random acceleration has been replaced by the white-noise process $W(\tau)$ where the Wong-Zakai [19] correction term is zero. The autocorrelation function of $W(\tau)$ is defined by the well-known relation

$$
R_w(\tau') = E[W(\tau) W(\tau + \tau')] = 2D\delta(\tau') \tag{9}
$$

where $2D$ is the spectral density, and $\delta(\ )$ is the Dirac delta function.

In view of the complexity of the state equations (8) it is not expected to obtain a stationary solution for the corresponding Fokker-Planck equation. Instead, it is possible to generate a general differential equation for all possible moments by using the Ito stochastic calculus [20] or the Fokker-Planck equation [21]. It is not difficult to show that the differential equation of the response joint moments is given in the form

$$
\begin{aligned}
m_{ijkl}' &= i m_{i-1,j,k+1,l} + j m_{i,j-1,k,l+1} + k[-m_{i+1,j,k-1,l} \\
&\quad - 2\zeta_1 m_{i,jkl} - a_4 m_{i+2,j,k-1,l} - (r^2 a_5 \\
&\quad + a_6) m_{i+1,j+1,k-1,l} - r^2 a_7 m_{i,j+2,k-1,l} - 2\zeta_1 a_4 m_{i+1,jkl} \\
&\quad - 2\zeta_2 r a_5 m_{i+1,j,k-1,l+1} - 2\zeta_1 a_6 m_{i,j+1,kl} \\
&\quad - 2\zeta_2 r a_7 m_{i,j+1,k-1,l+1} + a_8 m_{ijk+1,l} + a_9 m_{ijk,l+1} \\
&\quad + a_{10} m_{ij,k-1,l+2}] + l[-r^2 m_{i,j+1,k,l-1} - 2\zeta_2 r m_{ijkl} \\
&\quad - b_4 m_{i+2,jk,l-1} - (r^2 b_5 + b_6) m_{i+1,j+1,k,l-1} \\
&\quad - r^2 b_7 m_{i,j+2,k,l-1} - 2\zeta_1 b_4 m_{i+1,j,k+1,l-1} \\
&\quad - 2\zeta_2 r b_5 m_{i+1,jkl} - 2\zeta_1 b_6 m_{i,j+1,k+1,l-1} \\
&\quad - 2\zeta_2 r b_7 m_{i,j+1,kl} + b_8 m_{ij,k+2,l-1} + b_9 m_{ij,k+1,l} \\
&\quad + b_{10} \mathrm{d} m_{ijk,l}] + k(k-1)[D A_1^2 m_{ij,k-2,l} \\
&\quad + 2DA_1 A_2 m_{i+1,j,k-2,l} + 2DA_1 A_3 m_{i,j+1,k-2,l} + D(2A_1 A_4 \\
&\quad + A_2^2) m_{i+2,j,k-2,l} + 2D(A_1 A_5 + A_2 A_3) mi+1, j+1, k-2, l \\
&\quad + D(A_3^2 + 2A_1 A_6) m_{i,j+2,k-2,l}] + kl[2DA_1 B_1 m_{ij,k-1,l-1} \\
&\quad + 2D(A_1 B_2 + A_2 B_1) m_{i+1,j,k-1,l-1} + 2D(A_1 B_3 \\
&\quad + A_3 B_1) m_{i,j+1,k-1,l-1} + 2D(A_1 B_4 + A_4 B_1 \\
&\quad + A_2 B_2) m_{i+2,j,k-1,l-1} + 2D(A_1 B_5 + A_5 B_1 + A_2 B_3 \\
&\quad + \ \ {}_2) m_{i+1,j+1,k-1,l-1} + 2D(A_3 B_3 + A_1 B_6 \\
&\quad + A_6 B_1) m_{i,j+2,k-1,l-1}] + l(l-1)[DB_1^2 m_{ijk,l-2} \\
&\quad + 2DB_1 B_2 m_{i+1,jk,l-2} + 2DB_1 B_3 m_{i,j+1,k,l-2} + D(2B_1 B_4 \\
&\quad + B_2^2) m_{i+2,jk,l-2} + 2D(B_1 B_5 + B_2 \mathrm{d} B_3) m_{i+1,j+1,k,l-2} \\
&\quad + D(B_3^2 + 2B_1 B_6) m_{i,j+2,k,l-2}]
\end{aligned} \tag{10}
$$

where the definition

$$
\begin{aligned}
m_{ijkl} &= \int_{-\infty}^{\infty} \ldots \int X_1^i X_2^j X_3^k X_4^l p(\mathbf{X}, \tau) dX_1 \ldots dX_4 \\
&= E[X_1^i X_2^j X_3^k X_4^l]
\end{aligned}
$$

has been adopted.

It is seen that a moment equation of order $n = i + j + k + l$ contains moments of order n and $n+1$. In order to solve for the steady-state response the moment equations must be closed. The response moments will be determined by using Gaussian and non-Gaussian closure schemes.

Gaussian Closure Solution

From the general differential equation (10), one can generate four equations for the first-order moments and ten equations for the second-order moments. These equations are, however, coupled through third-order moment terms. In this section, the 14 equations will be closed by making the assumption that the system nonlinearities are too small to the extent that the response can be regarded as nearly Gaussian. In this case, the cubic semi-invariants vanish and third-order moment terms can be written in terms of lower-order moments, i.e.

$$
\begin{aligned}
\lambda_3[X_i X_j X_k] &= E[X_i X_j X_k] - \sum^{3} E[X_i] E[X_j X_k] \\
&\quad + 2E[X_i] E[X_j] E[X_k] = 0
\end{aligned} \tag{11}
$$

where the number over the summation sign refers to the number of terms generated by the indicated expression without allowing permutation of indices.

The closed 14 coupled equations are solved numerically by using the IMSL-DVERK Routine (Runge-Kutta-Verner fifth and sixth-order numerical integration method). The transient and steady-state responses of the system mean square displacements $E[Y_1^2]$ and $E[Y_2^2]$ are plotted in Fig. 2 for internal resonance ratio $r = 0.5$, mass ratio $m_2/m_1 = 0.2$, beams length ratio $l_2/l_1 = 0.6$, and $\epsilon = 0.02$. It is seen that the steady-state response fluctuates between two boundaries which will be referred to as lower and upper limits. Repeating the numerical integration for various values of the internal resonance parameter $r = 0.5 \pm \epsilon$, one can examine the effect of the system parameters upon the response mean squares.

The effect of damping ratios ζ_1 and ζ_2 is shown in Fig. 3(a). It is seen that the region of autoparameteric interaction becomes wider as the damping ratios decrease. Figure 3(b) shows the influence of the nonlinear coupling ϵ. For very small

ϵ the system does not reflect any autoparametric coupling for the whole range of internal resonance ratio. As ϵ increases the system enters the region of autoparametric interaction. This region becomes wider as ϵ increases. The effect of the mass ratio is shown in Fig. 3(*c*).

Non-Gaussian Closure Solution

Since the system is nonlinear, the response process is not Gaussian distributed and the corresponding third and higher-order semi-invariants will not vanish. These higher semi-invariants give a measure to the deviation of the response from normality. However, their contribution diminishes as their order increases if the process is slightly deviated from Gaussian. Thus one can establish a better approximation if fifth and higher-order semi-invariants will be equated to zero, i.e.

$$\begin{aligned}
\lambda_5[X_iX_jX_kX_lX_m] &= E[X_iX_jX_kX_lX_m] \\
&- \sum^{5} E[X_i]E[X_jX_kX_lX_m] \\
&+2 \sum^{10} E[X_i]E[X_j]E[X_kX_lX_m] \\
&-6 \sum^{10} E[X_i]E[X_j]E[X_k]E[X_lX_m] \\
&+2 \sum^{15} E[X_i]E[X_jX_k]E[X_lX_m] \\
&- \sum^{10} E[X_iX_j]E[X_kX_lX_m] \\
&+24E[X_i]E[X_j]E[X_k]E[X_l]E[X_m] = 0 \qquad (12)
\end{aligned}$$

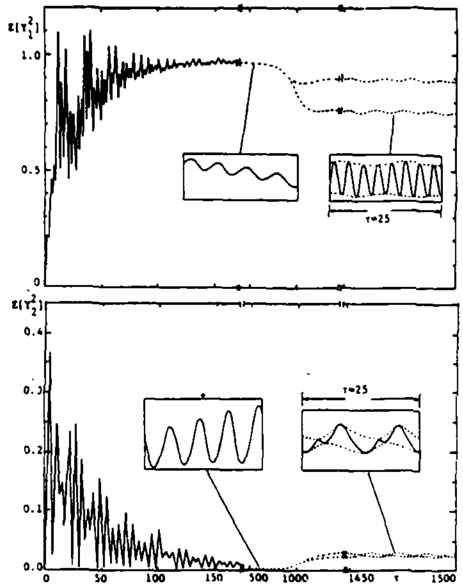

Fig. 2 Transient and steady-state responses based on Gaussian closure solution; (r = 0.5, $\zeta_1 = \zeta_2$ = 0.02, m_2/m_1 = 0.2, ϵ = 0.02)

From equation (10), one can generate moment equations of order up to four. This will result in 69 equations which are coupled and contain fifth-order moment terms. Replacing fifth-moment terms in terms of lower-order moments by using relations (12), the 69 equations will be closed. The resulting 69 coupled differential equations are solved numerically by using the IMSL-DVERK subroutine. Figure 4 exemplifies the time history response of the displacement mean squares for internal resonance ratio r = 0.5 and damping ratios $\zeta_1 = \zeta_2 = 0.02$. During the transient period the mean square of the first normal mode displacement grows until it reaches a peak value at τ = 60 then drops to a lower level at τ = 150. The mean square of the second normal mode displacement grows much slower until it reaches it peak at τ = 150 which is the time at which the first normal mode mean square reaches its minimum value. This feature reflects the fact that the two normal modes exchange energy during a transient period after which each mode shows a complete stationary response. Unlike the Gaussian closure solution described in the previous section, the non-Gaussian closure solution brings the system into a stationary state. The stationarity of the solution is confirmed by setting the left-hand sides of the closed 69 equations to zero

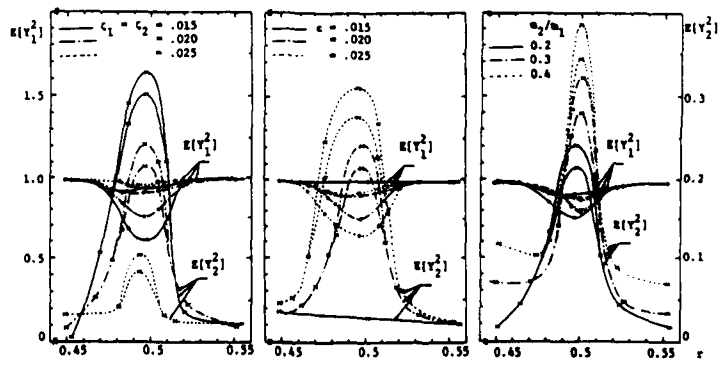

(a) m_2/m_1 = 0.2, ϵ = 0.02 (b) $\zeta_1 = \zeta_2$ = 0.02, m_2/m_1 = 0.2 (c) $\zeta_1 = \zeta_2$ = 0.002, ϵ = 0.02

Fig. 3 Gaussian closure solution for various system parameters

and the resulting nonlinear algebraic equations were solved numerically by using the ZSCNT subroutine which is basically the Secant method for simultaneous nonlinear equations. The algebraic solution is found identical to the stationary solution obtained by numerical integration. Originally, the authors tried to obtain an algebraic solution for the 14 equations closed by the Gaussian closure scheme. However, the solution did not converge for all possible guessing values. This shows that the Gaussian closure scheme is not adequate to model the system nonlinearity and thus results in a nonstationary solution. The validity of the stationarity was previously verified by Schmidt [15] who obtained a stationary solution of the Fokker-Planck equation of a nonlinear two-degree-of-freedom system via the stochastic averaging method. However, Schmidt did not determine the constant of integration from the normalized condition.

The numerical integration of the 69 closed differential resonance ration $r = 0.5 \pm \epsilon$. The influence of the damping ratios, nonlinear coupling parameter ϵ, and mass ratio are shown in Figs. 5(*a–c*), respectively. The effect of these parameters on the response mean squares is similar to their effect in the Gaussian solution curves; however, the response curves have one branch which is located within the limiting curves of the Gaussian solution.

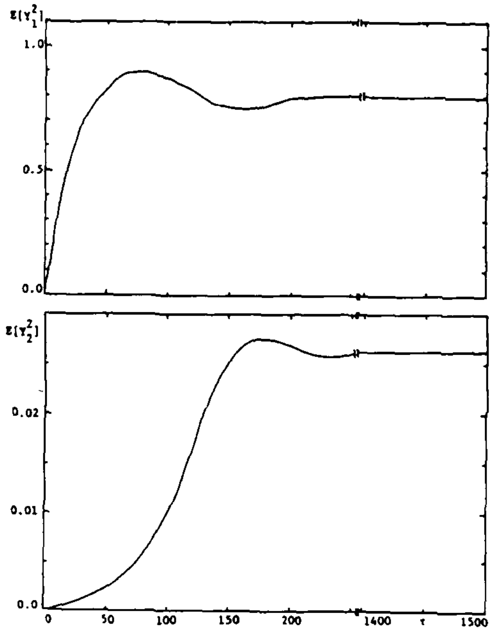

Fig. 4 Transient and steady-state responses based on non-Gaussian closure solution; (r = 0.5, ζ_1 = ζ_2 = 0.02, m_2/m_1 = 0.2, ϵ = 0.02)

Conclusions

The random response of a coupled beam system with quadratic autoparametric interaction is investigated in the neighborhood of the critical region of internal resonance. A general differential equation of the response moments of any order has been derived and found to represent an infinite hierarchy set. Two closure techniques have been employed. These are the Gaussian and non-Gaussian closures. The Gaussian closure led to a set of 14 coupled nonlinear equations for the first and second moments of the system responses. The non-Gaussian closure gave 69 coupled nonlinear equations for the first through fourth moments. The two sets of differential equations were solved by a numerical integration algorithm. The Gaussian closure solution led to a nonstationary response for all even order moments while the non-Gaussian closure solution showed that the system reached a stationary state. The influence of the system parameters upon the response mean squares were examined over a range of internal resonance within which the system autoparametric interaction took place.

Acknowledgment

This research is supported by a grant from AFOSR under grant No. AFOSR-85-0008.

References

1 Dowell, E. H., 1966, "Nonlinear Oscillations of a Fluttering Plate," *AIAA Journal*, Vol. 4, pp. 1267–1275.

2 Dzygadlo, Z., 1965, "Parametric Self-Excited Vibration of a Simply Supported Plate in Supersonic Flow," *Proceedings of Vibration Problems*, Vol. 6, pp. 353–365.

3 Dzygadlo, Z., 1967, "Nonstationary Parametric and Parametric Self-Excited Vibration of a Plate of Finite Length in Plane Supersonic Flow," *Proceedings of Vibration Problems*, Vol. 8, pp. 381–393.

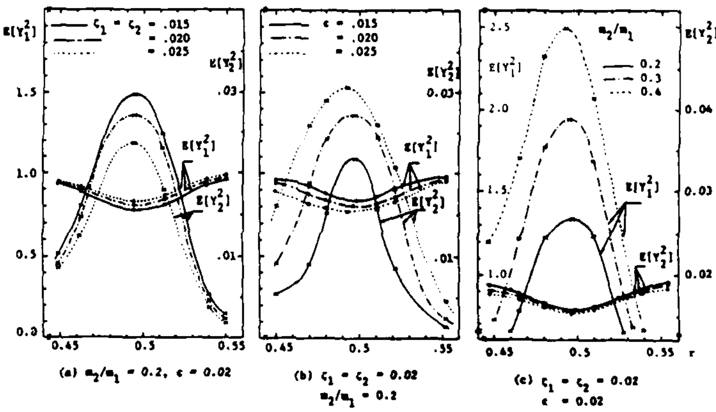

Fig. 5 Non-Gaussian closure solution for various system parameters

4 Dżygadło, Z., 1969, "Forced Parametrically-Excited Vibration of a Plate of Finite Length in Plane Supersonic Flow," *Proceedings of Vibration Problems*, Vol. 10, pp. 2313-245.

5 Eastep, F. E., and McIntosh, S. C., Jr., "Analysis of Nonlinear Panel Flutter and Response Under Random Excitation or Nonlinear Aerodynamic Loading," *AIAA Journal*, Vol. 9, pp. 411-418.

6 Ibrahim, R. A., and Barr, A. D. S., 1978, "Parametric Vibration, Part II: Mechanics of Nonlinear Problems," *The Shock and Vibration Digest*, Vol. 10(2), pp. 9-24.

7 Barr, A. D. S., 1980, "Some Developments in Parametric Stability and Nonlinear Vibration," *Proceedings, International Conference on Recent Advances in Structural Dynamics*, Institute of Sound and Vibration Research, University of Southampton, pp. 545-568.

8 Barr, A. D. S., and Done, G. T. S., 1971, "Parametric Oscillations in Aircraft Structure," *Aeronautical Journal*, Vol. 75, pp. 654-658.

9 Barr, A. D. S., and Ashworth, R. P., December 1977, "Parametric and Nonlinear Mode Interaction Behavior in the Dynamics of Structures," Final Report, AFOSR74-2723, (EOARD), London, Department of Mechanical Engineering, University of Dundee.

10 Ibrahim, R. A., 1978, "Parametric Vibration, Part III: Current Problems (1)," *The Shock and Vibration Digest*, Vol. 10(3), pp. 41-57.

11 Ibrahim, R. A., 1978, "Parametric Vibration, Part IV: Current Problems, (2)," *The Shock and Vibration Digest*, Vol. 10(4), pp. 19-47.

12 Evan-Iwanowski, R. M., 1976, *Resonance Oscillations in Mechanical Systems*, Elsevier Science, New York.

13 Nayfeh, A. H., and Mook, D. T., 1979, *Nonlinear Oscillations*, John Wiley Interscience, New York.

14 Ibrahim, R. A., and Roberts, J. W. 1976, "Broad-Band Random Excitation of a Two Degree-of-Freedom System With Autoparametric Coupling," *Journal of Sound Vibration*, Vol. 44(3), pp. 335-348.

15 Schmidt, G., 1977, "Probability Densities of Parametrically Excited Random Vibrations," *Proceedings IUTAM Symposium*, Stochastic Problems in Dynamics, edited by B. L. Clarkson, Pitman, London, pp. 197-213.

16 Wu, W F., and Lin, Y. K., 1984, "Cumulant-Neglect Closure for Nonlinear Oscillations Under Random Parametric and External Excitations," *International Journal of Nonlinear Mechanics*, Vol. 19, pp. 349-362.

17 Lin, Y. K., and Wu, W. F., 1984, "Applications of Cumulant Closure to Random Vibration Problems," *Proceedings ASME WAM on Random Vibrations*, AMD Vol. 65, pp. 113-125.

18 Ibrahim, R. A., and Soundararajan, A., 1985, "An Improved Approach for Random Parametric Response of Dynamic Systems With Nonlinear Inertia," *International Journal of Nonlinear Mechanics*, Vol. 20, pp. 309-323.

19 Wong, E., and Zakai, M., 1965, "On the Relation Between Ordinary and Stochastic Differential Equations," *International Journal of Engineering Science*, Vol. 3, pp. 213-229.

20 Arnold, L., 1974, *Stochastic Differential Equations: Theory and Applications*, Wiley, New York.

21 Melsa, J. L., and Sage, A. P., 1973, *An Introduction to Probability and Statistical Processes*, Prentice-Hall, Inc., New Jersey.

22 Schmidt, G., 1975, *Parametererregte Schwingungen*, *Deutscher Verlag der Wissenschaften*, Berlin, 1975.

23 Froys, A., and Niziol, J., 1984, *Internal Resonance in a Plane System of Rods*," *Journal of Sound Vibration*, Vol. 95, pp. 361-374.

APPENDIX

Modal matrix $[R]$

$$[R] = \begin{bmatrix} 1 & 1 \\ \phi_1 & \phi_2 \end{bmatrix}$$

where

$$\phi_1 = \frac{\omega_{11}^2 - \omega_1^2}{\omega_1^2 \cdot \dfrac{m_{12}}{m_{11}}}$$

$$\phi_2 = \frac{\omega_{11}^2 - \omega_2^2}{\omega_2^2 \cdot \dfrac{m_{12}}{m_{11}}}$$

$$\omega_{ii}^2 = \frac{K_{ii}}{m_{ii}}$$

$$m_{11} = 1 + \frac{m_2}{m_1}\left[1 + 2.25\left(\frac{l_2}{l_1}\right)^2\right]$$

$$m_{12} = 1.5\,\frac{l_2}{l_1}\,\frac{m_2}{m_1}$$

$$\omega_{1,2}^2 = \frac{1}{2\mu}\,\{\omega_{11}^2 + \omega_{22}^2 \pm [(\omega_{11}^2 + \omega_{22}^2)^2 - 4\mu\omega_{11}^2\omega_{22}^2]^{1/2}\}$$

$$\mu = 1 - \frac{m_{12}}{m_{11}}\,\frac{m_{12}}{m_{22}}$$

$$m_{22} = m_2/m_1$$

Stochastic modal interaction in linear and nonlinear aeroelastic structures

R. A. Ibrahim and Z. Hedayati*

Texas Tech. University, Department of Mechanical Engineering, Lubbock, Texas 79409, USA

The linear and autoparametric modal interactions in a three defree-of-freedom structure under wide band random excitation are examined. For a structure with constant parameters the linear response is obtained in a closed form. When the structure stiffness matrix involves random fluctuations, the governing equations of motion, in terms of the normal coordinates, are found to be coupled through parametric terms. The structural response is mainly governed by the condition of mean square stability. The boundary of stable-unstable responses is obtained as a function of the internal detuning parameter. The results of the linear system with constant parameters are used as a reference to measure the deviation of the system response when the nonlinear inertia coupling is included. In the neighbourhood of combination internal resonance the system random response is determined by using the Fokker Planck equation approach together with the Gaussian closure scheme. This approach results in 27 coupled first order differential equations in the first and second response moments. These equations are solved numerically. The response is found to deviate significantly from the linear solution when the system internal detuning is close to the exact internal resonance. The autoparametric interaction is found to depend significantly on the system damping ratios and a nonlinear coupling parameter. In the vicinity of combination internal resonance, the second normal mode mean square exhibits an increase associated with a corresponding decrease in the first and third normal modes.

I. INTRODUCTION

The modal analysis of aerolastic structures is usually carried out by using one of the available computer codes for eigenvalues and eigenvectors. These computer algorithms are useful in determining the structural dynamic behavior under various types of excitations. The first step usually involves the determination of eigenvalues and eigenvectors. With this information one can determine the linear response to deterministic or random excitations. For systems with constant parameters the mean square response to external white noise is linearly proportional to the excitation spectral density. If the excitation is acting parametrically to the system the equilibrium state could be stable or unstable in a stochastic sense. In certain situations the structure may not behave according to the linear theory of small oscillations and a number of complex response characteristics such as amplitude jump, internal resonance, saturation phenomenon, and chaotic motion[1,2] may be observed. These new characteristics owe their origin to the system inherent nonlinearities which should not be ignored in dynamic analysis.

In aircraft structures several types of nonlinearities have been reported. Breitbach[3] classified structural nonlinearities into distributed and concentrated. Distribution nonlinearity is induced by elastic deformation in riveted, screwed and bolted connections as well as within the structural components themselves. Concentrated nonlinearity acts locally lumped in control mechanisms or in the connecting parts between wing and external stores. This nonlinearity results from back-lash in the linkage elements of the control system, dry friction in control cable and push rod ducts, kinematic limitation of the control surface deflection, and application of spring tab system provided for relieving pilot operation. Breitbach[4] determined the flutter boundaries for three different configurations distinguished by different types of nonlinearities in the rudder and aileron control system of a sailplane. It was shown that the influence of hysteretic damping results in a considerable stabilizing effect and an increase in the flutter speed. However, this special type of non-linearity does not bring the structural response into a bounded limit cycle. Similar effects of nonlinearities due to friction and back-lash were considered by De Ferrari *et al.*[5], Peloubet *et al.*[6], Reed *et al.*[7] and Desmarais and Reed[8] examined the effects of control system nonlinearities, such as actuator force or deflection limits, on the performance of an active flutter suppression system. It was shown[7] that a nonlinear system which is stable with respect to small disturbances may be unstable with respect to large ones. Another important feature was that a store on a pylon with low pitch stiffness can provide substantial increase in flutter speed and reduce the dependency of flutter on the mass and inertia of stores relative to that of stiff-mounted stores.

In structural dynamics, the nonlinearity may take one of three classes[9,10]: elastic, inertia, and damping nonlinearities. Elastic nonlinearity stems from nonlinear

* Currently PhD student, Massachusetts Institute of Technology, Department of Mechanical Engineering, Cambridge, MA 02139, USA
Received September 1986. Discussion closes February 1987.

0266-8920/86/040182-10$2.00

strain-displacement relations which are inevitable. Inertia nonlinearity is derived, in Lagrangian formulation, from the kinetic energy. In multi-degree-of-freedom systems the normal modes may involve nonlinear inertia coupling which may give rise to what are effectively parametric instability phenomena within the system. The parametric action is not due to the external loading, as in the case of parametric vibration, but to the motion of the system itself and, hence, is described as autoparametric[11]. The main feature of autoparametric coupling is that responses of one component of the structure give rise to loading of another component through time-independent coefficients in the corresponding equation of motion. The deterministic autoparametric interactions in two and three freedom systems were examined by Barr and Ashworth[12], Haddow *et al.*[13], Ibrahim *et al.*[14], and Ibrahim and Woodal[15]. These studies have shown that the mode which is externally excited exhibits a saturation phenomenon in which energy is transferred to other modes involved in the nonlinear coupling. The stochastic aspects of parametric and autoparametric vibrations have recently been documented in a recent research monograph by Ibrahim[16].

To the authors' knowledge the random response of systems with autoparametric coupling has been restricted to two-degree-of-freedom systems. This paper deals with the linear and nonlinear modal interactions of a three degree-of-freedom aeroelastic structure subjected to random excitation. The deterministic responses of this model under various internal resonance conditions $\sum k_i\omega_i=0$ (where k_i are integers and ω_i are the system normal mode frequencies) have been determined by Ibrahim *et al.*[14,15]. The system involves quadratic nonlinear inertia which couples the system normal modes. It was shown that under principal internal resonance, the mode which is directly excited is suppressed and energy is transferred to the other mode. When the structure possess combination internal resonance of the summed type the normal mode amplitudes did not achieve a steady state and the response is characterized by energy exchange between the three modes.

The main objectives of this paper are to present the linear, parametric and autoparametric random responses of the same aeroelastic model considered in Refs 14 and 15. The mean square responses will be evaluated for a model with constant parameters and for a model with random variations in its stiffness matrix. The nonlinear random response of the system in the neighbourhood of combination internal resonance of the summed type will be determined by using the Fokker Planck equation approach together with a Gaussian closure scheme. The effects of the system nonlinearity and damping coefficients on the mean square responses will be examined.

II. BASIC MODEL AND EQUATIONS OF MOTION

Fig. 1 shows a schematic diagram of an analytical model of an aircraft subjected to random excitation $F(t)$. The fuselage is represented by the main mass m_3, linear spring K_3, and dashpot C_3. Attached to the main mass on each side are two coupled beams with tip masses m_1 and m_2, stiffnesses K_1 and K_2, and lengths l_1 and l_2. In the analysis

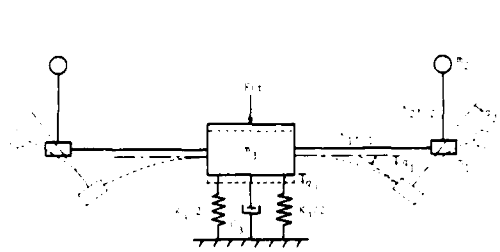

Fig. 1. Schematic diagram of an aeroelastic Structure and Coordinate System

of the shown system only the symmetric motions of the two sides of the model are considered. Under random excitation the system response will be described by the generalized coordinates q_1, q_2, and q_3 as shown in the figure. The equations of motion are derived by applying Lagrange's equation

$$\frac{d}{dt}\left\{\frac{\partial L}{\partial \dot{q}}\right\}-\left\{\frac{\partial L}{\partial q}\right\}=2\{Q_{NC}\} \tag{1}$$

where $L=T-V$.

The kinetic energy T is given by the expression[17]

$$\begin{aligned}T=&\frac{1}{2}\left\{m_1+m_2\left[1+\left(\frac{3l_2}{2l_1}\right)^2\right]\right\}\dot{q}_1^2+\frac{1}{2}m_2\dot{q}_2^2\\&+\frac{1}{2}(m_1+m_2+m_3)\dot{q}_3^2+\frac{3m_2l_2}{2l_1}\dot{q}_1\dot{q}_2\\&+(m_1+m_2)\dot{q}_1\dot{q}_3+\frac{9m_2l_2}{20l_1^2}(q_1\dot{q}_1^2+5q_1\dot{q}_1\dot{q}_3)\\&+\frac{3m_2}{2l_1}\left(\frac{q_1\dot{q}_1\dot{q}_2}{5}+q_1\dot{q}_2\dot{q}_3+\dot{q}_1q_2\dot{q}_3+\dot{q}_1^2q_2\right)\\&+\frac{6m_2}{5l_2}(q_2\dot{q}_2\dot{q}_3+\dot{q}_1q_2\dot{q}_2)\end{aligned} \tag{2}$$

where a dot denotes differentiation with respect to time t. Neglecting the gravitational effects, the potential energy V is given by

$$V=1/2(k_1q_1^2+k_2q_2^2+k_3q_3^2) \tag{3}$$

Substituting for T and V in equation (1), and considering $F(t)$ as the only nonconservative force (damping forces will be introduced later) results in the equations of motion in terms of the nondimensional coordinates $\bar{q}_i$,

$$\omega_3^2\begin{bmatrix}m_{11} & m_{12} & m_{13}\\ m_{12} & m_{22} & 0\\ m_{13} & 0 & m_{33}\end{bmatrix}\begin{Bmatrix}\bar{q}_1''\\ \bar{q}_2''\\ \bar{q}_3''\end{Bmatrix}+\begin{bmatrix}k_1 & 0 & 0\\ 0 & k_2 & 0\\ 0 & 0 & k_3\end{bmatrix}\begin{Bmatrix}\bar{q}_1\\ \bar{q}_2\\ \bar{q}_3\end{Bmatrix}$$
$$=\frac{1}{q_3^{\circ}}\begin{Bmatrix}0\\ 0\\ F(\tau/\omega_3)\end{Bmatrix}-\frac{m_2q_3^{\circ}\omega_3^2}{l_1}\begin{Bmatrix}\bar{\psi}_1\\ \bar{\psi}_2\\ \bar{\psi}_3\end{Bmatrix} \tag{4}$$

where

$$\bar{q}_i=q_i/q_3^{\circ}, \qquad \tau=\omega_3 t$$

q_3° is taken as the root-mean-square of the main mass when all other parts are locked under forced excitation,

ω_3 is taken as the third eigenvalue of the system, and

$$m_{11} = m_1 + m_2[1 + 2.25(l_2/l_1)^2]$$
$$m_{22} = m_2$$
$$m_{33} = m_1 + m_2 + m_3$$
$$m_{12} = 1.5 m_2 (l_2/l_1)$$
$$m_{13} = m_1 + m_2$$

$$\bar{\bar{\psi}}_1 = m_2[0.45(l_2 l_1^2)(2q_1\ddot{q}_1 + \dot{q}_1^2 + 5q_1\ddot{q}_3) + (1.5/l_1)(0.2q_1\ddot{q}_2 + q_2\ddot{q}_3 + 2q_2\ddot{q}_1 + 2\dot{q}_1 q_2) + (1.2/l_2)(q_2\ddot{q}_2 + \dot{q}_2^2) \quad (5)$$

where a prime denotes differentiation with respect to the dimensionless time τ.

III. EIGENVALUES OF THE SYSTEM

The system eigenvalues are determined from the conservative linear part of the equations of motion

$$[m]\{q\} + [k]\{q\} = \{0\} \quad (6)$$

The characteristic equation of (6) is

$$\mathrm{Det}|[k] - \omega^3[m]| = 0 \quad (7)$$

where ω is the eigenvalue of the mode in question.

Expanding the determinant gives the cubic equation

$$\left(-1 + \frac{m_{12}^2}{m_{11}m_{22}} + \frac{m_{13}^2}{m_{11}m_{33}}\right)\left(\frac{\omega}{\omega_{33}}\right)^6 + \left[\left(\frac{\omega_{11}}{\omega_{33}}\right)^2 + \left(\frac{\omega_{22}}{\omega_{33}}\right)^2\left(1 - \frac{m_{13}^2}{m_{11}m_{33}}\right) + \left(1 - \frac{m_{12}^2}{m_{11}m_{22}}\right)\right]\left(\frac{\omega}{\omega_{33}}\right)^4 - \left[\left(\frac{\omega_{11}}{\omega_{33}}\right)^2\left(\frac{\omega_{22}}{\omega_{33}}\right)^2 + \left(\frac{\omega_{11}}{\omega_{22}}\right)^2 + \left(\frac{\omega_{22}}{\omega_{33}}\right)^2\right]\left(\frac{\omega}{\omega_{33}}\right)^2 + \left(\frac{\omega_{11}}{\omega_{33}}\right)^2\left(\frac{\omega_{22}}{\omega_{33}}\right)^2 = 0 \quad (8)$$

where the frequency parameters $\omega_{ii} = K_i/m_{ii}$, are the natural frequencies of the individual components of the structure. The IMSL (International Mathematical and Statistical Library) Subroutine ZPOLR (Zeros of a Polynomial with Real Coefficients) is used to find the roots of equation (8) numerically. Fig. 2 shows a sample of the dependence of the natural frequency ration $r = \omega_3/(\omega_1 + \omega_2)$ on the ratios ω_{11}/ω_{33} and ω_{22}/ω_{33} for beams length ratio $l_2/l_1 = 0.25$, and mass ratios $m_2/m_1 = 0.5$, and $m_3/m_1 = 5.0$. Other sets of curves for different system parameters are obtained and reported in Ref. 17. The importance of these curves is to define the critical points where the structure possesses internal combination resonance $r = 1.0$. It is seen that the most critical region is located for the curves of $\omega_{22}/\omega_{33} = 1$ and 2. For the analysis hereafter the following parameters will be used: $l_2/l_2 = 0.25$, $\omega_{22}/\omega_{33} = 1.4$.

IV. TRANSFORMATION INTO NORMAL COORDINATES

Equations (4) include linear and nonlinear dynamic couplings. The linear coupling is eliminated by transforming equations (4) into normalized coordinates

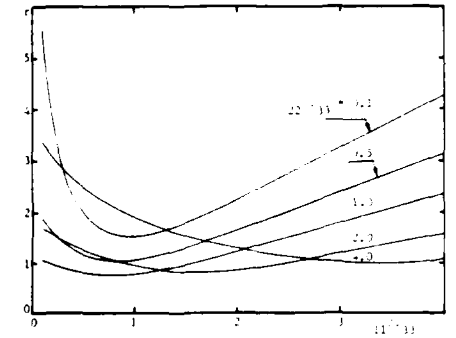

Fig. 2. Dependence of frequency ratio on system parameters for $l_2/l_1 = 0.25$, $m_2\ m_1 = 0.5$, $m_3\ m_1 = 5$

Y_i, by using the transformation

$$\{q_i\} = [R]\{Y\} \quad (9)$$

where $[R]$ is the modal matrix consisting of the normalized eigenvectors.

$$[R] = \begin{bmatrix} 1 & 1 & 1 \\ n_1 & n_2 & n_3 \\ \bar{n}_1 & \bar{n}_2 & \bar{n}_3 \end{bmatrix} \quad (10)$$

the elements of matrix (10) are determined by using the decomposition method[18] and are listed in Ref. 17.

Rewriting equations (4) in the matrix form and using transformation (9) gives

$$[m][R]\{Y''\} + [k][R]\{Y\} = \{F\} - \{\bar{\psi}\} \quad (11)$$

Premultiplying equation (11) by the transpose of the modal matrix results in diagonalizing the mass and stiffness matrices. The resulting equations involve nonlinear coupling and have the form

$$m_1\omega_3^2 \begin{bmatrix} M_{11} & 0 & 0 \\ 0 & M_{22} & 0 \\ 0 & 0 & M_{33} \end{bmatrix} \begin{Bmatrix} y_1'' \\ y_2'' \\ y_3'' \end{Bmatrix} + k_1 \begin{bmatrix} k_{11} & 0 & 0 \\ 0 & k_{22} & 0 \\ 0 & 0 & k_{33} \end{bmatrix} \begin{Bmatrix} y_1 \\ y_2 \\ y_3 \end{Bmatrix} = \frac{1}{q_3^5} \begin{Bmatrix} \bar{n}F(\tau/\omega_3) \\ \bar{n}_2 F(\tau/\omega_3) \\ \bar{n}_3 F(\tau/\omega_3) \end{Bmatrix} - \frac{m_2 q_3 \omega_3^2}{l_1} \begin{Bmatrix} \psi_1 \\ \psi_2 \\ \psi_3 \end{Bmatrix} \quad (12)$$

where

$$M_{ii} = 1 + \alpha(1 + 2.25\beta^2 + 3\beta n_i + 2\bar{n}_i + n_i^2 + \bar{n}_i^2) + [1 + m_3/_1 m)]\bar{n}_i^2 + 2\bar{n}$$

$$k_{ii} = 1 + (k_2/k_1)n_i^2 + (k_3/k_1)n_i^2$$

$$\psi_i = y_1''(L_{i11}y_1 + L_{i21}y_2 + L_{i31}y_3) + y_2''(L_{i12}y_1 + L_{i22}y_2 + L_{i32}y_3) + y_3''(L_{i13}y_1 + L_{i23}y_2 + L_{i23}y_2 + L_{i33}y_3) + M_{i11}y_1'^2 + M_{i22}y_2'^2 + M_{i33}y_3'^2 + M_{i12}y_1'y_2' + M_{i13}y_3' + M_{i23}y_2'y_3'$$

$$\alpha = m_2/m_1, \qquad \beta = l_1/l_1$$

$$\begin{aligned}
L_{ijk} &= 0.9\beta + 2.25\beta\bar{n}_k + 0.3n_k + 1.5n_j\bar{n}_k + 3n_j \\
&\quad + (1.2/\beta)n_jn_k + n_i[0.3 + 1.5\bar{n}_k + (1.2/\beta)n_j(1+\bar{n}_k)] \\
&\quad + \bar{n}_i[2.25\beta + 1.5(n_j+n_k) + (1.2/\beta)n_jn_k] \\
M_{ijk} &= 0.9\beta + 3(n_j+n_K) + (2.4/\beta)n_jn_k \\
&\quad - 2.4n_i + \bar{n}_i[4.5\beta + 3(n_j+n_k) + (2.4/\beta)n_jn_k] \\
&\quad (j \neq k) \\
M_{ill} &= 0.45\beta + 3n_l + (1.2/\beta)n_l^2 \\
&\quad - 1.2n_i + \bar{n}_i[2.25\beta + 3n_l + (1.2/\beta)n_l^2] \\
&\quad (j = k = l)
\end{aligned} \tag{13}$$

V. DYNAMIC MOMENT EQUATIONS

The response coordinates can be approximated as a Markov vector if the random excitation is approximated as a zero mean physical white noise $W(\tau)$ having the autocorrelation function

$$R_w(\Delta\tau) = E[W(\tau)W(\tau+\Delta\tau)] = 2D\delta(\Delta\tau) \tag{14}$$

where $2D$ is the spectral density intensity and $\delta(\ )$ is the Dirac delta function. This modelling is justified as long as the relevant Wong-Zakai[16] correction term is introduced. The non-linear functions ψ_i contain acceleration terms coupled with displacement coordinates such as $Y_i''Y_j$. These terms are removed from equations (12) by successive elimination by using MACSYMA software. Equations (12) take the new form

$$Y_i'' + 2\zeta_i r_{i3}Y_i' + r_{i3}^2 Y_i = f_i W(\tau) + \varepsilon g_i(\mathbf{Y}, \mathbf{Y}') \tag{15}$$

where linear viscous damping terms have neen introduced to account for energy dissipation, and

$$\omega_i^2 = (k_{ii}/M_{ii})(k_1/m_1), \qquad r_{i3} = \omega_i/\omega_3,$$
$$f_i = \bar{n}_i/M_{ii}, \qquad \varepsilon = q_3/l_i$$

$$W(\tau) = \frac{1}{q_3^2\omega_3^2 m_1} F(\tau/\omega_3)$$

Introducing the transformation into the Markov state vector $\mathbf{X}$

$$\{Y_1, Y_1', Y_2, Y_2', Y_3, Y_3'\} = \{X_1, X_2, \ldots, X_6\} \tag{16}$$

equations (15) may be written in the standard form of Stratonovich differential equations

$$\mathrm{d}X_i = F_i(\mathbf{X}, \tau)\,\mathrm{d}\tau + \sum_{j=1}^{6} G_{ij}(\mathbf{X}, \tau)\,\mathrm{d}B_j(\tau) \tag{17}$$

where the white noise $W(\tau)$ has been replaced by the formal derivative of the Brownian motion process $B(\tau)$, i.e.,

$$W(\tau) = \sigma\,\mathrm{d}B(\tau)/\mathrm{d}\tau, \qquad \sigma^2 = 2D$$

Alternatively, equations (17) may in turn be transformed into the Ito type equation

$$\mathrm{d}X_i = \left[F_i(\mathbf{X}, \tau) + \frac{1}{2}\sum_{k=1}^{6}\sum_{j=1}^{6} G_{kj}(\mathbf{X}, \tau)\frac{\partial G_{ij}(\mathbf{X}, \tau)}{\partial X_k}\right]\mathrm{d}\tau + \sum_{j=1}^{6} G_{ij}(\mathbf{X}, \tau)\,\mathrm{d}B_j(\tau) \tag{18}$$

where the double summation expression is called the Wong-Zakai correction term[16].

The system *stochastic Ito equations* are

$$\mathrm{d}X_1 = X_2\,\mathrm{d}\tau, \qquad \mathrm{d}X_3 = X_4\,\mathrm{d}\tau, \qquad \mathrm{d}X_5 = X_6\,\mathrm{d}\tau$$

$$\begin{aligned}
\mathrm{d}X_2 = -\Big\{ & 2\zeta_1 r_{13}X_2 + r_{13}^2 X_1 + \frac{\varepsilon\alpha}{M_{11}}[(-2\zeta_1 r_{13}X_2 - r_{13}^2 X_1) \\
& \times (L_{111}X_1 + L_{121}X_3 + L_{131}X_5) \\
& - (2\zeta_2 r_{23}X_4 + r_{23}^2 X_3) \\
& \times (L_{112}X_1 + L_{122}X_3 + L_{132}X_5) - (+2\zeta_3 X_6 + X_5) \\
& \times (L_{113}X_1 + L_{123}X_3 + L_{133}X_5) + M_{111}X_2^2 \\
& + M_{122}X_4^2 + M_{133}X_6^2 \\
& + M_{112}X_2X_4 + M_{113}X_2X_6 + M_{123}X_4X_6]\Big\}\,\mathrm{d}\tau \\
+ \Big\{ & f_1 - \frac{\varepsilon\alpha}{M_{11}}[f_1(L_{111}X_1 + L_{121}X_3 + L_{131}X_5) \\
& + f_2(L_{112}X_1 + L_{122}X_3 + L_{132}X_5) \\
& + f_3(L_{113}X_1 + L_{123}X_3 + L_{133}X_5)] \\
& + \frac{\varepsilon^2\alpha^2}{M_{11}M_{22}}[f_1(L_{211}X_1 + L_{221}X_3 + L_{231}X_5) \\
& + f_2(L_{212}X_1 + L_{222}X_3 + L_{232}X_5) \\
& + (f_3(L_{213}X_1 + L_{223}X_3 \\
& + L_{233}X_5)](L_{112}X_1 + L_{122}X_3 + L_{132}X_5) \\
& + \frac{\varepsilon^2\alpha^2}{M_{11}M_{33}}[f_1(L_{311}X_1 + L_{321}X_3 + L_{331}X_5) \\
& + f_2(L_{312}X_1 + L_{322}X_3 \\
& + L_{322}X_5) + f_3(L_{313}X_1 + L_{323}X_3 \\
& + L_{333}X_5)] + L_{113}X_1 \\
& + L_{123}X_3 + L_{133}X_5)\Big\}\,\mathrm{d}B
\end{aligned}$$

$$\begin{aligned}
\mathrm{d}X_4 = -\Big\{ & 2\zeta_2 r_{23}X_4 + r_{23}^2 X_3 + \frac{\varepsilon\alpha}{M_{22}}[(-2\zeta_1 r_{13}X_2 - r_{13}^2 X_1) \\
& \times (L_{211}X_1 + L_{122}X_3 + L_{231}X_5) \\
& - (2\zeta_2 r_{23}X_4 + r_{23}^2 X_3) \\
& \times (L_{212}X_1 + L_{222}X_3 + L_{232}X_5) \\
& - (2\zeta_3 X_6 + X_5) \\
& \times (L_{213}X_1 + L_{223}X_3 + L_{233}X_5) \\
& + M_{211}X_2^2 + M_{222}X_4^2 + M_{233}X_6^2 \\
& + M_{212}X_2X_4 + M_{213}X_2X_6 + M_{223}X_4X_6]\Big\}\,\mathrm{d}\tau \\
+ \Big\{ & f_2 - \frac{\varepsilon\alpha}{M_{22}}[f_1(L_{211}X_1 + L_{221}X_3 + L_{231}X_5) \\
& + f_2(L_{212}X_1 + L_{222}X_3 + L_{232}X_5) \\
& + f_3(L_{213}X_1 + L_{223}X_3 \\
& + L_{233}X)] + \frac{\varepsilon^2\alpha^2}{M_{22}M_{11}}
\end{aligned}$$

$$
\begin{aligned}
&\times[f_1(L_{111}X_1+L_{121}X_3+L_{131}X_5)\\
&+f_2(L_{112}X_1+L_{122}X_3+L_{132}X_5)\\
&+f_3(L_{113}X_1+L_{123}X_3+L_{133}X_5)]\\
&\times(L_{211}X_1+L_{221}X_3+L_{231}X_5)+\frac{\varepsilon^2\alpha^2}{M_{22}M_{33}}\\
&\times[f_1(L_{311}X_1+L_{321}X_3+L_{331}X_5)\\
&+f_2(L_{312}X_1+L_{322}X_3+L_{332}X_5)\\
&+f_3(L_{313}X_1+L_{323}X_3+L_{333}X_5)]\\
&\left.\times(L_{213}X_1+L_{23}X_3+L_{233}X_5)\right\}\mathrm{d}B
\end{aligned}
$$

$$
\begin{aligned}
\mathrm{d}X_6=-\Big\{&2\zeta_3X_6+X_5+\frac{\varepsilon\alpha}{M_{33}}[(-2\zeta_1r_{13}X_2-r_{13}^2X_1)\\
&\times(L_{311}X_1+L_{321}X_3+L_{331}X_5)\\
&-(2\zeta_2r_{23}X_4+r_{23}^2X_3)\\
&\times(L_{312}X_1+L_{322}X_3+L_{332}X_5)\\
&-(2\zeta_3X_6+X_5)(L_{313}X_1\\
&\times L_{323}X_3+L_{333}X_5)\\
&+M_{311}X_2^2+M_{322}X_4^2+M_{333}X_6^2\\
&+M_{312}X_2X_4+M_{313}X_2X_6M_{323}X_4X_6]\Big\}\mathrm{d}\tau\\
&+f_3-\frac{\varepsilon\alpha}{M_{33}}[f_1(L_{311}X_1+L_{321}X_3+L_{331}X_5)\\
&+f_2(L_{312}X_1+L_{322}X_3+L_{332}X_5)\\
&+f_3(L_{313}X_1+L_{323}X_3+L_{333}X_5)]\\
&+\frac{\varepsilon^2\alpha^2}{M_{33}M_{11}}[f_1(L_{111}X_1+L_{121}X_3+L_{131}X_5)\\
&+f_2(L_{112}X_1+L_{122}X_3+L_{132}X_5)\\
&+f_3(L_{113}X_1+L_{123}X_3+L_{133}X_5)]\\
&\times(L_{311}X_1+L_{321}X_3+L_{331}X_5)\\
&+\frac{\varepsilon^2\alpha^2}{M_{33}M_{22}}[f_1(L_{211}X_1+L_{221}X_3+L_{231}X_5)\\
&+f_2(L_{212}X_1+L_{222}X_3+L_{232}X_5)\\
&+f_3(L_{213}X_1+L_{223}X_3+L_{233}X_5)]\\
&\times(L_{312}X_1+L_{322}X_3+L_{332}X_5)\}\,\mathrm{d}B \qquad (19)
\end{aligned}
$$

The evolution of the response probability density function is described by the Fokker-Planck equation

$$
\frac{\partial p(\mathbf{X},\tau)}{\partial\tau}=-\sum_{i=1}^{6}\frac{\partial}{\partial X_i}[a_i(\mathbf{X},\tau)p(\mathbf{X},\tau)]+\frac{1}{2}\sum_{i=1}^{6}\sum_{j=1}^{6}\frac{\partial^2}{\partial X_i\partial X_j}[b_{ij}(\mathbf{X},\tau)p(\mathbf{X},\tau)] \qquad (20)
$$

where $p(\mathbf{X},\tau)$ is the response joint probability density function, and $a_i(\mathbf{X},\tau)$ and $b_{ij}(\mathbf{X},\tau)$ are the first and second incremental moments evaluated as follows

$$
\begin{aligned}
a_i(\mathbf{X},\tau)&=\lim_{\Delta\tau\to 0}\frac{1}{\Delta\tau}E[X_i(\tau+\Delta\tau)-X_i(\tau)]\\
b_{ij}(\mathbf{X},\tau)&=\lim_{\Delta\tau\to 0}\frac{1}{\Delta\tau}E[\{X_i(\tau+\Delta\tau)-X_i(\tau)\}\\
&\quad\times\{X_j(\tau+\Delta\tau)-X_j(\tau)\}] \qquad (21)
\end{aligned}
$$

The coefficients a_i and b_{ij} are evaluated for the present system with the aid of MACSYMA program. It is not possible to solve the resulting Fokker Planck equation even for the stationary case. Instead, one may generate a general first order differential equation describing the evolution of response moments of any order. This equation is obtained by multiplying both sides of the system Fokker Planck equation by the scalar function $\Phi(\mathbf{X})$

$$
\Phi(\mathbf{X})=X_1^{k_1}X_2^{k_2}X_3^{k_3}X_4^{k_4}X_5^{k_5}X_6^{k_6} \qquad (22)
$$

and integrating by parts over the entire state space $-\infty<\mathbf{X}<\infty$. The following boundary conditions are used

$$
p(\mathbf{X}\to-\infty)=p(\mathbf{X}\to\infty)=0 \qquad (23)
$$

Due to space limitation the system moment equation will not be listed in this paper. The reader may refer to Ref. 17 for more details. However, the general form of the resulting differential equation is

$$
m'_N=F_N(m_1,m_2,\ldots,m_N,m^{N+1}) \qquad (24)
$$

where $N=\sum_{i=1}^{6}k_i$.

In deriving the system moment differential equation the following notation is adopted

$$
m_{k_1k_2\ldots k_6}=\int_{-\infty}^{\infty}\cdots\int p(\mathbf{X},\tau)\Phi(\mathbf{X})\,\mathrm{d}X_1\,\mathrm{d}X_2\ldots\mathrm{d}X_6 \qquad (25)
$$

It is found that the differential equation of order N contains moment terms of order N and $N+1$. The source of this infinite hierarchy is the system nonlinear functions ψ_i in equations (12). If these nonlinear functions are dropped the system becomes linear and the response moment equations are consistent. In the present study the following three cases will be examined:

(i) Linear response of constant coefficients structure.
(ii) Linear response of the structure with random stiffness.
(iii) Response of the structure with autoparametric interaction involving the internal combination internal resonance $\omega_3\cong\omega_1+\omega_2$.

VI. STRUCTURE WITH CONSTANT PARAMETERS

The equations of motion for this case are obtained from equations (11) by excluding the nonlinear functions ψ_i. The resulting equations of motion are

$$
\begin{bmatrix}1&0&0\\0&1&0\\0&0&1\end{bmatrix}\begin{Bmatrix}Y_1''\\Y_2''\\Y_3''\end{Bmatrix}+\begin{bmatrix}2\zeta_1r_{13}&0&0\\2\zeta_2r_{23}&0&0\\0&2\zeta_3&\end{bmatrix}\begin{Bmatrix}Y_1'\\Y_2'\\Y_3'\end{Bmatrix}+\begin{bmatrix}r_{13}^2&0&0\\0&r_{23}^2&0\\0&0&1\end{bmatrix}\begin{Bmatrix}Y_1\\Y_2\\Y_3\end{Bmatrix}=W(\tau)\begin{Bmatrix}f_1\\f_2\\f_3\end{Bmatrix} \qquad (26)
$$

For this linear case the response moment differential equations are consistent. The mean squares of the stationary response is obtained in the closed form

$$E[Y_1^2]=Df_1^2\,(2\zeta_1 r_{13}^3),\qquad E[Y_1'^2]=Df_1^2\,(2\zeta_1 r_{13}),$$
$$E[Y_2^2]=Df_2^2\,(2\zeta_2 r_{23}^3),\qquad E[Y_2'^2]=Df_2^2\,(2\zeta_2 r_{23}),$$
$$E[Y_3^2]=Df_3^2\,(2\zeta_3),\qquad E[Y_3'^2]=Df_3^2\,(2\zeta_3)$$

Before presenting the linear response graphically, it would be useful to recall that the generalized coordinates q_i were nondimensionalized with respect to the root-mean square of the main mass response when the coupled system was locked under forced excitation. The value of q_3 can be estimated from the single degree of freedom equation of motion

$$(m_1+m_2+m_3)\ddot{q}_3+C_3\dot{q}_3+k_3q_3=F(t) \tag{28}$$

which has the stationary response

$$E[q_3^2]=E[\dot{q}_3^2]=D\,2\zeta_3 \tag{29}$$

and therefore

$$q_3=\sqrt{D\,2\zeta_3} \tag{30}$$

The excitation parameter level $D\,2\zeta_3$ is chosen so that q_3 is chosen so that q_3 is unity and as a result any deviation from unity gives a measure of the dynamic interaction (linear or nonlinear) with other modes. For the analysis hereafter the excitation level will be chosen such that

$$D\,2\zeta_3=1 \tag{31}$$

In this case the mean square response (27) is reduced to the simple form

$$E[Y_1^2]=\frac{\zeta_1}{\zeta_3}\frac{f_1^2}{r_{13}^3},\qquad E[Y_1'^2]=\frac{\zeta_1}{\zeta_3}\frac{f_1^2}{r_{13}},$$
$$E[Y_2^2]=\frac{\zeta_2}{\zeta_3}\frac{f_2^2}{r_{23}^3},\qquad E[Y_2'^2]=\frac{\zeta_2}{\zeta_3}\frac{f_2^2}{r_{23}},$$
$$E[Y_3^2]=E[Y_3'^2]=f_3^2 \tag{32}$$

The linear response for both normalized and generalized coordinates is determined for various damping ratios. Figs 3 and 4 show the mean square responses as a function of the frequency ratio r for two sets of damping ratios. It is seen that both the first and second normal mode mean square responses decrease faster than the

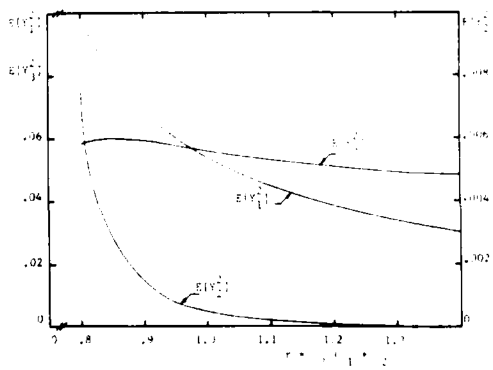

Fig. 3. Mean square response of normal modes for $\zeta_1=\zeta_2=0.005$, $\zeta_3=0.01$

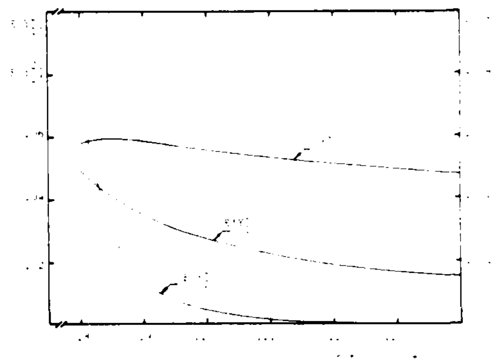

Fig. 4. Mean square response of normal modes for $\zeta_1\zeta_2=0.01$, $\zeta_3=0.01$

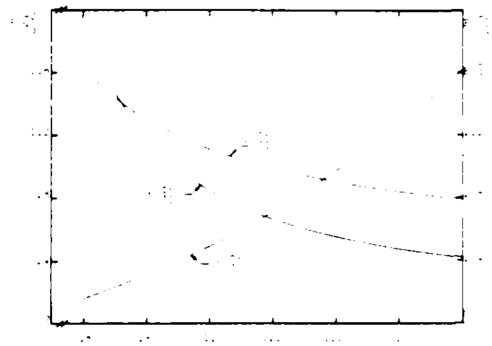

Fig. 5. Mean square response of generalized coordinates for $\zeta_1=\zeta_2=0.005$, $\zeta_3=0.01$

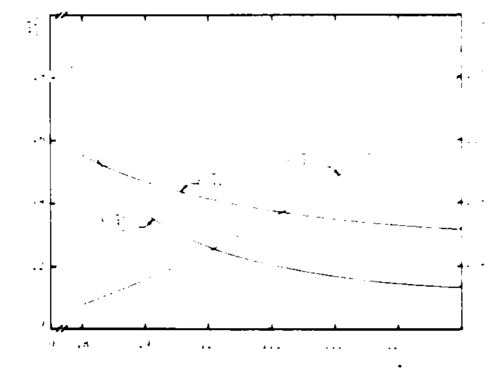

Fig. 6. Mean square response of generalized coordinates for $\zeta_1=\zeta_2=0.01$, $\zeta_3=0.01$

third mode as the frequency ratio increases. In terms of generalized coordinates, Figs 5 and 6 shows that the mean square displacement increases while the two beam displacements decrease with the frequency ratio. The two sets of figures show the well known control damping effect on the mean square responses.

VII. STRUCTURE WITH RANDOM STIFFNESS

The equations of motion of this case are obtained by including a random component to each stiffness in the original linear equations of motion.

The equations of motion take the

$$\begin{bmatrix} m_{11} & m_{12} & m_{13} \\ m_{12} & m_{22} & 0 \\ m_{13} & 0 & m_{33} \end{bmatrix} \begin{Bmatrix} \ddot{q}_1 \\ \ddot{q}_2 \\ \ddot{q}_3 \end{Bmatrix} + \begin{bmatrix} k_1 + S_1(t) & 0 & 0 \\ 0 & k_2 + S_2(t) & 0 \\ 0 & 0 & k_3 + S_3(t) \end{bmatrix} \begin{Bmatrix} q_1 \\ q_2 \\ q_3 \end{Bmatrix} = \begin{Bmatrix} 0 \\ 0 \\ F(t) \end{Bmatrix} \tag{33}$$

Introducing the same dimensionless parameters listed in Sections II and III, the equations of motion in terms of the normal coordinates after introducing linear damping are:

$$\begin{aligned} y_1'' + 2\zeta_1 r_{13} y_1' + r_{13}^2 y_1 + [s_{11} W_1(\tau) + s_{12} W_2(\tau) \\ + s_{13} W_3(\tau)] y_1 = f_1 W(\tau) \\ y_2'' + 2\zeta_2 r_{23} y_2' + r_{23}^2 y_2 + [s_{21} W_1(\tau) + s_{22} W_2(\tau) \\ + s_{23} W_3(\tau)] y_2 = f_2 W(\tau) \\ y_3'' + 2\zeta_3 y_3' + y_3 + [s_{31} W_1(\tau) + s_{32} W_2(\tau) \\ + s_{33} W_3(\tau)] y_3 = f_3 W(\tau) \end{aligned} \tag{34}$$

where

and $W_i(\tau)$ are zero mean white noise processes with spectral densities $2D_i$. Equations (34) constitute a set of coupled differential equations. The response mean squares are obtained by solving the stationary moment equations. The analytical solution for the stationary response is

$$\begin{aligned} E[Y_1^2] &= Df_1^2 / \{2\zeta_1 r_{13}^3 - D_1 s_{11}^2 - D_2 s_{12}^2 - D_3 s_{13}^2\}, \\ E[Y_1'^2] &= r_{13}^2 E[Y_1^2] \\ E[Y_2^2] &= Df_2^2 / \{2\zeta_2 r_{23}^3 - D_1 s_{21}^2 - D_2 s_{22}^2 - D_3 s_{23}^2\}, \\ E[Y_2'^2] &= r_{23}^2 E[Y_2^2] \\ E[Y_3^2] &= Df_3^2 / \{2\zeta_3 - D_1 s_{31}^2 - D_3 s_{32}^2 - D_3 s_{33}^2\}, \\ E[Y_3'^2] &= E[Y_3^2] \end{aligned} \tag{35}$$

This solution indicates that the system may be unstable depending on the values of D_i. The fact that the mean square must always be positive provides the stability criteria for mean squares given by (35). These criteria are obtained by keeping the denominators of (35) always positive, i.e.,

$$\begin{aligned} 2\zeta_1 r_{13}^3 &> (D_1 s_{11}^2 + D_2 s_{12}^2 + D_3 s_{13}^2) \\ 2\zeta_2 r_{23}^3 &> (D_1 s_{21}^2 + D_2 s_{22}^2 + D_3 s_{23}^2) \\ 2\zeta_3 &> (D_1 s_{31}^2 + D_2 s_{32}^2 + D_3 s_{33}^2) \end{aligned} \tag{36}$$

The stability boundaries represented by conditions (36) are shown in Fig. 7 as a function of the internal resonance frequency ratio r. For simplicity the excitation levels D_i, $2\zeta_i$ of the random stiffness perturbations are assumed to be equal. Samples of the response means squares as function of the excitation level $D/2\zeta$ are shown in Figs 8

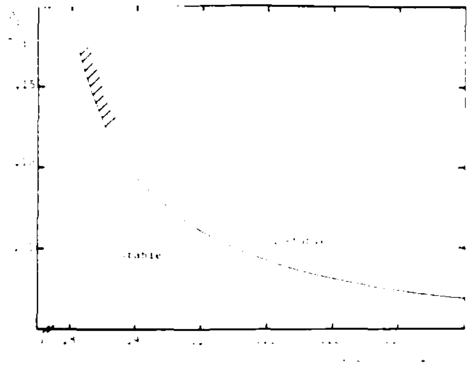

Fig. 7. Mean square stability boundary of the structure with random stiffness, for $\zeta_i = 0.01$

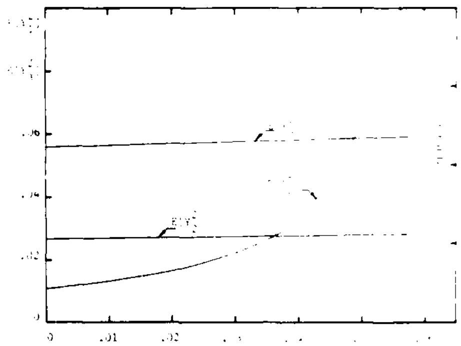

Fig. 8. Mean square response of normal modes with random stiffness for $r = 1.0$, $\zeta_i = 0.01$

and 9 in terms of normal and generalized coordinates, respectively. It is observed that the response of tip mass of the vertical cantilever is the main source of instability.

VIII. AUTOPARAMETRIC INTERACTION

In this case the influence of nonlinear modal coupling on the system response will be examined by including the functions in the analysis. These functions are only significant if the structure is tuned internally such that the normal mode frequencies have a linear relationship. For the present system it is found that the following three internal resonance conditions can take place[15]

$$\omega_3 = \omega_1 + \omega_2$$
$$\omega_3 = 2\omega_1 \quad \text{and} \quad \omega_3 = 2\omega_2 \tag{37}$$

The random response of the system will be exmined under the first internal resonance condition. As mentioned in Section III the response moment equations involve infinite coupling which must be closed in order to solve for the response statistics. It is known that the response of any nonlinear system to a random Gaussian excitation will be non-Gaussian. The deviation of the response from normality depends on the degree of the system nonlinearity. Generally, closure schemes are

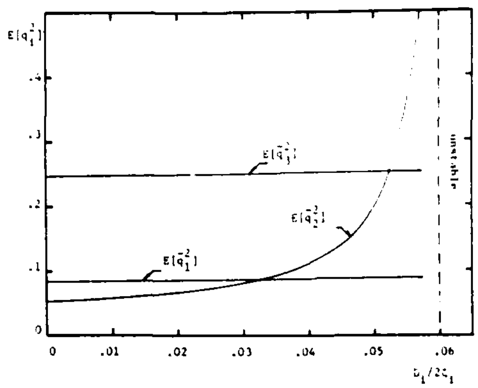

Fig. 9. Mean square response of generalized coordinates for same conditions of Fig 8

classified into Gaussian and non-Gaussian[16]. The Gaussian schemes are useful for dynamic systems with weak nonlinearity. However, in certain situations the application of Gaussian closures may lead to stochastic stability boundaries which are different from those derived by other techniques such as Stratonovich stochastic averaging or non-Gaussian closure approaches. This type of contradiction has been reported for nonlinear systems under parametric random excitations[16]. For two degree-of-freedom systems the Gaussian closure scheme yields nonstationary response while non-Gaussian closure gives strictly stationary response. However, the main response characteristics are found identical as predicted by both methods.

This Section examines the nonlinear response as obtained by using a Gaussian closure scheme which is based on the properties of the cumulants. For the present system 27 equations for the first and second order moments will be generated. The moment equations are closed by setting all third order cumulants to zero, i.e.,

$$\lambda_3[X_iX_jX_k] = E[X_iX_jX_k] - \sum^{3} E[X_i]E[X_jX_k] + 2E[X_i]E[X_j]E[X_k] = 0 \qquad (38)$$

where the number over summation sign refers to the number of terms generated in the form of the indicated expression without allowing permutation of indices. Relation (38) is used to obtain expressions for the third order moments in terms of first and second order moments.

The solution of the closed 27 coupled moment equations is obtained numerically by using the IMSL DVERK Subroutine (Runge-Kutta-Verner fifth and sixth numerical integration method). Depending on the value of internal detuning parameter r the system response may be reduced to the same linear response of section VI or may become quasi-stationary which deviates significantly from the linear solution. The response of autoparametric interaction is found to take place in regions of internal resonance ratio slightly deviated from the exact tuning $r = 1$. The deviation may be attributed to the contribution of nonlinearities incurred during the Gaussian closure procedure. Surprisingly, exact internal resonance yields linear response characteristics which are displayed in Fig. 10. It is seen that the response fluctuates between two limits during the transient period, then converges to a stationary values which corresponds exactly to the linear solution of Section VI. The effect of different initial conditions is examined and it is found that regardless of the initial conditions the solution reaches the same steady state value. For internal resonance ratio $r = 1.175$, Fig. 11 shows another set of time history responses. In this case the response mean squares do not achieve a stationary state. During the transient period the frequency of the third mode is approximately 1.17 times the sum of the first two mode frequencies. The quasi-stationary behaviour, although present for all three modes, is most prominent for the second mode.

To further illustrate the departure of the nonlinear response from the linear one, Figs 12–15 display the dependence of the normalized mean squares on the internal resonance for various system parameters. The mean squares are normalized by the corresponding linear solution. The subscript G/L refers to the ratio of the nonlinear Gaussian solution to the linear response. In the regions near critical internal resonance the upper and lower envelopes of the quasi-stationary response are plotted. A general trend is observed to exist in all figures. There is a sharp increase in the displacement mean square

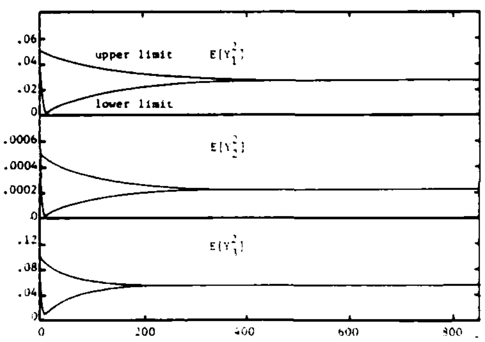

Fig. 10. Time history response of normal coordinates for $\zeta_1 = 0.01$, $\varepsilon = 0.025$, $r = \omega_3/(\omega_1 + \omega_2) = 1.0$

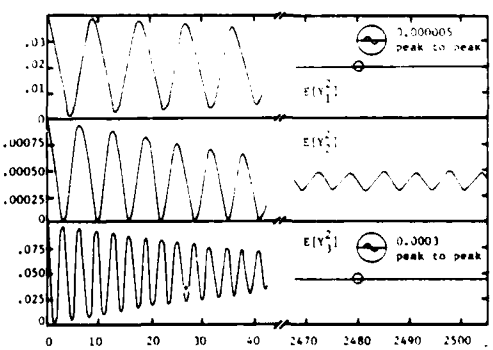

Fig. 11. Time history response of normal coordinates showing autoparametric interaction, for $\zeta_1 = 0.01$, $\varepsilon = 0.025$, $r = \omega_3/(\omega_1 + \omega_2) = 1.175$

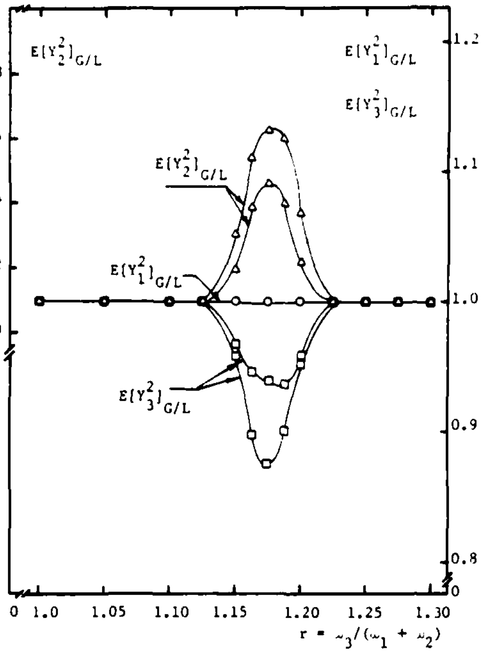

Fig. 12. Mean square resonse of normalized coordinates as function of internal resonance ratio r, for $\zeta_1=\zeta_2=0.005$, $\zeta_3=0.01$, $\varepsilon=0.025$

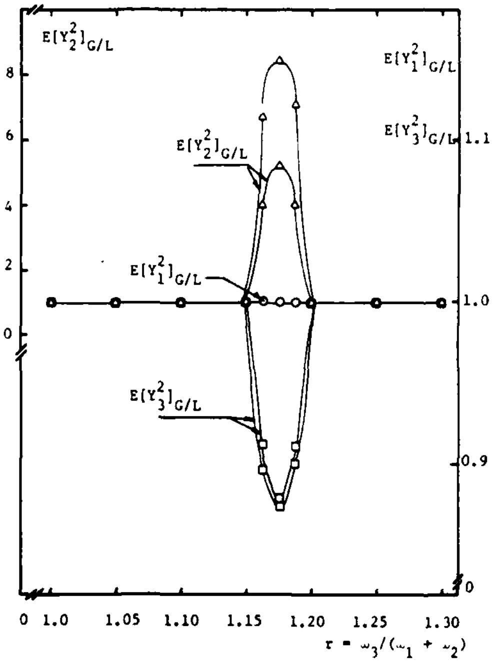

Fig. 13. Mean square response of normalized coordinates as function of internal resonance ratio r, for $\zeta_i=0.01$, $\varepsilon=0.025$

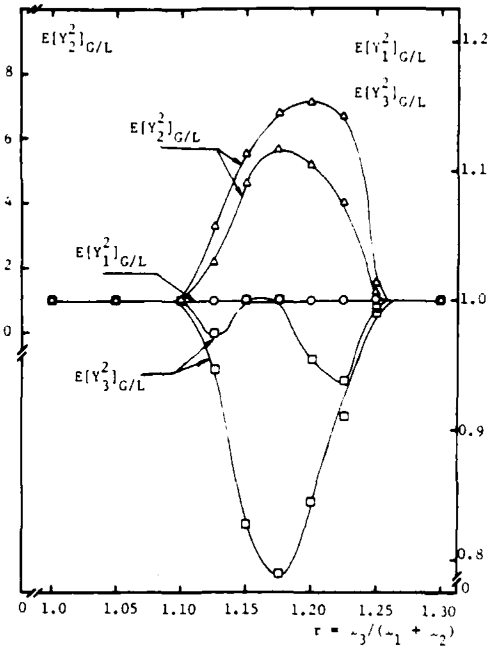

Fig. 14. Mean square response of normalized coordinates as function of internal resonance ratio r, for $\zeta_1=\zeta_2=0.005$, $\zeta_3=0.01$, $\varepsilon=0.05$

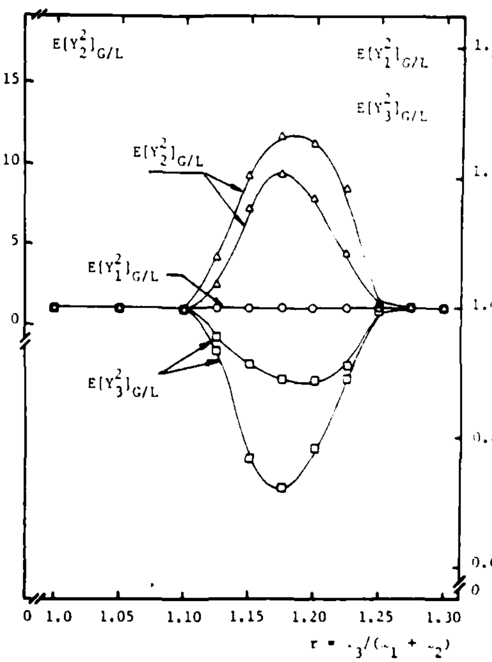

Fig. 15. Mean square response of normalized coordinates as function of internal resonance ratio r, for $\zeta_i=0.01$, $\varepsilon=0.05$

of the second mode associated with a corresponding decrease in the mean square of the third normal mode and very slight drop in the first mode. This feature is similar to a great extent to the deterministic nonlinear absorbing effect reported by Ibrahim and Woodall[15]. Figs 12 and 13 show the effect of damping ratios of the system response. It is seen that any increase in damping results in narrowing the region of autoparametric interaction. The nonlinear coupling parameter ε has a direct influence on the degree of the response deviation from the linear solution as shown in Figs 12–15. As ε increases from 0.025 to 0.05 the region of autoparametric interaction becomes more wider.

IX. CONCLUSIONS

The linear and nonlinear modal interactions of a three-degree-of-freedom structure subjected to random excitation is examined. For the linear modelling the response is determined for two cases of structure parameters. The first case is when the parameters are constant coefficients. The mean square response of this case is obtained in terms of the excitation spectral density and the internal detuning parameter. The second case involves random parametric excitations in the stiffness matrix. These excitations result in modal parametric coupling of the normal coordinates. The mean square responses are governed by the spectral densities of parametric excitations which also result in the conditions of mean square stability. The results of the first case are used as a reference to measure the effects of nonlinear inertia coupling of normal modes on the mean square response of the system in the neighbourhood of combination internal resonance. It is found that the critical internal resonance occurs at a value close to $r = 1.175$ which is deviated from the exact value $r = 1$. The nonlinear modal interaction results in an increase of the second normal mode mean square response and in an associated decrease of the first and third normal modes.

ACKNOWLEDGEMENT

This research is supported by a grant from the Air Force Office of Scientific Research under grant no. AFOSR-85-0008. Dr A. Amos is the Program director.

REFERENCES

1 Nayfeh, A. H. and Mook, D. T. *Nonlinear Oscillations*, John Wiley and Sons, New York, 1979
2 Schmidt, G. and Tondl, A. *Nonlinear Vibration*, Cambridge University Press, Cambridge, 1985
3 Breitbach, E. J. Effect of structural nonlinearities on aircraft vibration and flutter, Advisory Group for Aerospace Research and Development of NATO, AGARD Report No. 665, September 1977
4 Breitbach, E. J. Flutter analysis of an airplane with multiple structural nonlinearities in the control system, NASA Technical Paper 1620, 1980
5 De Ferrari, G., Chesta, L., Sensburg, O. and Lotze, A. Effects of nonlinearity on wing-store flutter, Advisory Group for Aerospace Research and Development of NATO, AGARD-R-687, 1980
6 Peloubet, R. P., Jr, Haller, R. L. and Bolding, R. M. F-16 Flutter suppression system investigation, *Proceedings of the AIAA ASME/ASCE/AHS 21st Structures, Strucutral Dynamics and Materials Conference*, Seattle, Washington, 1980, 620–634
7 Reed, W. H. III, Foughner, J. T., Jr and Runyan, H. L. Decoupler pylon: A simple effective wing/store suppressor, *J. Aircraft*, 1980, **17**(3), 206–211
8 Desmarais, R. N. and Reed, W. H., III Wing/store flutter with non-linear pylon stiffness, *J. Aircraft*, 1981, **18**(11), 984–987
9 Bolotin, V. V. *The Dynamic Stability of Elastic Systems*, Holden-Day, Inc., San Francisco, 1964
10 Barr, A. D. S. Some developments in parametric stability and nonlinear vibration, *Proceedings of International Conference of Recent Advances in Structural Dynamics*, Southampton, England, 1980, 545–568
11 Minorsky, N. *Nonlinear Oscillations*, Van Nostrand, New York, 1962
12 Barr, A. D. S. and Ashworth, R. P. Parametric and nonlinear mode interaction behavior in the dynamics of structures, AFOSR Final Report, Department of Mechanical Engineering, University of Dundee, December 1977
13 Haddow, A. G., Barr, A. D. S. and Mook, D. T. Theoretical and experimental study of modal interaction in a two-degree-of-freedom structure, *J. Sound and Vibration*, 1984, **97**(3), 451–473
14 Ibrahim, R. A., Woodall, T. D. and Heo, H. Modal analysis of structural systems involving nonlinear coupling, *Shock and Vibration Bulletin*, 1984, **54**(1), 19–27
15 Ibrahim, R. A. and Woodall, T. D. Linear and nonlinear modal analysis of aeroelastic structural systems, *Computers and Structures*, 1986, **22**(4), 699–707
16 Ibrahim, R. A. *Parametric Random Vibrations*, John Wiley and Sons, New York, 1985
17 Hedayati, Z. Random modal interaction of a nonlinear aeroelastic structure, MS Thesis, Texas Technical University, August 1985
18 Craig, R. R. *Structural Dynamics – An Introduction to Computer Methods*, John Wiley and Sons, New York, 1981

Stochastic Response of Nonlinear Structures with Parameter Random Fluctuations

R. A. Ibrahim* and H. Heo†
Texas Tech University, Lubbock, Texas

The random response of a nonlinear structural system is examined when its parameters are experiencing random fluctuations with time. The treatment is based on the recent developments in the mathematical theory of stochastic differential equations. These include the *Ito* stochastic calculus and the Fokker-Planck equation approach to derive a general differential equation that describes the evolution of the statistical moments of the response coordinates. The differential equation is found to constitute an infinite coupled set of differential equations that are closed via two different closure schemes. The system response is determined in the neighborhood of internal resonance condition and for various random intensities of the system parameters. It is found that the random modal interaction is governed mainly by the internal resonance ratio and the stiffness fluctuation intensity. The effect of the random damping fluctuation on the system response is found to be very small *compared to the stiffness fluctuation effect.*

I. Introduction

THE dynamic behavior of lightweight structures is of main concern to aeronautical engineers involved in the design and reliability of aerospace structures. These structures are usually made up of composite materials that are nonhomogeneous and exhibit fluctuations in their dynamic properties. The fluctuations of these properties are random in nature and thus result in random eigenvalues and responses. Depending on the analytical modeling of such structures, the interaction between aerodynamic, inertia, and elastic forces may give rise to a number of aeroelastic phenomena. For example, classical flutter can occur due to a linear interaction of these three forces. Classical flutter may also involve the coupling of two or more degrees of freedom. However, the linear mathematical modeling fails to predict a number of observed dynamic characteristics such as amplitude jump, limit cycles, parametric instability, internal resonance, multiple solutions, and saturation phenomena. These complex characteristics owe their origin to the inherent nonlinearity of the structure.

The amplitude jump, limit cycles, and parametric instability are common features of nonlinear single- and multi-degree-of-freedom systems. Parametric instability[1] takes place when the external excitation appears as a coefficient in the homogeneous part of the equation of motion. It occurs when the *excitation frequency is twice the natural frequency of the* system. Internal resonance[2] and saturation phenomena[3] may occur only in nonlinear dynamic systems with more than one degree of freedom. Internal resonance implies the existence of a linear relationship between the normal mode frequencies of the structure and results in a nonlinear interaction between the normal modes in a form of energy exchange. Under external excitation, the mode that is directly excited exhibits, in the beginning, the same features of the response of a linear single-degree-of-freedom system, and all other modes remain dormant. As the excitation amplitude reaches a certain critical level, the other modes become unstable, and the originally excited mode reaches an upper bound. This mode is said to be saturated, and the energy is then transferred to other modes. This type of modal interaction is referred to in the literature as autoparametric interaction,[4] since one mode acts as a parametric excitation to other modes. Barr and Done[5] conducted a ground resonance test and applied a sinusoidal excitation at one or more points to find out the conditions under which parametric and autoparametric instabilities could occur. The autoparametric resonance was found to take place when the directly excited mode frequency is twice the indirectly excited mode. Barr and Done[5] observed several combinations of normal mode interaction. For example, when the exciting mode was wing bending, the excited mode was found to be one of the following: 1) wing store pylon bending, 2) wing store pylon twisting, 3) engine pod mounting structure bending, or 4) engine mounting structure twisting.

In structural dynamics, the nonlinearity is represented in three different forms:[1,6] elastic, inertia, and damping nonlinearities. Elastic nonlinearity stems from nonlinear strain-displacement relations, which are inevitable. Inertia nonlinearity is derived, in a Lagrangian formulation, from kinetic energy The equations of motion of a discrete mass dynamic system, *with holonomic scleronomic constraints, in terms of the generalized coordinates* q_i, are usually written in the form[7]

$$\sum_{j=1}^{n} m_{ij} q_j + \sum_{j=1}^{n} \sum_{\ell=1}^{n} [j\ell, i] q_i q_\ell + \frac{\partial V}{\partial q_i} = Q_i,$$

$$i = 1, 2, \ldots, n$$

where V is potential energy, Q_i represents all nonconservative forces, and $[j\ell, i]$ is the Christoffel symbol of the first kind and is given by the expression

$$[j\ell, i] = \frac{1}{2}\left(\frac{\partial m_{ij}}{\partial q_\ell} + \frac{\partial m_{i\ell}}{\partial q_j} - \frac{\partial m_{j\ell}}{\partial q_i}\right)$$

The metric tensor m_{ij} and the Christoffel symbol are generally functions of the q_k, and for motion about the equilibrium configuration they can be expanded in a Taylor series about that state. Thus, from inertia sources, quadratic, cubic, and higher-power nonlinearities can arise.

Received Feb. 20, 1986; presented as Paper 86-0962 at the AIAA/ASME/ASCE/AHS 27th Structures, Structural Dynamics and Materials Conference, San Antonio, TX, May 19-21, 1986; revision received July 11, 1986.

*Professor, Department of Mechanical Engineering. Member AIAA.

†Graduate Student, Department of Mechanical Engineering; currently Senior Research Specialist, Agency for Defense Development, Korea.

Other types of nonlinearities, such as distributed and concentrated nonlinearities, are encountered in aeroelastic flutter problems.[8] Distributed nonlinearity is induced by elastic deformations in riveted, screwed, and bolted connections, as well as the structural components themselves. Concentrated nonlinearity acts locally in control mechanisms or in the connecting parts between wing and external stores. This nonlinearity is caused by backlash in the linkage elements of the control system, dry friction in control cable and push rod ducts, kinematic limitation of the control surface deflection, and application of spring tab systems provided for relieving pilot operation. Breitbach[9] determined the flutter boundaries for three different configurations distinguished by different types of nonlinearities in the rudder and aileron control system of a sailplane. It was shown that the influence of hysteretic damping results in a considerable stabilizing effect and an increase in the flutter speed. Similar effects of nonlinearities due to friction and backlash were reported in Ref. 10. Peloubet et al.,[11] Reed et al.,[12] and Desmarais and Reed[13] examined the effect of control system nonlinearities, such as actuator force or deflection limits, on the performance of an active flutter suppression system. It was shown[12] that a nonlinear system that is stable with respect to small disturbances may be unstable with respect to large ones. Another important feature was that a store mounted on a pylon with low pitch stiffness can provide substantial increase in flutter speed and reduce the dependency of flutter on the mass and inertia of stores relative to that of still-mounted stores.

It is clear that, in mathematical modeling, the aeroelastician should consider various types of nonlinearities in order to understand the origin of any unusual structural behavior under various types of aerodynamic loadings. Under deterministic unsteady aerodynamic forces, these phenomena can be predicted by one of the standard perturbation techniques of nonlinear differential equations.[14,15] However, aerospace structures are usually subjected to turbulent airflow, and the analyst encounters aerodynamic loads that are random in nature. Furthermore, once the structure starts to vibrate, its parameters, such as damping and stiffness, experience random fluctuations with the passage of time. The dynamic analysis of these structures is not a simple task, and it requires an advanced background in probability theory and stochastic differential equations.

It is very important at this stage to distinguish between two different problems encountered in structural dynamics. These are the random response of dynamic systems to random parametric excitation[16] and the random response of structural systems whose parameters are random variables described in a probabilistic sense. In the former case, the system equations of motion are stochastic differential equations with coefficients that are random processes while, in the latter case, the equations of motion are differential equations with parameter uncertainties. The methods of treating dynamic systems under parametric random excitations are different from those used in solving differential equations with parameter uncertainties. Parametric random vibration is basically a combination of the theory of stochastic processes, stochastic differential equations, and applied dynamics. On the other hand, systems with parameter uncertainties (referred to in the literature as disordered systems)[17] involve random boundary-value problem and random field theory. Within the framework of the linear theory of random vibration of disordered systems, the engineer encounters problems of random eigenvalues, random eigenvectors, random responses, normal mode localization, optimum design, and reliability. These issues have recently been reviewed by the author in Ref. 18.

This paper deals with the random response of a nonlinear two-degree-of-freedom structural model when its damping and stiffness coefficients involve random time variation. The model consists of two coupled beams with tip concentrated masses as shown in Fig. 1. The deterministic response of this model to harmonic support motion has been examined by Barr and Ashworth,[19] and Haddow et al.[20] Their studies showed that the system exhibits a number of nonlinear response phenomena under conditions of internal resonance, high excitation level, and low damping ratios. The authors of the present paper have recently determined the random response of this system to random support motion when its parameters are time-independent.[21] In fact, as the structure oscillates, the damping and stiffness coefficients may experience random time variations. The random variations of the structural parameters and the random support excitation will be assumed Gaussian-independent wide-band processes. The Fokker-Planck equation approach will be used to generate a general first-order differential equation for the statistical moments of the response coordinates. In view of the system nonlinearity, the response processes will be non-Gaussian-distributed, and the moment equations will form an infinite coupled set of moment equations, which will be closed via two independent closure schemes referred to as Gaussian and non-Gaussian closure schemes.[16] These closure schemes are based on the semi-invariant properties of the response processes. The Gaussian closure scheme is only valid if the system is linear with time-invariant coefficients and is subjected to Gaussian excitation. The application of Gaussian closure to nonlinear systems is analogous to the linearization solutions of deterministic nonlinear differential equations. The non-Gaussian closure scheme is more accurate since it takes into account the effect of the system nonlinearity on the response probability density function. More details of closure schemes may be found in a recent research monograph[16] by the first author. The results will be compared with the response statistical moments of the same system when its coefficients are constants.

II. Theoretical Analysis

Equations of Motion and Response Markov Vector

Figure 1 shows a schematic diagram of an analytical model of a nonlinear aeroelastic structural system, which represents a wing with external store. It consists of two coupled beams with tip masses m_1 and m_2. The present study will examine the nonlinear random interaction between the first two normal modes under random support motion $\xi_0(t)$ when the dynamic properties of the system experience random fluctuations. The mathematical modeling of the system was derived in Ref. 22. In terms of the nondimensional normal coordinates Y_1 and Y_2, the system equations of motion are

$$
\begin{aligned}
&\begin{bmatrix} 1 & 0 \\ 0 & 1 \end{bmatrix} \begin{Bmatrix} Y_1'' \\ Y_2'' \end{Bmatrix} \\
&+ \begin{bmatrix} 2\zeta_1[1+\xi_{c1}(\tau)] & 0 \\ 0 & 2r\zeta_2[1+\xi_{c2}(\tau)] \end{bmatrix} \begin{Bmatrix} Y_1' \\ Y_2' \end{Bmatrix} \\
&+ \begin{bmatrix} 1+\xi_{k1}(\tau) & 0 \\ 0 & r^2[1+\xi_{k2}(\tau)] \end{bmatrix} \begin{Bmatrix} Y_1 \\ Y_2 \end{Bmatrix} = -\xi_0''(\tau) \begin{Bmatrix} a_1 \\ b_1 \end{Bmatrix} \\
&- \epsilon\xi_0''(\tau) \begin{bmatrix} a_2 & a_3 \\ b_2 & b_3 \end{bmatrix} \begin{Bmatrix} Y_1 \\ Y_2 \end{Bmatrix} + \begin{Bmatrix} \psi_1(Y, Y', Y'') \\ \psi_2(Y, Y', Y'') \end{Bmatrix} \qquad (1)
\end{aligned}
$$

where $\{Y_1, Y_2\} = \{y_1, y_2\}/q_1^0$, and q_1^0 is the response root-mean-square of the system when the vertical beam is locked and the horizontal beam behaves as a single degree of freedom with end mass $m_1 + m_2$.

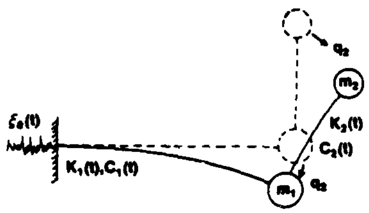

Fig. 1 Schematic diagram of a structural model with random parameters under random support motion.

The normal coordinates y are related to the generalized coordinates q through the transformation

$$\{q\} = [R]\{y\} \tag{2}$$

where $[R]$ is the system modal matrix that is defined in Ref. 21. The small parameter $\epsilon = q_1^0/\ell_1$ is the nonlinear coupling parameter, $r = \omega_2/\omega_1$ is the frequency ratio where ω_1 and ω_2 are the normal mode frequencies (in the present paper it is considered that $\omega_2 < \omega_1$). A prime denotes differentiation with respect to the nondimensional time parameter $\tau = \omega_1 t$.

The nonlinear functions $\psi_i(Y, Y', Y'')$ are given by the expressions

$$\psi_1(Y, Y', Y'') = a_4 Y_1 Y_1'' + a_5 Y_1 Y_2'' + a_6 Y_2 Y_1'' + a_7 Y_2 Y_2'' + a_8 Y_1'^2 + a_9 Y_1' Y_2' + a_{10} Y_2'^2$$

$$\psi_2(Y, Y', Y'') = b_4 Y_1 Y_1'' + b_5 Y_1 Y_2'' + b_6 Y_2 Y_1'' + b_7 Y_2 Y_2'' + b_8 Y_1'^2 + b_9 Y_1' Y_2' + b_{10} Y_2'^2$$

The coefficients a_i and b_i depend on the system parameters and are defined in Ref. 22. These functions involve quadratic nonlinearities of the inertia type. They include autoparametric coupling terms such as $Y_1 Y_2''$ in which the acceleration Y_2'' of the second mode acts as a parametric excitation to the first mode. The first expression on the right-hand sides of Eqs. (1) represents the nonhomogeneous part of the excitation, while the second expression is the parametric action of the excitation that couples the two modes parametrically. $\xi_{ci}(\tau)$ and $\xi_{ki}(\tau)$ represent the random fluctuations in the damping and stiffness terms, respectively. These functions and the support acceleration are assumed to be Gaussian wide-band random processes with zero means. The spectral densities of these processes are assumed to cover a frequency band that includes the first two normal mode frequencies and to be well below any other higher normal mode frequency. In the limiting case, as the correlation time of $\xi_i(\tau)$ becomes very small compared with any characteristic period of the system, the response coordinates approach a Markov process. In order to represent Eqs. (1) as a Markov vector, the acceleration terms Y'', which appear in the nonlinear terms $\psi_i(Y, Y', Y'')$, must be removed by successive elimination. This process has been performed by using the MACSYMA software. Having eliminated Y'', Eqs. (1) can be written in the Stratonovich form[16]

$$X_i' = f_i(X, \tau) + \sum_{j=1}^{4} G_{ij}(X, \tau)\xi_j(\tau), \qquad j = 1, \ldots, 4 \tag{3}$$

through the coordinate transformation

$$\{Y_1, Y_2, Y_1', Y_2'\} = \{X_1, X_2, X_3, X_4\} \tag{4}$$

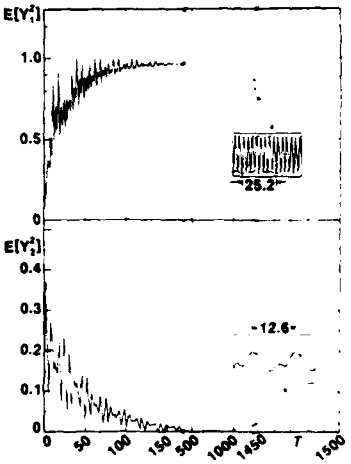

Fig. 2 Time-history response of normal mode mean squares according to Gaussian closure solution.

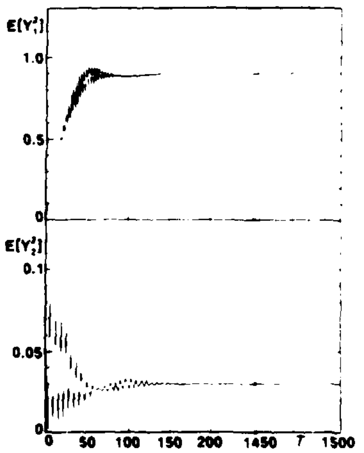

Fig. 3 Time-history response of normal mode mean squares according to non-Gaussian closure solution.

Alternatively, the system equations of motion can be written in terms of the Ito-type equation

$$\mathrm{d}X_i = \left[f_i(X, \tau) + \frac{1}{2} \sum_{k=1}^{4} \sum_{j=1}^{4} G_{kj}(X, \tau) \frac{\partial G_{ij}(X, \tau)}{\partial X_k} \right] \mathrm{d}\tau + \sum_{j=1}^{4} G_{ij}(X, \tau)\, \mathrm{d}B_j(\tau) \tag{5}$$

where the double summation expression is referred to the Ito (or the Wong-Zakai) correction term,[16] which is a result of replacing the physical wide-band random process $\xi_i(\tau)$ by the white noise $W_i(\tau)$. In Eq. (5) the white-noise processes $W_i(\tau)$

have been replaced by the formal derivative of the Brownian motion $B_i(\tau)$, i.e.,

$$W_i(\tau) = \mathrm{d}B_i(\tau)/\mathrm{d}\tau \tag{6}$$

The statistical properties of $B_i(\tau)$ are

$$E[\mathrm{d}B_i(\tau)] = 0 \tag{7a}$$

$$E\left[\mathrm{d}B_i^2(\tau)\right] = 2D_i\,\mathrm{d}\tau \tag{7b}$$

$$E\left[\mathrm{d}B_i(\tau)\,\mathrm{d}B_j(\tau)\right] = 0 \qquad \text{for } i \neq j \tag{7c}$$

where $2D_i$ is the spectral density of the Brownian motion process $B_i(\tau)$. The equations of motion can now be written in terms of the Markov vector coordinates X, as

$$\mathrm{d}X_1 = X_3\,\mathrm{d}\tau$$

$$\mathrm{d}X_2 = X_4\,\mathrm{d}\tau$$

$$\begin{aligned}
\mathrm{d}X_3 = \Big\{ & -X_1 - 2\zeta_1 X_3 - a_4 X_1^2 - (a_6 + r^2 a_5) X_1 X_2 - r^2 a_7 X_2^2 - 2\zeta_1 a_4 X_1 X_3 - 2\zeta_2 r a_5 X_1 X_4 - 2\zeta_1 a_6 X_2 X_3 - 2\zeta_2 r a_7 X_2 X_4 + a_8 X_3^2 \\
& + a_9 X_3 X_4 + a_{10} X_4^2 \underline{+ 4D_{c_1}\zeta_1^2 (X_3 + 2a_4 X_1 X_3 + 2a_6 X_2 X_3 + a_6^2 X_1^2 X_3 + 2a_4 a_6 X_1 X_2 X_3 + a_6^2 X_2 X_3)} \\
& \underline{+ 4D_{c_2}\zeta_2^2 r^2 \left[a_5 X_1 X_4 + a_7 X_2 X_4 + a_5 b_5 X_1^2 X_4 + (a_5 b_7 + a_7 b_5) X_1 X_2 X_4 + a_7 b_7 X_2^2 X_4 \right]} \Big\}\,\mathrm{d}\tau - X_1\,\mathrm{d}B_{k_1}(\tau) \\
& - r^2 (a_5 X_1 X_2 + a_7 X_2 X_4)\,\mathrm{d}B_{k_2}(\tau) - 2\zeta_1 (X_3 + a_4 X_1 X_3 + a_6 X_2 X_3)\,\mathrm{d}B_{c_1}(\tau) - 2\zeta_2 r (a_5 X_1 X_4 + a_7 X_2 X_4)\,\mathrm{d}B_{c_2}(\tau) \\
& - (A_1 + A_2 X_1 + A_3 X_2 + A_4 X_1^2 + A_5 X_1 X_2 + A_6 X_2^2)\,\mathrm{d}B_0(\tau) \\
\mathrm{d}X_4 = \Big\{ & -r^2 X_2 - 2\zeta_2 r X_4 - b_4 X_1^2 - (b_6 + r^2 b_5) X_1 X_2 - r^2 b_7 X_2^2 - 2\zeta_1 b_4 X_1 X_3 - 2\zeta_2 r b_5 X_1 X_4 - 2\zeta_1 b_6 X_2 X_3 - 2\zeta_2 r b_7 X_2 X_4 \\
& + b_8 X_3^2 + b_9 X_3 X_4 + b_{10} X_4 + 4D_{c_1}\zeta_1^2 [b_4 X_1 X_3 + b_6 X_2 X_3 \underline{+ a_4 b_4 X_1^2 X_3 + (a_4 b_6 + b_4 a_6) X_1 X_2 X_3 + a_6 b_6 X_2^2 X_3]} \\
& \underline{+ 4D_{c_2}\zeta_2^2 r^2 (X_4 + 2b_5 X_1 X_4 + 2b_7 X_2 X_4 + b_5^2 X_1^2 X_4 + 2b_5 b_7 X_1 X_2 X_4 + b_7^2 X_2^2 X_4)} \Big\}\,\mathrm{d}\tau - 2\zeta_1 (b_4 X_1 X_3 + b_6 X_2 X_3)\,\mathrm{d}B_{c_1}(\tau) \\
& - r^2 (X_2 + b_5 X_1 X_2 + b_7 X_2^2)\,\mathrm{d}B_{k_2}(\tau) - 2\zeta_2 r (X_4 + b_5 X_1 X_4 + b_7 X_2 X_4)\,\mathrm{d}B_{c_2}(\tau) \\
& - (B_1 + B_2 X_1 + B_3 X_2 + B_4 X_1^2 + B_5 X_1 X_2 + B_6 X_2^2)\,\mathrm{d}B_0(\tau)
\end{aligned} \tag{8}$$

where the underlined expressions are the Wong-Zakai correction terms.

Dynamic Moment Equations

The joint probability density function $p(X, \tau)$ of the response coordinates can be determined by applying the Fokker-Planck equation

$$\frac{\partial}{\partial \tau} p(X, \tau) = -\sum_{i=1}^{4} \frac{\partial}{\partial X_i}\left[a_i(X, \tau)\, p(X, \tau)\right] + \frac{1}{2}\sum_{i=1}^{4}\sum_{j=1}^{4} \frac{\partial^2}{\partial X_i \partial X_j}\left[b_{ij}(X, \tau)\, p(X, \tau)\right] \tag{9}$$

where $a_i(X, \tau)$ and $b_{ij}(X, \tau)$ are the first and second incremental moments of the Markov process $X(\tau)$. These are defined as follows:

$$a_i(X, \tau) = \lim_{\delta\tau \to 0} \frac{1}{\delta\tau} E\{ X_i(\tau + \delta\tau) - X_i(\tau) \} \tag{10a}$$

$$b_{ij}(X, \tau) = \lim_{\delta\tau \to 0} \frac{1}{\delta\tau} E \times \left\{ [X_i(\tau + \delta\tau) - X_i(\tau)][X_j(\tau + \delta\tau) - X_j(\tau)] \right\} \tag{10b}$$

provided that all limits exist and $X(\tau) = X$.

It is found that the system Fokker-Planck equation cannot be solved for the response probability density in a closed form. However, it is possible to generate a general differential equation for the response joint moments of any order N by multiplying both sides of the system Fokker-Planck equation by the scaler function

$$\Phi = X_1^i X_2^j X_3^k X_4^\ell \tag{11}$$

where $i + j + k + \ell = N$, and integrating by parts over the entire space $-\infty < X < \infty$. The following notation is adopted to denote the various response moments:

$$m_{i,j,k,\ell} = \iiiint_{-\infty}^{+\infty} X_1^i X_2^j X_3^k X_4 p(X, \tau)\,\mathrm{d}X_1, \mathrm{d}X_2\,\mathrm{d}X_3\,\mathrm{d}X_4 \tag{12}$$

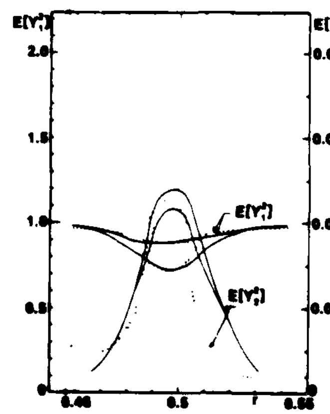

Fig. 4 Mean-square response of normal modes according to Gaussian closure solution vs internal resonance: ——, deterministic system; ---, system with random damping, $D_{c_1} = D_{c_2} = 0.1 D_0$, $2D_0 = 0.08$.

The resulting differential equation of the response joint moments is

$$
\begin{aligned}
m'_{i,j,k,\ell} = {} & i m_{i-1,j,k+1,\ell} + j m_{i,j-1,k,\ell+1} + k\Big[-m_{i+1,j,k-1,\ell} + \zeta_1(\zeta_1 D_{c_1} - 2) m_{i,j,k,\ell} - a_4 m_{i+2,j,k-2,\ell} \\
& - (a_6 + r^2 a_5) m_{i+1,j+1,k-1,\ell} - r^2 a_7 m_{i,j+2,k-1,\ell} + 2\zeta_1 a_4(\zeta_1 D_{c_1} - 1) m_{i+1,j,k,\ell} + \zeta_2 r a_5(\zeta_2 r D_{c_2} - 2) m_{i+1,j,k-1,\ell+1} \\
& + 2\zeta_1 a_6(\zeta_1 D_{c_1} - 1) m_{i,j+1,k,\ell} + \zeta_2 r a_7(\zeta_2 r D_{c_2} - 2) m_{i,j+1,k-1,\ell+1} + a_8 m_{i,j,k+1,\ell} + a_9 m_{i,j,k,\ell+1} + a_{10} m_{i,j,k-1,\ell+2}\Big] \\
& + \ell\Big[-r^2 m_{i,j+1,k,\ell-1} + (\zeta_2 r D_{c_2} - 2) m_{i,j,k,\ell} - b_4 m_{i+2,j,k,\ell-1} - (r^2 b_5 + b_6) m_{i+1,j+1,k,\ell-1} - r^2 b_7 m_{i,j+2,k,\ell-1} \\
& + \zeta_1 b_4(\zeta_1 D_{c_1} - 2) m_{i+1,j,k+1,\ell-1} + 2\zeta_2 r b_5(\zeta_2 r D_{c_2} - 1) m_{i+1,j,k,\ell} + \zeta_1 b_6(\zeta_1 D_{c_1} - 2) m_{i,j+1,k+1,\ell-1} \\
& + 2\zeta_2 r b_7(\zeta_2 r D_{c_1} - 1) m_{i,j+1,k,\ell} + b_8 m_{i,j,k+2,\ell-1} + b_9 m_{i,j,k+1,\ell} + b_{10} m_{i,j,k,\ell+1}\Big] + k(k-1)\Big\{ D_0 A_1^2 m_{i,j,k-2,\ell} \\
& + 2 D_0 A_1 A_2 m_{i+1,j,k-2,\ell} + 2 D_0 A_1 A_3 m_{i,j+1,k-2,\ell} + \big[D_{k_1} - D_0(2 A_1 A_4 + A_2^2)\big] m_{i+1,j,k-2,\ell} \\
& + 2 D_0(A_1 A_5 + A_2 A_3) m_{i+1,j+1,k-2,\ell} + D_0(A_3^2 + 2 A_1 A_6) m_{i,j+2,k-2,\ell} + 4 D_{c_1}\zeta_1^2 m_{i,j,k,\ell}\Big\} + k\ell\Big[2 D_0 A_1 B_1 m_{i,j,k-1,\ell-1} \\
& + 2 D_0(A_1 B_2 + A_2 B_1) m_{i+1,j,k-1,\ell-1} + 2 D_0(A_1 B_3 + A_3 B_1) m_{i,j+1,k-1,\ell-1} + 2 D_0(A_1 B_4 + A_4 B_1 + A_2 B_2) m_{i+2,j,k-1,\ell-1} \\
& + 2 D_0(A_1 B_5 + A_5 B_1 + A_2 B_3 + A_3 B_2) m_{i+1,j+1,k-1,\ell-1} + 2 D_0(A_3 B_3 + A_1 B_6 + A_6 B_1) m_{i,j+2,k-1,\ell-1}\Big] \\
& + \ell(\ell-1)\Big\{ 2 D_0 B_1^2 m_{i,j,k,\ell-2} + 2 D_0 B_1 B_2 m_{i+1,j,k,\ell-2} + 2 D_0 B_1 B_3 m_{i,j+1,k,\ell-2} + D_0(2 B_1 B_4 + B_2^2) m_{i+2,j,k,\ell-2} \\
& + 2 D_0(B_1 B_5 + B_1 B_3) m_{i+1,j+1,k,\ell-2} + \big[D_{k_2} r^2 + D_0(B_3^2 + 2 B_1 B_6)\big] m_{i,j+2,k,\ell-2} + 4 D_{c_2}\zeta_2^2 r^2 m_{i,j,k,\ell}\Big\}
\end{aligned}
\tag{13}
$$

Gaussian Closure Solution

It is seen that any moment equation of order N includes terms of order $N+1$ on the right-hand side of Eq. (13) which, in this case, constitutes an infinite coupled set of moment equations. In order to close this infinite hierarchy, two different closure schemes will be applied. These schemes are based on the properties of the joint cumulant (or semi-invariants). It should be noticed that the response coordinates are not Gaussian-distributed, and any closure scheme should take into account the deviation of the response from being Gaussian. However, if the response coordinates are assumed to be "nearly" Gaussian, then all joint cumulants of order greater than 2 vanish identically, and the response statistics can be described in terms of first- and second-order moments. This approach is referred to as Gaussian closure scheme and is applied for the present system by setting the third-order joint cumulant to zero, i.e.,

$$
\begin{aligned}
\lambda_3[X_i X_j X_k] = {} & E[X_i X_j X_k] \\
& - \sum^{3} E[X_i] E[X_j X_k] + 2 E[X_i] E[X_j] E[X_k] = 0
\end{aligned}
\tag{14}
$$

where the number over the summation sign refers to the number of terms generated by the indicated expression without allowing permutation of indices. For example,

$$
\begin{aligned}
\sum^{3} E[X_i] E[X_j X_k] = {} & E[X_i] E[X_j X_k] + E[X_j] E[X_i X_k] \\
& + E[X_k] E[X_i X_j]
\end{aligned}
\tag{15}
$$

The Gaussian closure scheme will lead to 14 closed moment equations, which consist of four equations for the first-order moments and ten equations for the second-order moments. These equations will be integrated numerically by using the IMSL (International Mathematical and Statistical Library) DVERK subroutine (Runge-Kutta-Verner fifth- and sixth-order numerical integration method). The results of this solution will be presented in Sec. III.

Non-Gaussian Closure Solution

The Gaussian closure solution is analogous to the linearized solution of nonlinear mechanics problems. In view of the inherent nonlinearity of the system (as well as the random time coefficients), the response processes will be non-Gaussian and, in this case, all higher-order cumulants of order greater than 2 will not vanish. The probability density of non-Gaussian processes can be expressed in terms of the Gram-Charlier expansion or Edgeworth asymptotic series. It has been shown (in Ref. 23) that rapid convergence in the Edgeworth expansion can be achieved by retaining the first few terms in the series. In this paper the non-Gaussian closure solution will be obtained by setting the fifth-order joint cumulant to zero, i.e.,

$$
\begin{aligned}
\lambda_5[X_i X_j X_k X_\ell X_m] = {} & E[X_i X_j X_k X_\ell X_m] \\
& - \sum^{5} E[X_i] E[X_j X_k X_\ell X_m] \\
& + 2\sum^{10} E[X_i] E[X_j] E[X_k X_\ell X_m] \\
& - 6\sum^{10} E[X_i] E[X_j] E[X_k] E[X_\ell X_m] \\
& + 2\sum^{15} E[X_i] E[X_j X_k] E[X_\ell X_m] \\
& - \sum^{10} E[X_i X_j] E[X_k X_\ell X_m] \\
& + 24 E[X_i] E[X_j] E[X_k] E[X_\ell] E[X_m]
\end{aligned}
\tag{16}
$$

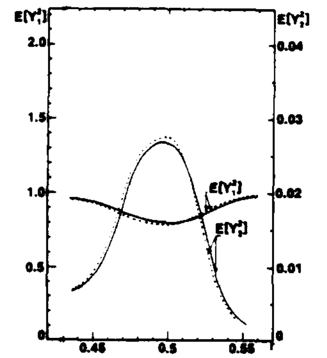

Fig. 5 Mean-square response of normal modes according to non-Gaussian closure solution vs internal resonance: ——, deterministic system; ---, system with random damping, $D_{c_1} = D_{c_2} = 0.1 D_0$, $2D_0 = 0.08$.

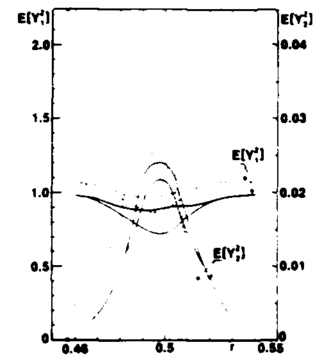

Fig. 6 Mean-square response of normal modes according to Gaussian closure solution vs internal resonance: ——, deterministic system; ---, system with random stiffness, $D_{c_1} = D_{c_2} = 0.1 D_0$, $2D_0 = 0.08$.

This procedure requires that 69 differential equations be generated from Eq. (13). These equations consist of 4 equations for first-order moments, 10 equations for second-order moments, 20 equations for third-order moments, and 35 equations for fourth-order moments. These equations will be solved by numerical integration by using the IMSL DVERK subroutine. The results of this solution, together with the Gaussian closure solution, will be discussed in Sec. III.

III. Statistics of the System Response

The statistics of the system response are determined for three different cases of system parameter uncertainties. These are 1) damping random variation, 2) stiffness random variation, and 3) damping and stiffness variations. The results of the numerical integration are presented and discussed in the following sections.

Response of the System with Random Damping

The time-history response of the displacement mean squares of the system normal coordinates is shown in Figs. 2 and 3 according to the Gaussian and non-Gaussian closure solutions, respectively. These figures display both the transient and steady-state responses for exact internal tuning ratio $r = 0.5$, damping ratios $\zeta_1 = \zeta_2 = 0.02$, mass ratio $m_1/m_2 = 0.2$, excitation spectral density $2D_0 = 0.08$, and damping variation density $D_{c_1} = D_{c_2} = 0.1 D_0$. Both responses show that the transient response level is greater than the steady-state level. It is seen that after a response period of $\tau = 1000$, the mean squares fluctuate between two limits for the Gaussian closure solution while they are strictly stationary for the non-Gaussian closure solution. This difference between the two solutions is due to the fact that the non-Gaussian closure more adequately models the system nonlinearity. The stationarity of the response of coupled nonlinear systems was verified by Schmidt,[24] who used the stochastic averaging method. The influence of the initial conditions on the time-history response is found to have no effect on the steady-state response for both solutions; however, the effect exists only during the transient period.

The numerical integration has been repeated for various values of internal detuning parameter r in the neighborhood of the exact internal resonance $r = 0.5$. The results are shown in Figs. 4 and 5 for Gaussian and non-Gaussian closure solutions, respectively. These figures include response curves for the case of deterministic system (i.e., the system with constant damping coefficients) for comparison. The Gaussian closure solution is indicated by two curves (for each mode),

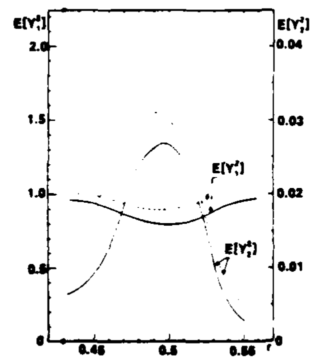

Fig. 7 Mean-square response of normal modes according to non-Gaussian closure solution vs internal resonance: ——, deterministic system; ---, system with random stiffness, $D_{k_1} = D_{k_2} = 0.1 D_0$, $2D_0 = 0.08$.

which represent the upper and lower limits of the quasi-stationary response as reflected in the steady-state time-history response shown in Fig. 2. The non-Gaussian solution, on the other hand, is shown by one curve for each mode since the response achieves a stationary response. It is seen that the mean square of the first normal mode approaches the response of the single degree of freedom as the internal detuning is well removed from the exact internal resonance $r = 0.5$. The damping random variation has a remarkable effect on the Gaussian closure solution, and the effect is less pronounced in the non-Gaussian closure solution. In the non-Gaussian solution, the damping variation results in a slight decrease in the mean-square response of the first mode and a corresponding increase in the second mode mean-square response for $r < 0.5$. For $r > 0.5$ the effect is reversed. It is found that the damping fluctuation does not have a uniform effect on the response in the case of Gaussian closure solution; however, the region of the autoparametric interaction becomes narrower.

Response of the System with Random Stiffness

Figures 6 and 7 provide a comparison between the mean-square response of the system as obtained by Gaussian and non-Gaussian closure solutions, respectively. The response of

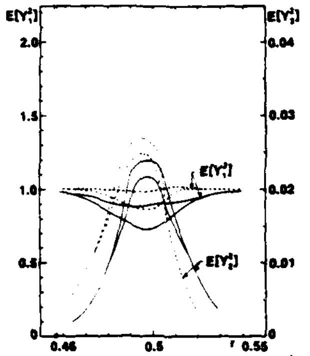

Fig. 8 Mean-square response of normal modes according to Gaussian closure solution vs internal resonance: ——, deterministic system; --, system with random damping and stiffness, $D_{ci} = D_{ki} = 0.1D_0$, $2D_0 = 0.08$.

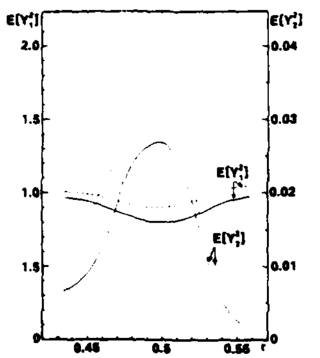

Fig. 9 Mean-square response of normal modes according to non-Gaussian closure solution vs internal resonance: ——, deterministic system; --, system with random damping and stiffness, $D_{ci} = D_{ki} = 0.1D_0$, $2D_0 = 0.08$.

the system with stiffness random fluctuation is shown by dotted curves, while solid curves belong to the response of the deterministic system. It is seen that, for both solutions, a small random fluctuation in the system stiffness ($D_{k_1} = D_{k_2} = 0.1D_0$) results in a substantial dispersion of the response statistics. It is known that under random stiffness variation the system eigenvalues will be random.[25] Previous investigations[26-29] of the response of linear systems (with parameters represented by random variables) showed that a small dispersion in the stiffness resulted in a considerable dispersion in the system response. It is also evident from both Figs. 6 and 7 that the effect of the stiffness random variation is to increase the level of the response mean squares and to widen the region of autoparametric interaction. However, the characteristics of the autoparametric vibration absorber[30,31] are less effective in the presence of stiffness random variation.

Combined Damping and Stiffness Variations

The system mean-square responses of the system with equal levels of spectral densities of the damping and stiffness random parameters ($D_{ci} = D_{ki} = 0.1D_0$) are shown in Figs. 8 and 9, according to Gaussian and non-Gaussian closure solutions, respectively. Based on the results of the previous two cases, it is clear that the system response is mainly dominated by the stiffness random variation.

IV. Conclusions

The influence of the damping and stiffness random variation on the random response of structural systems with autoparametric interaction has been determined. The Fokker-Planck equation approach has been used to derive a general differential equation for the response moments. This equation constitutes an infinite coupled set of moment equations, which are truncated by two closure schemes. These closure schemes are based on the properties of the statistical cumulants. The first, referred to as Gaussian closure, assumes that the response distribution does not deviate significantly from normal. The other scheme takes into account the deviation of the response distribution from being Gaussian. The results of both solutions are calculated and represented as function of the internal detuning parameter. The Gaussian closure solution results in a quasi-stationary response, while the non-Gaussian closure solution is strictly stationary. It has also been found that the random variation of the system stiffness has more considerable effect than the effect of damping variation on the response mean squares. One last point is that the model selected in this study is a simple structural system in which several characteristics resemble those encountered in aeroelastic structures, such as a wing with external store. However, the investigation did not consider the interaction with random aerodynamic forces that results in stochastic nonlinear flutter. Currently, the authors are involved in a research program supported by the AFOSR to examine the stochastic flutter of real nonlinear models wings and panels under random aerodynamic loading.

Acknowledgments

This research is supported by a grant from the Air Force Office of Scientific Research under Grant AFOSR-85-0008 Dr. Anthony Amos is the program director.

References

[1] Bolotin, V.V., *The Dynamic Stability of Elastic Systems*, Holden-Day, San Francisco, CA, 1964.

[2] Evan-Iwanowski, R.M., *Resonance Oscillations in Mechanical Systems*, Elsevier, New York, 1976.

[3] Nayfeh, A.H. and Mook, D.T., *Nonlinear Oscillations*, Wiley-Interscience, New York, 1979.

[4] Minorsky, N., *Nonlinear Oscillations*, Van Nostrand, New York, 1962.

[5] Barr, A.D.S. and Done, G.T.S., "Parametric Oscillations in Aircraft Structures," *Aeronautical Journal*, Vol. 75, 1971, pp. 654-658.

[6] Barr, A.D.S., "Some Developments in Parametric Stability and Nonlinear Vibration," *Proceedings of the International Conference of Recent Advances in Structural Dynamics*, Southampton, England, 1980, pp. 545-568.

[7] Greenwood, D.T., *Classical Dynamics*, Prentice-Hall, Englewood Cliffs, NJ, 1977.

[8] Breitbach, E.J., "Effect of Structural Nonlinearities on Aircraft Vibration and Flutter," AGARD Rep. 665, Sept. 1977.

[9] Breitbach, E.J., "Flutter Analysis of an Airplane with Multiple Structural Nonlinearities in the Control System," NASA TP 1620, 1980.

[10] De Ferrari, G., Chesta, L., Sensburg, O., and Lotze, A., "Effects of Nonlinearity on Wing-Store Flutter," AGARD-R-687, 1980.

[11] Peloubet, R.P. Jr., Haller, R.L., and Bolding, R.M., "F-16 Flutter Suppression System Investigation," *Proceedings of the AIAA/ASME/ASCE/AHS 21st Structures, Structural Dynamics and Materials Conference*, Seattle, WA, May 1980, pp. 620-634.

[12] Reed, W.H. III, Foughner, J.T. Jr., and Runyan, H.L., "Decoupler Pylon: A Simple, Effective Wing/Store Suppressor," *Journal of Aircraft*, Vol. 17, March 1980, pp. 206-211.

[13] Desmarais, R.N. and Reed, W.H. III, "Wing/Store Flutter with Nonlinear Pylon Stiffness," *Journal of Aircraft*, Vol. 18, Nov. 1981, pp. 984-987.

[14] Struble, R.A., *Nonlinear Differential Equations*, McGraw-Hill, New York, 1962.

[15] Nayfeh, A.H., *Perturbation Methods*, Wiley, New York, 1973.

[16] Ibrahim, R.A., *Parametric Random Vibration*, Research Studies Press, Wiley, New York, 1985.

[17] Soong, T.T., *Random Differential Equations in Science and Engineering*, Academic Press, Orlando, FL, 1973.

[18] Ibrahim, R.A., "Structural Dynamics with Parameter Uncertainties," *Applied Mechanics Reviews*, Vol. 40, March 1987.

[19] Barr, A.D.S. and Ashworth, R.P., "Parametric and Nonlinear Mode Interaction Behavior in the Dynamics of Structures," Department of Mechanical Engineering, University of Dundee, Scotland, Rep. AFOSR 74-2723, Dec. 1977.

[20] Haddow, A.G., Barr, A.D.S., and Mook, D.T., "Theoretical and Experimental Study of Modal Interaction in a Two-Degree-of-Freedom Structure," *Journal of Sound and Vibration*, Vol. 97, No. 3, 1984, pp. 451-473.

[21] Ibrahim, R.A. and Heo, H., "Autoparametric Vibration of Coupled Beams under Random Support Motion," *Journal of Vibration, Acoustics, Stress, and Reliability*, Vol. 108, 1986, pp. 421-426.

[22] Heo, H., "Nonlinear Stochastic Flutter of Aeroelastic Structural Systems," Ph.D. Thesis, Texas Tech University, Lubbock, TX, Dec. 1985.

[23] Ibrahim, R.A., Soundararajan, A., and Heo, H., "Stochastic Response of Nonlinear Dynamic Systems Based on a Non-Gaussian Closure," *Journal of Applied Mechanics*, Vol. 52, No. 4, 1985, pp. 965-970.

[24] Schmidt, G., "Probability Densities of Parametrically Excited Random Vibrations," *Proceedings of the IUTAM Symposium on Stochastic Problems in Dynamics*, edited by B.L. Clarkson, Pitman, London, 1977, pp. 197-213.

[25] Scheidt, J. and Purkert, W., *Random Eigenvalue Problems*, Elsevier, New York, 1983.

[26] Bogdanoff, J.L. and Chenea, P.F., "Dynamics of Some Disordered Linear Systems," *International Journal of Mechanical Science*, Vol. 3, 1961, pp. 157-169.

[27] Chen, P.C. and Soroka, W.W., "Impulse Response of a Dynamic System with Statistical Properties," *Journal of Sound and Vibration*, Vol. 31, 1973, pp. 309-314.

[28] Chen, P.C. and Soroka, W.W., "Multi-Degree Dynamic Response of a System with Statistical Properties," *Journal of Sound and Vibration*, Vol. 37, 1974, pp. 547-556.

[29] Prasthofer, P.H. and Beadle, C.W., "Dynamic Response of Structures with Statistical Uncertainties in Their Stiffnesses," *Journal of Sound and Vibration*, Vol. 42, 1975, pp. 447-493.

[30] Haxton, R.S. and Barr, A.D.S., "The Autoparametric Vibration Absorber," *Journal of Engineering for Industry*, Vol. 94, 1972, pp. 119-125.

[31] Ibrahim, R.A. and Roberts, J.W., "Broad Band Random Excitation of a Two Degree-of-Freedom System with Autoparametric Coupling," *Journal of Sound and Vibration*, Vol. 44, 1976, pp. 335-348.

Structural dynamics with parameter uncertainties

R A Ibrahim

Department of Mechanical Engineering, Texas Tech University, Lubbock TX 79409

The treatment of structural parameters as random variables has been the subject of structural dynamicists and designers for many years. Several problems have been involved during the last few decades and resulted in new theorems and interesting phenomena. This paper reviews a number of topics pertaining to structural dynamics with parameter uncertainties. These include direct problems such as random eigenvalues and random responses of discrete and continuous systems. The impact of these problems on related areas of interest such as sensitivity of structural performance to parameter variations, design optimization, and reliability analysis is also addressed. The paper includes the results of experimental investigations, the phenomenon of normal modes localization, and the effect of mistuning of turbomachinery blades on their flutter and forced response characteristics.

1. INTRODUCTION

The concept of uncertainty plays an important role in the investigation of various engineering and physical chemistry problems. In fluid mechanics, for example, the inaccuracy of measurements is called "uncertainty" which differs from the concept of error (Kline, 1985). An error in measurement is the difference between the true value and the measured value. On the other hand, an uncertainty is a possible value that the error might take on in a given measurement. Because the uncertainty can take on various values over a range, it is inherently random. In control theory, the differential equations of control systems often involve uncertain bounded state variables. The parameters of transfer functions of certain models usually vary with a certain degree of uncertainty (Ashworth, 1982). Thus a probabilistic transfer function can be defined with uncertain parameters and can lie anywhere within the ranges which are determined from simulation tests. The identification of uncertain parameters has recently been examined by Skowronski (1981, 1984).

Another class of problems involving parameter uncertainties is the random heterogeneity of real media which possess properties that are described in a probabilistic sense. More specifically, these properties vary randomly with respect to time and position, and thus constitute a random field. The theory of wave propagation in random media is very complicated and involves partial differential equations whose coefficients are random functions of space and time. The difficulty of random wave propagation problems stems from the fact that the solution of a linear partial differential equation depends nonlinearly upon the coefficients (Chernov, 1960; Frisch, 1968; Sobczyk, 1985).

In physical chemistry the problem of determining the vibrational properties of randomly disordered crystal lattices involves the calculations of the frequency spectrum, electronic energy levels of binary alloys, thermodynamic properties of alloys, isotropic mixtures, and other solid state phenomena. Of particular importance is the "normal localization" or "confinement" phenomenon which was first reported by Anderson (1958). Anderson showed that the electron eigenstates in a disordered solid may become localized and results in a reduction of metallic conductivity. In structural dynamics with parameter uncertainties, irregularities may inhibit the propagation of vibration within the structure and the vibration modes become localized. The similarities between the propagation of vibration in an elastic system and the conduction of electrons in a solid is discussed by Hodges (1982), Hodges and Woodhouse (1983), and Pierre et al (1986). Several problems in physics and physical chemistry pertaining to crystal lattice dynamics were reviewed by Elliot et al (1974) and recently documented in a monograph by Bottger (1983).

In structural dynamics, uncertainties arise from two main sources (Prasthofer and Beadle, 1975). The first is a statistical one and is due, for example, to the stiffness or damping fluctuations caused by random variations in material properties, randomness in boundary conditions, and variations caused by manufacturing and assembly techniques. The second is nonstatistical and is due, for example, to the inaccuracies and assumptions introduced in the mathematical modeling of the structure. In the first class the mechanical properties of dynamic systems are subject to a certain degree of uncertainty because the physical properties of their elements are not measured exactly. In addition, the physical properties can experience variations with the passage of time as a result of wear and tear or just inherent deterioration. These properties should be modeled as random variables with a probability distribution representing the distribution of the measured values. This modeling results in random eigenvalues, eigenvectors, and random responses of the system in question. The analysis of random eigenvalues and eigenvectors has been a subject of several studies by mathematicians and engineers and will be reviewed in section 3.

Figure 1 shows five examples of structural systems involving parameter and load uncertainties. They include "almost" periodic structures, similar component subsystems, multi-span beams, rocket fins, and turbomachinery rotors. The rocket fins

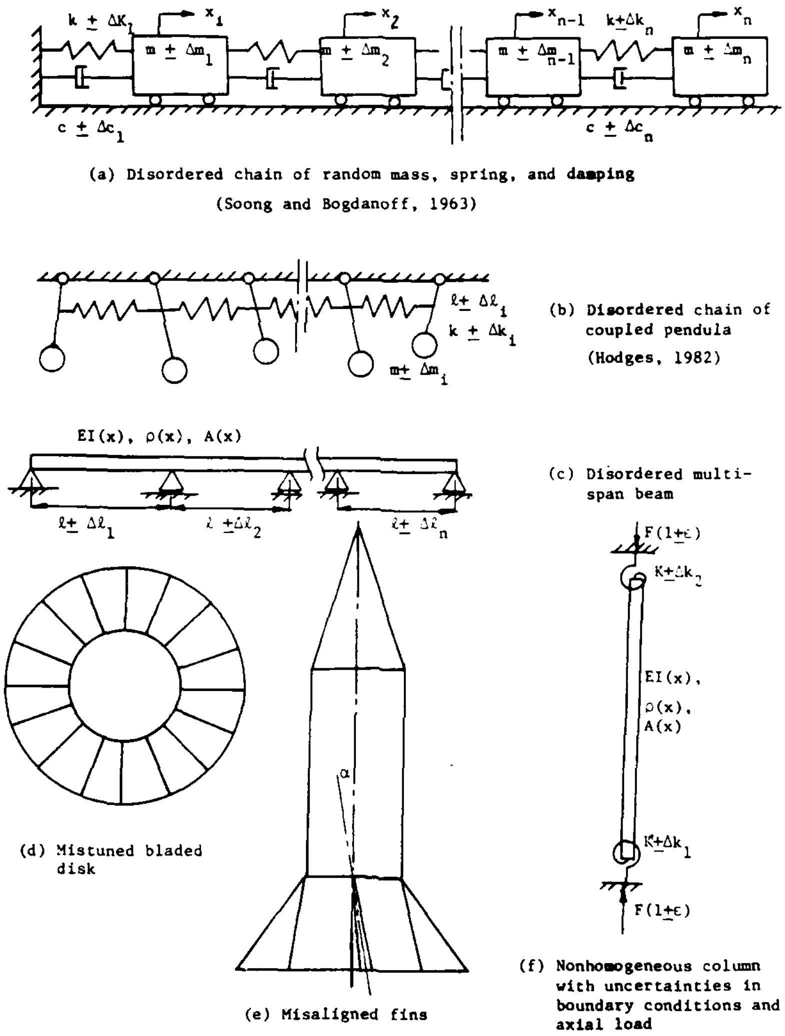

FIG. 1. Examples of disordered systems.

are not usually identical in their areas and each fin has some misalignment with the rocket longitudinal axis. For the case of turbomachinery rotors, there is always some mass and stiffness eccentricity in the disks. Parameter variations exist in disk blades and result in corresponding variations in the individual natural frequencies of the blades. This problem is known as mistuning (Srinivasan, 1984) which may have a significant effect on the forced response amplitude of the blades and also in the value of the flow speed at which flutter of the blades occurs. Other examples include buried pipelines, railroad tracks, and interconnected girders. The uncertainties in these systems affect to a large extent their design and operating performance.

It should be noted that parameter irregularities may cause significant changes in the dynamic characteristics of structural systems. In particular, they may cause the occurrence of mode localization which can be used as a means of passive control of vibrations. In civil engineering the mechanical and strength properties of the material vary from one point to another point and are seldom prone to certain *in situ* measurements but only to indirect estimat . (Augusti et al, 1984). The uncertainty of these properties has a direct relationship to the reliability of such structures. These uncertainties are usually manifested in the applied loads, stiffness, and theoretical models that are used to describe and relate loading and resistance. The design of structures under conditions of uncertainty implies a balancing decision between risk of failure and cost or weight (Ang and Tang, 1984; Frangopol, 1986). The risk is an unavoidable consideration for structural optimization problems. It has been customary in most reliability studies to measure the risk by the probability of failure (ie, the likelihood of occurrence of some specified limit state). On the other hand, when restrictions and constraints of the design are imprecisely described, the design objective functions become fuzzy (Zadeh, 1965, 1973; Brown, 1980; Brown and Yao, 1983). Recently, the fuzzy set theory has been applied in multi-objective fuzzy optimization design of ship grillage structures (Gangwu and Suming, 1986).

The degree of sensitivity of structures to either deterministic design changes, or stochastic parameter variations is of great importance to the structural dynamicist. In particular, it is essential to determine if small perturbations can result in significant changes of the free or forced response amplitudes. This sensitivity analysis is of great concern to those who are involved in the control of large flexible space structures (Meirovitch et al, 1983; Nurre et al, 1984). These structures possess several modes densely packed at low frequencies. When they are descretized, model errors occur and the free modes of vibration cannot be determined accurately. Thus when a control system is designed for natural frequencies whose values are assumed to be exact, the model errors and structural uncertainties may deteriorate the performance of the control loop, and may even make the system unstable. This problem results in what is known as robustness, ie, a control system is termed robust if it is relatively insensitive to model errors and structural uncertainties.

This paper provides a review of the recent theorems and results pertaining to structural dynamics with parameter uncertainties. An early account of the subject was provided by Soong and Cozzarelli (1976). Three main problems will be addressed. These are:

1. Random eigenvalues,
2. Random response characteristics, and
3. Design optimization and reliability.

Before reviewing these three problems the differences between parametric random vibration and structural dynamics with parameter uncertainties will be discussed first.

2. BETWEEN PARAMETRICALLY EXCITED AND DISORDERED SYSTEMS

It is very important to distinguish between two types of parameter variations encountered in structural dynamics. The first type arises due to random parametric excitation of systems with essentially fixed properties while the second class is internal and is associated with the system when its parameters are represented in a probabilistic sense. In the former case the system equations of motion are stochastic differential equations with random coefficients represented by random processes (Ibrahim, 1985), while in the latter case the equations of motion are differential equations with random parameters represented by random variables (Soong, 1973). The methods of treating dynamic systems under parametric random excitations are different from those used in solving differential equations with random variable coefficients. Parametric random vibration is basically a combination of the theory of stochastic processes, stochastic differential equations, and applied dynamics. Systems with parameter uncertainties (referred to in the literature as "disordered systems"), on the other hand, involve boundary-value problem and random field theory (Vanmarcke, 1984). The term "disorder" has been extensively used in the literature to distinguish between the case of random perturbation of the system parameters (described by a probabilistic law) and the case when these parameters are perturbed in a deterministic sense.

3. RANDOM EIGENVALUES

3.1. Basic concept of random eigenvalue

The value of the natural frequency of simple single degree-of-freedom systems is given by the square root of the stiffness to mass ratio. This value is assumed by constant for identical systems. However, experiments have shown that this value varies randomly (Mok and Murray, 1965) because in reality the physical properties of the elements can neither be measured exactly nor manufactured exactly. Thus, the eigenvalues are random variables whose statistical properties are determined by the random coefficients of the inertia and stiffness terms of the equations of motion. Consider for example the natural frequency of a simple mass-spring system

$$\lambda = \omega^2 = k/m.$$

the variation of λ due to variations in stiffness $k = \bar{k} + \delta k$ and mass $m = \bar{m} + \delta m$, may be expressed as a Taylor series

$$\delta\lambda = \lambda - \bar{\lambda} = -\frac{\partial \lambda}{\partial k}\delta k + \frac{\partial \lambda}{\partial m}\partial m + \frac{1}{2}\frac{\partial^2 \lambda}{\partial k^2}(\delta k)^2 + \frac{1}{2}\frac{\partial^2 \lambda}{\partial m^2}(\delta m)^2 + \cdots, \quad (1)$$

where overbar quantities refer to mean values and $\bar{\lambda} = \bar{k}/\bar{m}$

When the variations δm and δk are random variables the natural frequency will be a random variable. The mean and variance of λ can be evaluated as follows

$$E[\lambda] = \bar{\lambda} + \frac{1}{2}\frac{\partial^2 \lambda}{\partial k^2}E[\delta k^2] + \frac{1}{2}\frac{\partial^2 \lambda}{\partial m^2}E[\delta m^2] + \cdots \quad (2)$$

and

$$E\left[(\lambda - \bar{\lambda})^2\right] = \left(\frac{\partial \lambda}{\partial m}\right)^2 E[\delta k^2] + \left(\frac{\partial \lambda}{\partial m}\right)^2 E[\delta m^2] + 2\frac{\partial \lambda}{\partial k}\cdot\frac{\partial \lambda}{\partial m}E[\delta k \cdot \delta m] + \frac{1}{4}\left(\frac{\partial^2 \lambda}{\partial k^2}\right)^2 E[\delta k^4] + \frac{1}{4}\left(\frac{\partial^2 \lambda}{\partial m^2}\right)^2 E[\delta m^4] + \frac{1}{2}\left(\frac{\partial^2 \lambda}{\partial k^2}\right)\left(\frac{\partial^2 \lambda}{\partial m^2}\right)E[\delta k^2 \cdot \delta m^2] + \cdots \quad (3)$$

The same is applied when the mass moment of inertia is included in the equations of motion. Collins and Thomson (1967) derived the statistical characteristics of principal moments of inertia and principal axes directions.

Generally, the structural dynamicist is interested in determining the probability that one or more eigenvalues lie in a given range or less than a certain value (Boyce, 1968). However, the probabilistic description of the eigenvalues and the eigenvectors has been examined for a limited and simple class of problems. In most cases, it is possible to calculate the statistical functions (such as expectations, variances, and covariance functions) of the eigenvalues and eigenvectors.

The random eigenvalue problem has been examined for a limited number of linear discrete and continuous systems. The treatment of these systems is based on the analysis of random matrices and random differential operators (Scheidt and Purkert, 1983). The next subsections will review the methods and main results reported in the literature.

3.2. Random eigenvalues of discrete systems

The statistics of random eigenvalues and eigenvectors of discrete systems may be determined by using one of three main approaches. These are the transfer matrix method, the random perturbation method, and the Monte Carlo numerical simulation algorithm. The transfer matrix method (Kerner 1954, 1956; Soong, 1962) utilizes a perturbational expansion of the random eigenvalues in terms of the random perturbations of the system parameters. The perturbation method is based on an asymptotic expansion and combines the ordinary perturbation and multivariate statistical analysis. The multivariate establishes the probability distributions of random eigenvalues in terms of the distributions of the matrix coefficients in the equations of motion. The Monte Carlo method, on the other hand, generates a random sample of the system random parameters which are used for computing numerically the eigenvalues and eigenvectors for each set of parameters in the sample. Monte Carlo simulations are expensive since they require a large number of numerical solutions to define the probability level at the tails of the distribution. This disadvantage becomes evident when one deals with large or medium size systems where numerical simulations become unrealistic on conventional digital computers. The first two methods will be outlined in the next two sections.

3.2.1. Transfer matrix method

This method was first developed for disordered periodic lattice systems by Kerner (1954, 1956). It was adopted by Soong and Bogdanoff (1963) to examine the statistics of the random eigenvalues of disordered spring-mass chain of N degrees of freedom of the type shown in Figure 1(a). Basically the method is an extension of the transfer matrix developed originally for free vibration of deterministic discrete systems (Thomson, 1981). The method transfers the displacement vector $\{\mathbf{X}\}_j$ of the jth mass into next mass displacement vector $[X]_{j+1}$, ie

$$\{\mathbf{X}\}_j = [\mathbf{I}+\mathbf{T}]_{j+1}\{\mathbf{X}\}_{j+1}, \tag{4}$$

where $\mathbf{I}$ is the unit matrix and $[\mathbf{I}+\mathbf{T}]$ is the transfer matrix. The first displacement vector $\{\mathbf{X}\}_0$ is related to the last displacement vector $\{\mathbf{X}\}_N$ by the relationship

$$\{\mathbf{X}\}_0 = \left[\prod_{j=1}^{N}[\mathbf{I}+\mathbf{T}]_j\right]\{\mathbf{X}\}_N. \tag{5}$$

In order to demonstrate the method, a periodic disordered chain with random masses and constant equal springs of stiffness K will be considered. Let the random mass be defined by the expression

$$m_j = \bar{m}(1+\epsilon_j), \tag{6}$$

where $\bar{m}$ is the mean value of the mass and ϵ_j is a small random variable with zero mean.

The transfer matrix can be written in the form

$$[\mathbf{I}+\mathbf{T}]_j = [\mathbf{I}+\mathbf{T}]_j + [\mathbf{E}]_j, \tag{7}$$

where $[\mathbf{E}]_j$ is a perturbational transfer matrix which results from the random perturbations ϵ_j.

The characteristic equation can be established from eq. (5). The roots of this equation are the system eigenvalues ω_n. In order to determine the statistical properties of the eigenvalues it is necessary to express ω_n in terms of the random variables ϵ_j. It will be assumed that the range over which the values of ϵ_j are distributed is small and ω_n can be explained in powers of the random variables ϵ_j:

$$\omega_n = \bar{\omega}_n + \sum_{j=1}^{N}\omega_{1j}\epsilon_j + \sum_{j=1}^{N}\omega_{2j}\epsilon_j^2 + \sum_{j=1}^{N-1}\sum_{\substack{k=2\\k>j}}^{N}\omega_{1jk}\epsilon_j\epsilon_k + \cdots, \tag{8a}$$

$$\cong \bar{\omega}_n + \sum_{j=1}^{N}\omega_{1j}\epsilon_j \quad \text{for small } \epsilon_j, \qquad n = 1, 2, \ldots, N \tag{8b}$$

Let the random variables ϵ_j be statistically independent, identically and normally distributed with zero mean. This means that the probability density function of each is

$$p(\epsilon) = \frac{1}{\sigma_\epsilon\sqrt{2\pi}}\exp\{-\epsilon^2/2\sigma_\epsilon^2\}, \tag{9}$$

where σ_ϵ^2 is the variance of the random variable ϵ.

From the theory of random processes (Laning and Battin, 1956), it is known that if the random variables ϵ_j are independent and normally distributed the random eigenvalues will be normaly distributed with mean value $\bar{\omega}_n$ and variance $\sigma_\epsilon^2\sum_{j=1}^{N}\omega_{1j}^2$. These two statistical parameters provide the elements of the probability density function of ω_n^2, ie

$$p(\omega_n) = \frac{1}{\sigma_\omega\sqrt{2\pi}}\exp\{-(\omega_n-\bar{\omega}_n)^2/2\sigma^2\omega\}. \tag{10}$$

Figure 2 shows $p(\omega_n)$ and the standard deviation σ_ω for a spring-mass chain of 10 degrees of freedom with $\sigma_\epsilon = 0.05$. It is seen that the randomness of the masses results in a considerable dispersion in the high frequency region. The standard deviation of the random eigenvalues increases with the standard deviation of the mass perturbations ϵ_j according to the formula (Soong, 1962)

$$\sigma_\omega/\sigma_\epsilon = \left\{\sum_{j=1}^{N}\omega_{1j}^2\right\}^{1/2}. \tag{11}$$

3.2.2. Random perturbation method

The perturbation method for the deterministic eigenvalue problem is well documented (Cole, 1968; Meirovitch, 1980). The method has recently been extended for random eigenvalues by Scheidt and Purkert (1983). The eigenvalues of discrete systems are usually determined from the conservative part of the system equations of motion whose eigenvalue equation is given in the form

$$[\mathbf{K}(s) - \lambda\mathbf{M}(s)]\{x\} = \{0\}, \tag{12}$$

where $\mathbf{K}(s)$ and $\mathbf{M}(s)$ are symmetric stiffness and mass matrices, respectively. The elements of these matrices are taken from the entire sample space S, ie, $s \subset S$. λ_j and $\{\mathbf{x}\}_j$ are the jth eigenvalue and eigenvector, respectively. The random matrices $\mathbf{K}(s)$ and $\mathbf{M}(s)$ can be written as the sum of deterministic and random matrices

$$\mathbf{K}(s) = \bar{\mathbf{K}} + \tilde{\mathbf{k}}(s),$$
$$\mathbf{M}(s) = \bar{\mathbf{M}} + \tilde{\mathbf{m}}(s), \tag{13}$$

where $\tilde{\mathbf{k}}(s)$ and $\tilde{\mathbf{m}}(s)$ represent random fluctuations in the stiffness and mass matrices, respectively, with zero means such that

$$|\tilde{\mathbf{k}}(s)| = \left\{\sum_{i,j=1}^{n}\tilde{k}_{ij}^2(s)\right\}^{\frac{1}{2}} < \epsilon_k,$$

and

$$|\tilde{\mathbf{m}}(s)| = \left\{\sum_{i,j=1}^{n}\tilde{m}_{ij}^2(s)\right\}^{\frac{1}{2}} < \epsilon_m. \tag{14}$$

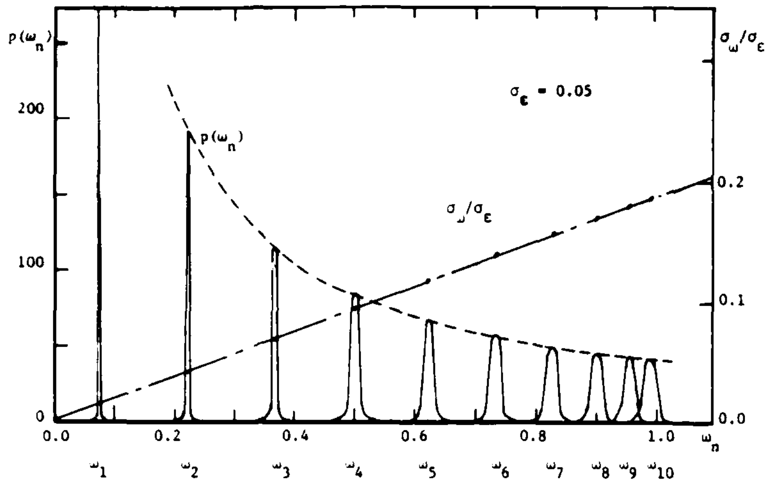

FIG. 2. Probability density functions and standard deviation of ω_n

Alternatively, the problem can be stated by transforming eq. (12) into the standard form

$$[\mathbf{A} - \lambda \mathbf{I}]\{\mathbf{x}\} = \{0\}, \tag{15}$$

where A is the system dynamic matrix which is symmetric positive and has the random perturbational form

$$\mathbf{A}(s) = \bar{\mathbf{A}} + \mathbf{a}(s). \tag{16}$$

The deterministic matrix $\bar{\mathbf{A}}$ has the simple eigenvalues

$$\bar{\lambda}_1 < \bar{\lambda}_2 < \cdots < \bar{\lambda}_n. \tag{17}$$

while the random matrix $\mathbf{A}(s)$ has the random eigenvalues

$$\lambda_1(s) < \lambda_2(s) < \cdots < \lambda_n(s). \tag{18}$$

it is clear that the existence of the first two moments of the eigenvalues $\lambda_j(s)$ is implied by the existence of the first two moments of the elements of $\mathbf{A}(s)$.

The eigenvectors $\{\mathbf{x}\}_j$ are normalized by the relation

$$(\mathbf{x}_j, \mathbf{x}_j) = 1, \tag{19}$$

where $(\mathbf{x}_j, \mathbf{x}_j)$ denotes the scalar (or inner) product of the same vector $\mathbf{x}_j$, ie $\{x\}_j^T\{\mathbf{x}\}_j$. Introducing the two expansions

$$\lambda_j(s) = \bar{\lambda}_j + \sum_{k=1}^{\infty} \bar{\lambda}_{jk}(s) \tag{20}$$

$$\{\mathbf{x}(s)\}_j = \{\bar{\mathbf{x}}\}_j + \sum_{k=1}^{\infty} \{\bar{\mathbf{x}}(s)\}_{jk} \tag{21}$$

where $\{\bar{\mathbf{x}}\}_j = (0, 0, \ldots, 0, 1^j, 0, \ldots, 0)$ is the normalized eigenvector associated with $\bar{\lambda}_j$. $\bar{\lambda}_{jk}(s)$ and $\{\bar{\mathbf{x}}(s)\}_{jk}$ are the contributions due to the perturbed elements of $\mathbf{a}(s)$. From the analytical dependence of λ_j and $\{\mathbf{x}\}_j$ on the elements of $\mathbf{a}(s)$, Scheidt and Purkert (1973) showed that expansions (20) and (21) converge at least for sufficiently small values of the elements of $\mathbf{a}(s)$. The homogeneous terms $\lambda_{jk}(s)$ and $\{\mathbf{x}(s)\}_{jk}$ up to fourth order are given by Scheidt and Purkert (1983). These terms can then be used to determine the expectations and correlation relations of the random eigenvalues and eigenvectors. If the correlation between the elements of $\mathbf{a}(s) = [\mathbf{a}_{ij}]$ are only given, then up to first-order perturbation the means of the eigenvalues and eigenvectors are

$$E = [\lambda_j(s)] = \bar{\lambda}_j + \sum_{\substack{i=1 \\ i \neq j}}^{n} E[a_{ij} a_{ji}]/\bar{\lambda}_{ji} + \cdots, \tag{22}$$

$$E[\mathbf{x}(s)_j] = \left(1 + \frac{1}{2} E\left[(\bar{\mathbf{x}}_{j1}, \bar{\mathbf{x}}_{j1})\right]\right)\bar{\mathbf{x}}_{j0} + E[\{Z\}_{j2}] + \cdots. \tag{23}$$

where $\bar{\lambda}_{ij} = \bar{\lambda}_i - \bar{\lambda}_j$, $\{Z\}_{j2} = \{Z_{21}, Z_{22}, \ldots, Z_{2n}\}^T$, and the elements of $\{Z\}_{j2}$ are given by the expression

$$(Z_{2i})_j = \frac{1}{\bar{\lambda}_{ij}} \left\{ \sum_{\substack{k=1 \\ k \neq j}}^{n} \frac{1}{\bar{\lambda}_{kj}} a_{ik} a_{kj} - \frac{1}{\bar{\lambda}_{ij}} a_{ij} a_{jj} \right\}$$

for $i \neq j$ and $(Z_{2j})_j = 0$

On the other hand, the correlation relations of the eigenvalues and eigenvectors up to the $(k+1)$-th order in the perturbations a_{ij} are

$$\begin{aligned} R_\lambda(j, k) = E[\lambda_j \lambda_k] &= E[a_{jj} a_{kk}] \\ &+ \sum_{\substack{i=1 \\ i \neq j}}^{n} \frac{1}{\bar{\lambda}_{ij}} E\left[a_{ij} a_{ji} a_{kk}\left(1 + \frac{a}{\bar{\lambda}}\right)\right] \\ &+ \sum_{\substack{i=j \\ i \neq k}}^{n} \frac{1}{\bar{\lambda}_{ik}} E\left[a_{ik} a_{ki} a_{jj}\left(1 + \frac{a_{kk}}{\bar{\lambda}_k}\right)\right] \\ &+ \sum_{\substack{i,l=1 \\ i,l \neq j}}^{n} \frac{1}{\bar{\lambda}_{ij} \bar{\lambda}_{lj}} E[a_{ij} a_{jl} a_{li} a_{kk}] \\ &+ \sum_{\substack{i,l=1 \\ i,l \neq j}}^{n} \frac{1}{\bar{\lambda}_{ik} \bar{\lambda}_{lk}} E[a_{ki} a_{il} a_{lk} a_{jj}] \\ &+ \sum_{\substack{i,l=1 \\ i \neq j \\ l \neq k}}^{n} \frac{1}{\bar{\lambda}_{ij} \bar{\lambda}_{lk}} \{ E[a_{ij} a_{ji} a_{lk} a_{kl}] \\ &- E[a_{ij} a_{ji}] E[a_{lk} a_{kl}] \} \end{aligned} \tag{24}$$

The analysis is called first order perturbation if first-order terms in expansions (20) and (21) are retained and higher-order terms are excluded. It is second order if terms up to second order are kept. However, second-order perturbation is tedious and involves multivariate statistical analysis. Most of the analyses reported in the literature deal with the first-order perturbation.

Problems involving a random symmetric matrix with multiple eigenvalues of the unperturbed matrix have been treated by Scheidt and Purkert (1983). The analysis consists in the formulation of a convergence condition for the perturbation expansions.

Collins (1967) and Collins and Thomson (1969) considered first-order perturbation and derived the eigenvalue and eigenvector statistics of a multi-degree-of-freedom system in terms of the covariance matrix of the system elements. With reference to the eigenvalue eq. (12) they showed that the variations in the mass and stiffness matrices result in the following first order variations in the eigenvalue and eigenvector, respectively:

$$\lambda_i - \bar{\lambda}_i = \sum_{j=1}^{n^2} \frac{\partial \lambda_i}{\partial k_j}(k_j - \bar{k}_j) + \sum_{l=1}^{n^2} \frac{\partial \lambda_i}{\partial m_l}(m_l - \bar{m}_l) + \cdots, \quad (25)$$

$$x_{ri} - \bar{x}_{ri} = \sum_{j=1}^{n^2} \frac{\partial x_{ri}}{\partial k_j}(k_j - \bar{k}_j) + \sum_{l=1}^{n^2} \frac{\partial x_{ri}}{\partial m_l}(m_l - \bar{m}_l) + \cdots \quad (26)$$

If the elements of the mass and stiffness matrices of eq. (12) are random variables with means $\bar{k}_j$ and $\bar{m}_j$ and variances $\sigma_{k_j}^2$ and $\sigma_{m_j}^2$, then the expected eigenvalues and eigenvectors are $\bar{\lambda}_i$ and $\bar{x}_{ri}$, respectively, and the variance of the eigenvalue is

$$\sigma_{\lambda_i}^2 = \mathrm{Var}(\lambda_i) = \sum_{j=1}^{n^2}\sum_{l=1}^{n^2} \frac{\partial \lambda_i}{\partial k_j}\cdot\frac{\partial x_i}{\partial_{kl}}\mathrm{cov}(k_j, k_l)$$
$$+2\sum_{j=1}^{n^2}\sum_{l=1}^{n^2} \frac{\partial \lambda_i}{\partial k_j}\cdot\frac{\partial \lambda_i}{\partial m_l}\mathrm{cov}(k_j, m_l)$$
$$+\sum_{j=1}^{n^2}\sum_{l=1}^{n^2} \frac{\partial \lambda_i}{\partial m_j}\cdot\frac{\partial \lambda_i}{\partial m_l}\mathrm{cov}(m_j, m_l) \quad (27)$$

where

$$\mathrm{cov}(k_j, k_l) = \int_{-\infty}^{\infty}\int (k_j - \bar{k}_j)(k_l - \bar{k}_l)\, p(k_j, k_l)\, dk_j\, dk_l$$
$$= \rho_{jl}\sigma_{k_j} f \sigma_{k_l}. \quad (28)$$

and $p(k_j, k_l)$ is the joint probability density function for K_j and K_l, and ρ_{jl} is the correlation coefficient for k_j and k_l. Expressions for $\mathrm{cov}(k_j, m_l)$ and $\mathrm{cov}(m_j, m_l)$ follow the same format of relation (8).

For a simple chain of equal springs and masses with uncorrelated random masses or with random uncorrelated stiffnesses, Collins and Thomson showed that the standard deviation of the frequency is governed linearly with the standard deviations of the masses and stiffnesses. The results were confirmed by an independent Monte Carlo simulation and were very close to those obtained earlier by Soong and Bogdanoff (1963). However, these linear relationships disappear when correlation exists in the masses or stiffnesses and the eigenvalues are not closely spaced. Recently Pierre (1985) considered two different discrete systems and employed a first-order perturbation to solve for the statistics of their eigenvalues. The first system is a mass-spring chain with random mass and the second is a chain of coupled pendula with random lengths. His results were found identical to those obtained by Soong and Bogdanoff.

Schiff and Bogdanoff (1972a, b) derived an estimator for the standard deviation of a natural frequency in terms of second-order statistical properties of the system parameters. The derivation was based on the mean square approximation developed by Bogdanoff (1965, 1966).

It may be noticed that the statistical properties of random eigenvalues are usually based on the assumption of normal distribution of the system random parameters. However, for correlated non-Gaussian parameters the analysis can be performed in terms of another set of Gaussian random parameters which are evaluated by using the Rosenblatt (1952) transformation. This transformation has extensively been used in reliability analysis when the performance function is nonlinear. This issue will be addressed in detail in section 5.1.

3.3. Random eigenvalues of continuous systems

3.3.1. *Methods of analysis*

Continuous systems may involve uncertainties from two main sources. These are (Boyce and Goodwin 1964):

(*i*) Uncertainties in the geometry and the material properties. The random variation in space dependent parameters results in variations of the differential operators governing the free vibrations of the structure.

(*ii*) Uncertainties in the support mechanism of the system (or the boundary conditions).

The uncertainties of the first class constitute a random field. According to Vanmarcke (1984) the behavior of disordered systems is governed by two general laws. The first is a statement of "conservation of uncertainty" as measured by the product of the variance by the scale of fluctuation of the property in the random field. The scale of fluctuation is taken as the area under the correlation function. This product remains invariant under linear transformation that preserves the mean. The second law states that the degree of disorder of a homogeneous random field, as measured by the direction-dependent bandwidth measure, tends to increase when a random field is subjected to local aggregation.

For the two classes of uncertainties the random eigenvalue has been determined for a limited class of dynamical systems. These include elastic strings and bars (Boyce, 1962; Goodwin and Boyce, 1964) and elastic beams (Boyce and Goodwin 1964; Bliven and Soong, 1969; Hoshiya and Shah, 1971; Shinozuka and Astill, 1972; Vaicaitis 1974). Boyce (1968) outlined a number of techniques for determining the statistics of the eigenvalues of systems described by partial differential equations and boundary conditions involving uncertainty in their parameters. These differential equations are of order $2n$ and usually written in the form

$$\mathscr{L}w(x) = \mathscr{M}w(x), \quad (29)$$

subject to the boundary conditions

$$\Psi_i(w) = 0, \quad i = 1, 2, \ldots, 2n, \quad (30)$$

where $\mathscr{L}$, $\mathscr{M}$, and Ψ_i are differential operators (with respect to the spatial coordinate x) whose coefficients are random variables. $w(x)$ is the displacement of the system at x. Equation (29) involves values of w and its first $2n - 1$ derivatives at the end points of the interval in which solutions are sought. The eigenvalue problem defined by eqs. (29) and (30) is assumed to be self-adjoint and positive definite. The investigation of random eigenvalues has been carried out via analytical or numerical approaches. The numerical methods include the Monte Carlo simulation and stochastic finite element methods. The analytical treatment of the random eigenvalue problem of systems described by eqs. (29) and (30) is outlined by Boyce (1968) and Scheidt and Purkert (1983). The mathematical methods which have been used to determine the statistical moments of eigenvalues are classified according to whether the statistical or nonstatistical part of the analysis is performed first. One class consists of first expressing the solution in terms of the system parameters, without regard to whether these parameters are random or deterministic. Having obtained such a solution, the statistical properties are then determined. According to Keller (1962, 1964) this approach is referred to as "honest" and the solution can be determined by using one of the following techniques (Boyce, 1968; Scheidt and Purkert, 1983):

(*i*) Perturbation methods.
(*ii*) Variational methods.
(*iii*) Asymptotic estimate methods.
(*iv*) Integral equation methods.

The "honest" approach does not provide an exact solution and the above four methods are not suitable for every problem. For example, the variational methods are not suitable for structures with random boundary conditions. Variational methods and integral equation methods are limited because they only lead to statements for the first eigenvalue of the system. Moreover, in order to apply the integral equation methods, very strong conditions for the calculation of the mean of the eigenvalues are required. Under certain conditions pertaining to the spatial correlation function, the asymptotic methods and perturbation techniques lead to the same results. The perturbation methods have less restrictions and are extensively used in the literature.

The approach, on the other hand, is called "dishonest" (Boyce, 1967) if the statistics of the eigenvalue problem are directly determined by performing averaging analysis to the system's partial differential equation and its associated boundary conditions. The statistics can be evaluated by using one of the following methods:

(*i*) Iteration methods.
(*ii*) Hierarchy methods (Haines, 1965, 1967; Adomian, 1983).

The iteration methods are based on some assumptions for the correlation relations in order to solve the averaged integral equations of the random eigenvalue. The hierarchy methods take into consideration further equations so that all statistical functions in question can be calculated.

In a series of papers by Purkert and Scheidt (1977, 1979a, b), a number of theorems pertaining to functionals of weakly correlated processes encountered in the eigenvalue problems, boundary value problems, and initial value problems were established. They treated the stochastic eigenvalue problem for ordinary differential equations with deterministic boundary conditions. The coefficients of the differential operator were independently weakly correlated processes of small correlation spatial length. They showed that as the *correlation length* becomes very small, the eigenvalues and eigenvectors possess Gaussian distributions. This result has recently been confirmed by Boyce and Xia (1983). When the random terms are not small the perturbation method is no longer valid and the second term in the Hermite-Chebychev expansion (Ibrahim, 1985) of the distribution function will not vanish. This implies that the distribution of the eigenvalue will not be normal. Boyce and Xia (1985) obtained the upper bounds for the mean of eigenvalues through a variational characterization of the eigenvalues. For stochastic boundary value problems Linde (1969) and Boyce (1966, 1980) considered a Sturm-Liouville problem with a stochastic nonhomogeneous term. In their recent monograph Sheidt and Purkert (1983) analyzed the moments of the eigenvalues and mode shapes of random matrices and random ordinary differential operators. The calculations of these moments were based on perturbation expansions, and so required the random terms to be appropriately small. Day (1980) developed a number of asymptotic expansions for the random eigenvalues and eigenvectors of continuous systems.

The concept of the Wiener field, which is obtained by replacing the time variable of the Wiener process by a space coordinate, was adopted by Wedig (1976, 1977) as a basic model for randomly distributed loadings or imperfections of continuous structural systems. The solution of such boundary value problems may thus be described by integral equations defined on the Wiener field and thus possesses the Markov properties. Wedig showed that these integral equations may be interpreted in the mean square sense via the boundary and eigenvalue problems of elastic structures with random distributed imperfections or loadings.

3.3.2 Applications

The random eigenvalue of a column under axial force F, shown in Figure 1(f), is described by the second order partial differential equation

$$\frac{\partial^2}{\partial x^2}\mathrm{EI}(x)^2\frac{\partial^2 w(x,t)}{\partial x^2}+F\frac{\partial^2 w(x,t)}{\partial x^2}+A(x)\frac{\partial^2 w(x,t)}{\partial t^2}=0 \tag{31}$$

and the boundary conditions:

$$\begin{aligned}\mathrm{EI}(0)\frac{\partial^2 w(x,t)}{\partial x^2}\Big|_{x=0}-K_1\frac{\partial w(x,t)}{\partial x}\Big|_{x=0}&=0,\\ w(0,t)&=0;\\ \mathrm{EI}(L)\frac{\partial^2 w(x,t)}{\partial x^2}\Big|_{x=L}+K_2\frac{\partial w(x,t)}{\partial x}\Big|_{x=L}&=0,\\ w(L,t)&=0,\end{aligned} \tag{32}$$

where $w(x,t)$ is the lateral displacement at distance x and time t, L is the length of the column, $\mathrm{EI}(x)$ is the flexural stiffness, and $\rho A(x)$ is the column mass per unit length. K_1 and K_2 are the stiffnesses of the end springs. For simple supports $K_1=K_2=0$, and for fixed supports $K_1=K_2=\infty$.

The solution of eq. (31) may be expressed in the form

$$w(x,t)=\sum U_j(X)\exp(i\omega t) \tag{33}$$

Introducing the following substitutions

$$\begin{aligned}X&=x/L,\\ I(X)&=\bar{I}[1+\alpha(X)],\\ A(X)&=\bar{A}[1+a(X)],\\ \mu&=FL^2/\mathrm{E\bar{I}},\\ \lambda&=\rho\bar{A}L^4\omega^2/\mathrm{EI},\end{aligned}$$

where $a(X)$ and $\alpha(X)$ are random variables, eq. (31) and the boundary conditions (32) for mode j become:

$$\{[1+\alpha(X)]U''(X)\}''+\mu U''(X)-\lambda[1+a(X)]U(X)=0, \tag{34}$$

$$\begin{aligned}&[1+\alpha(0)]U''(0)-(K_1L/\mathrm{EI})U'(0)=0, \quad U(0)=0;\\ &[1+\alpha(1)]U''(1)+(K_2L/\mathrm{EI})U'(1)=0, \quad U(1)=0,\end{aligned} \tag{35}$$

where a prime denotes differentiation with respect to X, and subscript j, indicating the mode number in expansion (33), is removed.

Hoshiya and Shah (1971) employed the standard perturbation analysis to determine the expected value and variance of the eigenvalue of the nth mode by using a linearized perturbation technique. They found that the variance of the nth natural frequency is proportional to the variances of the stiffness coefficients at the boundaries and the axial load. This linear relationship implies that the principle of superposition can be applied in a modified form. For the buckling case, ie, when $\lambda = 0$, the eigenvalue problem is reduced to determine the statistics of the buckling eigenvalue (Augusti et al, 1981, 1984). Shinozuka and Astill (1972) considered the case when both K_t and K_2 are random variables.

The natural frequencies of transverse vibration of elastic beams were analyzed by Boyce and Goodwin (1964). They considered the geometry of the cross-section of the beam and its support mechanism as random variables. The statistics of the eigenvalues were determined by using three different techniques. These were the perturbation method, the method of integral equations, and numerical solution. Bliven and Soong (1969) determined the statistics of the natural frequencies of a simply supported elastic beam with random imperfections in the beam stiffness. The beam was modeled as a lumped-parameter model and the properties of the frequencies were derived by using a perturbation method. The stiffness random variation was represented by the relation

$$\mathrm{EI} = \overline{\mathrm{EI}}/[1 + \alpha(x)],$$

where $\overline{\mathrm{EI}}$ is the mean value of the beam stiffness and (x) is a stationary random field process with zero mean and autocorrelation function given by the relation

$$E[\alpha(x_1), \alpha(x_2)] = \sigma^2 \exp(-|x_1 - x_2|/d), \tag{36}$$

where d is a non-negative constant known as the correlation distance.

The standard deviation of the natural frequency of the beam was obtained in the closed form

$$\sigma_\omega(n) = \bar{\omega}(n)\sigma\sqrt{g(n)}, \tag{37}$$

where $\bar{\omega}(n)$ is the nth mode natural frequency of the uniform beam $= n^2\pi^2\sqrt{\overline{\mathrm{EI}}/mL^4}$.

$$g(n) = \int_0^1\int_0^1 \sin^2(n\pi x_1)\sin^2(n\pi x_2) \times \exp[-|x_1 - x_2|/d]\,dx_1\,dx_2,$$

and $\bar{m}$ is the beam mass per unit length.

Bliven and Soong found that when the stiffness fluctuation has zero correlation distance $d = 0$, the natural frequency standard deviation vanishes. The standard deviation was found to reach the value of $\sigma_\omega(n) = 0.5\bar{\omega}(n)\sigma$ when the stiffness variation is perfectly correlated ($d \to \infty$).

The random eigenvalue of a beam-column supported at its ends by a rotary springs was examined by Shinozuka and Astill (1972). The spring supports and axial applied force were treated as random variables. The distribution of material and geometric properties were considered correlated homogeneous random functions. The distributions of these properties were generated by using a Monte Carlo simulation for multivariate and multidimensional random processes developed originally by Shinozuka (1971). The mean and variance of the eigenvalues were determined by using the perturbation analysis and Monte Carlo simulation. It was found that the application of approximate methods, such as the perturbation technique based on exact or an assumed mode shape, causes a considerably greater error for the buckling case than in the vibration case. Furthermore, the perturbation solution for the eigenvalue variance can be approximated reasonably well by using an assumed mode shape in place of the unperturbed mode shape. Vaicaitis (1974) employed a two-variable perturbation expansion procedure to determine the eigenvalues and normal modes of beams with random and/or nonuniform characteristics which do not deviate considerably from the beam mean properties. A Monte Carlo simulation was used to determine the statistical averages of beam eigenvalues and mode shapes. Two cases of random fluctuations of beam cross section were considered. For one particular case there was significant deviation attributed mainly to the fact that gradual change in the beam stiffness was permitted. In this case the beam is "soft" at one end and "hard" at the other end.

Hart and Collins (1970), Collins et al (1971), and Hasselman and Hart (1971, 1972) developed a numerical method for computing the variance of structural dynamic mode properties by using component mode synthesis which was formulated originally by Hurty (1964, 1965). Numerical solution provided reasonable results for lower modes even when a relatively small percentage of available component modes is used. Hart (1973) developed a general algorithm for calculating the statistics of the natural frequencies and mode shapes of structures acted upon by an external static loading. This type of problems involves considerable calculations due to the fact that the proportionate axial load in each member of the structure is dependent upon the structural parameters which are random variables. For the two-bar truss shown in Figure 3 Hart determined the first natural frequency's mean and standard deviation. The influence of the static load on the statistics of the first natural frequency is shown in Figure 4. It is seen that the standard deviation of the natural frequency increases with the axial load. The implication of this increase was further demonstrated in Figure 5 by using normal probability density function. The observed flattening shape of the probability density function with increased compressive loading shows a marked decrease in confidence with the magnitude of loading.

The random eigenvalue problem of disordered periodic beam was considered by Lin and Yang (1974). They used a first-order perturbation procedure to derive expressions for the variances of natural frequencies and normal modes for different cases of random bending stiffness and span lengths. The natural frequencies were found to be more sensitive to span variations than to bending stiffness fluctuation. It was shown that if the random variations in bending stiffness for different spans are uncorrelated then there is no effect on the statistics of the eigenvalues. The effect exists only when there is a correlation in the random variation in the individual spans. For a random variation in the span lengths it was shown that the variance of the natural frequency is inversely proportional to the number of

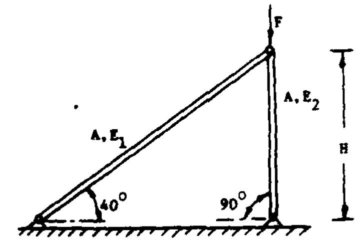

FIG. 3. Two bar truss (Hart, 1973).

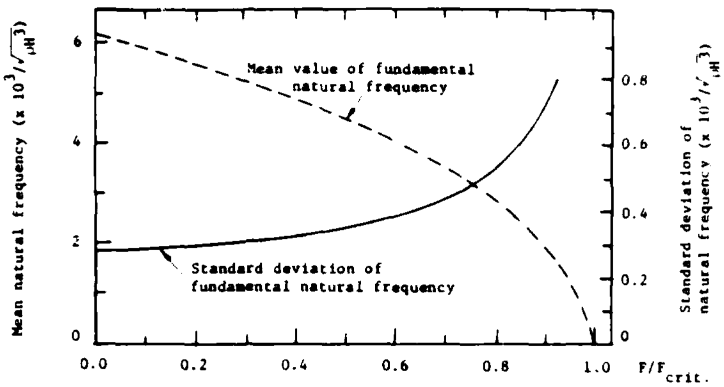

FIG 4 Variation in fundamental natural frequency statistics with applied load (Hart, 1973)

spans. The random imperfections in spatial periodicity also resulted in variability in the normal modes. However, due to the arbitrary choice of modal amplitude the variance of the normal mode was not a unique function of space.

The statistics of natural frequencies of mistuned blades of a circumferentially closed packet of turbomachinery were examined by Ewins (1973) and Huang (1982). When the bladed disk assembly is tuned and all the blades are identical the natural frequencies and mode shapes are quite regular. Each mode may be described as having a particular number of nodal diameters, just as for an unbladed disk. However, when the blades are mistuned to a degree which might well exist in service, the mode shapes and frequencies become irregular. In this case the natural frequencies of the individual blades can be randomly different from one another. This problem is belonging to systems with periodic random parameters and such systems are modeled by a stiff ring supported by transverse springs with randomly distributed stiffness and mass parameters. Huang adopted an exponential form for the auto- and cross-correlation function of the random structural parameters. This form was originally assumed by Hoshiya and Shah (1971). The analysis of Huang was based on a spectral analysis method. He found that the mean of the natural frequency of the structure with random parameters is identical to the natural frequency of the structure with homogeneous parameters. The standard deviation of the natural frequency of mth mode was expressed in terms of the $(2m)$th Fourier coefficients of the random parameters and was represented as a vector sum of their standard deviations. While the normal modes of a homogeneous structure have a shape of harmonic waves with symmetrically located nodal diameters, for a structure with random parameters the mode shapes are complicated and the nodal diameters are located unsymmetrically. It was shown that these modes have a shape involving not only the main harmonic, but also an infinite number of harmonics. In addition, these random normal modes are orthogonal despite their complicated form. Another important feature was that the phase angles of random normal modes are not arbitrary (as in the case of a homogeneous structure) but are random variables independent of the initial conditions.

Recently, the stochastic finite element method has been used by Nakagiri et al (1985) to determine the uncertain eigenvalue of fiber reinforced plastic (FRB) laminated plates. These composite materials usually exhibit anisotropy and heterogeneity. The elastic constants may fluctuate around the mean values due to some slackness during the manufacturing process which causes spatial distribution of the volume fraction. In addition, another parameter known as the stacking sequence is usually used as a major design parameter of the FRB laminated plates

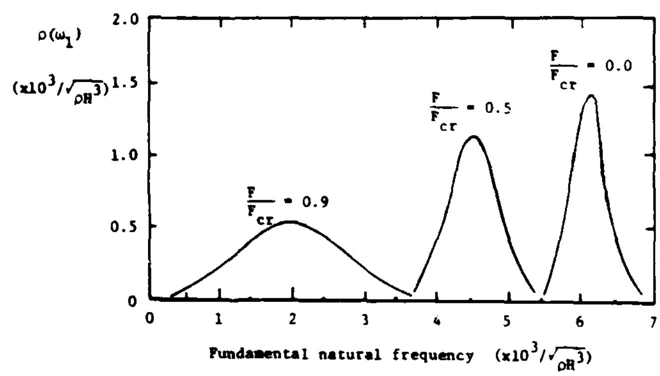

FIG 5 Probability density function variation with applied load (Hart, 1973)

The stacking sequence (Vinson and Chou, 1975) implies a group of parameters such as elastic constants, layer number, fiber orientation, and layer thickness. Nakagiri et al considered the effect of the fluctuation of the overall stiffness due to uncertain variation of the stacking sequence. The uncertain stacking sequence was treated as a set of random variables for the case of simply-supported graphite/epoxy plates. It was found that the eigenvalue is more sensitive to the standard deviation of the fiber orientation, and the effect of the stacking sequence is more pronounced for the rectangular plate than for the square one.

3.3.3. Normal mode localization

Periodic structures with slight variations in their periodicity can exhibit a phenomenon known as normal mode localization. This phenomenon takes place in a manner that vibrational energy injected into the structure by an external source cannot propagate to arbitrarily large distances, but is instead substantially confined to a region close to the source. Hodges (1982) called this phenomenon as "Anderson localization" due to Anderson (1958) who discovered mode localization in solid state physics in an attempt to understand electrical conduction processes in disordered solids. The effect of irregularities has a similar effect to damping in that it limits the propagation of vibrations at large distances from the excitation source. This effect is mainly caused by confinement of the energy close to the source, not by dissipation of the energy as it propagates out.

The phenomenon of mode localization can be well understood by using the coupled pendula example [Fig. 1(b)] which was adopted by Hodges (1982). Hodges provided an excellent explanation of mode localization: If all pendula are identical so that their individual natural frequencies are precisely equal, then the normal modes of oscillation when these pendula are coupled together extend throughout the system, the amplitude of oscillation of each pendulum varies sinusoidally with its position in space. On the other hand, if the natural frequency of oscillation varies from pendulum to pendulum in some kind of random fashion, then in the limit of zero coupling, normal modes consist of oscillation of individual pendula at frequencies equal to their natural frequencies. For small coupling the normal modes remain localized close to individual pendula and the normal mode frequencies approximate the natural frequencies of the pendula. Thus for a particular mode one pendulum is oscillating close to its natural frequency with a large motion. Its nearest neighbors, unlike the ordered system, are driven off resonance, and since the coupling is weak they respond with much smaller amplitudes. These neighbors in turn drive pendula further out and so on, but at each step the driving force and response tend to diminish in magnitude. A typical mode shape diagram is shown in Figure 6. In terms of forced oscillations, mode localization implies localization of the response in the vicinity of the excitation point.

The effect of mode localization was examined by Bendiksen (1984a, b) and Valero and Bendiksen (1985) who showed that irregularities in shrouded blades of jet engine rotors can result in a stabilizing mechanism which is closely connected with the phenomenon of mode localization. In the framework of localization theory, the stabilizing mechanism is explained based on the fact that the original monochromatic flutter wave is scattered into waves of different and more stable wavelengths and inter-blades phase angles. While the effect of mistuning between turbomachinery blades is favorable in flutter (see also Kaza and Kielb, 1982) it can lead to an increase in amplitude on at least one blade in forced vibration situation as will be shown in section 4.1.2.

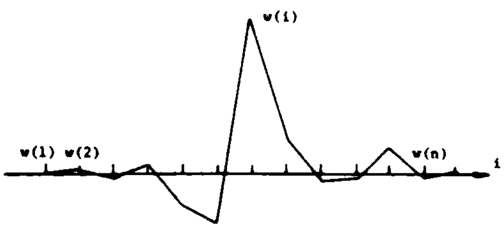

FIG. 6. Schematic diagram of the site amplitude $w(i)$ for a localized normal mode (Hodges, 1982).

For periodic multispan beams Miles (1956) showed that the natural frequencies are clustered in an infinite number of groups, or bands, with n frequencies in each band, where n is the number of spans. If a torsional spring is placed at the $n-1$ intermediate support location, then the width of the frequency bands diminishes as the spring constant k increases. In the limit as the spring constant goes to infinity, the beam becomes clamped at the constraint locations and the width of the frequency bands is reduced to zero. Pierre et al (1986) established an internal coupling parameter which is equivalent to the inverse of the torsional spring constant $1/k_\theta$. For $k_\theta = 0$ the spans are fully coupled. For large values of the spring constant and irregular spacing between supports, a multispan beam can be regarded as a disordered chain of weakly coupled subsystems. Pierre (1985) and Pierre and Dowell (1986) developed a theoretical analysis for the mode localization phenomenon and indicated that the free modes of vibration are susceptible to becoming localized and the natural frequencies of the multispan beam are in bands of small width if the spring constant is large. They proposed a general criterion stating that localization may occur if the width of the frequency band of the ordered system is of the order of, or smaller than, the spread in individual natural frequencies of the disordered component systems.

Pierre et al (1986) determined the free modes of transverse vibration of a disordered two-span beam by using a Rayleigh Ritz formulation with the constraint conditions enforced by means of Lagrange multipliers. They developed a modified perturbation method to analyze the localized modes. Figure 7 shows the mode shapes for tuned and mistuned beam for torsional spring parameter $c = 1000$, where $c = 2lk_\theta/EI$, l is the length of the beam and E and I are the Young's modulus and area moment of inertia of the beam, respectively. For a mistuned beam it is seen that mode localization is manifested in that the peak deflection is much larger in one span than in the other one.

4. RANDOM RESPONSE

The response of linear structural components with uncertain parameters can be determined by using standard techniques such as the impulse and frequency response functions and perturbation methods, or numerical approaches such as stochastic finite methods and Monte Carlo simulation. The results reported in the literature will be reviewed in the next two subsections.

4.1. Standard techniques

4.1.1. Simple structural components

In an attempt to examine certain aspects of the dynamical response of statistically defined systems, Chenea and Bogdanoff (1958) and Bogdanoff and Chenea (1961) considered a linear single degree-of-freedom system with independent discrete distributions in the mass, damping, and stiffness coefficients. The analysis of Bogdanoff and Chenea was based on a partial

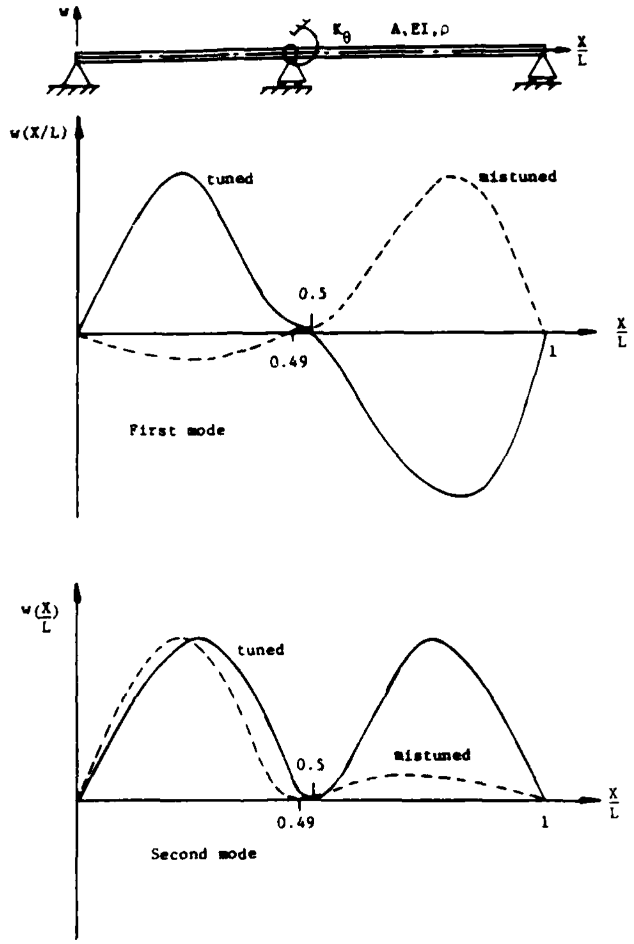

FIG 7 First two mode shapes for tuned (—) and mistuned (- - -) two-span beam $\Delta l = 0.01$, $c = 1000$ (Pierre et al. 1986)

differential equation for the response joint density function (Kozin, 1961). This equation is known as the Liouville equation (Soong, 1973) and is identical to the Fokker–Planck equation with zero diffusion coefficient. Small dispersions in the system parameters were found to result in a considerable dispersion in the frequency response. The impulse response of the same system was determined by using the perturbation method by Chen and Soroka (1973). They considered a linear system described by the differential equation

$$\ddot{X} + 2\zeta\omega_n\dot{X} + \omega_n^2 X = f(t), \tag{38}$$

where the natural frequency is considered random $\omega_n = \bar{\omega}_n + \epsilon\tilde{\omega}_n$, $\bar{\omega}_n$ is a constant and the perturbation $\tilde{\omega}_n$ is a random variable with zero mean, ϵ is a small perturbational parameter and $f(t)$ is an impulse excitation. Chen and Soroka derived the solution of equation (38) by using a perturbational technique. Figure 8 shows a sample of the time history response curves for damping ratio $\zeta = 0.05$. It is seen that both the mean and standard deviation of the response amplitude are nonstationary and the standard deviation is 90 degrees out of phase from the mean. The amplitude of the response standard deviation increases with time, and gradually dampens out after it reaches a certain level. For systems with a very high natural frequency, the uncertainty in the natural frequency was found to have very small effect on the response statistics. However, the effect is significant if the natural frequency is low. As the damping factor decreases, the dispersion from the mean became substantial.

The response of multi-degree-of-freedom systems with random parameters was examined by Soong and Bogdanoff (1963, 1964) and Chen and Soroka (1974). Soong and Bogdanoff determined the statistics of the impulse admittance and frequency response of a linear chain with random masses distributed in a small range. Chen and Soroka developed a method which relates the statistics of response parameters to the statistics of the system eigenvalues and eigenvectors. They showed

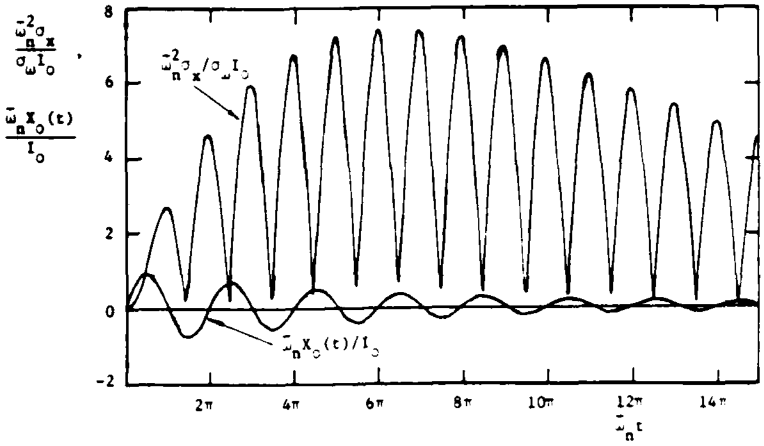

FIG. 8. Mean and standard deviation of impulse function $I_0\delta(t)$ for $\zeta = 0.05$ (Chen and Soroka, 1973)

that the response statistics of disordered systems are higher than those of purely deterministic systems. The instantaneous transient response statistics of an undamped linear multi-degree-of-freedom system, with random stiffness, subjected to arbitrary but deterministic forcing functions was investigated by Prasthofer and Beadle (1975). For the case of an impulsive excitation, they found that the growth of the response uncertainty is exponential. As the standard deviation of the stiffness increases the response mean square increases rapidly with time. For a multi-degree-of-freedom system the response decay rate decreases as the correlation coefficient between the stiffness elements increases. The influence of damping uncertainty on the frequency response of a linear multi-degree-of-freedom system was examined by Caravani and Thomson (1973). They determined the mean and standard deviation of the response by using a linearization technique and a Monte Carlo simulation. They pointed out that an accurate estimate of the damping coefficients for lightly damped systems, in the neighborhood of a natural frequency, is very important in determining the mean and standard deviation of the system response.

The means and variances of the frequency response functions of a disordered periodic beam were studied by Yang and Lin (1975). Two types of excitation were considered. These were a concentrated force (or moment) and a distributed force convected at a constant velocity. It was shown that the magnitude of the statistical average of the frequency response function can be considerably greater than the value computed without taking into account the random variation in the span lengths. In the neighborhood of resonance frequencies the standard deviation of the frequency response function becomes quite large, indicating greater uncertainty in such regions. In the case of convected loading the use of a perfect periodic model cannot account for the response in certain vibration modes while these modes can be induces in a disordered periodic beam.

4.1.2 Mistuned bladed disks

It has been indicated in section 3.3.3 that the mistuning of turbomachinery bladed disks could have beneficial effect in the case of blade flutter. However, the effect is reversed in the case of forced vibration (Whitehead, 1966; Ewins, 1969; Stange and MacBain, 1983). It is believed that Tobias and Arnold (1957) have made the first attempt to understand the effect of blade mistuning on the response of stationary waves (modes traveling opposite to the direction of disk rotation so as to appear stationary to a fixed observer). An interesting and important structural phenomenon resulting from mistuning is the splitting of a bladed disk's diametral modes of vibration (modes having 1, 2, ..., n nodal diameters) into "twin" or "dual" modes. The presence of dual modes characteristics in a bladed disk can significantly affect either or both of its aeroelastic stability and resonant response characteristics. Whitehead (1966) showed that there is an upper limit to the effect of mistuning and is given approximately by the factor of $(1 + \sqrt{N})/2$, where N is the number of blades in the row. This upper limit was obtained under the assumption that the damping forces are substantially less than the aerodynamic coupling forces. Jay and Burns (1984) conducted a series of rotating and unrotating test to identify mistuning, damping, split factors for various diametral patterns and dynamic strains signatures from resonant tests of a shrouded fan blade disk. System mode responses to various distortion patterns were found to involve standing waves and traveling waves.

A number of lumped mass models of bladed disk assemblies have also been used to study the effects of various blade mistune distributions on the maximum resonant response of the blades (Wagner, 1967; Dye and Henry, 1969; El-Bayoumy and Srinivasan, 1975; MacBain and Whaley, 1984). The nature of the lumped parameter models used in these studies is such that individual blade response was studied in terms of single- or two-degree-of-freedom blade modes whose vibratory response was altered by mechanical coupling via the disk portion of the models. Hence, the basis or starting point for these lumped mass models was the individual blade resonant frequencies. The results showed how much greater or smaller the individual blade response would be for a set of mistuned blades compared to the response of a tuned set of blades. For a given mistuning distribution and excitation, the response of the mistuned set of blades was found to be many times greater or smaller (depending upon the disk circumferential location) than the response of tuned blades. Ewins and Han (1984) conducted a sereis of case studies to examine the influence of various parameters on the resonant response levels of individual blades on a disk. They found, for the case of a 33-bladed disk, that mistuning always increases the highest resonant response level from that experienced by a tuned system but while some blades are more highly stressed, others suffered a lower level and the mean value is roughly constant. It was also concluded that the highest response is always experienced by a blade of extreme mistune.

Analytical investigations of mistuning fall into three categories (Griffin and Hoosac, 1984): deterministic (Dye and Henery, 1969; Ewins, 1973; El-Bayoumy and Srinivasan, 1975), statistical (Huang, 1982), and combined and statistical approaches (Sogliero and Srinivasan, 1980; Kazan and Kielb, 1982; Muszynska et al, 1981). Basu and Griffin (1986) used a deterministic/statistical approach and developed a model involving aerodynamic and structural interaction for studying the effect of mistuning on bladed disk vibration. They found that the mistuning effect significantly decreases as the density of the gas flowing through the turbine is decreased. On the other hand the effect was found to increase linearly with the number of blades on the disk.

4.2. Stochastic finite element methods

Recent developments of stochastic finite element methods have promoted the analysis of structural dynamics with uncertain parameters. These techniques could be broadly classified into statistical and nonstatistical (Liu et al, 1985b). The statistical approach is based on numerical simulation via Monte Carlo, stratified sampling, and Latin Hypercube sampling. A comparative discussion of these techniques is provided by Mckay et al (1979). All simulation methods require that the joint probability distributions of the excitation and random parameters be available. However, these distributions are seldom to be available. Instead, one usually may assume that the input random variables are mutually independent and Gaussian. If these random inputs are non-Gaussian distributed, one may use the Rosenblatt (1952) transformation to transform non-Gaussian correlated variables to Gaussian uncorrelated ones. Nonstatistical approaches include numerical integration (Liu et al, 1985a, 1986), second moment analysis (Cornell 1972) and stochastic finite element methods (Nakagiri et al, 1984; Liu et al, 1985a, b; Hisada and Nakagiri, 1982; Hisada et al, 1983). A major advantage of these methods is that the multivariate distribution functions are not required but only the first two moments. Recently several stochastic finite element approaches have been developed by Vanmarcke and Grigoriu (1983), Liu et al (1985a, b), Dias and Nagtegaal (1985), and Mori and Ukai (1986). Linear problems in structural mechanics with uncertain parameters have been solved by second-moment analysis (Contreras, 1980; Nakagiri et al, 1984).

Astill et al (1972) examined the problem of impact loading of structures with random geometric and material properties. Their approach is a combination of finite element method and a Monte Carlo simulation. For the case of an axisymmetric concrete cylinder they assumed spatial distributions of Young's modulus and density for each realization of the test cylinder. Each test cylinder was subjected to the same axial impact loading. The algorithm gave a sample of 100 maximum stress intensities from which the sample mean and standard deviation were computed. For a certain intermediate location of the test cylinder it was found that the axial stress is always different from the corresponding stress in a uniform cylinder.

Vanmarcke and Grigoriu (1983) developed a stochastic finite element analysis for solving first- and second-order statistics of the deflection of structural members whose properties vary randomly along their axis. The covariance matrix of these element averages was obtained by simple algebraic operations on the variance function which in turn depends primarily on the scale fluctuation. Although this approach was used to determine the free end deflection of elastic members, Vanmarcke and Grigoriu claimed that it can be applied to determine the response statistics to external dynamic excitations even when the statistical information about spatial variation of material properties is limited. Recently Liu et al (1985a, b, 1986) developed a number of probabilistic finite elements methods for nonlinear structural dynamics. These methods are applicable for correlated and uncorrelated discrete random variables. For elastic-plastic bar with end load, they (Liu et al, 1985b) computed the mean and variance of the displacement at the free end by using the probabilistic finite element and Monte Carlo simulation. The solutions of the two methods compared very well, however, the probabilistic finite element approach required much less computer time than the Monte Carlo simulation. Unfortunately these results did not reflect the influence of parameter uncertainties on the random response.

The dynamic response of random parametered structures under random excitation has been examined in a number of studies by Paez and his group (Chang, 1985; Bennett, 1985; Branstetter and Paez, 1986). These studies provide computer programs in a finite element framework to establish response moments on a step-by-step basis. These numerical algorithms evaluate the system response characteristics at an advance time by using the statistical information about response structural characteristics, and excitation at a previous time. Branstetter and Paez (1986) examined their computer programs for several damped single degree-of-freedom systems and several undamped two degree-of-freedom systems. The responses of these systems to white noise excitations were obtained for random stiffness parameters while all other system parameters were fixed. It was shown that single-degree-of-freedom systems display greater response variance than systems with deterministic stiffness. The difference in response variance is found to be small when the structure initial conditions are zero. The difference increases and assumes an oscillatory character when the initial conditions depart from zero. The mean response is nonzero for structures with nonzero initial conditions and/or nonzero mean load.

Bennett (1985) considered uncertainties in the stiffness and damping of single- and multi-degree-of-freedom structural systems. The random variables of the system parameters were replaced by a deterministic component (equal to the mean of the original random variable) and a random component with zero mean and with variance equal to that of the original random variable. For a single-degree-of-freedom system Bennett found that the value of the peak response increases monotonically with the standard deviation of the stiffness. For lightly damped systems which do not have zero mean, the effects of the damping randomness on the response are less pronounced than those obtained when the stiffness was random. The standard deviation of the response at the time of peak response was found to increase with the correlation between the stiffness and damping.

5. DESIGN OPTIMIZATION AND RELIABILITY

5.1. Reliability-based design

The study of response of disordered systems is very important for design purposes. These responses can help the designer to establish acceptable tolerances on system components. The main problem which concerns the designer is how to govern the fluctuations of the system parameters for safe operations. For example when the values of the elastic displacement of a structure are significant, the problem is to set up an optimum standard of manufacturing the structure components

Here the permissible fluctuation in the structure parameters becomes a restrictive condition. Generally, design optimization of structures subject to reliability requirements is regarded as the ultimate goal of any design procedure. The basic approach in most reliability-based structural optimization is to impose a set of constraints on overall system reliability or probability of failure (Ang and Tang, 1975, 1984; Moses, 1973; Parmi and Cohn, 1978). Another approach suggests to minimize the total cost or weight for a specified allowable overall failure probability (Frangopol, 1984a; Hilton, 1960; Moses and Kinser, 1967).

One of the main objectives of the designer is to establish an acceptable probability of failure. Several procedures for the analysis of probability of failure of structures have been developed (Frangopol, 1984a, b, 1985a, b; Frangopol and Nakib, 1986; Kam, 1986; Moses, 1974; Moses and Kinser, 1967; Moses and Stevenson, 1970). In order to establish a probability of failure consider a structural system subjected to a number of external loads. The structure is said to survive if the applied stress σ_D in the built-in section due to all external loads is smaller than an ultimate limit stress σ

$$\sigma_d \leq \sigma \tag{39}$$

The equality sign in eq. (39) corresponds to the state of the collapse threshold of the structure. In general, for each limit state, it is possible to establish a critical inequality similar to eq (39) and identify, in the space of the relevant parameters, a "safe region $\mathscr{S}$ (or success region)", where the critical inequality holds, and unsafe region $\mathscr{F}$ (or failure region), where it does not hold. These regions are shown in Figure 9(a) according to Augusti et al (1984), where

$$S = \sigma_D \quad \text{and} \quad R = \sigma \tag{40}$$

In most cases the applied load $S = S(t)$ is a random process, *while the resistance R, which is calculated or measured, is a* random variable. For each actual structure, the resistance takes up a constant value R_0, although uncertain, and the representative point (R, S) moves in time up and down the solid line in Figure 9(a). Figure 9(b) shows a possible realization of the random loading process $S(t)$. The limit state is attained when $S(t)$ violates the threshold R_0. The time to failure t_{fail} can be used as a measure of the structure reliability. Alternatively, one can consider a time interval $(0, t)$ and then check the critical inequality in the worst possible condition. This can be formulated in probabilistic terms by stating that the probability of failure P_{fail} and the complementary probability of success (reliability) $r = P_{suc}$ coincide respectively with the probability that the critical inequality is violated at least once in the interval $(0, t)$. In space random variables, the probability that a point Q, which represents the significant input and system parameters, falls either in the failure region $\mathscr{F}$ or in the success region $\mathscr{S}$. Symbolically, these states are

$$P_{fail} = \text{Prob}[\,Q \subset \mathscr{F}\,], \quad \text{and} \quad P_{suc} = \text{Prob}[\,Q \subset \mathscr{S}\,] \tag{41}$$

Among the basic formulations of reliability calculations are the level 1 and level 2 approaches. In level 1 one simply applies the characteristic safety factor $\gamma = R/S$. In level 2 one needs to determine a reliability index β which measures, in units of standard deviation, the distance between the average point and the boundary of failure region. This means that larger values of β imply smaller probability of failure. The probability of failure is found (August et al, 1984) to be less dependent on the coefficient fo variation $\delta_s = \sigma(S)/E[S]$ of external excitation of the corresponding coefficient of resistance $\delta_R = \sigma(R)/E[R]$ is relatively large, where $\delta(S)$ and $\delta(R)$ are the standard deviations of the applied stress and the resisting stress, respectively. Level 2 reliability methods include the estimation of the minimum distance β which is regarded as a safety measure of the smallest distance of the surface separating the safe and unsafe regions from the origin in the space of random variables Q.

Generally the level of performance of any structural system depends on the properties of the system. Thus, it is possible to characterize a function $g(Q)$ known as the performance function such that

$$\begin{aligned} g(Q) > 0 &= \text{the safe state, and} \\ g(Q) < 0 &= \text{the failure state} \end{aligned} \tag{42}$$

Geometrically the limit-state equation $g(Q) = 0$ is an n-dimensional surface that is referred to as the "failure surface." The performance function could be linear or nonlinear. The evaluation of the exact probability of safety for nonlinar performance function is generally involved and the determination of the required reliability index would not be as simple as in the linear *performance function (Ang and Tang, 1984). For correlated* non-Gaussian random variables, the safety index may be evaluated in terms of another set of independent Gaussian variables through the Rosenblatt transformation (1952). Hohenbichler and Rackwitz (1981) developed an algorithm to determine the safety index by using the Rosenblatt transformation.

Tanaka and Onishi (1980) developed a method of regulating the deviations of random parameters and derived a restrictive conditional formula in terms of the permissible displacement (or natural frequency) fluctuation. The method is based on the linear deviation analysis with partial differential analysis together with sequential linear programming (SLP) for a number of restrictive conditions. Tanaka et al (1982) treated the optimization problem of the allowable variance of random parameters by using a perturbation method and Monte Carlo simulation. They computed the deviation of the steady state response of

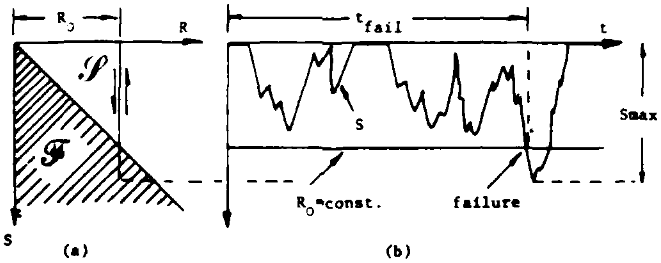

FIG. 9 (a) Safe and unsafe regions for (b) realization of $S(t)$ (Augusti et al, 1984) structural systems involving random parameters with the purpose of regulating the deviation of the random parameters when the deviation of the response is specified.

The techniques of mathematical programming have been extensively used to minimum-weight design of deterministic structures subject to constraints on stresses, displacements, dynamic response, and stiffness (Moses and Kinser, 1967); Moses and Stevenson, 1970; Moses 1973, 1974). The stochastic programming of dynamically loaded structures was developed originally by Charnes and Cooper (1959) and is well documented by Rao (1979). The basic idea of this method is to convert the probabilistic problem into an equivalent deterministic one by minimizing the expected value of the objective function subject to certain constraints. Davidson et al (1977) applied the mathematical programming techniques for optimization of structures subject to reliability requirements. Their work resulted in a general formulation of the minimum-weight optimization for indeterminate structures with random parameters. Jozwiak (1985, 1986) applied the stochastic programming based on expected values in the problem of optimization of dynamically loaded structures with random parameters. The mean values of joint displacements and their derivatives were determined by solving the equations of motion of the structure under the constraints of minimum weight.

Other techniques such as multi-objective optimization methods (Rao, 1982, 1984; and Schy and Giesy, 1981) and fuzzy sets (Zadeh 1965, 1973; Brown, 1980; Brown et al, 1983) have been employed to the design of simple structural elements and aeroplane control systems involving uncertain parameters and stochastic processes. The basic idea in multi-objective design is to include all important objectives in a vector objective function. The problem of optimizing structural systems involving dynamic restrictions, random parameters, stochastic processes, and multi-objectives has been outlined by Rao (1982). By considering the imprecision of the restricitons such as use, design, construction, one may assume that, some of the constraints and goals for each of the objective functions are fuzzy or imprecise in multi-objective fuzzy optimization design. If the corresponding expectation functions for objective and admission for constraint are introduced it is possible to quantify the fuzzy objectives and constraints. Guangwu and Suming (1986) employed the concept of multi-objective fuzzy design optimization for ship grillage structures.

5.2. Design sensitivity to parameter variations

5.2.1. Basic concept of sensitivity analysis

The sensitivity of a structural system to variations of its parameters is one of the basic aspects in the design of structures. The sensitivity theory is a mathematical problem which investigates the change in the system behavior due to parameter variations. The basic concepts of sensitivity theory are well documented in several books, see, eg, Frank (1978). The sensitivity problem can be stated by defining the actual system parameters represented by the vector $\boldsymbol{\alpha} = \{\alpha_1, \alpha_2, \ldots, \alpha_n\}^T$ which differ from the nominal value $\boldsymbol{\alpha}_0$ by a deviation $\Delta\boldsymbol{\alpha}$. These parameters are related to a certain vector $\mathbf{x}$ which characterizes the dynamic behavior of the system. In structural dynamics the vector $\mathbf{x}$ can be taken as the system response vector. The mathematical model of the system response can be written in terms of the first order differential equations

$$\{\dot{\mathbf{x}}\} = \{f(\mathbf{x}, \boldsymbol{\alpha}, t, \mathbf{F})\}, \quad \{\mathbf{x}(t_0)\} = \{\mathbf{x}^0\}, \tag{43}$$

where $\mathbf{F}$ represents the input vector.

Generally a unique relationship between the parameter vector and the response vector is assumed. However, this is not possible in real problems because they cannot be identified exactly. It is a common practice in sensitivity theory to define a *sensitivity function* $\mathbf{S}$ which relates the elements of the set of the parameter deviations $\Delta\boldsymbol{\alpha}$ to the elements of the set of the parameter-induces errors of the system function $\Delta\mathbf{x}$ by the linear relationship

$$\Delta\mathbf{x} = \mathbf{S}(\boldsymbol{\alpha}_0)\,\Delta\boldsymbol{\alpha} \tag{44}$$

This relation is a linear approximation of eq. (43) and is valid only for small parameter variations, ie, $\|\Delta\boldsymbol{\alpha}\| \ll \|\boldsymbol{\alpha}_0\|$. $\mathbf{S}$ is a matrix function known as the trajectory sensitivity matrix which can be established either by a Taylor series expansion or by partial differentiation of the state equation with respect to the system nominal parameters.

When the system is random, the function $\mathbf{S}$ is referred to as stochastic sensitivity function. Szopa (1984) developed equations for stochastic sensitivity functions to determine the influence of changes in the initial conditions on the response. These functions were aplied to a stochastic nonlinear oscillator with a limit cycle. It was found that the mean values and the variances of the stochastic sensitivity functions converge to zero. Szopa (1986) used the sensitivity theory to investigate the influence of changes in system parameters on solutions of dynamical systems. The statistics of the stochastic sensitivity functions were found to have finite values when the response exhibit chaotic characteristics.

5.2.2. Design derivatives

Consider the eigenvalue problem given by eq. (15). It will be assumed that the eigenvalues λ_i of the system matrix $\mathbf{A}$ are distinct. The elements of $\mathbf{A}$ are function of the system parameters $\boldsymbol{\alpha}$. The sensitivity of the free vibration the structure as well as the sensitivity of its relative stability with respect to any parameter of $\mathbf{A}$ can be characterized by the sensitivity of the eigenvalues λ_i with respect to the parameters.

The partial derivative

$$S_\alpha^\lambda = \partial\lambda_i/\partial\alpha_j|_{\alpha_0} \tag{45}$$

is known as the eigenvalue sensitivity or the eigenvalue derivative.

The eigenvector sensitivity (or derivative) of the system matrix is also given by the partial differentiation

$$S_\alpha^x = \partial x_i/\partial\alpha_j|_{\alpha_0} \tag{46}$$

The eigenvalue sensitivity has been examined mathematically by McCalley (1960), Mantey (1968), and Reddy (1969). Frank (1978) developed a number of formulae to determine the eigenvalue sensitivity. The derivatives of the eigenvalues and eigenvectors are very helpful in design optimization of structures under dynamic response restrictions. They have been extensively used in studying vibratory systems with symmetric mass, damping, and stiffness properties (Fox and Kapoor, 1968; Kiefling, 1970) and in nonself-adjoint systems (Rogers, 1970; Plaut and Huseyin, 1973; Rudisill, 1974). For distributed parameter systems, design derivatives of eigenvalues were first encountered in optimization studies by Haug and Rousselet (1980) and Reiss (1986). Reiss used a relatively simple method to determine explicit results for the design derivatives of eigenvalues and eigenvectors. He expressed self-adjoint operator equations in terms of integral form by using Green's function (Reiss, 1983). Recently Kuo and Wada (1986) developed the nonlinear sensitivity coefficients and correction terms, usually eliminated during the linearization process in the Taylor expansion. The nonlinear correction terms were found significant in problems involving many finite element analyses where the size of the eigenmatrix is of order 10E06 and the difference in the eigenvectors may be of order 0.01.

Lund (1979) developed a method to calculate the sensitivity of critical speeds of a conservative rotor to changes in the design using a state vector–transfer matrix formulation. Fritzen and Nordman (1983) have developed the eigenvalue and eigenvector derivatives for general vibratory system (with nonsymmetric system matrices) and used them in evaluating stability behavior due to parameter changes in rotor dynamics. Palazzolo et al (1983) presented a generalized receptance approach for eigensolution reanalysis of rotor dynamic systems. Their method has the advantage of accomodating system modificaion of arbitrary magnitude and treats the modifications simultaneously. Rajan et al (1986) developed the eigenvalue derivatives for the damped natural frequencies of whirl of general linear rotor systems modeled by finite element discretization. For underdamped modes, the eigenvalue derivative is complex. The real part represents the damping sensitivity coefficient while the imaginary part gives the whirl speed sensitivity. Rajan et al showed that the combination of design parameter and whirl frequency sensitivity coefficients may be used to evaluate the damped critical speed sensitivity coefficients.

In reliability-based design optimization it is useful to examine the results to sensitivity analysis in order to determine the influence of the statistical parameters on the optimum solutions. The essential objectives of sensitivity analysis of any system is to establish a measure of the way each response quantity varies with changes in the parameters that define the system (Grierson, 1983). Recently, Arora and Haug (1979) and Frangopol (1985a) have developed a technique for determining the reliability-based optimum design sensitivity of redundant ductile structures. Frangopol investigated the sensitivity of an optimum design to changes in the statistical parameters that define the loading and resistance strength of the structure.

6. EXPERIMENTAL RESULTS

The first attempt to measure the statistics of structural modal frequencies is believed to be made by Mok and Murray (1965). They carried out a series of free flexural vibration tests of a bar with a stepped profile and a maximum variation in the cross section of 50%. The predicted and measured results were found very close. Twenty years later, Paez et al (1985, 1986) conducted a series of experimental investigations to measure the random variation of the natural frequency of a cantilever beam. One end of the beam was mounted on a fixture through a screw and two washers, and the other end carries a concentrated mass. The torque in the screw establishes a preload which governs the stiffness of the beam at the fixture. Paez et al conducted 19 experiments each with different values of base torque and stiffness. The variation of the fundamental frequency with the base stiffness was obtained experimentally and numerically (by using a finite element program). It was shown that the standard deviation of modal frequency increases with the mean modal frequency. Another interesting feature observed by Paez et al was that the magnitude of random variation in modal frequency can become greater than the spacing between modal frequencies as the frequency order increases.

The phenomenon of normal mode localization was first examined experimentally by Hodges and Woodhouse (1983). Their model was a thin high-tensile steel wire stretched between two supports. Seven small lead weights were securely attached initially at equal lengths and then were shifted slightly to give a controlled amount of irregularity. Under a step function force with repeatable amplitude the string motion was observed and measurements were taken for the energy transmission from end to end of the string. Levels of energy attenuation in the disordered case were found in some cases quite large (99%) with only 2.4% standard deviation in the mass positions.

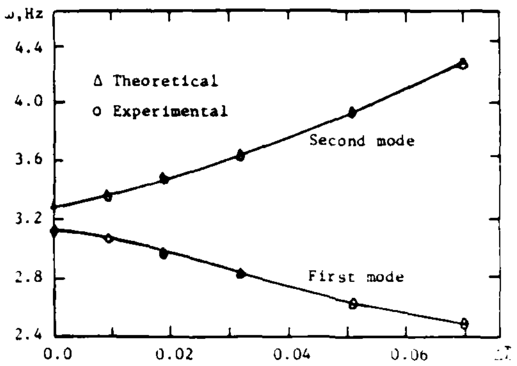

FIG 10. Comparison of experimental and theoretical natural frequencies of the first two modes for c = 281.8 (Pierre et al, 1986)

Pierre et al (1986) conducted an experimental investigation to verify the existence of localized modes for two disordered two-span beams shown in Figure 7. The beam was pinned at both ends while the third support with variable torsional stiffness was located near the mid-span. This middle support can be moved to various locations. A pure excitation torque was applied to the specimen beam near its intermediate support. Figure 10 shows the comparison between theoretical and experimental natural frequencies of the first two modes versus mistuning parameter $\delta l = \Delta l / l$, where l is the length of the beam, and Δl is the variation from the middle of the beam. The coupling parameter $c = 2k_\theta l / EI$, where k_θ is the stiffness of the torsional spring, E and I are the Young's modulus and the area moment of inertia of the beam, respectively. The degree of localization of a mode is expressed by the ratio $A = A \;\; A$ which represents the peak deflection in one span to the peak deflection in the other span, such that the numerator of this ratio corresponds to the span with smaller peak deflection. This peak ratio is shown in Figure 11 for the two modes for two different values of torsional spring constant c. The mode shapes of tuned and mistuned beams are shown in Figure 12. It was reported that for $\delta l = 2\%$ and $c = 281.8$, the first mode of the mistuned beam is strongly localized in the second span, whereas the one of the tuned beam is collective, that is the peak deflection is the same in both spans.

A comprehensive experimental and theoretical investigations were conducted by Ewins (1976) to determine the effects of turbomachinery blades mistuning. His bladed disk testpiece model consists of 24 blades. A provision for adjusting the tune of each blade individually was accomplished by adding a number of washers to a nut and bolt attached near the tip of each blade. The test piece was excited by placing an electromagnet close to its surface and passing an alternating current through the magnet. The response of the bladed disk was detected by a set of strain gages fixed near the root of each blade. The natural frequencies were then measured by adjusting the frequency of the magnet so as to produce a large response in the strain gage outputs. The shape of each mode was determined by examination of the relative amplitudes of all the blades. It was observed that there was a distinct, though complex, pattern linking the basic (tuned) mode shape with the mistuned mode shape and the mistuned pattern, particularly for the lower diametral modes. Jay and Burns (1986) conducted a series of rotating and non-

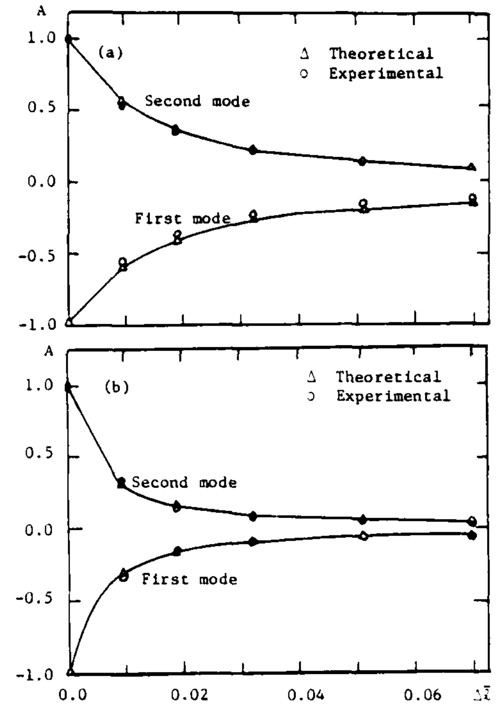

FIG. 11. Comparison of experimental and theoretical peak ratio A of the first two modes for (a) c = 90.4, (b) c = 281.8 (Pierre et al. 1986)

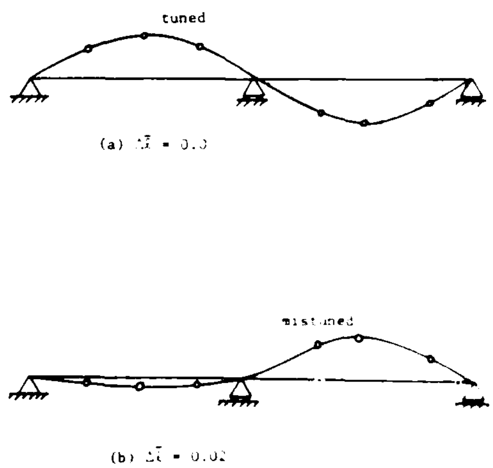

FIG. 12. Measures first mode shape for tuned (a) and mistuned (b) two-span beam for c = 281.8 (Pierre et al. 1986)

rotating tests to identify individual blade frequencies, mode shapes, mistuning, damping, and split factors for diametral patterns of the 3, 4, 5, and 6 diametral mode families. The first harmonic of the normalized axial velocity deficit at the proper mass flow rate was used to construct a gust perturbation velocity. These spanwise gust perturbation velocities multiplied by the product of the density and the relative velocity squared results in the normalized force parameter. It was found that any increase in the perturbation force parameter results in an increase in the dynamic stress in the bladed disk. In addition the perturbation parameter does account for the interaction between the wake and modal response of the system as they are changed by aerodynamic loading.

7. CONCLUSIONS

Several problems in structural dynamics involving parameter uncertainties have been treated in the literature. These problems include the random eigenvalue of disordered systems, normal mode localization, random response, design optimization, and reliability. The mathematical theory of the random eigenvalue has reached the maturity stage, however, this theory has not been fully implemented to treat real engineering problems. It is observed that some progress has been made towards the development of numerical algorithms such as stochastic finite element methods and Monte Carlo simulations to determine the response of structural elements. These developments have promoted the investigation of several problems including mistuned turbomachinery bladed disks, reliability-based design and derivatives of eigenvalues in design optimization. Few attempts have been made to employ new approaches such as multi-objective optimization and fuzzy sets in design optimization problems. It is believed that these techniques will have new research avenues in many design problems. Another area of potential future research is the optimum design sensitivity in reliability-based design under multilevel reliability constraints to evaluate the significance of various uncertainties and approximations on the optimum solutions.

The problems treated in the literature have been restricted within the framework of the linear theory. The limitations of the linear formulation need to be defined to provide the structural dynamicist the influence of nonlinearities as a source of uncertainty. Future studies should include the influence of geometric and material nonlinearities. Experimental investigations are also very important to examine the influence of parameter uncertainties of composite structures on their dynamic performance.

Acknowledgments

This paper was prepared during the course of a research project supported by the Air Force Office of Scientific Research under Grant No. AFOSR-85-0008. Dr Anthony Amos is the Program Director. The author would like to thank Professors T T Soong, W E Boyce, D Frangopol, C Pierre, Dr T Paez, and the reviewers for their comments and references which were of great help in adding new dimensions to this review.

REFERENCES

Adomian G (1983), *Stochastic systems*, Academic, New York.
Anderson P W (1958), Absence of diffusion in certain random lattices, *Phys Rev* **109** 1492-1505.
Ang A H S and Tang W H (1975), *Probability concepts in engineering planning and design, Volume I, Basic principles*, Wiley, New York.

Ang, A H-S. and Tang, W H (1984). *Probability concepts in engineering planning and design, volume II: Decision, risk, and reliability*. Wiley, New York.
Arora, J S. and Haug E J (1979). Methods of design sensitivity analysis in structural optimization. *AIAA J* **17**(9), 970–974.
Ashworth, M J (1982). *Feedback design of systems with significant uncertainty*. Research Studies Press, Wiley, Chichester, UK.
Astill, C J, Nosseir, S B and Shinozuka, M (1972). Impact loading on structures with random properties. *J Struct Mech* **1**(1), 63–77.
Augusti, G, Borri, A, and Casciati F (1981). Structural design under random uncertainties: Economical return and 'intangible' quantities. *Proc 3rd int conference on structural safety and reliability* (Icossar 81), Trondheim. Elsevier, Amsterdam, p 483–494.
Augusti, G, Baratta, A, and Casciati, F (1984). *Probabilistic methods in structural engineering*. Chapman and Hall, London.
Basu, P, and Griffin, J H (1986). The effect of limiting aerodynamic and structural coupling in models of mistuned bladed disk vibration. *J Vib Acoust Stress Reliab Des* **108**, 132–139.
Bendiksen, O O (1984a). Flutter of mistuned turbomachinery rotors. *J Eng Gas Turbines Power* **106**(1), 25–33.
Bendiksen, O O (1984b). Aeroelastic stabilization by disorder and imperfection. Abstract of a paper presented at the XVIth int congress of theoretical and applied mechanics, Lyngby, Denmark, Aug 19–25, 1984, paper no 583.
Bennett, R (1985). Reliability of protective structures. PhD thesis, Univ of New Mexico.
Bliven, D O, and Soong, T T (1969). On frequencies of elastic beams with random imperfections. *J Franklin Inst* **287**, 297–304.
Bogdanoff, J L (1965). Mean square approximate systems and their application in estimating response in complex disordered linear systems. *J Acoust Soc Am* **38**, 244–252.
Bogdanoff, J L (1966). Uniqueness of mean-square approximate systems. *J Acoust Soc Am* **39**(2), 261–268.
Bogdanoff, J L, and Chenea, P F (1961). Dynamics of some disordered linear systems. *Int J Mech Sci* **3**, 157–169.
Bottger, H (1983). *Principles of the theory of lattice dynamics*. VCH Publishers, Deerfield Beach FL.
Boyce, W E (1962). Random vibration of elastic strings and bars. *Proceedings of the 4th US national congress of applied mechanics* (Berkeley CA), ASME, New York, p 77–85.
Boyce, W E (1966). Stochastic nonhomogeneous Sturm–Liouville problem. *J Franklin Inst* **282**, 206–215.
Boyce, W E (1967). A "dishonest" approach to certain stochastic eigenvalue problem. *SIAM J Appl Math* **15**, 143–152.
Boyce, W E (1968). Random eigenvalue problems. In *Probabilistic methods in applied mathematics*, A T Bharucha-Reid (Ed), vol 1, Academic, New York, p 1–73.
Boyce, W E (1980). On a conjecture concerning the means of the eigenvalues of random Sturm–Liouville boundary value problems *Q Appl Math* **38**, 241–245.
Boyce, W E, and Goodwin, B E (1964). Random transverse vibrations of elastic beams. *J Soc Ind Appl Math* **12**, 613–629.
Boyce, W E, and Xia, N-M (1983). The approach to normality of the solutions of random boundary and eigenvalue problems with weakly correlated coefficients. *Q Appl Math* **40**, 419–445.
Boyce, W E, and Xia, N-M (1985). Upper bounds for the means of eigenvalues of random boundary value problems with weakly correlated coefficients. *Q Appl Math* **42**(4), 439–454.
Branstetter, L J, and Paez, T L (1986). Dynamic response of random parametered structures with random excitation. Sandia Report SAND85-1175. Sandia National Laboratories, Albuquerque NM
Brown, C B (1980). The merging of fuzzy and crisp information *J Eng Mech* **106** (EM1), 123–133.
Brown, C B, and Yao, J T P (1983). Fuzzy sets and structural engineering *J Struct Eng* **109**(5), 1211–125
Caravani, P, and Thomson, W T (1973). Frequency response of a dynamic system with statistical damping. *AIAA J* **11**(2), 170–173
Chang, F (1985). Probabilistic dynamics of elasto-plastic structures PhD thesis, Univ of New Mexico
Charnes, A, and Cooper, W W (1959) Chance constrained programming *Management Sci* **6**, 73–79
Chen, P-C, and Soroka, W W (1973) Impulse response of a dynamic system with statistical properties *J Sound Vib* **31**, 309–314
Chen, P-C, and Soroka, W W (1974) Multi-degree dynamic response of a systems with statistical properties *J Sound Vib* **37**(4), 547–556
Chenea, P F, and Bogdanoff, J L (1958). Impedance of some disordered systems *ASME colloquium on mechanical impedance methods for mechanical vibration*, ASME, New York, p 125–128
Chernov, L A (1960). *Wave propagation in random medium* McGraw-Hill, New York.
Cole, J D (1968). *Perturbation methods in applied mathematics*. Blaisdell, Waltham MA.
Collins, J D (1967) The eigenvalue problem for systems with statistical properties. PhD thesis, UCLA.
Collins, J D, Hart, G C, and Kennedy, B (1971) Statistical analysis of the modal properties of large structural systems Society of Automotive Engineers, National aeronautics and space engineering and manufacturing meeting, Los Angeles CA, 28–30 Sep, SAE paper 710785
Collins, J D, and Thomson W T (1967) Statistics of rigid body moment of inertia computation. *J Spacecraft Rockets* **4**(12), 1673–1675
Collins, J D, and Thomson, W T (1969) The eigenvalue problem for strutural systems with statistical properties. *AIAA J* **7**(4), 642–648
Contreras, H (1980). The stochastic finite element method. *Comput Struct* **12**, 341–348.
Cornell, C A (1972). First order analysis of model and parameter uncertainty int symp on uncertainties in hydodogic and water resource systems. Univ of Arizona, Tucszon.
Davidson, J W, Felton, L P, Hart, G C (1977) Optimization design of structures with random parameters. *Comput Struct* **7**, 481–486
Day, W B (1980). Asymptotic expansions of eigenvalues and eigenfunctions of random boundary-value problems *Q Appl Math* **38**, 169–177
Dias, J B, and Nagtegaal, J C (1985) Efficient algorithm for use in probabilistic finite element analysis. *Proc advances in aerospace structural analysis*, vol AD-09, O H Burnside and C H Parr (Eds), ASME Winter Annual Meeting, p 37–50
Dye R C F, and Henry, T A (1969). Vibration of compressor blades resulting from scatter in blade natural frequencies. *J Eng Power* **91**, 182
El-Bayoumy, L E, and Srinivasan, A V (1975). The effect of mistuning on rotor blade vibration. *AIAA J* **13**(4), 460–464
Elliot, R J, Krumhansl, J K, and Leath, P L (1974) The theory and properties of randomly disordered crystals and related physical systems *Rev Modern Phys* **46**, 465–543
Ewins, D J (1969). The effects of dentuning upon the forced vibrations of bladed disks. *J Sound Vib* **9**, 65–79
Ewins, D J (1973) Vibration characteristics of bladed disk assemblies *J Mech Eng Sci* **15**(3), 165–186
Ewins, D J (1976). Vibration modes of mistuned bladed disks *J Eng Power* **98**(3), 349–355
Ewins, D J, and Han, Z S (1984) Resonant vibration levels of a mistuned bladed disk *J Vib Acoust Stress Reliab Des* **106**, 211–217
Fox, R L, and Kapoor, M P (1968) Rates of change of eigenvalues and eigenvectors. *AIAA J* **6**(12), 2426–2429
Frangopol, D M (1984a). A reliability-based optimization technique for automatic plastic design. *Comput Methods Appl Mech Eng* **44**, 105–117
Frangopol, D M (1984b) Sensitivity studies in reliability-based plastic design. *Eng Comput* **1**(3), 237–246.
Frangopol, D M (1985a) Sensitivity of reliability-based optimum design *J Struct Eng* **111**, 1703–1721.
Frangopol, D M (1985b). Structural optimization using reliability concepts *J Struct Eng* **111**, 2288–2301
Frangopol, D M (1986) Computational experience gained in structural optimization under uncertainty *Proc of the 1st int conference on computational mechanics*, vol 2, G Yagawa and S N Atluri (Eds), Springer-Verlag, Tokyo, p X.53–X.58
Frangopol, D M, and Nakib, R (1986) Analysis and optimum design of non-deterministic structures under random loads *Proc of the 9th conference on electronic computation*, Committee on Elec Comp ST Div/ASCE/ Birmingham AL, p 483–493
Frank, P M (1978) *Introduction to system sensitivity theory* Academic, New York
Frisch, U (1968) Wave propagation in random media In *Probabilistic methods in applied mathematics*, vol 1, A T Bharucha-Teid (Ed), Academic, New York, p 75–198
Fritzen, C P, and Nordman, R (1982) Influence of parameter changes to stability behavior of rotors NASA conference publication 2250 *Rotor dynamic instability problems in high-performance turbomachinery*, TAMU p 284–297
Goodwin, B E, and Boyce, W E (1964) Vibrations of random elastic strings Method of integral equations *Q Appl Math* **22**, p 261–266
Grierson, D E (1983) The intelligent use of structural analysis *Perspectives Comput* **3**(4), 32–39
Griffin, J H, and Hoosac, T M (1984) Model development and statistical investigation of turbine blade mistuning *J Vib Acoust Stress Reliab Des* **106**, 204–210
Guangwu, Z and Suming, S (1986) Interactive multiobjective fuzzy optimization design of ship grillage structure *Proc of the 1st int conference on computational mechanics*, vol 2, G Yagawa and S N Atluri (Eds), Springer Verlag, Tokyo, p X 129–X 134
Haines, C W (1965) An analysis of stochastic eigenvalue problems PhD thesis, RPI
Haines, C W (1967) Hierarchy methods for random vibrations of elastic strings and beams *J Eng Math* **1**, 293–305
Hart, G C (1973) Eigenvalue uncertainty in stressed structures *J Eng Mech* **99**(EM3), 481–494
Hart, G C, and Collins, J D (1970) The treatment of randomness in finite element modeling. Society of Automotive Engineers, Aerospace fluid power conference, National aeronautic and space engineering and manufacturing meeting, Los Angeles CA Oct 5–9, SAE paper 700842
Hasselman, T K, and Hart, G C (1971) Dynamic analysis of structures with random properties by component mode synthesis Society of Automotive Engineers, National aeronautic and space engineering and manufacturing meeting, Los Angeles CA, 28–30 Sep, SAE paper 710786
Hasselman, T K, and Hart, G C (1972). Modal analysis of random structural systems *J Eng Mech* **98**(EM3), 561–579

Haug, E J, and Rousselet, B (1980). Design sensitivity analysis in structural mechanics. *J Struct Mech* **8**(2), 161–186.

Hilton, H H, and Feigen, M (1960). Minimum weight analysis based on structural reliability. *J Aerospace Sci* **27**(9), 641–652.

Hisada, T, and Nakagiri S (1982). Stochastic finite element analysis of uncertain structural systems. *4th Int conference on finite element method*. Australia, p 133–137.

Hisada, T, Nakagiri, S, and Nagasaki, T (1983). Stochastic finite element analysis of buckling of frame structure with uncertain initial stresses. *Trans JSME* **49**.

Hodges, C H (1982). Confinement of vibration by structural irregularity. *J Sound Vib* **82**(3), 411–424.

Hodges, C H, and Woodhouse, J (1983). Vibration isolation from irregularity in a nearly periodic structure: Theory and measurements. *J Acoust Soc Am* **74**(3), 894–905.

Hohenbichler, M, and Rackwitz, R (1981). Non-normal dependent vectors in structural safety. *J Eng Mech* **107**(EM6), 1227–1238.

Hoshiya, M, and Shah, H C (1971). Free vibration of stochastic beam-column. *J Eng Mech* **97**, 1239–1255.

Huang, Wen-hu (1982). Vibration of some structures with periodic random parameters. *AIAA J* **20**(7), 1001–1008.

Hurty, W C (1964). Dynamic analysis of structural systems by component mode synthesis. Jet Propulsion Lab, Pasadena CA, report 32-530, Jan 15.

Hurty, W C (1965). Dynamic analysis of structural systems using component modes. *AIAA J* **3**(4), 678–685.

Ibrahim, R A (1985). *Parametric random vibration*. Research Studies Press, Wiley, New York.

Ray, R L, and Burns, D W (1986). Characteristics of the diametral resonant response of a shrouded fan under a prescribed distortion. *J Vib, Acoust Stress Reliab Des* **108**, 125–131.

Jozwiak, S F (1985). Optimization of structures with random parameters. *Proc IVth int. conference on engineering software*, London.

Jozwiak, S F (1986). Optimization of dynamically loaded structures with random parameters. *Proc of the 1st int conference of computational mechanics*, vol 2, G Yagawa and S N Atluri (Eds), Springer-Verlag, Tokyo, p X 159–X 164.

Kam, T Y (1986). Optimal design of brittle structures with reliability constraint. *Proc of the 1st int conference on computational mechanics*, vol 2, G Yagawa and S N Atluri (Eds), Springer-Verlag, Tokyo, p X 65–X 70.

Kaza, K R V, and Kielb, R E (1982). Effects of mistuning on bending-torsion flutter and response of a cascade in incompressible flow. *AIAA J* **20**(8), 1120–1129.

Keller, J B (1962). Wave propagation in random media. *Am Math Soc*, Providence R I, 217–246.

Keller, J B (1964). Stochastic equations in random media. *Am Math Soc*, Providence R I, 145–170.

Kerner, E H (1954). Periodic impurities in a periodic lattice. *Phys Rev* **95**(3), p 687.

Kerner, E H (1956). The band structure of mixed linear lattice. *Proc of the Phys Soc* **69A**(433A), 234.

Kiefling, L A (1970). Comment on "the Eigenvalue problem for structural systems with statistical properties." *AIAA J* **8**(7), 1371–1372.

Kline, S J (1985). The purposes of uncertainty analysis. *J Fluids Eng* **107**(2), 153–160.

Kozin, F (1961). On the probability densities of the output of some random systems. *A J Appl Mech* **28**, 161–165.

Kuo, C P, and Wada, B K (1986). Nonlinear sensitivity coefficients and corrections in system identification. *AIAA/ASME ASCE AHS 27th structures, structural dynamics and materials conference*, part 2, San Antonio TX, Paper no 86-0967, p 576–584.

Laning, J H, Jr, and Battin, R H (1958). *Random processes in automatic control*. McGraw-Hill, New York.

Lin, Y K, and Yang, J N (1974). Free vibration of a disordered periodic beam. *J Appl Mech* **41**, 383–391.

Linde, Van Der R H (1969). Eigenfunctions of random eigenvalue problems and their statistical properties. *SIAM J Appl Math* **17**(6), 1298–1304.

Liu, W K, Belytschko, T, and Mani, A (1985a). A computational method for the determination of the probabilistic distribution of the dynamic response of structures. *Comput-Aided Eng, ASME PVP* **9**(5), 243–248.

Liu, W K, Belytschko, T, and Mani, A (1985b). Probabilistic finite elements for transient analysis in nonlinear continua. *Advances in aerospace structural analysis*, Proceedings of ASME WAM, Miami Beach FL, O H Burnside and C H Parr (Eds), vol AD-09, p 9–24.

Liu, W K, Belytschko, T, and Mani, A (1986). Probabilistic finite element methods in nonlinear structural dynamics. *Comput Methods Appl Mech Eng*.

Lund, J W (1979). Sensitivity of the critical speeds of a rotor to changes in the design. *J Mech Des* **102**, 115–121.

Macbain, J C, and Whaley, P W (1984). Maximum resonant response of mistuned bladed disks. *J Vib Acoust Stress Reliab Des* **106**, 218–223.

Mantey, P E (1968). Eigenvalue sensitivity and state variable selection. *IEEE Trans Autom Control* **13**.

McCalley, R B Jr, (1960). Error analysis for eigenvalue problems. *ASCE 2nd Conference on Electronic Computation*, Pittsburgh, PA, Conference papers, ASME New York.

McKay, M D, Beckman, R J, and Conover, W J (1979). A comparison of three methods for selecting values of input variables in the analysis of output from a computer code. *Technometrics* **21**(2).

Meirovitch, L (1980). *Computational methods in structural dynamics*. Sijthoff-Noordhoff Co, Netherlands.

Meirovitch, L, Baruh, H, and Oz, H (1983). A comparison of control techniques for large flexible systems. *J Guidance Control Dyn* **6**, 302–310.

Miles, J W (1956). Vibration of beams on many supports. *J Eng Mech* **82**(EM1), 1–9.

Mok, C-H, and Murray, E A, Jr (1965). Free vibrations of a slender bar with non-uniform characteristics. *J Acoust Soc Am* **40**, 385–389.

Mori, M, and Ukai, O (1986). A numerical technique on structural analysis of uncertain shape structure by S.FEM. *Proc of the 1st international conference of computational mechanics*, vol 2, G Yagawa and S N Atluri (Eds), Springer-Verlag, Tokyo, p XI 173–X 179.

Moses, F (1973). Design for reliability concepts and applications. In *Optimum structural design theory and applications*, R H Gallaghar and O C Zienkiewicz (Eds), chapter 13, Wiley, London.

Moses, F (1974). Reliability of structural systems. *ASCE Trans J Struct Eng* **100**, 1813–1820.

Moses, F, and Kinser, D E (1967). Optimum structural design with failure probability constraints. *AIAA J* **5**(6), 1152–1158.

Moses, F, and Stevenson, J (1970). Reliability-based structural design. *J Struct Eng* **96**(ST2), 221–244.

Muszynska, A, Jones, D I G, Lagnes T, and Whitford, L (1981). On nonlinear response of multiple bladed systems. *Shock Vib Bull* **51**(3), 88–110.

Nakagiri, S, Hisada, T, and Toshimitsu, K (1984). Stochastic time-history analysis of structural vibration with uncertain damping. *J PVP* **93**, 109–120.

Nakagiri, S, Takabatake, H, and Tani, S (1985). Uncertain eigenvalue analysis of composite laminated plates by the stochastic finite element method. In *Advances in aerospace structural analysis*, ASME Aerospace Division AD-09, O H Burnside and C H Parr (Eds), p 1–7.

Nurre, G S, Ratner, M J, and Lyons, M G (1984). Structural control for a circular plate. *J Guidance Control Dyn* **7**, 535–545.

Paez, T L, Branstetter, L J, and Gregory, D L (1985). Modal randomness by boundary conditions. *Proc of the SAE aerospace technology*.

Paez, T L, Branstetter, L J, and Gregory, D L (1986). Random vibration of modal frequencies: Experiments and analysis. *Shock Vib Bull* **56**.

Palazzolo, A B, Wang, P O, and Pilkey, W D (1983). Eigensolution reanalysis of rotor dynamic systems by the generalized receptance method. *J Eng Power* **105**, 543–550.

Parimi, S R, and Cohn, M Z (1978). Optimal solutions in probabilistic structural design. *J Mec Appl* **2**(1), 47–92.

Pierre, C (1985). Analysis of structural systems with parameter uncertainties. PhD thesis, Duke Univ, Durham NC.

Pierre, C, and Dowell, E H (1987). Localization of vibrations by structural irregularity. *J Sound Vib* **114**(3).

Pierre, C, Tang, D-M, and Dowell, E H (1986). Localized vibrations of disordered multi-span beams: Theory and experiment. *AIAA/ASME/ASCE/AHS 27th structures, structural dynamics and materials conference*, San Antonio TX, Part 2, Paper no 86-0934, p 445–455.

Plaut, R H, and Husevin, K (1973). Derivatives of eigenvalues and eigenvectors in non-self-adjoint systems. *AIAA J* **11**(2), 250–251.

Prasthofer, P H, and Beadle, C W (1975). Dynamic response of structures with statistical uncertainties in their stiffness. *J Sound Vib* **42**(4), 477–493.

Purkert, W, and vom Scheidt, J (1977). On the approximate solution of the mean value problems for the eigenvalue of stochastic differential operator (in German). *Z Angew Math Mech* **57**, 515–525.

Purkert, W and von Scheidt, J (1979a). On the dispersion of the Stochastic eigenvalue problems. *Z Angew Math Mech* **59** 611–623.

Purkert, W, and von Scheidt, J (1979b). Stochastic eigenvalue problems for differential equations. *Rep Math Phys* **15**, 205–227.

Rajan, M, Nelson, H D, and Chen, W J (1986). Parameter sensitivity in the dynamics of rotor-bearing systems. *J Vib Acoust Stress Reliab Des* **108**, 197–206.

Rao, S S (1979). *Optimization: Theory and applications*. Wiley, New York.

Rao, S S (1982). Optimization of structures under shock and vibration environment. *Shock Vib Digest* **14**(12), 9–15.

Rao, S S (1984). Multiobjective optimization in structural design with uncertain parameters and stochastic processes. *AIAA J* **22**(11), 1670–1678.

Reddy, D C (1969). Eigenfunction sensitivity and the parameter variation problem. *Int J Control* **9**, 561–568.

Reiss, R (1983). On the design derivative of Green's functional. *Proc 18th midwestern mechanics conference*, Iowa City IA, p 145–147.

Reiss, R (1986). Design derivatives of eigenvalues and eigenfunctions for self-adjoined distributed parameter systems. *AIAA J* **24**(7), pp 1169–1172.

Rogers, L C (1970). Derivatives of eigenvalues and eigenvectors. *AIAA J* **8**(5), 943–944.

Rosenblatt, M (1952). Remarks on multivariate transformation. *Annals of Mathematical Statistics* **23**(3), 470–472.

Rudisill, C S (1974). Derivatives of eigenvalues and eigenvectors for general matrix. *AIAA J* **12**(5), 721–722.

Scheidt, J and Purkert, W (1983). *Random Eigenvalue Problems*. Elsevier, New York.

Schiff, A J and Bogdanoff, J L (1972a). An estimator for the standard deviation of a natural frequency-Part 1. *ASME J Appl Mech* **39**, 535–538.

Schiff, A J and Bogdanoff, J L (1972b). An estimator for the standard

deviation of a natural frequency-Part 2. *ASME J Appl Mech* **39**, 539–544
Schy, A A and Giesy, P D (1981) Multiobjective insensitive design of airplane control systems with uncertain parameters. AIAA Paper, Aug 1981, 262–271
Shinozuka, M (1971) Simulation of multivariate and multidimensional random processes. *Acoustical Society of America Journal* **49**(1), Pt 2, 357–367
Shinozuka, M and Astill, C A (1972). Random eigenvalue problems in structural analysis. *AIAA J* **10**(4), 456–462.
Skowronski, J M (1981) Adaptive identification of models stabilizing under uncertainty. In *Lecture notes in biomathematics*, vol 40, Springer, Berlin, p 64–78
Skowronski, J M (1984). Parameter and state identification in non-linearizable uncertain system. *Int J Nonlinear Mech* **19**(5), 421–429
Sobczyk, K (1985) *Stochastic wave propagation*. Fundamental studies in engineering **6**, Elsevier, Amsterdam
Sogliero, G. and Srinivasan, A V (1980) Fatigue life estimates of mistuned blades via a stochastic approach. *AIAA J* **18**(3), 318–323
Soong, T T (1962) On the dynamics of a disordered linear chain. PhD thesis, Purdue Univ, Indiana
Soong, T T (1973) *Random differential equations in science and engineering*. Academic, New York
Soong, T T, and Bogdanoff, J L (1963) On the natural frequencies of a disordered linear chain of N degrees of freedom. *Int J Mech Sci* **5**(3), 237–265
Soong, T T, and Bogdanoff, J L (1964). On the impulsive admittance and frequency response of a disordered linear chain of N degrees of freedom. *Int J Mech Sci* **6**(3), 225–237
Soong, T T, and Cozzarelli, F A (1976) Vibration of disordered structural systems. *Shock Vib Digest* **8**(5), 21–35
Srinivasan, A V (1984) Vibrations of bladed-disk assemblies—A selected survey. *J Vib Acoust Stress Reliab Des* **106**, 165–168
Strange, W A, and MacBain, J C (1983) An investigation of dual mode phenomena in a mistuned bladed disk. *J Vib Acoust Stress Reliab Des* **105**(3), 402–407
Szopa, J (1984) Sensitivity of stochastic systems to initial conditions. *J Sound Vib* **97**(4), 645–649
Szopa, J (1986). Application of stochastic sensitivity functions to chaotic systems. *J Sound Vib* **104**(1), 176–178
Tanaka, K, and Onishi, H (1980) Regulating calculation of random parameters in structural mechanics. *Bull JSME* **23**(176), part I, 255–259, part II pp 260–264
Tanaka, K, Onishi, H, and Kaga, M (1982) Estimation of the variance of steady vibration response of structures with random parameters and method to compute the allowable variance of the parameters. *Comput Struct* **15**(3), 329–334
Thomson, W T (1981) *Theory of vibration with applications*, 2nd ed. Prentice-Hall, Englewood Cliffs NJ
Tobias, S A, and Arnold, R N (1957) The influence of dynamical imperfection on the vibration of rotating disks. *Proc Inst Mech Eng* **171**, 669–690
Vaicaitis, R (1974) Free vibrations of beams with random characteristics. *J Sound Vib* **35**, 13–21
Valero, N A, and Bendiksen, O O (1985) Vibration characteristics of mistuned shrouded blade assemblies. ASME paper no 85-GT-115
Vanmarcke, E (1984) *Random fields: Analysis and synthesis*. MIT Press, Cambridge MA
Vanmarcke, E, and Grigoriu, M (1983) Stochastic finite element analysis of simple beams. *J Eng Mech* **109**(5), 1203–1214
Vinson, J R, and Chou, T W (1975) *Composite materials and their use in structures*. Applied Sciences Publishers, London
Wagner, J T (1967) Coupling of turbomachine blade vibrations through the rotor. *J Eng Power* **89**(4), 502–513
Wedig, W (1976) Moments and probability densities of dynamical systems under stochastic parameter excitation. *Proc of the VII int conference on nonlinear oscillations*, Berlin, p 469–492
Wedig, W (1977) Stochastic boundary and eigenvalue problems. In *Stochastic problems in dynamics*, B L Clarkson (Ed), Pitman, London, p 54–66
Whitehead, D S (1966) Effect of mistuning on vibrations of turbomachine blades induced by wakes. *J Mech Eng Sci* **8**(1), 15–21
Yang, J N, and Lin, Y K (1975) Frequency response functions of a disordered periodic beam. *J Sound Vib* **38**(3), 317–340
Zadeh, L (1965) Fuzzy sets. *Info Control* **8**, 338–353
Zadeh, L (1973) Outline of a new approach to the analyses of complex systems and decision processes. *IEEE Trans Syst Man Cybernetics* SMC **3**(1), 28–44

Raouf A Ibrahim *is a professor of Mechanical Engineering at Texas Tech University. He received his BSc and MSc in Aeronautical Engineering in 1963 and 1969, respectively, from Cairo University (Egypt). He received his PhD in Mechanical Engineering from the University of Edinburgh in 1974. From 1963 through 1971, he worked as a research engineer at the Aerospace Research Center of rockets industry in Egypt. His research activities in nonlinear random vibration began in 1974 when he collaborated with J W Roberts of the University of Edinburgh. From 1976 through 1979, he was appointed Senior Research Specialist at Sakr Factory in Cairo, and worked as Adjunct Assistant Professor at Cairo University. In 1979 he moved to the United States and worked at Shaker Research Corporation, New York. Dr Ibrahim joined the Department of Mechanical Engineering at Texas Tech University in 1980. He is a recipient of two Halliburton Awards of Excellence in 1983 and 1986, and Pi Tau Sigma Outstanding Professor Award in 1982. He has published more than forty technical papers and a recent research monograph entitled* Parametric Random Vibration, *(Wiley, New York, 1985). He is a Registered Professional Engineer in the State of Texas and a member of ASME, AIAA, ASEE, and AAM.*

AIAA'87

AIAA-87-0779-CP

Experimental Investigation of Structural Autoparametric Interaction Under Random Excitation

R.A. Ibrahim and D.G. Sullivan, Texas Tech Univ., Lubbock, TX

AIAA/ASME/ASCE/AHS 28th Structures, Structural Dynamics and Materials Conference

April 6-8, 1987/Monterey, California

87-0779

EXPERIMENTAL INVESTIGATION OF STRUCTURAL AUTOPARAMETRIC INTERACTION UNDER RANDOM EXCITATION

R. A. Ibrahim* D. G. Sullivan**
Texas Tech University
Lubbock, Texas 79409

ABSTRACT

The paper presents the results of an experimental investigation of random excitation of a nonlinear two-degree-of-freedom structural model. The model normal mode frequencies are adjusted to have the ratio of 2 to 1. This ratio meets the condition of internal resonance of the analytical model. When the first normal mode is externally excited by a band limited random excitation, the system mean square response is found to be linearly proportional to the excitation spectral density up to a certain level above which the two normal modes exhibit discontinuity governed mainly by the internal detuning parameter and the system damping ratio. The results are completely different when the second normal mode is externally excited. For small levels of excitation spectral density the response is dominated by the second normal mode. For higher levels of excitation spectral density the first normal mode attends and interacts with the second normal mode in a form of energy exchange. A number of deviations from theoretical results are observed and discussed.

I. INTRODUCTION

The last two decades have witnessed an increasing interest in the study of dynamic behavior of nonlinear systems under deterministic and random excitations. Under certain conditions these systems may experience complex response characteristics such as jump phenomenon, limit cycles, internal resonance, saturation phenomenon, and chaotic motion. These nonlinear phenomena have been predicted theoretically[1-3] and observed experimentally[4-6] under harmonic excitations. However, most of the predicted random response characteristics, including response stochastic stability and statistics,[7,8] have not been verified experimentally. Very few experimental investigations of random vibration of nonlinear systems have been reported in the literature.[7] The lack of experimental verifications may be due to several reasons. These include difficulties in generating the same properties of the random excitation as represented theoretically, and the limitations of experimental equipment. Recently, Bolotin[9] discussed a number of experimental difficulties encountered in experimental measurements of stochastic stability of parametric excited systems.

In deterministic nonlinear vibrations; the amplitude jump, limit cycles, and parametric instability are common features of nonlinear single- and multi-degree-of-freedom systems. Parametric instability takes place when the external excitation appears as a coefficient in the homogeneous part of the equation of motion. It occurs when the excitation frequency is twice (or multiple) of the system natural frequency. Internal resonance and saturation phenomenon may occur only in nonlinear systems with more than one degree-of-freedom. Internal resonance implies the existence of a linear relationship between the system natural frequencies and causes nonlinear normal mode interaction in the form of energy exchange. Under external harmonic excitation, the mode which is directly excited, exhibits in the beginning, the same features of a single-degree-of freedom system response and all other modes remain dormant. As the excitation amplitude reaches a certain critical level, the other modes become unstable and the originally excited mode reaches an upper bound. In this case, the mode is said to be saturated and energy is transferred into other modes. This interesting phenomenon takes place only in systems with quadratic nonlinear coupling which results in a third order internal resonance.

Under deterministic unsteady aerodynamic forces, most nonlinear characteristics can be predicted by one of the standard techniques of nonlinear differential equations. However, aerospace structures are usually subjected to turbulent air flow, and the aeroelastician is confronted with aerodynamic loads which are random in nature. These loads vary in a highly irregular fashion and can be described in terms of statistical quantities such as means, mean squares, autocorrelation functions and spectral density functions. Ibrahim and Roberts[10,11] and Ibrahim and Heo[12,13] considered nonlinear two degree-of-freedom structural systems and applied Gaussian and non-Gaussian closure techniques to predict the response statistics and response stochastic stability. These studies revealed that a system with internal resonance may experience nonlinear characteristics such as autoparametric interaction. Roberts[14] conducted a series of experimental tests to measure the mean square stability boundaries of a unimodal response of a coupled two-degree-of-freedom system. Roberts reported a number of difficulties in measuring the stability boundaries. Based on the authors experience and other investigators work, it is understood that experimental investigation of nonlinear random vibration is not a simple task and requires careful planning and advanced equipment preparations.

The purpose of the present paper is to report the results of an experimental investigation to measure the response mean squares of a nonlinear two degree-of-freedom structural model under band limited random excitation. The same model was analytically examined by Haddow, et al.[5] under harmo-

---

* Professor, Department of Mechanical Engineering
Member AIAA.
** Graduate Student

nic excitation, and by Ibrahim and Heo[12,13] under wide band random excitation. Agreements and disagreements with theoretical predictions will be discussed together with recommendations for future experimental work.

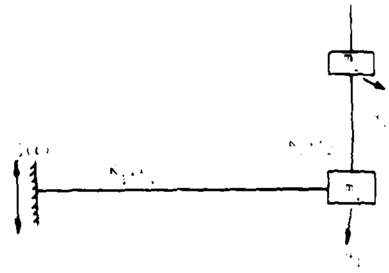

Fig. (1) Model of coupled two beams

II. ANALYTICAL BACKGROUND

The random response of a two degree-of-freedom elastic structure has been determined analytically in references [12,13]. The analytical model shown in fig (1) consists of two beams with end masses. Under vertical support motion $\zeta(t)$ the response of the two beams is mainly governed by linear dynamic and parametric couplings. However, if the system is designed such that the first two normal mode frequencies ω_1 and ω_2 satisfy the internal resonance condition $\omega_2 \approx 2\omega_1$, the nonlinear inertia forces become dominant and the system dynamic response deviates from the linear response. In terms of the non-dimensional normal coordinates $\underset{\sim}{Y}$ the system equations of motion are:

$$[I]\{Y''\} + [\zeta]\{Y'\} + [r^2]\{Y\} =$$

$$\zeta''(\tau)\{a\} + \varepsilon\zeta''(\tau)[b]\{Y\} + \varepsilon\{\psi\} \qquad (1)$$

where a prime denotes differentiation with respect to the nondimensional time parameter $\tau = \omega_1 t$, and the coordinates $\underset{\sim}{Y}$ are related to the dimensional normal coordinates $\underset{\sim}{y}$ by the relation $\{Y_1, Y_2\} = \{y_1, y_2\}/q_1^*$. q_1^* is taken as the response root mean square of the system when the length of the vertical beam shrinks to zero, i.e. the response root mean square of the main beam with end mass (m_1+m_2). The elements of the vector $\{a\}$ and matrix $[b]$ are constants depending on the system properties. The small parameter $\varepsilon = q_1^*/\ell_1$. The matrix $[r^2]$ is diagonal with elements 1 and $(\omega_2/\omega_1)^2$. The vector $\{\psi\}$ contains all quadratic nonlinear terms which encompasses two groups: nonlinear terms of the same mode and autoparametric terms of the type $Y_i Y_j''$. It is the autoparametric coupling which gives rise to the internal resonance condition $r = \omega_2/\omega_1 = 2$.

The random acceleration $\zeta''(\tau)$ was assumed to be Gaussian wide band process with zero mean and a smooth spectral density 2D up to some frequency higher than any characteristic frequency of the system. The acceleration terms in the nonlinear functions ψ_i were removed by successive elimination and the system equations of motion was transformed into a Markov vector via the coordinates transformation

$$\{Y_1, Y_2, Y_1', Y_2'\} = \{X_1, X_2, X_3, X_4\} \qquad (2)$$

A set of first order differential equations of the response statistical moments were generated by using the Fokker-Planck equation approach.[7] These equations were found to be coupled through higher order moments and were closed via two approaches: Gaussian and non-Gaussian closures. These closure techniques are based on the cumulant properties. The Gaussian closure is established by equating all cumulants λ of order greater than two to zero, i.e.

$$\lambda_{N>2}[X_1^{k_1} X_2^{k_2} \ldots X_n^{k_n}] = 0, \qquad N = \sum_{i=j}^{n} k_i \qquad (3)$$

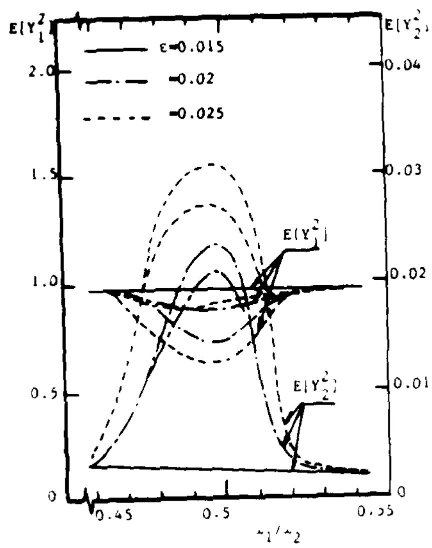

Fig. (2) Gaussian closure solution for various values of nonlinear coupling parameter ε

This approach resulted in fourteen coupled differential equations for first and second order moments of the response coordinates. The numerical integration of these equations revealed that the response mean squares fluctuate between two limits. This fluctuation means that the response does not achieve a stationary state. The autoparametric interaction took place in the neighborhood of internal resonance and was manifested by an energy exchange between the mean squares of the two normal modes. Figure (2), taken from reference 12, shows a sample of the mean square response of the system normal modes against the internal detuning parameter.

The second method takes into account the effect of the response non-normality. As a first order non-Gaussian approximation all cumulants of order greater than four were equated to zero, i.e.

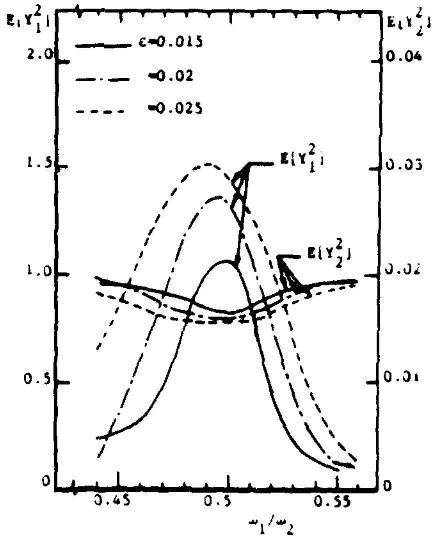

Fig. (3) Non-Gaussian closure solution for various values of nonlinear coupling parameter ε

$$\dot{N}_{N>4}[X_1^{k_1} X_2^{k_2} \cdots X_n^{k_n}] = 0, \qquad N = \sum_{i=1}^{n} k_i \qquad (4)$$

This approach resulted in 69 first order differential equations, in the first through the fourth order moments, which were solved numerically. The solution reaches a stationary state after a transient period and exhibits the same nonlinear interaction as predicted by the Gaussian closure solution. Figure (3) shows the stationary mean square response of the normal coordinates against the internal detuning parameter.

Although the two approaches yielded common features to those predicted by deterministic theory[5] of nonlinear vibration such as autoparametric suppression effect, the random analysis did not verify the existence of saturation phenomenon. The saturation phenomenon[2] is a well known feature for multi-degree-of-freedom systems involving quadratic nonlinear coupling subjected to harmonic forced excitation.

It is well known that the predicted results are approximate and their validity has not been examined. The next section reports the measured results of a series of experimental tests of the same model under band limited random excitation.

III. EXPERIMENTAL INVESTIGATION

III.1 Experimental Model and Equipment

The model is similar to a great extent to the experimental model used by Haddow, et al.[5] It consists of a horizontal beam of cross section of 0.111"x1.0", length 7.5", and carries a tip mass of 0.015 slug. The tip mass has a provision for clamping the vertical beam which has cross section 0.054"x1.0". The length of the vertical beam can be adjusted by changing the location of its top mass (0.0127 slug). The deflections of the two beams are measured by strain gages fixed at the root of each beam. Two gages are mounted on the horizontal beam in a two arm bridge. Four gages are mounted on the vertical beam in a four arm bridge. The fixed end of the horizontal beam is clamped by a fixture which is bolted on the top of the shaker armature. The shaker is a Caldyne model A88 of thrust 100 lb and provides 1" peak-to-peak stroke. The shaker is powered by a Ling Electronics Model RA-250 power supply and receives a random signal through a GenRad Type 1381 Random Noise generator. The random signal is filtered to a desired band width with a Krohn-Hite Model 3343 Variable Electric Filter. The filtered signal is amplified via a Calex Model 176 Instrument Amplifier. Figure (4) shows a schematic diagram of the instrumentation used in this investigation. The acceleration of the shaker platform is measured by a PCB Piezotronic Model 302A02 shock accelerometer. The accelerometer is powered by a PCB Piezotronic Model 480C06 power unit.

The first two normal mode frequencies of the system are determined theoretically and measured experimentally as a function of the beams length ratio ℓ_2/ℓ_1 as shown in fig. (5). This figure shows that the internal resonance $\omega_2/\omega_1 = 2$ is obtained in two locations of the length ratio. At these mass locations the normal mode frequencies are:

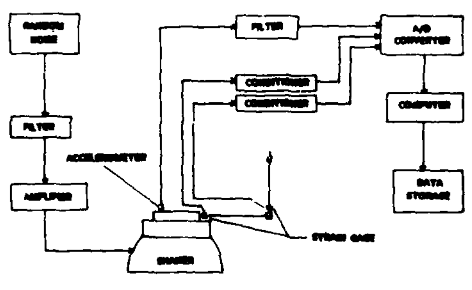

Fig. (4) Arrangement of experimental equipment

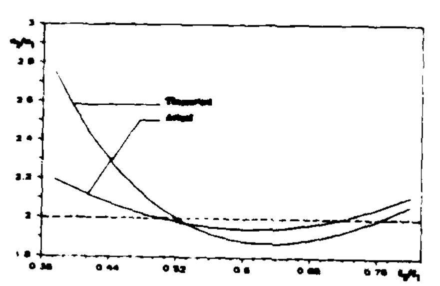

Fig. (5) Measured and theoretical frequency ratio of the first two normal modes.

$$\ell_2/\ell_1 = 0.485: \quad f_1 = 9.1 \text{ Hz}, \quad f_2 = 18.2 \text{ Hz} \qquad (5a)$$

$$\ell_2/\ell_1 = 0.707: \quad f_1 = 7.45 \text{ Hz}, \quad f_2 = 14.9 \text{ Hz} \qquad (5b)$$

The analog signals of the excitation and responses are read and converted into binary numbers using a Data Translation Model DT-3752 Intelligent Analog Peripheral (IAP). This IAP is capable of reading either 8 channels (±10v) or 16 channels (0-10v) of input. It can also read and convert analog signals at up to 40k points per second. This unit is mounted in an expansion slot of an IBM System 9001 Benchtop Computer. The control and programming of the Analog/Digital (A/D) system are accomplished through the software controlled registers and field selectable (hardware) options. The software controlled registers are the control registers, status register, and gain/channel register. The control register controls the operation and mode of the A/D system. The modes which are used in this investigation are direct memory transfer and increment mode operation. Direct memory transfer places converted data directly into the memory of the computer. The increment mode allows the A/D to increment the input channel number automatically before each A/D conversion. This allows data to be taken from sequential channels without requiring a program to specify each channel. The status register reports the complete status of the A/D system during the operation. The gain/channel register selects the desired channels from which the data is to be taken and sets a programmable gain for all input signals. This gain is set to one for all tests. The computer controls the DT-3752 through a *Fortran program*. Analog signals are converted for a specified amount of time or until the computer memory is full. When the computer has completed collecting data, the data is transferred to a floppy disk for future processing.

The data processing is performed at equally spaced intervals. The problem of determining this time interval is well discussed in Bendat and Piersol.[15] Generally, if sampling is prepared at points which are too close together, it will yield correlated and redundant data. This will unnecessarily increase the labor and cost of calculations. Sampling at points which are too far will lead to the problem of aliasing. The aliasing is mainly a confusion between the low and high frequency components in the original data. In order to eliminate the problem of aliasing, a sampling rate should be chosen to be at least two time the maximum frequency that the model will experience. In order to get a good sample data, a sampling rate is chosen which is roughly eight times the maximum frequency. In the present investigation, the sampling rate is chosen to be 80 Hz per channel for the first mode excitation and 160 Hz per channel for the second mode and wide band excitation. Data processing involves another problem known as quantization which is the conversion of data values at the sampling points into digital form. The infinite number of values of the continuous analog signal must be approximated by a fixed set of digital levels. A choice between two consecutive levels will be required because the scale is finite. The accuracy of the approximating process is a function of the available levels which is dependent upon the analog to digital converter resolution. The accuracy of the DT-3752 is the value of the least significant bit which corresponds to a voltage of ±0.0049v. This resolution is analogous to a deflection of the horizontal beam beam of ±0.00073-in and the vertical of ±0.00097-in and an acceleration of ±0.00044-g for the excitation.

The experimental model is tested under various levels of excitation spectral density. This is achieved by keeping the input signal level constant (Master Gain on Ling Amplifier) for the range of internal detuning of the model. The level of amplification is adjusted to five levels for testing of both the first and second normal frequency bandwidths. Another series of tests are conducted for excitation spectral density that covers both normal mode frequencies.

III.2 Experimental Results

The experimental results include sample records of time history responses and the mean square responses in terms of generalized coordinates and normal coordinates. The mean square response will be represented against the internal detuning parameter r and the excitation spectral density level. The bandwidth of the random excitation depends on the mode under investigation.

III.2.1 First Mode Excitation

The first mode is excited by a limited bandwidth random excitation of bandwidth 5Hz and a central frequency very close to the first normal mode natural frequency. The frequency content of this random process is selected such that it does not excite any higher structural modes. For the five *levels of excitation spectral density*, the system response is governed mainly by the first mode which does not show any nonlinear coupling. Figure (6) shows a sample of the time history response under excitation spectral level $S_o = 0.0142$ (g^2/Hz) when the model is internally tuned to the resonance condition $\omega_2/\omega_1 = 2.0$. It is seen that the response is characterized by a narrow band random process of frequency close to the first normal mode - 7.5 Hz.

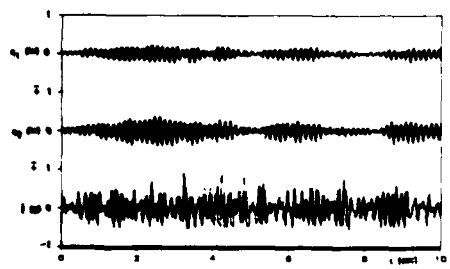

Fig. (6) Time history response of first normal mode excitation, level V, $S_o = 0.0142$ g^2/Hz.

Figure (7a) shows the mean square response of the generalized coordinates for the same excitation spectral density level of fig. (6). The empty points are measured when the mass of the vertical beam moves upward while the full points are obtained when the mass moves downward. Both groups

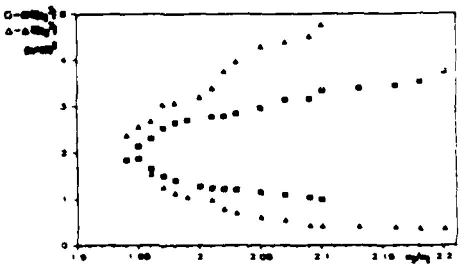

Fig. (7a) Mean square responses of generalized coordinates under first normal mode excitation.

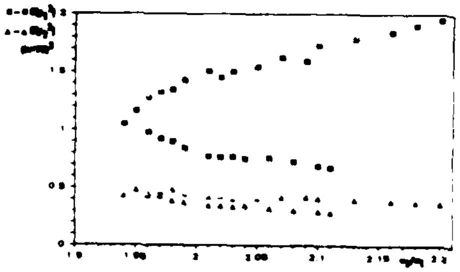

Fig. (7b) Mean square response of normal coordinates under first normal mode excitation.

Excitation level V: $S_o = 0.0142\ g^2/Hz$, empty points correspond higher position of the upper mass while full points correspond lower position.

are measured in the neighborhood of the system internal resonance. The group of full points indicates that the mean square of the horizontal beam increases while the mean square of the vertical beam decreases as the normal mode frequency ratio ω_2/ω_1 increases. This implies that the model behaves like a single degree-of-freedom system for $\omega_2/\omega_1 >> 2$. For the second group of results (empty points) the mean square response of the vertical beam increases and the mean square of the horizontal beam decreases. This feature is belonging to the characteristics of linear vibration absorbers due to inertia coupling. The corresponding response curves in normal coordinates are shown in fig. (7b). The square points (empty or full) are belonging to the first normal mode which obviously predominates the response. It is also seen that as the vertical mass moves downward, the model starts to behave like a linear single degree-of-freedom system whose mean square is given by the relationship[17]

$$E[y^2] = D/(\zeta\omega^3 m^2) \quad (6)$$

where m, ω and ζ are the mass, natural frequency, and damping ratio of the system, respectively. 2D

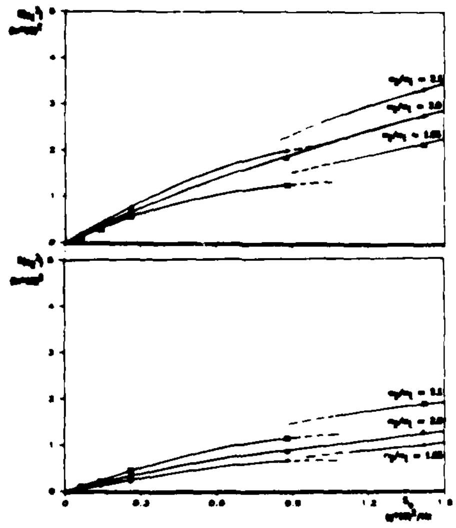

Fig. (8a) Relationship between mean square responses of generalized coordinates and the excitation spectral density for various values of internal detuning.

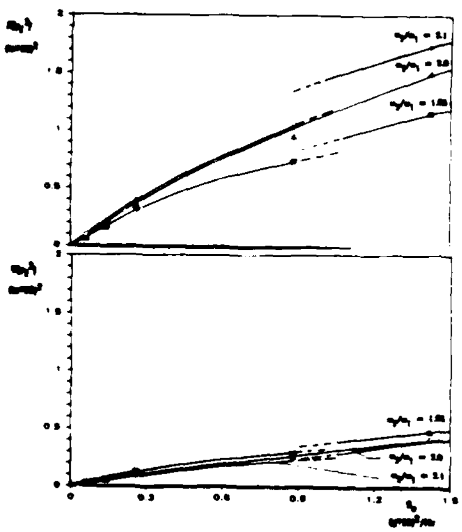

Fig. (8b) Relationship between mean square responses of normal coordinates and the excitation spectral density for various values of internal detuning.

(Measurements are taken for lower position of the upper mass).

is the excitation spectral density of a wide band random excitation.

It is clear that the trend of the full square points agrees with the linear solution (6) that the mean square response is inversely proportional to the cube of the first normal mode frequency.

In order to provide more insight to the system response statistics, the mean square response is plotted against the excitation spectral density level as shown in fig. (8a) for various values of internal detuning. It is seen that the mean squares of the two beams increase with the excitation spectral density up to a certain level above which the curves are discontinuous. The degree of discontinuity depends on the internal detuning. Any deviation from the exact internal detuning results in a strong discontinuity. This discontinuity means that the system is unstable in the mean square sense. Similar features were reported in the deterministic response of the same system by Haddow, et al.[5] The location of discontinuity is strongly dependent on the values of damping ratios and the internal detuning of the structure. Figure (8b) shows the mean square response of the normal coordinates against the excitation spectral density. The curves have the same trend of fig (8a).

III.2.2 Second Mode Excitation

The second normal mode is excited by a limited band random excitation of bandwidth 5 Hz and central frequency very close to the second normal mode frequency. Five levels of excitation spectral density ranging from 0.001 g^2/Hz to 0.022 g^2/Hz are selected. A general feature of the time history response records is that both amplitudes q_1 and q_2 increase with the levels of excitation as in the first mode excitation. The records also show that for all selected beam length ratios and for all levels of excitation spectral density, the vertical beam amplitude q_1 is always greater than the horizontal beam amplitude q_2. Another observation is that when the excitation level is held constant the amplitudes q_1 and q_2 increase slightly as the beam length ratio increases. For small levels of excitation spectral density, the second normal mode is observed to have no interaction with the first mode. However, above a certain level of excitation spectral density, it is found that the first mode appears for a certain period of time and then disappears as the second mode takes over, and so on as shown in fig. (9a). This nonlinear interaction of the two normal modes is more clarified in fig. (9b). Under harmonic excitation, Haddow, et al.[5] reported similar energy exchange between the two modes. Furthermore, it was shown that the directly excited mode becomes saturated and energy is transferred to the first mode. In the present investigation, the energy transfer takes place not only under high levels of excitation spectral density but also when the the internal resonance is approaching the value 2 as vertical beam length is increasing.

The mean square responses of the generalized and normal coordinates are plotted against the internal detuning parameter r in figs. (10a) and (10b), respectively. The suppression effect of the excited mode takes place only when the vertical mass is moved downward as shown in fig. (10b) by the full triangular points. The second mode mean square (empty triangular points) increases with a corresponding decrease in the first mode mean square (as the vertical mass moves upward).

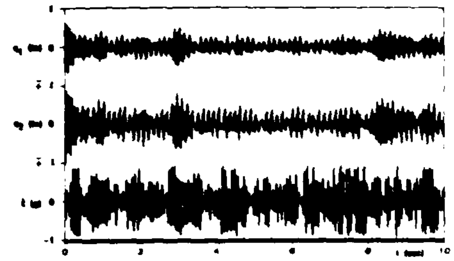

Fig. (9a) Time history response of second mode excitation under excitation spectral density of 0.022 g^2/Hz

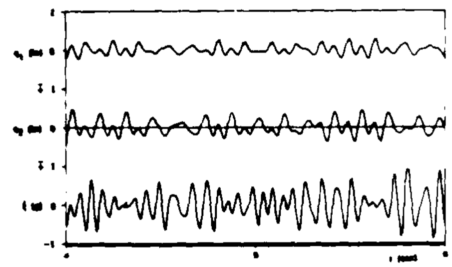

Fig. (9b) Magnification of time history response of second mode excitation showing attendance of first normal mode

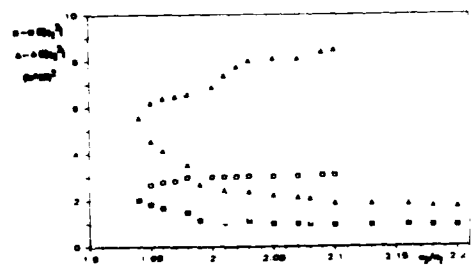

Fig. (10a) Mean square responses of generalized coordinates under second normal mode excitation

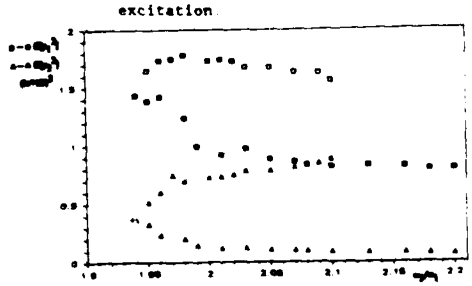

Fig. (10b) Mean square responses of normal coordinates under second normal mode excitation.

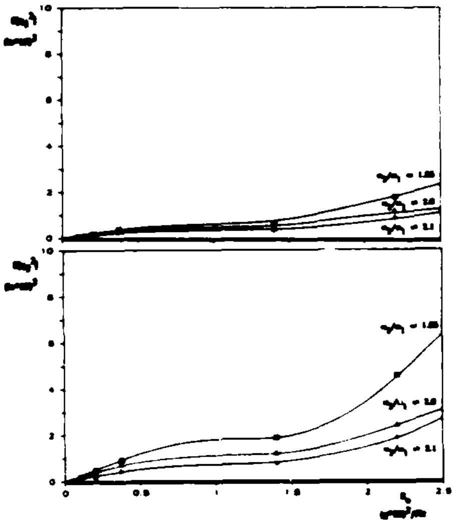

Fig. (11a) Relationship between mean square responses of generalized coordinates and excitation spectral density for various values of internal detuning.

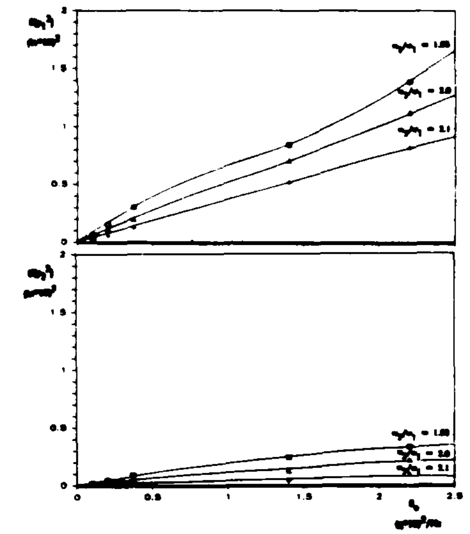

Fig. (11b) Relationship between mean square responses of normal coordinates and excitation spectral density for various values of internal detuning.

(Measurements are taken for lower position of the upper mass.)

Figures (11a) and (11b) show the influence of the excitation spectral density on the normal mode mean square responses of the generalized and normal coordinates, respectively. Figure (11b) indicates that the second normal mode mean square is relatively smaller than the first normal mode mean square response. This suppression effect is due to the nonlinear normal mode interaction. However, the saturation phenomenon, known in deterministic systems with quadratic nonlinearity, is not pronounced in the present results since the excitation is a random process which contains several frequencies each of which may excite the two modes. In deterministic excitation, the external and internal detunings are very important in establishing the saturation phenomenon.

III.2.3 TWO MODE EXCITATION

The purpose of these tests is to explore the behavior of the system under random excitation which covers both normal mode frequencies. Due to the shaker limitation the tests are conducted under single excitation spectral density level $S_o = 0.0026$ g^2/Hz. A sample of the time history response record is shown in fig. (12) which reveals the presence of the two modes. The amplitude of oscillation of each beam depends on the vertical mass location which yields the same internal resonance condition. Figures (13a) and (13b) show the dependence of the mean square response on the internal detuning in terms of generalized and normal coordinates, respectively. The full points reveal linear response characteristics while the empty points show a nonlinear interaction between the two modes.

IV. CONCLUSIONS AND DISCUSSION

The results of an experimental investigation of nonlinear modal interaction in a two-degree-of-freedom structural model under random excitation are reported. The modal equations of motion include linear and nonlinear inertia couplings of the generalized coordinates. The normal mode frequencies ω_1 and ω_2 of the model are adjusted to meet the internal resonance condition $r = 2.0$. This frequency ratio is found to exist at two beam length ratios $\ell_2/\ell_1 = 0.49$ and 0.71. At these locations the system response characteristics are completely different when the model is excited by a band limited random excitation. Three main series of tests are conducted to examine the system response behavior when the first and second modes are excited separately and when both modes are excited simultaneously.

When the first normal mode is externally excited it is found that the mean squares of the two modes are increasing monotonically with excitation spectral density. The response-excitation relationship is almost linear for small excitation levels. When the two beams are tuned to the exact internal resonance, the response-excitation relationship follows a continuous curve. For different internal detuning, the response curves exhibit a discontinuity. This feature is similar to the deterministic characteristics of the same model.[5]

When the second normal mode is externally excited, the system response is dominated by the second normal mode up to an excitation spectral density level above which the first normal mode attends and

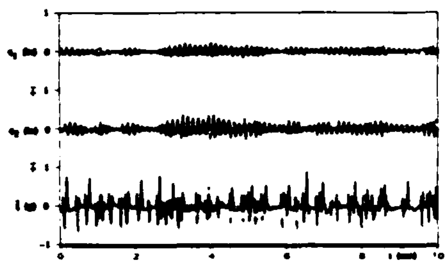

Fig. (12) Time history response of two normal modes excitation.

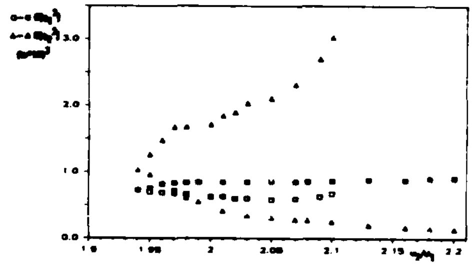

Fig. (13a) Mean square responses of generalized coordinates under band-limited random excitation of the two normal modes.

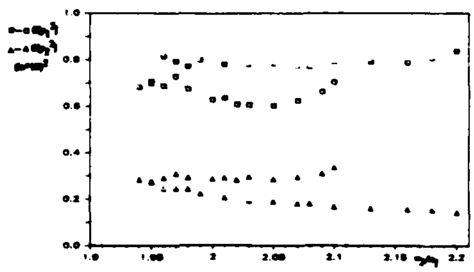

Fig. (13b) Mean square responses of normal coordinates under band-limited random excitation of the two normal modes.

[$S_o = 0.0026\ g^2/Hz$, points notation follows fig. (7)].

the two normal modes exhibit nonlinear interaction. Above this excitation level, the first normal mode shows large random motion which results in a suppression of the second mode. The results do not display any evidence for the existence of saturation phenomenon. The main features of the vibration autoparametric absorber effect reported theoretically by Ibrahim and Heo[12] are not exactly confirmed in the measured results. It is believed that the deviation from theory is attributed to the fact that the experimental excitation is a band limited random process, while in theory it is represented by a wide band random process. Another source of deviation is that the transformation into normal coordinates is not exact since it does not take into account the effect of structural damping. To eliminate this problem, it is convenient to adopt other models whose generalized and normal coordinates are the same. With new equipment and more powerful shakers the first author is currently undertaking an experimental research program supported by the NSF.

ACKNOWLEDGEMENT

This research is supported by a grant from the Air Force Office of Scientific Research under grant No AFOSR-85-0008. Dr. Anthony Amos is the program director.

REFERENCES

1. Evan-Iwanowski, R. M., "Resonance Oscillations in Mechanical Systems," Elsevier, New York, 1976.

2. Nayfeh, A. H. and Mook, D. T., "Nonlinear Oscillations," John Wiley & Sons, New York, 1979.

3. Schmidt, G. and Tondl, A., "Nonlinear Vibrations," Cambridge University Press, Cambridge, 1986.

4. Hatwal, H.; Mallik, A. K.; and Ghosh, A., "Forced Nonlinear Oscillations of an Autoparametric System, Part II: Chaotic Motion," ASME J. Applied Mechanics, Vol. 50(4), 1983, pp. 663-668.

5. Haddow, A. G.; Barr, A. D. S.; and Mook, D. T., "Theoretical and Experimental Study of Modal Interaction in a Two-Degree-of-Freedom Structure," J. Sound and Vibration, Vol. 97(3), 1984, pp. 451-473.

6. Bux, S. L. and Roberts, J. W., "Nonlinear Vibratory Interactions in Systems of Coupled Beams," J. Sound and Vibrations, Vol. 104(3), 1986, pp. 497-520.

7. Ibrahim, R. A., "Parametric Random Vibration," John Wiley & Sons, New York, 1985.

8. Piszczek, K. and Niziot, J., "Random Vibration of Mechanical Systems," John Wiley & Sons, New York, 1986.

9. Bolotin, V. V., "Random Vibration of Elastic Systems," Martinus and Nijhoff Publishers, The Hague, The Netherland, 1984.

10. Ibrahim, R. A. and Roberts, J. W., "Broad Band Random Excitation of a Two Degree-of-Freedom System with Autoparametric Coupling," J. Sound and Vibration, Vol. 44(3), 1976, pp. 335-348.

11. Ibrahim, R. A. and Roberts, J. W., "Stochastic Stability of the Stationary Response of a System with Autoparametric Coupling," Z. Angew Math Mech. (ZAMM), Vol. 57, 1976, pp. 643-649.

12. Ibrahim, R. A. and Heo, H., "Autoparametric Vibration of Coupled Beams under Random Support Motion," ASME J. Vibration, Acoustics, Stress, and Reliability in Design, Vol. 108, 1986, pp. 421-426.

13. Ibrahim, R. A. and Heo, H., "Stochastic Response of Nonlinear Structures with Parameter Random Fluctuations," AIAA Journal, Vol. 25(3), March 1987.

14. Roberts, J. W., "Random Excitation of a Vibratory System with Autoparametric Interaction," J. Sound and Vibration, Vol. 69(1), 1980, pp. 101-116.

15. Bendat, J. S. and Piersol, A. G., "Random Data: Analysis and Measurement Procedures," John Wiley & Sons, New York, 1971.

16. Lin, Y. K., "Probabilistic Theory of Structural Dynamics," McGraw-Hill Book Co., New York, 1967.

STRUCTURAL MODAL INTERACTION WITH COMBINATION INTERNAL RESONANCE UNDER WIDE BAND RANDOM EXCITATION

R. A. Ibrahim W. Li
Wayne State University
Department of Mechanical Engineering
Detroit, Michigan 48202

ABSTRACT.

This paper examines the nonlinear interaction of a three-degree-of-freedom structural model subjected to a wide band random excitation. The nonlinearity of the system results in different critical regions of internal resonance which have significant effect on the response statistics. With reference to combination internal resonance of the summed type the system response is analyzed by using the Fokker-Planck equation approach together with a non-Gaussian closure scheme. The non-Gaussian closure is based on the cumulant properties of order greater than three. As a first order approximation the scheme yields 209 first order differential equations in first through fourth order joint moments of the response coordinates. The analysis is carried out with the aid of the computer algebra software MACSYMA. The response statistics are determined numerically in the time and frequency (internal detuning) domains. Contrary to the Gaussian closure scheme the non-Gaussian closure solution yields a strictly stationary response in addition to a number of complex response characteristics not previously reported in the literature of the area of nonlinear random vibration. These include multiple solutions and jump phenomena (jump and collapse in the response mean squares) at internal detuning slightly shifted from the exact internal resonance condition. At exact internal resonance the system response possesses a unique limit cycle in a stochastic sense. The regions of multiple solutions are defined in terms of system parameters (damping ratios and nonlinear coupling parameter) and excitation spectral density level.

I. INTRODUCTION

The linear modeling of any dynamical system is commonly acceptable as long as the actual response characteristics to various types of loading follow the linear solution. However, under certain situations the system may experience certain complex characteristics that cannot be justified by the linear solution. These complex response features owe their origin to the system inherent nonlinearities. In structural dynamics the nonlinearity may take one of three classes [1,2]: elastic, inertia, and damping nonlinearities. Elastic nonlinearity stems from nonlinear strain-displacement relations which are inevitable. Inertia nonlinearity is derived, in Lagrangian formulation, from the kinetic energy. In multi-degree-of-freedom systems the normal modes may involve nonlinear inertia coupling which may give rise to what are effectively parametric instability phenomena within the system. The parametric action is not due to the external loading, as in the case of parametric vibration, but to the motion of the system itself and, hence, is described as autoparametric [3]. The main feature of autoparametric coupling is that the motion of one normal mode gives rise to loading of other modes through time-independent coefficients in the corresponding equation of motion. The natural frequencies of the normal modes involved in the autoparametric interaction are usually related by a linear algebraic relationship known as "internal resonance" condition.

According to the order of nonlinear coupling the system may exhibit certain types of response phenomena [4,5]. For example, systems with quadratic nonlinear inertia coupling may experience saturation phenomenon, amplitude jump, nonlinear resonance absorption effect, and multi-response behavior. For the case of two degree-of-freedom systems which possess third order internal resonance condition $\omega_2 = 2\omega_1$, it is found that if the second mode is externally excited it behaves, in the beginning, like a linear single degree-of-freedom system, and the first mode remains dormant. As the excitation amplitude reaches a certain critical level the first mode becomes unstable, and the second mode reaches an upper level. This mode is said to be saturated, and energy is then transferred to the first mode. This feature has been predicted theoretically and observed experimentally by Haxton and Barr [6] in their autoparametric vibration absorber; Nayfeh, et al. [7] and Mook, et al. [8] in ship dynamics involving nonlinear coupling between pitching and rolling motion; and Haddow, et al. [9] in nonlinear motion of coupled beams. For three degree-of-freedom systems possessing internal resonance of the summed type $\omega_3 = \omega_1 + \omega_2$ similar features were reported by Ibrahim and Woodall [10], Bux and Roberts [11] and Roberts and Zhang [12].

The response behavior of nonlinear systems under harmonic excitation may be changed if the excitation is a random process. The theory of nonlinear random vibration is not well developed as its deterministic counterpart. The theory of nonlinear random vibration requires advanced background in the theory of random processes and stochastic differential equations [13-15]. Few attempts have been made to predict the response statistics of nonlinear two-degree-of-freedom systems. These include the work of Ibrahim and Roberts [16,17], Schmidt [18], and Ibrahim and Heo [19,20] who examined the autoparametric interaction of two freedom systems subjected to wide band random excitations. The response statistics of these systems share a number of nonlinear characteristics of deterministic results such as nonlinear resonance absorption effect. However, the saturation phenomenon did not take place because the excitation contains a wide range of frequencies which result in a continuous variation of the external detuning. Recently, Ibrahim and Hedayati [21] have examined the effect of quadr ic nonlinear inertia coupling in a three-degree-of-freedom structure subjected to a wide band random excitation. They used the Fokker-Planck equation approach together with a Gaussian closure scheme. In the neighborhood of the combination internal resonance condition, $\omega_3 = \omega_1 + \omega_2$, the nonlinear interaction was found to take place between the second and third normal modes at an internal detuning parameter $r = \omega_3 / (\omega_1 + \omega_2) = 1.18$. At $r = 1.0$ all attempts converged to the linear random response statistics. The purpose of the present paper is to employ a non-Gaussian closure scheme which take into account the effect of the response deviation from normal distribution with the purpose of exploring three modal nonlinear interaction. For the sake of completeness a brief review of the results of reference [21] will be given in section VI. The effect of excitation spectral density level on the response characteristics will be examined in section VII.

II. BASIC MODEL AND EQUATIONS OF MOTION

Figure 1 shows a schematic diagram of an analytical model of an aircraft subjected to random excitation $F(t)$. The fuselage is represented by the main mass m_3, linear spring k_3 and dashpot c_3. Attached to the main mass on each side are two coupled beams with tip masses m_1 and m_2, stiffnesses k_1 and k_2, and lengths ℓ_1 and ℓ_2. In the analysis of the shown system only the symmetric motions of the two sides of the model are considered. Under random excitation the system response will be described by the generalized coordinates q_1, q_2, and q_3 as shown in the figure. The equations of motion are derived by applying Lagrange's equation

$$\frac{d}{dt}\left\{\frac{\partial L}{\partial \dot{q}}\right\} - \left\{\frac{\partial L}{\partial q}\right\} = \{Q_{NC}\} \tag{1}$$

where $L = T - V$,

The kinetic energy T is given by the expression

$$T = \frac{1}{2}\{m_1+m_2[1+(\frac{3\ell_2}{2\ell_1})^2]\}\,\dot{q}_1^2 + \frac{1}{2}\,m_2\dot{q}_2^2 + \frac{1}{2}(m_1+m_2+m_3)\dot{q}_3^2$$

$$+ \frac{3m_2\ell_2}{2\ell_1}\,\dot{q}_1\dot{q}_2 + (m_1+m_2)\dot{q}_1\dot{q}_3 + \frac{9m_2\ell_2}{20\ell_1^2}\,(q_1\dot{q}_1^2 + 5q_1\dot{q}_1\dot{q}_3) \tag{2}$$

$$+ \frac{3m_2}{2\ell_1}\,(\frac{q_1\dot{q}_1\dot{q}_2}{5} + q_1\dot{q}_2\dot{q}_3 + \dot{q}_1q_2\dot{q}_3 + \dot{q}_1^2\,q_2) + \frac{6m_2}{5\ell_2}(q_2\dot{q}_2\dot{q}_3 + \dot{q}_1q_2\dot{q}_2)$$

where a dot denotes differentiation with respect to time t. Neglecting the gravitational effects, the potential energy V is given by the elastic energy

$$V = 1/2(k_1q_1^2 + k_2q_2^2 + k_3q_3^2) \tag{3}$$

Substituting for T and V in equation (1) and bypassing energy dissipation due to damping (damping forces will be introduced later) yields the equations of motion in terms of the nondimensional coordinates $\bar{q}_i$

$$\omega_3^2 \begin{bmatrix} m_{11} & m_{12} & m_{13} \\ m_{12} & m_{22} & 0 \\ m_{13} & 0 & m_{33} \end{bmatrix} \begin{Bmatrix} \bar{q}_1'' \\ \bar{q}_2'' \\ \bar{q}_3'' \end{Bmatrix} + \begin{bmatrix} k_1 & 0 & 0 \\ 0 & k_2 & 0 \\ 0 & 0 & k_3 \end{bmatrix} \begin{Bmatrix} \bar{q}_1 \\ \bar{q}_2 \\ \bar{q}_3 \end{Bmatrix}$$

$$= \frac{1}{q_3^\circ} \begin{Bmatrix} 0 \\ 0 \\ F(\tau/\omega_3) \end{Bmatrix} - \frac{m_2q_3^\circ\omega_3^2}{\ell_1} \begin{Bmatrix} \bar{\Psi}_1 \\ \bar{\Psi}_2 \\ \bar{\Psi}_3 \end{Bmatrix} \tag{4}$$

where $\bar{q}_i = q_i/q_3^\circ$, $\quad \tau = \omega_3 t$

q_3° is taken as the root-mean-square of the main mass when all other parts are locked under forced excitation, ω_3 is taken as the third eigenvalue of the system, and

$$m_{11} = m_1 + m_2[1 + 2.25(\ell_2/\ell_1)^2], \qquad m_{22} = m_2$$

$$m_{33} = m_1 + m_2 + m_3, \qquad m_{12} = 1.5m_2(\ell_2/\ell_1)$$

$$m_{13} = m_1 + m_2$$

$$\begin{aligned}
\bar{\Psi}_1 &= 0.45\ (\ell_2/\ell_1)\ (2\bar{q}_1\bar{q}_1'' + \bar{q}'^2 + 5\bar{q}_1\bar{q}_3'') \\
&\quad + 1.5\ (0.2\bar{q}_1\bar{q}_2'' + \bar{q}_2\bar{q}_3'' + 2\bar{q}_2\bar{q}_1'' + 2\bar{q}_1'\bar{q}_2') \\
&\quad + 1.2\ (\ell_1/\ell_2)(\bar{q}_2\bar{q}_2'' + \bar{q}'^2) \\
\bar{\Psi}_2 &= 1.5\ (0.2\bar{q}_1\bar{q}_1'' - 0.8\bar{q}_1'^2 + \bar{q}_1\bar{q}_3'') \\
&\quad + 1.2(\ell_1/\ell_2)(\bar{q}_2\bar{q}_3'' + \bar{q}_2\bar{q}_1'') \\
\bar{\Psi}_3 &= 2.25(\ell_2/\ell_1)(q_1q_1'' + \bar{q}_1'^2) \\
&\quad + 1.5(\bar{q}_1\bar{q}_2'' + 2q_1'\bar{q}_2' + \bar{q}_2\bar{q}_1'') \\
&\quad + 1.2(\ell_1/\ell_2)(\bar{q}_2\bar{q}_2'' + \bar{q}_2'^2)
\end{aligned} \tag{5}$$

where a prime denotes differentiation with respect to the dimensionsionless time τ.

III. EIGENVALUES AND MODE SHAPES

The system eigenvalues are determined from the conservative linear part of the equations of motion

$$[m]\{\ddot{q}\} + [k]\{q\} = \{0\} \tag{6}$$

the characteristic equation of (6) is

$$\mathrm{Det}|[k] - \omega^2[m]| = 0 \tag{7}$$

where the roots of (7) give the eigenvalues ω_i of the system. Expanding the determinant gives the cubic equation

$$
\begin{aligned}
&\left(-1+\frac{m_{12}^2}{m_{11}m_{22}}+\frac{m_{13}^2}{m_{11}m_{33}}\right)\left(\frac{\omega}{\omega_{33}}\right)^6+\left[\left(\frac{\omega_{11}}{\omega_{33}}\right)^2\right. \\
&\left.+\left(\frac{\omega_{22}}{\omega_{33}}\right)^2\left(1-\frac{m_{13}^2}{m_{11}m_{33}}\right)+\left(1-\frac{m_{12}^2}{m_{11}m_{22}}\right)\right]\left(\frac{\omega}{\omega_{33}}\right)^4 \\
&-\left[\left(\frac{\omega_{11}}{\omega_{33}}\right)^2\left(\frac{\omega_{22}}{\omega_{33}}\right)^2+\left(\frac{\omega_{11}}{\omega_{33}}\right)^2+\left(\frac{\omega_{22}}{\omega_{33}}\right)^2\right]\left(\frac{\omega}{\omega_{33}}\right)^2+\left(\frac{\omega_{11}}{\omega_{33}}\right)^2\left(\frac{\omega_{22}}{\omega_{33}}\right)^2=0
\end{aligned}
\tag{8}
$$

where the frequency parameters $\omega_{ii}=\sqrt{k_i/m_{ii}}$ are the natural frequencies of the individual components of the model. The IMSL (International Mathematical and Statistical Library) subroutine ZPOLR (Zeros of a Polynomial with real coefficients) is used to find the roots of equation (8). Figure (2) shows a sample of the dependence of the natural frequency ratio $r=\omega_3/(\omega_1+\omega_2)$ on the ratios ω_{11}/ω_{33} and ω_{22}/ω_{33} for beams of length ratio $\ell_2/\ell_1=0.25$, and mass ratios $m_2/m_1=0.5$, and $m_3/m_1=5.0$. The importance of these curves is to define the critical points where the structure possesses internal combination resonance $r=1.0$. It is seen that the most critical region is located on the curves belonging to the values of ω_{22}/ω_{33} ranging from 1 to 2. For the present analysis the curve corresponding to $\omega_{22}/\omega_{33}=1.4$ will be adopted. The mode shapes of the model corresponding to the three eigenvalues which satisfy the internal resonance condition $r=1.0$ are evaluated by the method of matrix decomposition [22] and are shown in fig. (3). The eigenvectors of the system will be used in section IV to construct the modal matrix [R].

IV. TRANSFORMATION INTO NORMAL COORDINATES

Equations (4) include linear and nonlinear dynamic coupling. It is convenient to eliminate the linear dynamic coupling by transforming equation (4) into principal coordinates Y_i, by using the transformation

$$\{q\} = [R]\{Y\} \tag{9}$$

where [R] is the modal matrix whose columns are the eigenvectors,

$$[R] = \begin{vmatrix} 1 & 1 & 1 \\ n_1 & n_2 & n_3 \\ \bar{n}_1 & \bar{n}_2 & \bar{n}_3 \end{vmatrix} \tag{10}$$

Rewriting equations (4) in terms of the principal coordinates in the matrix form

$$[m][R]\{Y''\} + [k][R]\{Y\} = \{F(\tau)\} - \{\psi(\underset{\sim}{Y},\underset{\sim}{Y}',\underset{\sim}{Y}'')\} \tag{11}$$

Premultiplying equation (11) by the transpose of the modal matrix results in diagonalizing the mass and stiffness matrices. The resulting equations involve nonlinear coupling and have the form

$$m_1\omega_3^2 \begin{bmatrix} \bar{M}_{11} & 0 & 0 \\ 0 & M_{22} & 0 \\ 0 & 0 & M_{33} \end{bmatrix} \begin{Bmatrix} Y_1'' \\ Y_2'' \\ Y_3'' \end{Bmatrix} + k_1 \begin{bmatrix} \bar{k}_{11} & 0 & 0 \\ 0 & k_{22} & 0 \\ 0 & 0 & k_{33} \end{bmatrix} \begin{Bmatrix} Y_1 \\ Y_2 \\ Y_3 \end{Bmatrix}$$

$$= \frac{1}{q_3^\circ} \begin{Bmatrix} \bar{n}_1 F(\tau/\omega_3) \\ \bar{n}_2 F(\tau/\omega_3) \\ \bar{n}_3 F(\tau/\omega_3) \end{Bmatrix} - \frac{m_2 q_3^\circ \omega_3^2}{\ell_1} \begin{Bmatrix} \psi_1 \\ \psi_2 \\ \psi_3 \end{Bmatrix} \tag{12}$$

where

$$M_{ii} = 1 + \alpha(1 + 2.25\beta^2 + 3\beta n_i + 2\bar{n}_i + n_i^2 + \bar{n}_i^2) + [1 + m_3/m_1)]\ \bar{n}_i^2 + 2\bar{n}_i$$

$$k_{ii} = 1 + (k_2/k_1)\ n_i^2 + (k_3/k_1)\ \bar{n}_i^2$$

$$\begin{aligned}\psi_i &= Y_1''\ (L_{i11}Y_1 + L_{i21}Y_2 + L_{i31}Y_3) + Y''_2(L_{i12}Y_1 + L_{i22}Y_2 + L_{i32}Y_3) \\ &+ Y_3''\ (L_{i13}Y_1 + L_{i23}Y_2 + L_{i33}Y_3) + M_{i11}Y_1'^2 + M_{i22}Y_2'^2 + M_{i33}Y_3'^2 \\ &+ M_{i12}Y_1'Y_2' + M_{i13}Y_1'\ Y_3' + M_{i23}Y_2'\ Y_3'\end{aligned}$$

$$\alpha = m_2/m_1\ , \qquad \beta = \ell_2/\ell_1$$

$$\begin{aligned}L_{ijk} &= 0.9\beta + 2.25\beta\bar{n}_k + 0.3n_k + 1.5n_j\bar{n}_k + 3n_j + (1.2/\beta)n_jn_k \\ &+ n_i[0.3 + 1.5\bar{n}_k + (1.2/\beta)n_j(1+\bar{n}_k)] + \bar{n}_i[2.25\beta + 1.5(n_j+n_k) + (1.2/\beta)n_jn_k]\end{aligned}$$

$$\begin{aligned}M_{ijk} &= 0.9\beta + 3(n_j+n_k) + (2.4/\beta)n_jn_k - \qquad (j \neq k) \\ &-2.4n_i + \bar{n}_i[4.5\beta + 3(n_j+n_k) + (2.4/\beta)n_jn_k]\end{aligned} \tag{13}$$

$$\begin{aligned}M_{i\ell\ell} &= 0.45\beta + 3n_\ell + (1.2/\beta)n_\ell^2 - \\ &- 1.2n_i + \bar{n}_i[2.25\beta + 3n_\ell + (1.2/\beta)n_\ell^2] \qquad (j = k = \ell)\end{aligned}$$

V. DIFFERENTIAL EQUATIONS OF RESPONSE MOMENTS

The response coordinates can be approximated as a Markov vector if the random excitation is represented by a zero mean physical white noise $W(\tau)$ having the autocorrelation function

$$R_w(\Delta\tau) = E[W(\tau)W(\tau+\Delta\tau)] = 2D\delta(\Delta\tau) \tag{14}$$

where 2D is the spectral density and $\delta(\ )$ is the Dirac delta function. This modeling is justified as long as the relevant Wong-Zakai [14] coorection term is preserved. In order to construct the response Markov vector the acceleration terms involved in the nonlinear functions $\underset{\sim}{\Psi}$ must be removed by successive elimination. In view of the complexity of the equations of motion the elimination process is performed by using the symbolics manipulation software MACSYMA. Equation (12) takes the new form

$$Y''_i + 2\zeta_i r_{i3} Y'_i + r_{i3}{}^2 Y_i = f_i W(\tau) + \varepsilon g_i(\underset{\sim}{Y}, \underset{\sim}{Y}'), \qquad i = 1,2,3 \tag{15}$$

where linear viscous damping terms have been introduced to account for energy dissipation, and

$$\omega_i{}^2 = (k_{ii}/M_{ii})\ (k_1/m_1) \qquad \varepsilon = q_3^\circ / \ell_1$$

$$r_{i3} = \omega_i/\omega_3 \qquad W(\tau) = \frac{1}{q^\circ{}_3\,\omega_3{}^2 m_1} F(\tau/\omega_3)$$

$$f_i = \bar{n}_i/M_{ii}$$

Introducing the transformation into the Markov state vector $\underset{\sim}{X}$

$$\{Y_1,\ Y'_1,\ Y_2,\ Y'_2,\ Y_3,\ Y'_3\} = \{X_1,\ X_2,\ X_3,\ X_4,\ X_5,\ X_6\} \tag{16}$$

equation (15) may be written in the standard form of Stratonovich differential equation

$$dX_i = F_i(\underset{\sim}{X},\tau)d\tau + \sum_{j=1}^{6} G_{ij}(\underset{\sim}{X},\tau)dB_j(\tau) \tag{17}$$

where the white noise $W(\tau)$ has been replaced by the formal derivative of the Brownian motion process $B(\tau)$, i.e.

$$W(\tau) = \sigma\, dB(\tau)/d\tau, \qquad \sigma^2 = 2D$$

Alternatively, equation (17) may in turn be transformed into the Ito type equation

$$\begin{aligned} dX_i &= [F_i(\underset{\sim}{X},\tau) + \frac{1}{2}\sum_{k=1}^{6}\sum_{j=1}^{6} G_{kj}(\underset{\sim}{X},\tau)\frac{\partial G_{ij}(\underset{\sim}{X},\tau)}{\partial X_k}]\, d\tau \\ &\quad + \sum_{j=1}^{6} G_{ij}(\underset{\sim}{X},\tau)\, dB_j(\tau) \end{aligned} \tag{18}$$

where the double summation expression is the called the Wong-Zakai (or Ito) correction term [14].

The system stochastic Ito equations are

$$dx_1 = x_2 d\tau, \qquad dx_3 = x_4 d\tau, \qquad dx_5 = x_6 d\tau$$

$$\begin{aligned} dx_2 = \{&2\,\xi_1 r_{13} x_2 - r_{13}^2 x_1 + (2\, b_1 \xi_1 r_{13} x_2 + r_{13}^2 x_1)(L_{111}x_1 + L_{121}x_3 + L_{131}x_5) \\ &+ (2\, b_1 \xi_2 r_{23} x_4 + b_1 r_{23}^2 x_3)(L_{112}x_1 + L_{122}x_3 + L_{132}x_5) \\ &+ (2\, b_1 \xi_3 x_6 + b_1 x_5)(L_{113}x_1 + L_{123}x_3 + L_{133}x_5) \\ &+ b_1[- M_{111}x_2^2 - M_{122}x_4^2 - M_{133}x_6^2 - M_{112}x_2x_4 - M_{123}x_4x_6 - M_{113}x_2x_6]\}d\tau \\ + \{&f_1 + c_{11}x_1^2 + c_{12}x_3^2 + c_{13}x_5^2 + c_{14}x_1x_3 + c_{15}x_1x_5 + c_{16}x_3x_5 \\ &+ c_{17}x_1 + c_{18}x_3 + c_{19}x_5\}dB \end{aligned}$$

$$
\begin{aligned}
dx_4 = \{ & 2\,\xi_2 r_{23} x_4 - r_{23}^2 x_3 + (2\,b_2 \xi_1 r_{13} x_2 + r_{13}^2 x_1)(L_{211} x_1 + L_{221} x_3 + L_{231} x_5) \\
& + (2\,b_2 \xi_2 r_{23} x_4 + b_1 r_{23}^2 x_3)(L_{212} x_1 + L_{222} x_3 + L_{232} x_5) \\
& + (2\,b_2 \xi_3 x_6 + b_2 x_5)(L_{213} x_1 + L_{223} x_3 + L_{233} x_5) \\
& + b_2[- M_{211} x_2^2 - M_{222} x_4^2 - M_{233} x_6^2 - M_{212} x_2 x_4 - M_{223} x_4 x_6 - M_{213} x_2 x_6]\}dt \\
+ \{ & f_2 + c_{21} x_1^2 + c_{22} x_3^2 + c_{23} x_5^2 + c_{24} x_1 x_3 + c_{25} x_1 x_5 + c_{26} x_3 x_5 \\
& + c_{27} x_1 + c_{28} x_3 + c_{29} x_5\}dB
\end{aligned}
$$

$$
\begin{aligned}
dx_6 = \{ & 2\,\xi_3 x_6 - x_5 + (2\,b_3 \xi_1 r_{13} x_2 + r_{13}^2 x_1)(L_{311} x_1 + L_{321} x_3 + L_{331} x_5) \\
& + (2\,b_3 \xi_2 r_{23} x_4 + b_3 r_{23}^2 x_3)(L_{312} x_1 + L_{322} x_3 + L_{332} x_5) \\
& + (2\,b_3 \xi_3 x_6 + b_3 x_5)(L_{313} x_1 + L_{323} x_3 + L_{333} x_5) \\
& + b_3[- M_{311} x_2^2 - M_{322} x_4^2 - M_{333} x_6^2 - M_{312} x_2 x_4 - M_{323} x_4 x_6 - M_{313} x_2 x_6]\}dt \\
& + \{f_3 + c_{31} x_1^2 + c_{32} x_3^2 + c_{33} x_5^2 + c_{34} x_1 x_3 + c_{35} x_1 x_5 + c_{36} x_3 x_5 \\
& \quad + c_{37} x_1 + c_{38} x_3 + c_{39} x_5\}dB
\end{aligned}
\qquad (19)
$$

where

$$b_i = \varepsilon\alpha/M_{ii}$$

$$c_{i1} = b_i \sum_{k=1}^{3} (b_k \sum_{j=1}^{3} f_j L_{i1k} L_{k1j})$$

$$c_{i2} = b_i \sum_{k=1}^{3} (b_k \sum_{j=1}^{3} f_j L_{i2k} L_{k2j})$$

$$c_{i3} = b_i \sum_{k=1}^{3} (b_k \sum_{j=1}^{3} f_j L_{i3k} L_{k3j})$$

$$c_{i4} = b_i[\sum_{k=1}^{3} (b_k \sum_{j=1}^{3} f_j L_{i1k} L_{k2j}) + \sum_{k=1}^{3} (b_k \sum_{j=1}^{3} f_j L_{i2k} L_{k1j})]$$

$$c_{i5} = b_i[\sum_{k=1}^{3} (b_k \sum_{j=1}^{3} f_j L_{i1k} L_{k3j}) + \sum_{k=1}^{3} (b_k \sum_{j=1}^{3} f_j L_{i3k} L_{k1j})]$$

$$c_{i6} = b_i[\sum_{k=1}^{3} (b_k \sum_{j=1}^{3} f_j L_{i2k} L_{k3j}) + \sum_{k=1}^{3} (b_k \sum_{j=1}^{3} f_j L_{i3k} L_{k2j})]$$

$$c_{i7} = - b_i \sum_{j=1}^{3} f_j L_{i1j}$$

$$c_{i8} = - b_i \sum_{j=1}^{3} f_j L_{i2j}$$

$$c_{i9} = - b_i \sum_{j=1}^{3} f_j L_{i3j}$$

The evolution of the probability density of the joint response coordinates $\underset{\sim}{X}$ is described by the Fokker-Planck equation

$$\frac{\partial p(\underset{\sim}{X},\tau)}{\partial \tau} = -\sum_{i=1}^{6} \frac{\partial}{\partial X_i} [a_i(\underset{\sim}{X},\tau)\ p\ (\underset{\sim}{X},\tau)] + \quad (20)$$

$$+ \frac{1}{2} \sum_{i=1}^{6} \sum_{j=1}^{6} \frac{\partial^2}{\partial X_i \partial X_j} [b_{ij}(\underset{\sim}{X},\tau)\ p(\underset{\sim}{X},)]$$

where $p(\underset{\sim}{X},\tau)$ is the response joint probability density function, and $a_i(\underset{\sim}{X},\tau)$ and $b_{ij}(\underset{\sim}{X},\tau)$ are the first and second incremental moments evaluated as follows

$$a_i(\underset{\sim}{X},\tau) = \lim_{\Delta\tau\to 0} \frac{1}{\Delta\tau} E[X_i(\tau + \Delta\tau) - X_i(\tau)]$$

$$(21)$$

$$b_{ij}(\underset{\sim}{X},\tau) = \lim_{\Delta\tau\to 0} \frac{1}{\Delta\tau} E[\{X_i(\tau+\Delta\tau)-X_i(\tau)\}\{X_j(\tau+\Delta\tau)-X_j(\tau)\}]$$

In order to construct the Fokker-Planck equation of the present system the coefficients a_i and b_{ij} are evaluated. In view of the complicated analytical manipulations involved in this section and subsequent sections the MACSYMA programming is used throughout the analysis of this paper. It is obvious that the system Fokker-Planck equation cannot be solved even for the stationary case. Instead, one may generate a general first order differential equation describing the evolution of response joint moments of any order. This equation is obtained by multiplying both sides of the Fokker-Planck equation by the scalar function $\Phi(\underset{\sim}{X})$

$$\Phi(\underset{\sim}{X}) = X_1^{k1} X_2^{k2} \ldots X_6^{k6} \quad (22)$$

and integrating by parts over the entire state space $-\infty < \underset{\sim}{X} < +\infty$. The boundary conditions are used

$$p(\underset{\sim}{X} \to -\infty) = p(\underset{\sim}{X} \to \infty) = 0 \quad (23)$$

The resulting moment equation is very long and it will not be listed in this paper. However, the general form of this equation is

$$m'_N = F_N(m_1, m_2, \ldots, m_N, m_{N+1}) \tag{24}$$

In deriving the moment equation the following notation is adopted

$$m_{k1,k2\ldots,k6} = \int_{-\infty}^{\infty}\ldots\int \; p(\underset{\sim}{X},\tau)\,\Phi(\underset{\sim}{X})\, dX_1 dX_2 \ldots dX_6 \tag{25}$$

Equation (24) constitutes a set of infinite coupled equations. In other words, the differential equation of order N contains moment terms of order N and N+1. In reference [21], these equations were closed via a closure scheme based on the assumption that the response process is very close to a normal process. However, the system mean square responses revealed that the nonlinear interaction took place only between two normal modes, instead of three, although the system was tuned to the combination internal resonance. In order to clarify this deficiency the system response will be further examined by a non-Gaussian closure based on the concept of cumulant-neglect.

VI. GAUSSIAN CLOSURE SOLUTION

This section briefly reviews the main results obtained in reference [21] for the sake of completeness. The moment equations were closed by setting all third order cumulants to zero, i.e.

$$\lambda_3[X_iX_jX_k] = E[X_iX_jX_k] - \sum^{3} E[X_i]E[X_jX_k] + 2E[X_i]E[X_j]E[X_k] = 0 \tag{26}$$

where the number over summation sign refers to the number of terms generated in the form of the indicated expression without allowing permutation of indices. Relation (26) is used to obtain expressions for third order moments in terms of first and second order moments. These expressions are then used to close the second order moment equations generated from the general equation (24). In this case one can generate 27 coupled equations in the first (6 equations) and second (21 equations) order moments. The solution of the closed 27 coupled moment equations is obtained numerically by using the IMSL DVERK Subroutine (Runge-Kutta-Verner fifth and sixth numerical integration method. Depending on the value of internal detuning parameter r the system response may be reduced to the linear response or may become quasi-stationary which deviates significantly from the linear solution. The numerical integration is carried out on the IBM-3081 computer which takes 61.08 seconds CPU time with accuracy 0.1D-06 for the case of quasi-stationary solution ($r = 1.18$). Figure (4) presents the transient and steady-state responses for $\zeta_i = 0.01$, $\varepsilon = 0.05$, and $r = 1.12$. The steady state solution converges to the stationary linear solution derived in reference [21]. For $r = 1.18$ the response significantly deviates from the linear solution. Figures (5) and (6) show the transient and steady state responses indicated by the dotted curves (G) for excitation spectral density $D/2\zeta_3 = 1.0$, damping ratios $\zeta_i = 0.01$, and nonlinear coupling parameter $\varepsilon =$ 0.025 and 0.05, respectively. The transient response shows that the autoparametric coupling takes place between the second and third normal modes in a form of energy exchange. It is seen that the steady state response does not achieve a stationary value but fluctuates between two limits. The values of the two limits are divided by the linear solution and the ratios are plotted against the detuning parameter r as shown in figs. (7) and (8) for two different values of the nonlinear coupling parameter ε. The region of autoparametric interaction is seen to become wider as the nonlinear coupling parameter increases and as the damping ratios ζ_i decrease. These two figures reveal the fact that the nonlinear interaction takes place within a small range of internal detuning parameter around $r = 1.18$ which is well remote from the exact internal resonance $r = 1.0$. The authors have made several attempts to determine the response statistics under the condition of exact internal resonance $r = 1.0$. However, all numerical solutions converge to the linear response and the Gaussian closure fails to predict any nonlinear interaction between the three modes at $r = 1.0$. Inspection of the frequency ratios ω_3/ω_2, ω_3/ω_1, and ω_2/ω_1, shown in fig. (9), reveal that at $r = 1.18$ the second and third modes are in exact internal resonance, i. e. $\omega_3 = 2\omega_2$. If one considers only the equations of motion which govern the nonlinear coupling of the second and third modes with the condition $\omega_3 = 2\omega_2$, the system moment equations are then reduced to 69 equations whose numerical solutions coincides with the response presented in figs. (7) and (8). It is obvious that the Gaussian closure scheme is not adequate to predict the nonlinear three modal interaction and this is the main reason for considering the non-Gaussian closure approach in the next section.

VII. NON-GAUSSIAN CLOSURE SOLUTION

The non-Gaussian closure scheme takes into account the effect of non-normality of the response probability density and thus is expected to provide adequate modeling for the system nonlinear random response. As a first order approximation the third and forth order cumulants will be considered in the analysis and all higher order cumulants are set to zero. In this case one has to generate moment equations up to fourth order. Fifth order moments which appear in the fourth order moment equations will be replaced by fourth and lower order moments by using the relationship

$$\begin{aligned}\lambda_5[X_iX_jX_kX_\ell X_m] = {} & E[X_iX_jX_kX_\ell X_m] - \sum^{5} E[X_i]E[X_jX_kX_\ell X_m] \\ & + 2\sum^{10} E[X_i]E[X_j]E[X_kX_\ell X_m] - 6\sum^{10} E[X_i]E[X_j]E[X_k]E[X_\ell X_m] \\ & + 2\sum^{15} E[X_i]E[X_jX_k]E[X_\ell X_m] - \sum^{10} E[X_iX_j]E[X_kX_\ell X_m] \\ & + 24E[X_i]E[X_j]E[X_k]E[X_\ell]E[X_m] = 0\end{aligned} \tag{27}$$

The number N of moment equations of order K is given by the relationship [14]

$$N = n(n + 1)(n + 2)\ldots(n + K - 1)/K! \tag{28}$$

where n is the number of state coordinates $\underset{\sim}{X}$. For the present problem one needs to generate 6 equations for first order moments, 21 equations for second order, 56 equations for third order and 126 equations for fourth order, with a total of 209 first order differential equations which are closed by using relation (27).

The 209 differential equations are solved by numerical integration by using the DVERK subroutine on the IBM3081 computer. For one complete time history response the numerical integration took 748.48 seconds CPU time (i.e. over 12 times the CPU time of the Gaussian closure solution) with accuracy of 0.1D-06. Figures (5) and (6) show the transient and steady state responses indicated by solid curves (NG) for r =1.18 which corresponds to two-modal interaction between second and third modes. Again the transient response shows nonlinear interaction in a form of energy exchange between second and third normal modes. Contrary to the Gaussian closure solution, it is seen that the steady state response achieves a strictly stationary solution. The numerical integration is carried out for the 209 equations at r = 1.0 to find out if the non-Gaussian closure predicts nonlinear three modal interaction. Figure (10) shows the transient and steady state mean square response for $\zeta_i = 0.01$, $\varepsilon = 0.05$. The CPU time taken for one complete time history record is 1414 seconds which is much longer than the CPU time for Gaussian closure solution. The fluctuations observed in the transient response are entirely dependent on the the initial conditions introduced in the numerical algorithm. For example all response records obtained with zero initial conditions do not show any fluctuations in the transient period.

Since, the non-Gaussian closure scheme yields a stationary solution it is possible to solve only for the steady state by setting the left hand sides of the 209 equations to zero and solve the resulting nonlinear algebraic equations numerically. The numerical solution is carried out by using the ZSPOW (Solve a System of Nonlinear Equations) subroutine on the IBM-3081 computer. The solution is obtained by assuming initial guessing (approximate) values for the roots of the equations. Convergence of the solution is reached when the initial roots are close to the exact solution. The decision of accepting valid roots is based on two main criteria. The first is the non-negativeness of the even order moments, and the second is to satisfy Schwarz's inequality. Another important criterion is the positiveness of the joint probability density of the response coordinates especially at the tails. However, in view of the problem complexity the authors did not inspect this criterion. It is noteworthy to mention that once the solution is obtained for one point, the solution of all subsequent points is generated with less effort. The CPU time for one point solution varies between 40 and 60 seconds depending on the initial guessing values, with accuracy of 0.1D-06.

The steady state solution is plotted against the internal detuning parameter r for various values of system parameters and excitation spectral density level. Figures (11) through (15) show three- and two-modal nonlinear interactions which occur at $r = 1.0$ and 1.18, respectively. It is seen that the regions of autoparametric interaction become wider as the nonlinear coupling parameter ε and excitation level $D/2\zeta_3$ increase and as the damping ratios decrease. For most system and excitation parameters used in fig. (11) through (14) the two modal interaction is stronger than the three modal interaction. Significant three modal interaction arises for relatively larger values of the nonlinear coupling parameter ε and small damping ratios ζ_i as shown in fig. (15).

Since the main objective of this study is to examine the random response characteristics of three modal interaction, attention is focused on the response characteristics in the neighborhood of exact internal resonance $r = 1.0$. The mean square responses of the three normal modes are plotted in figs. (16) through (21) for various values of nonlinear coupling parameter ε and damping ratios ζ_i. These figures demonstrate the development of complex response characteristics as the nonlinear coupling parameter increases and as the damping ratios decrease. The autoparametric interaction occurs between the three modes in such a manner that the mean square responses of the first two normal modes is always greater than the linear solution (>1.0) while it is less for the third normal mode. This means that the nonlinear interaction takes place between the first and second modes on one hand and the third mode on the other hand. A new feature of considerable interest is the contrast in the form of the mean square response curves above the exact detuning ratio $r > 1.0$ for a certain combination of system parameters and excitation level as shown in figs. (18) through (21). This is indicated by the multiple solutions over a finite portion of the internal detuning parameter. At points of vertical tangency the response mean squares exhibit the jump and collapse phenomena indicated by the arrows AB and CD, respectively, see fig. (18). Those solutions shown by the upper and lower branches BC and AD are verified by numerical integration. However, all numerical integration attempts made at points very close to the middle branch AC converge to either the upper or lower branches. This implies that the middle solution is always unstable which is analogous to a great extent to deterministic solutions of nonlinear systems. For systems with quadratic nonlinearity, the deterministic theory of nonlinear vibrations predicts similar phenomena.

The well known saturation phenomenon reported by Nayfeh and Mook [4] does not take place for dynamic systems with quadratic nonlinearity subjected to wide band random excitation since the excitation includes a wide range of frequencies which always excite the system normal modes. The influence of the excitation spectral density level $D/2\zeta_3$ upon the response mean squares is shown in fig. (22) damping ratios $\zeta_i = 0.002$ and coupling parameter $\varepsilon = 0.05$. This figure shows that the system has three possible solutions for the same excitation level only if the internal detuning is slightly shifted from the exact internal resonance $r = 1.0$. At points of vertical tangency the response mean square will experience the jump and collapse phenomena as shown by the arrows AB and CD, respectively.

Figures (18) through (21) reveal that the region of internal detuning over which multiple solutions take place is dependent on the nonlinear coupling parameter and damping ratios of the three normal modes. In order to define the region of multiple solutions a parametric study is carried out. The results are shown in fig. (23) which displays a set of regions of multiple solutions for various values of damping ratios. The threshold value of ε^* where the mean square responses bifurcate into multiple solutions is plotted as a function of damping ratios ζ_i in fig. (24).

VIII. CONCLUSIONS

With the advent of computer algebra software, such as MACSYMA, REDUCE, and FORMAC, complicated analyses of dynamic systems can be performed with less human mistakes. In the area of nonlinear oscillations [5] computer symbolic manipulations are used to derive the basic differential equations of motion of nonlinear systems and to transfer these equations into principal coordinates. It is believed that the symbolic computation will be widely used in the near future to analyze nonlinear systems with large dimensions.

The MACSYMA software is used to analyze the nonlinear random modal interaction of a three-degree-of-freedom structural model in the neighborhood of combination internal resonance of the summed type. The Fokker-Planck equation approach together with a non-Gaussian closure scheme are used to determine the response statistics. Contrary to the Gaussian closure scheme results, the non-Gaussian closure yields several new features of response characteristics. These include weak and strong three modal interaction, multiple solutions, and jump phenomena. Multiple solutions only occur over a finite region of internal detuning parameter which is slightly greater than the exact internal resonance condition. At exact internal combination resonance the system possesses a unique stable limit cycle.

ACKNOWLEDGMENT

This research is supported by a grant from the Air Force Office of Scientific Research under grant no. AFOSR-85-0008. Dr. A. Amos is the program director.

References

1. V. V. Bolotin 1964 The Dynamic Stability of Elastic Systems. Holden-Day, Inc., San Francisco.

2. A. D. S. Barr 1980 Proceedings of International Conference of Recent Advances in Structural Dynamics, Southampton, England, 545-568. Some Developments in Parametric Stability and Nonlinear Vibration.

3. N. Minorsky 1962 Nonlinear Oscillations Van Nostrand, New York.

4. A. H. Nayfeh and D. T. Mook 1979 Nonlinear Oscillations. New York: Wiley-Interscience.

5. G. Schmidt and A. Tondl 1986 Ninlinear Vibrations. Cambridge University Press, Cambridge, England.

6. R. S. Haxton and A. D. S. Barr 1972 Journal of Engineering for Industry 94, 119-125. The autoparametric vibration absorber.

7. A. H. Nayfeh, D. T. Mook and L. R. Marshal 1973 Journal of Hydronautics 7, 145-152. Nonlinear coupling of pitch and roll modes in ship motions.

8. D. T. Mook, L. R. Marshall and A. H. Nayfeh 1974 Journal of Hydronautics 8, 32-40. Subharmonic and superharmonic resonances in the pitch and roll modes of ship motions.

9. A. G. Haddow, A. D. S. Barr and D. T. Mook 1984 Journal of Sound and Vibration 97(3), 451-473. Theoretical and experimental study of modal interaction in a two-degree-of-freedom structure.

10. R. A. Ibrahim and T. D. Woodall 1986 Computer & Structures 22(4), 699-707. Linear and nonlinear modal analysis of aeroelastic structural systems.

11. S. L. Bux and J. W. Roberts 1986 Journal of Sound and Vibration 104(3), 497-520. Nonlinear vibratory interactions in systems of coupled beams.

12. J. W. Roberts and J. Z. Zhang 1987 Proceedings of the 5th International Modal Analysis Conference, 427-434, Imperial College, London. Nonlinear resonance absorption in vibratory systems.

13. V. V. Bolotin 1984 Random Vibration of Elastic Systems. Martinus Nijhoff Publishers, The Netherlands.

14. R. A. Ibrahim 1985 Parametric Random Vibration. John Wiley & Sons, New York.

15. K. Piszczek and J. Niziot 1986 Random Vibration of Mechanical Systems. John Wiley & Sons, New York.

16. R. A. Ibrahim and J. W. Roberts 1976 Journal of Sound and Vibration 44(3), 335-348. Broad band random excitation of a two degree-of-freedom system with autoparametric coupling.

17. R. A. Ibrahim and Roberts 1977 Zeitschrift fur Angewandte Mathematik und Mechanik (ZAMM) 57(9), 643-649. Stochastic stability of the stationary response of a system with autoparametric coupling.

18. G. Schmidt 1977 Stochastic Problems in Dynamics, 197-213, edited by B. L. Clarkson, Pitman, London. Probability densities of parametrically excited random vibration.

19. R. A. Ibrahim and H. Heo 1986 Journal of Vibration, Acoustics, Stress, and Reliability in Design 108(4),421-426. Autoparametric vibration of coupled beams under random support motion.

20. R. A. Ibrahim and H. Heo 1987 American Institute of Aeronautics and Astronautics Journal 25(2), 331-338. Stochastic response of nonlinear structures with parameter random fluctuations.

21. R. A. Ibrahim and Z. Hedayati 1986 Probabilistic Engineering Mechanics 1(4). Stochastic modal interaction in linear and nonlinear aeroelastic structures.

22. R. R. Craig 1981 Structural Dynamics: An Introduction to Computer Methods. John Wiley & Sons, New York.

Fig. (1) Schematic diagram of the model.

Fig. (2) Normal mode frequency ratios $r = \omega_3/(\omega_1+\omega_2)$ versus system parameters ω_{11}/ω_{33} for various of ω_{22}/ω_{33}.

Fig. (3) Mode shapes corresponding to the combination internal resonance $\omega_3 = \omega_1+\omega_2$.

Fig. (4) Transient and steady mean square responses according to Gaussian closure solutions for $\zeta_i = 0.01$, $\varepsilon = 0.05$, and $r = 1.12$. The steady state response converges to the stationary linear solution at $r = 1.12$.

Fig. (5) Transient (a) and steady state (b) responses according to Gaussian (G) and non-Gaussian (NG) closure solutions, for $\zeta_i = 0.01$, $\varepsilon = 0.025$, $\omega_3/(\omega_1+\omega_2) = 1.18$, $D/2\zeta_3 = 1.0$.

Fig. (6) Transient (a) and steady state (b) responses according to Gaussian (G) and non-Gaussian (NG) closure solutions, for $\zeta_i = 0.01$, $\varepsilon = 0.05$, $\omega_3/(\omega_1+\omega_2) = 1.18$, $D/2\zeta_3 = 1.0$.

Fig. (7) Gaussian closure solution yields two-modal interaction between second and third normal modes ($\varepsilon = 0.025$, $\zeta_i = 0.01$, $D/2\zeta_3 = 1.0$)

Fig. (8) Gaussian closure solution yields two-modal interaction between the second and third normal modes ($\varepsilon = 0.05$, $\zeta_i = 0.01$, $D/2\zeta_3 = 1.0$)

Fig. (9) Frequency ratios of two and three normal modes versus system parameters for $\omega_{22}/\omega_{33} = 1.4$, $m_2/m_1 = 0.5$, $m_3/m_1 = 5.0$, $\ell_2/\ell_1 = 0.25$.

Fig. (10) Non-Gaussian closure of nonlinear three-modal interaction for $\varepsilon = 0.05$, $\zeta_i = 0.01$, $D/2\zeta_3 = 1.0$.

Fig. (11) Non-Gaussian closure solution showing two-modal interaction at $r = 1.18$, and weak three-modal interaction at $r = 1.0$, for $\varepsilon = 0.025$, $\zeta_i = 0.01$, $D/2\zeta_3 = 1.0$.

Fig. (12) Non-Gaussian closure solution showing two-modal interaction at $r = 1.18$, and weak three-modal interaction at $r = 1.0$, for $\varepsilon = 0.025$, $\zeta_i = 0.01$, $D/2\zeta_3 = 2.0$.

Fig. (13) Non-Gaussian closure solution showing two-modal interaction at $r = 1.18$, and weak three-modal interaction at $r = 1.0$, for $\varepsilon = 0.05$, $\zeta_i = 0.01$, $D/2\zeta_3 = 1.0$.

Fig. (14) Non-Gaussian closure solution showing two-modal interaction at $r = 1.18$, and weak three-modal interaction at $r = 1.0$, for $\varepsilon = 0.06$, $\zeta_i = 0.01$, $D/2\zeta_3 = 1.0$.

Fig. (15) Non-Gaussian closure solution showing two-modal interaction at $r = 1.18$, and three-modal interaction at $r = 1.0$, for $\varepsilon = 0.05$, $\zeta_i = 0.003$, $D/2\zeta_3 = 1.0$.

Fig. (16) Non-Gaussian closure solution showing strong three-modal interaction for $\varepsilon = 0.025$, $\zeta_i = 0.004$, $D/2\zeta_3 = 1.0$.

Fig. (17) Non-Gaussian closure solution showing strong three-modal interaction for $\varepsilon = 0.05$, $\zeta_i = 0.004$, $D/2\zeta_3 = 1.0$.

Fig. (18) Manifestation of multiple solutions and jump phenomenon in three modal interaction for $\varepsilon = 0.05$, $\zeta_i = 0.002$, $D/2\zeta_3 = 1.0$.

Fig. (19) Manifestation of multiple solutions and jump phenomenon in three modal interaction for $\varepsilon = 0.05$, $\zeta_i = 0.001$, $D/2\zeta_3 = 1.0$.

Fig. (20) Manifestation of multiple solutions and jump phenomenon in three modal interaction for $\varepsilon = 0.075$, $\zeta_i = 0.004$, $D/2\zeta_3 = 1.0$.

Fig. (21) Development of complex response in the third normal mode mean square for $\varepsilon = 0.075$, $\zeta_i = 0.002$, $D/2\zeta_3 = 1.0$.

Fig. (22) Dependancy of mean square responses on the excitation spectral density, a region of multiple solutions for $\varepsilon = 0.05$, $\zeta_i = 0.002$.

Fig. (23) Region of multiple solutions for various values of ζ_i.

Fig. (24) Threshold value of ε above where the mean square responses have multiple solutions.

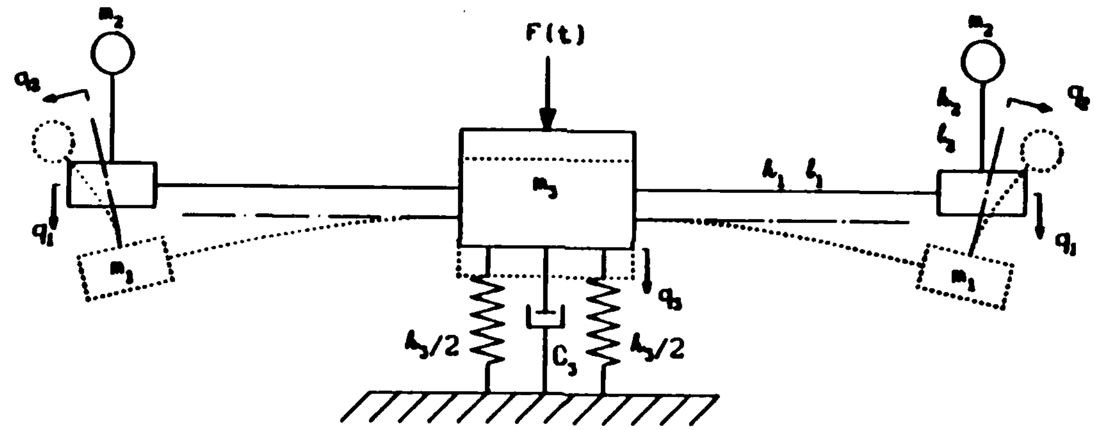

Fig (1)

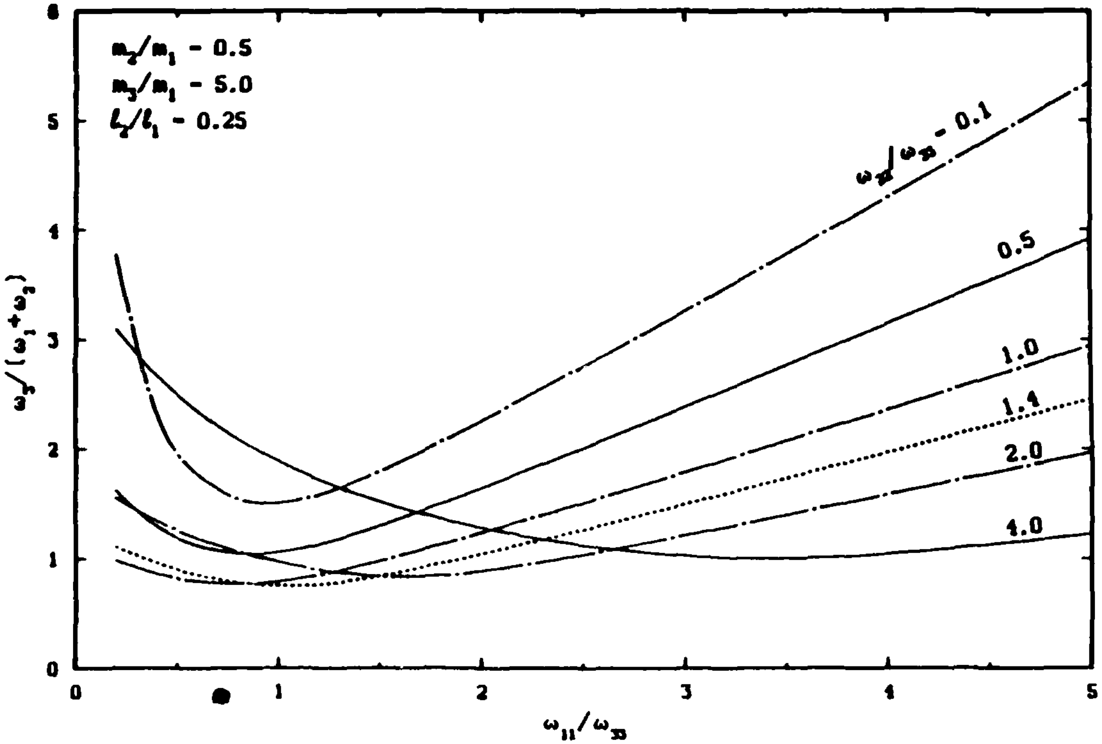
m_2/m_1 - 0.5
m_3/m_1 - 5.0
ℓ_2/ℓ_1 - 0.25
ω_{22}/ω_{33} - 0.1
0.5
1.0
1.4
2.0
4.0
$\omega_3/(\omega_1+\omega_2)$
ω_{11}/ω_{33}
0
1
2
3
4
5
6

Fig (2)

AD-A193 427 NONLINEAR STOCHASTIC INTERACTION IN AEROELASTIC STRUCTURES(U) TEXAS TECH UNIV LUBBOCK DEPT OF MECHANICAL ENGINEERING R A IBRAHIM 29 JAN 88 2/2

UNCLASSIFIED AFOSR-TR-88-0368 AFOSR-85-0008 F/G 20/4 NL

END

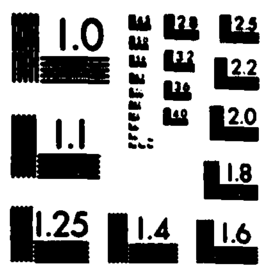
1.0
2.8
2.5
3.2
2.2
3.6
4.0
2.0
1.1
1.8
1.25
1.4
1.6

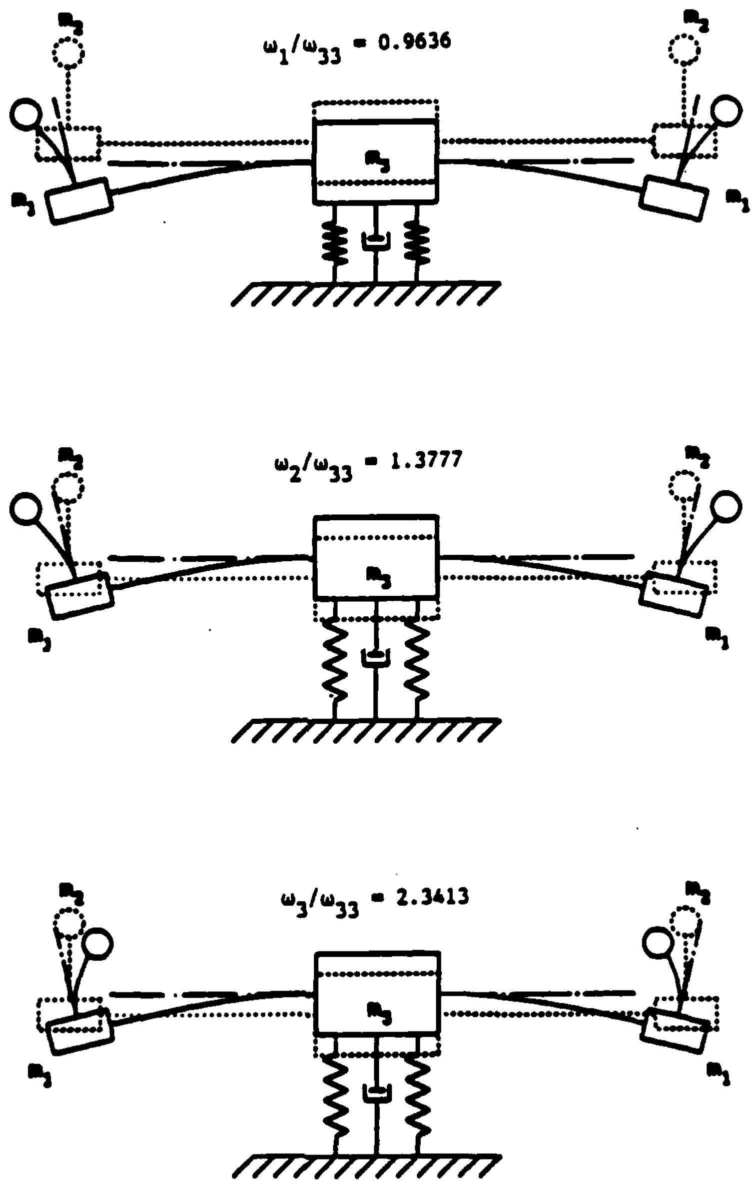

m2
ω1/ω33 = 0.9636
m2
m3
m1
m1
m2
ω2/ω33 = 1.3777
m2
m3
m1
m1
m2
ω3/ω33 = 2.3413
m2
m3
m1
m1

Fig. 3

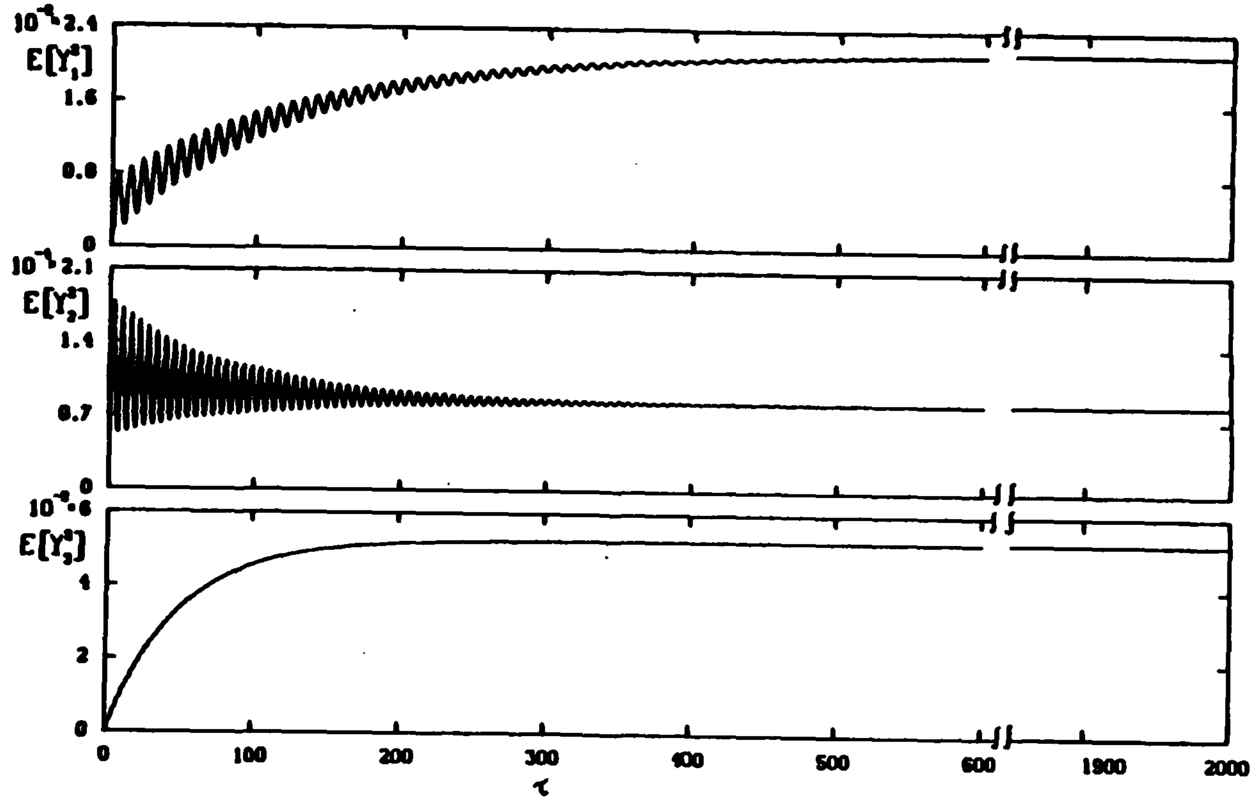

$E[Y_1^2]$
$E[Y_2^2]$
$E[Y_3^2]$
2.4
1.6
0.8
0
2.1
1.4
0.7
0
6
4
2
0
0
100
200
300
400
500
600
1900
2000
τ

Fig 4

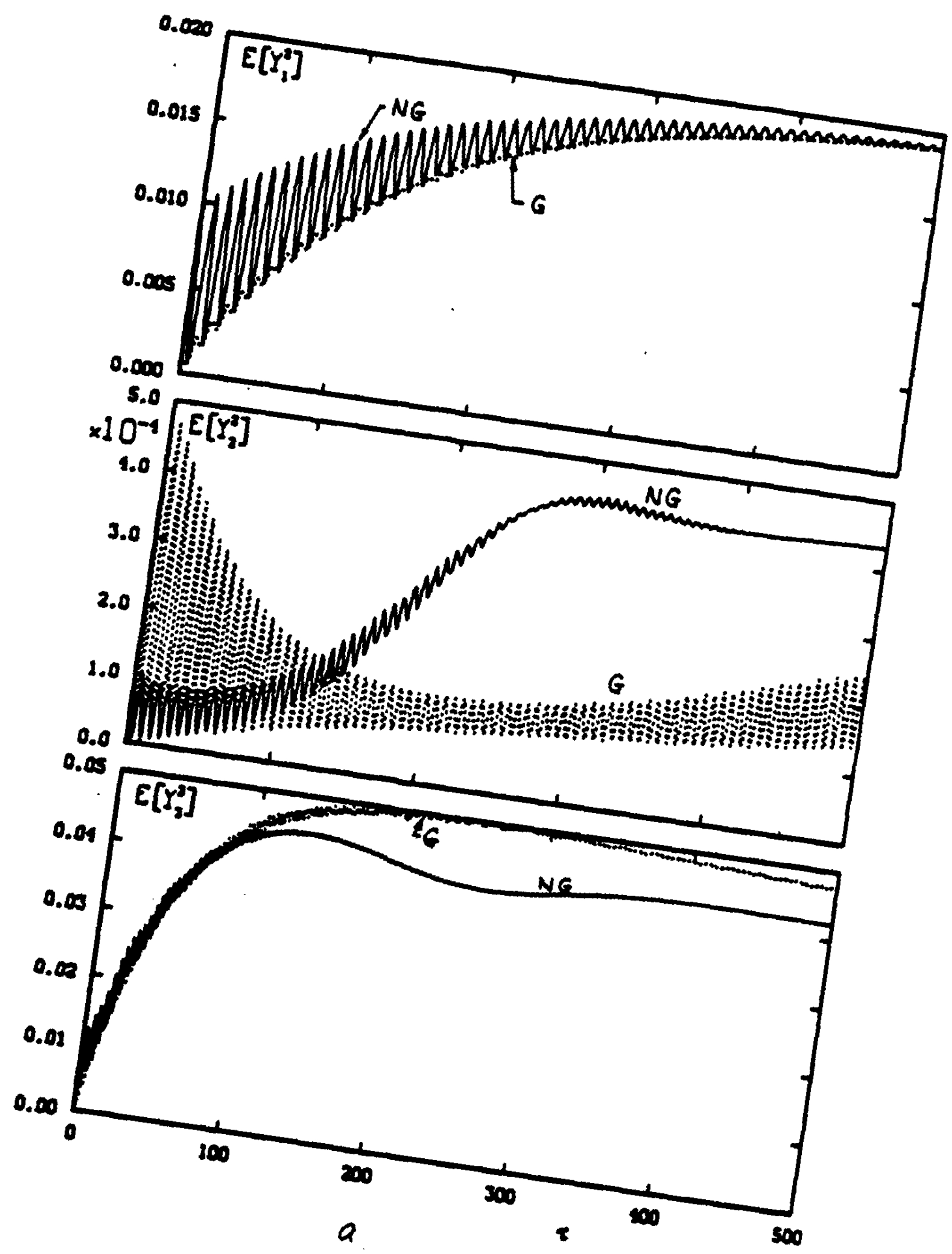
0.020
0.015
0.010
0.005
0.000
E[Y₁²]
NG
G
5.0
×10⁻⁴
4.0
3.0
2.0
1.0
0.0
E[Y₂²]
NG
G
0.05
0.04
0.03
0.02
0.01
0.00
E[Y₃²]
G
NG
0
100
200
300
400
500
τ
a

Fig. 5

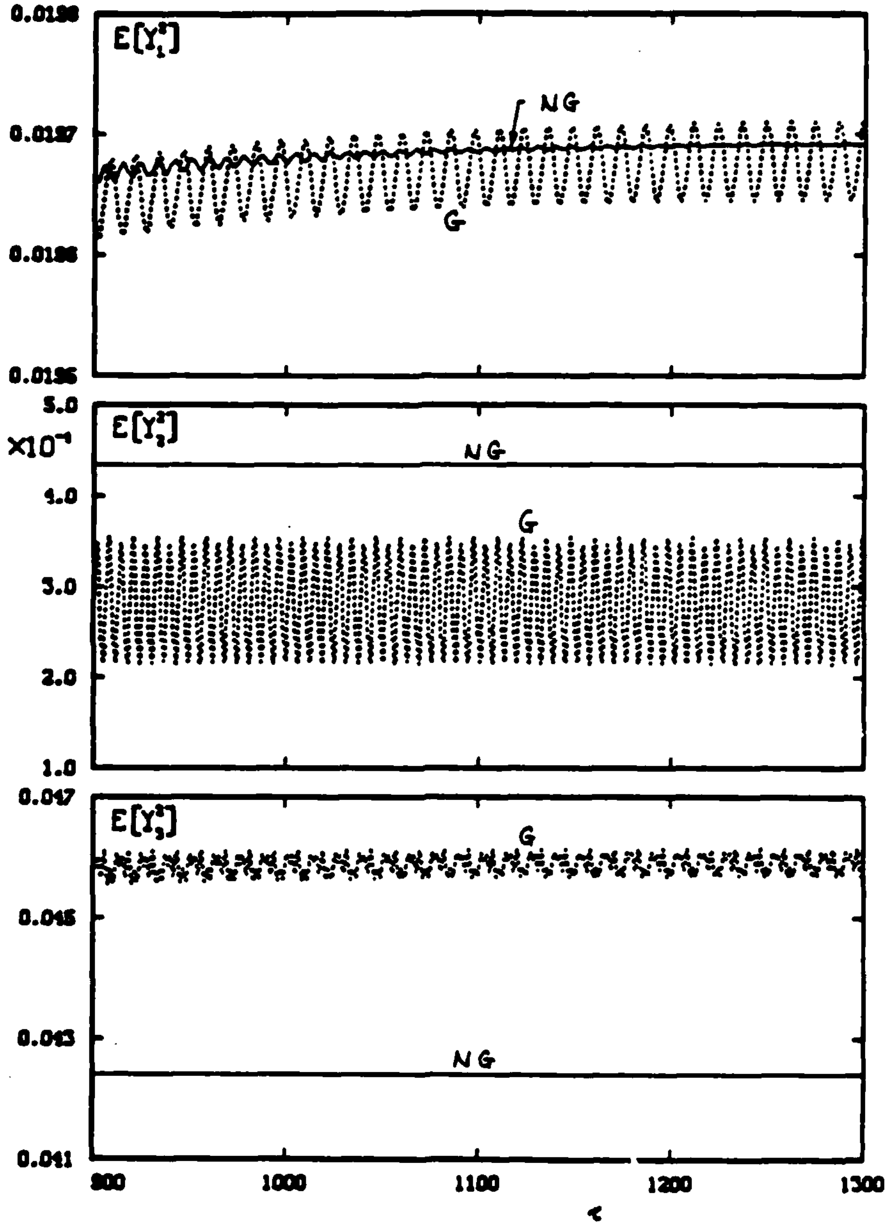
E[Y₁²]
NG
G
0.0188
0.0187
0.0186
0.0185
E[Y₂²]
×10⁻⁴
5.0
4.0
3.0
2.0
1.0
E[Y₃²]
0.047
0.045
0.043
0.041
900
1000
1100
1200
1300
t

b

Fig. 5

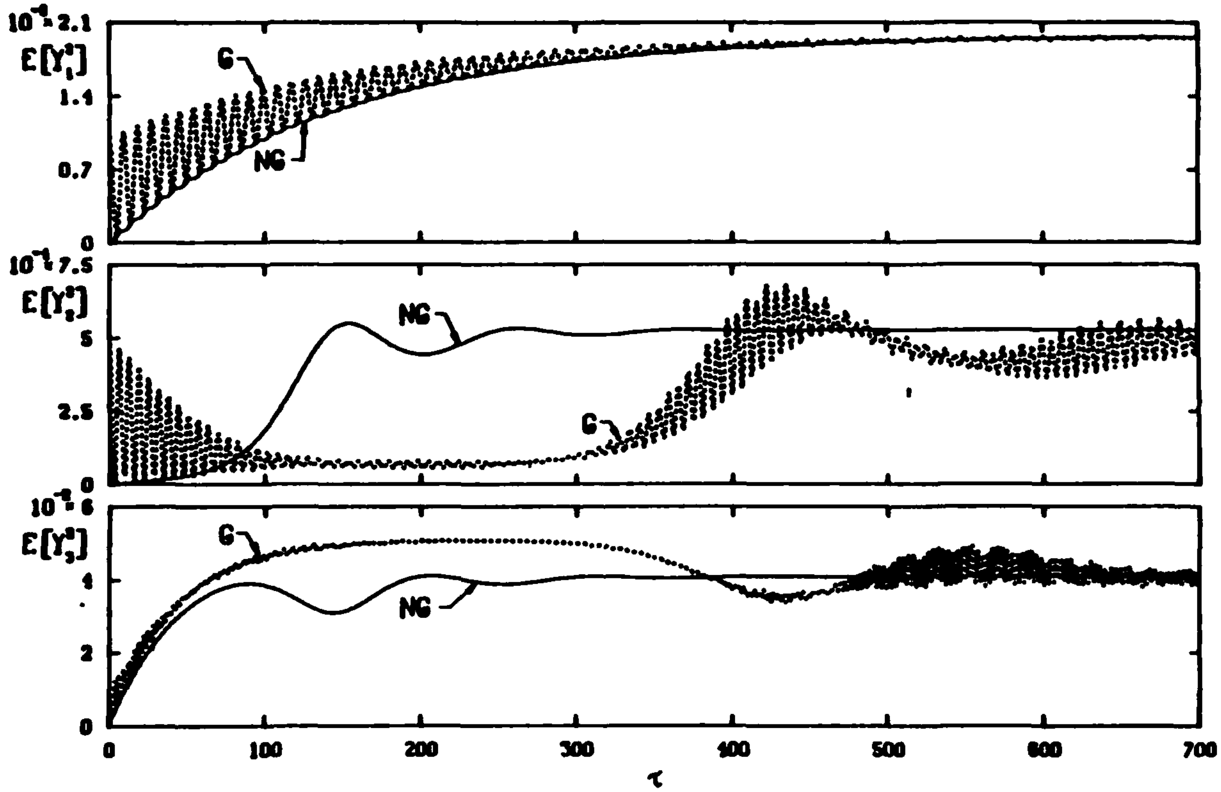

E[Y₁²]
2.1
1.4
0.7
0
G
NG
E[Y₂²]
7.5
5
2.5
0
E[Y₃²]
6
4
2
0
100
200
300
400
500
600
700
τ

(a)
Fig. 6

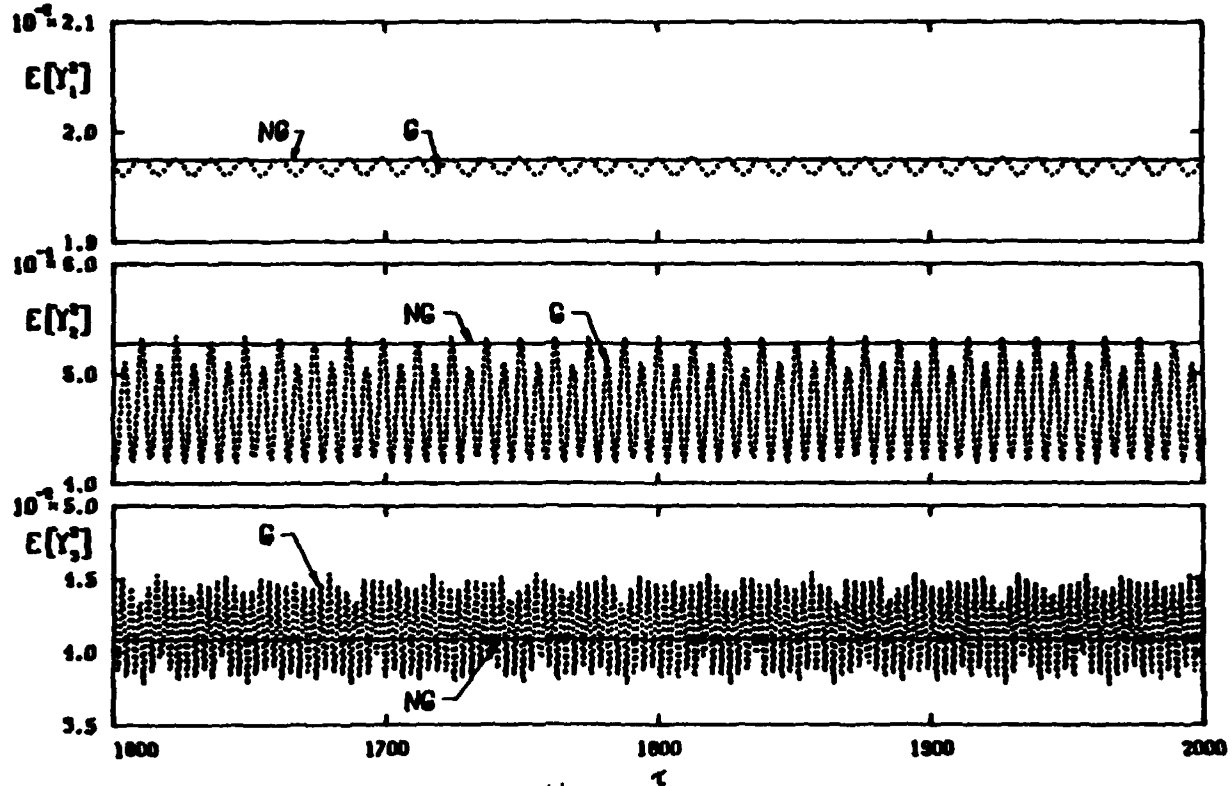

(b)

Fig 6

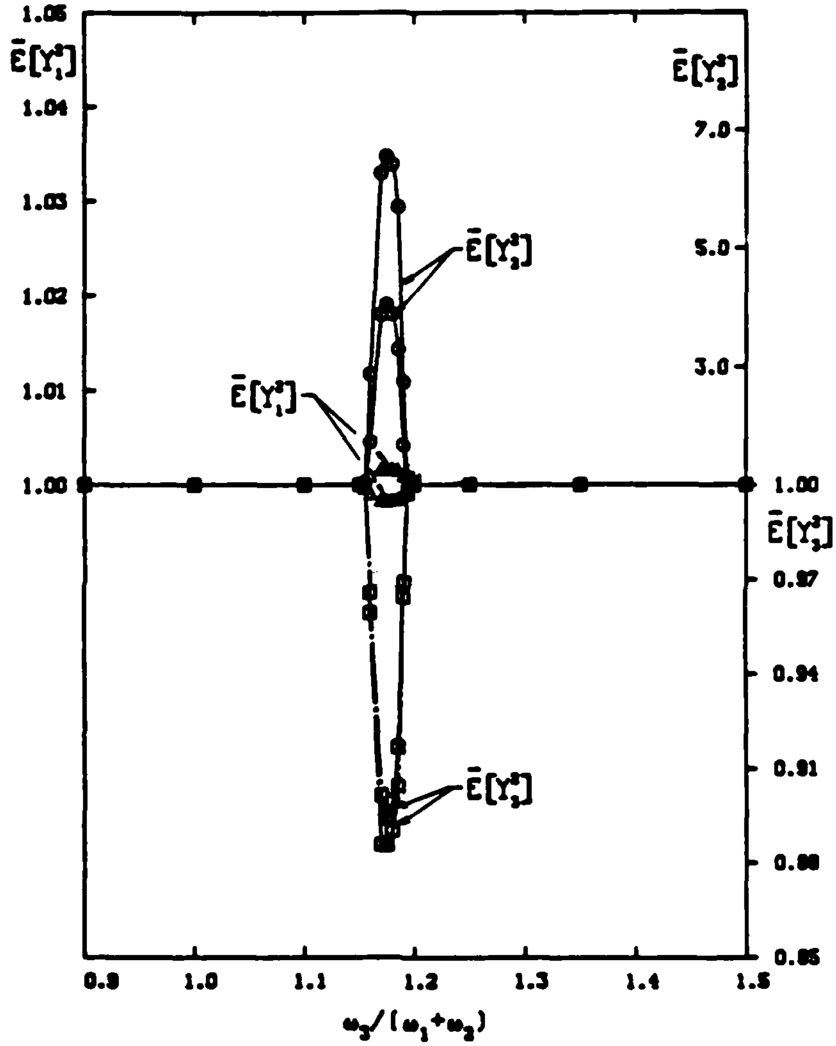

1.05
Ē[Y₁²]
1.04
1.03
1.02
1.01
1.00
Ē[Y₂²]
7.0
5.0
3.0
1.00
Ē[Y₃²]
0.97
0.94
0.91
0.88
0.85
Ē[Y₂²]
Ē[Y₁²]
Ē[Y₃²]
0.9
1.0
1.1
1.2
1.3
1.4
1.5
ω₃/(ω₁+ω₂)

Fig. 7

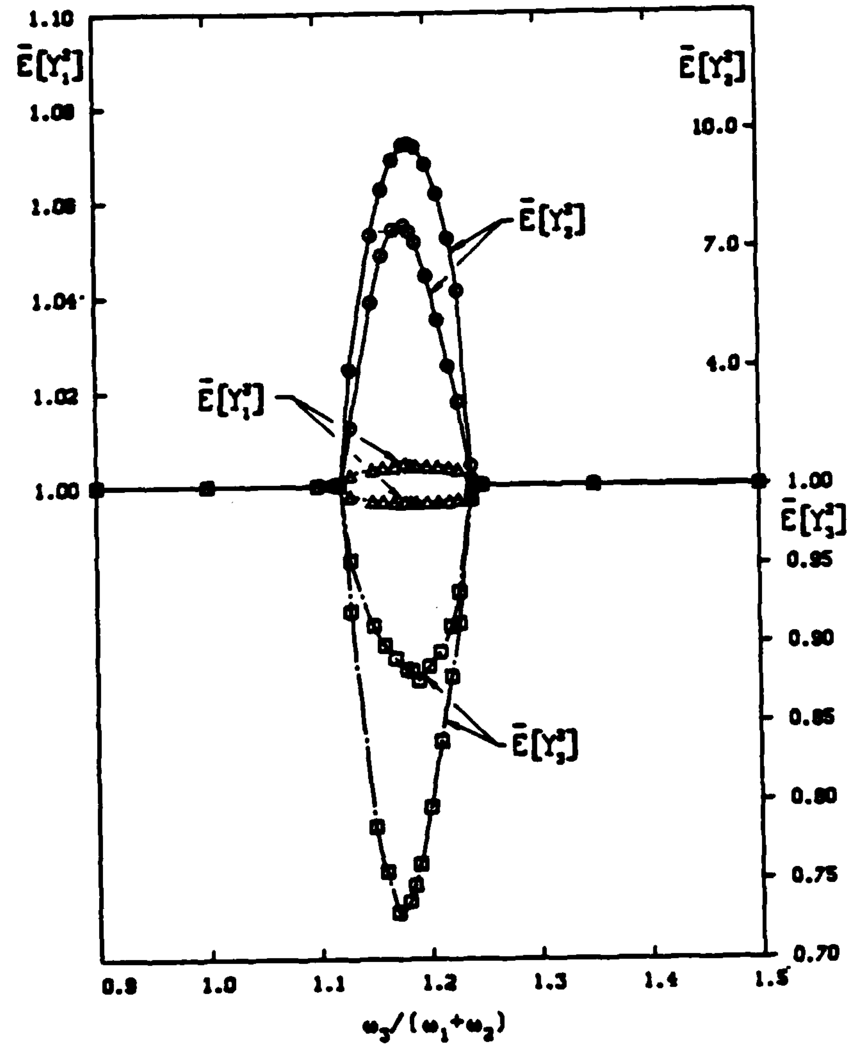
1.10
$\bar{E}[Y_1^2]$
1.08
1.06
1.04
1.02
1.00
$\bar{E}[Y_2^2]$
10.0
7.0
4.0
$\bar{E}[Y_2^2]$
$\bar{E}[Y_1^2]$
1.00
$\bar{E}[Y_3^2]$
0.95
0.90
0.85
0.80
0.75
0.70
$\bar{E}[Y_3^2]$
0.9
1.0
1.1
1.2
1.3
1.4
1.5
$\omega_3/(\omega_1+\omega_2)$

Fig. 8

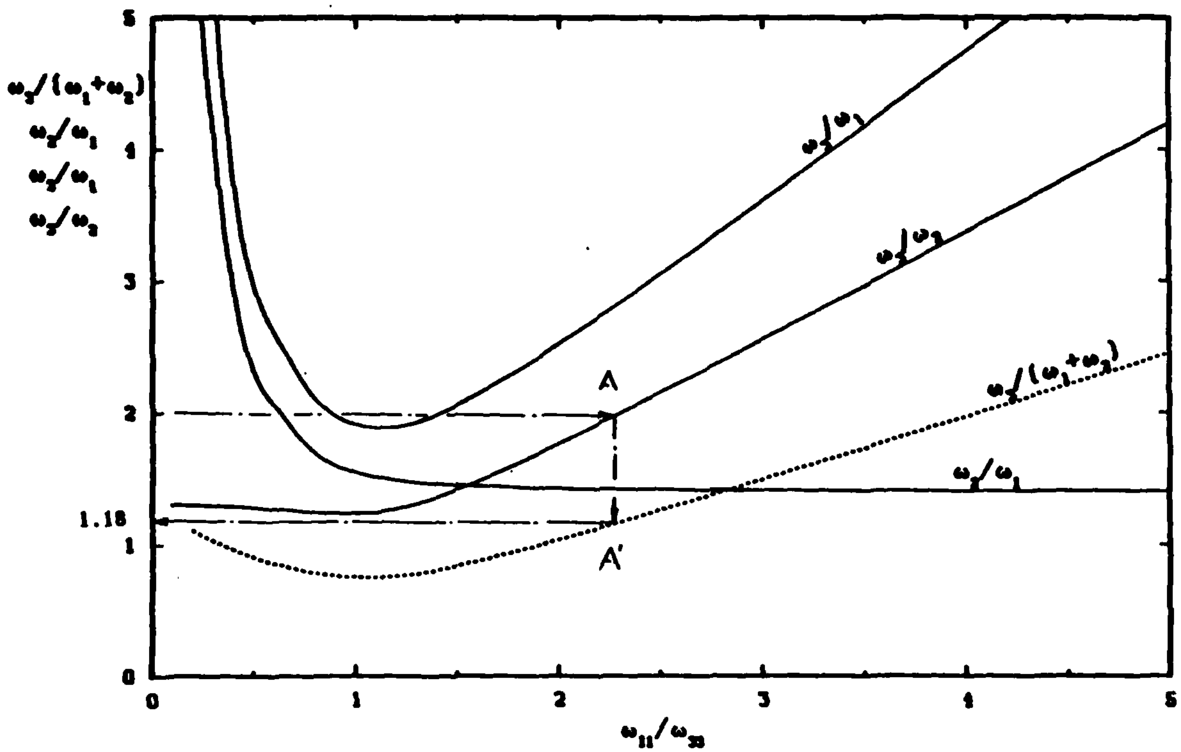

$\omega_3/(\omega_1+\omega_2)$
ω_3/ω_1
ω_2/ω_1
ω_3/ω_2
5
4
3
2
1.18
1
0
0
1
2
3
4
5
ω_{11}/ω_{33}
A
A'

Fig. 9

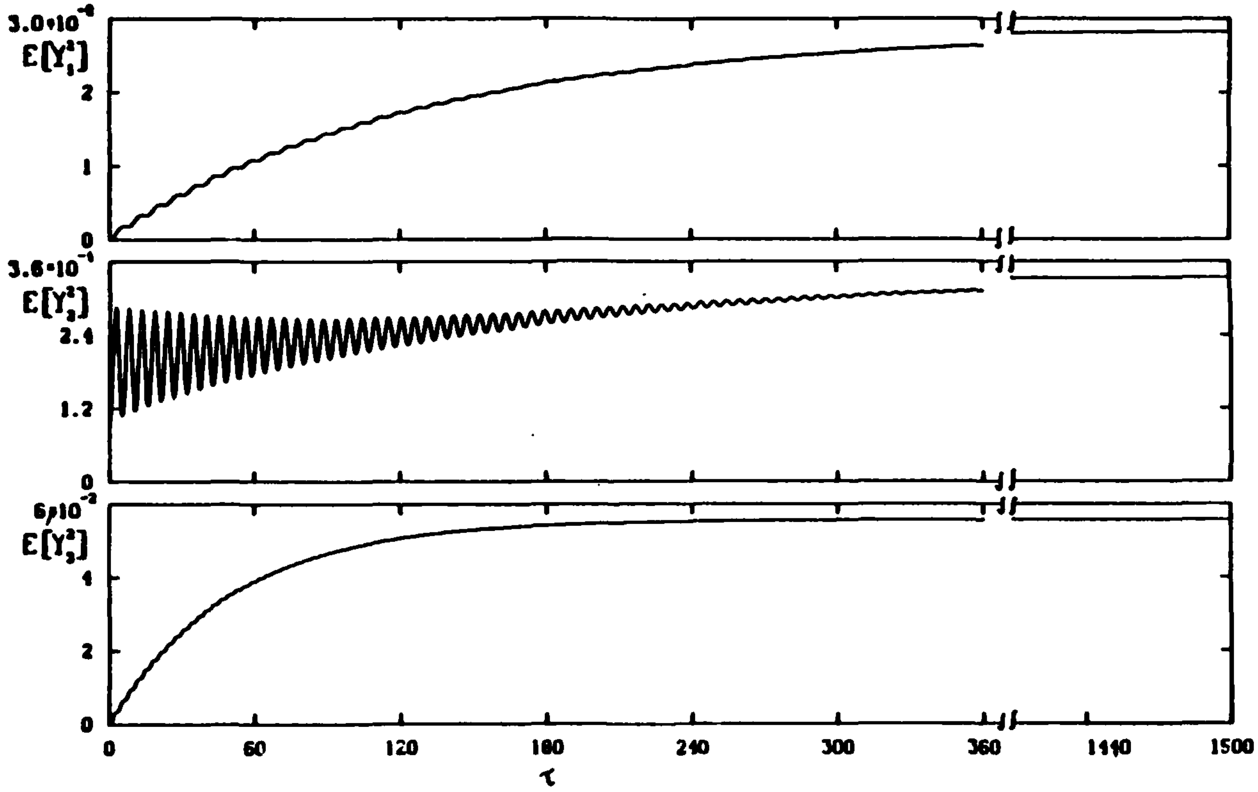
3.0·10^-4
E[Y_1^2]
2
1
0
3.6·10^-1
E[Y_2^2]
2.4
1.2
0
6·10^-2
E[Y_3^2]
4
2
0
0
60
120
180
240
300
360
1440
1500
τ

Fig. 10

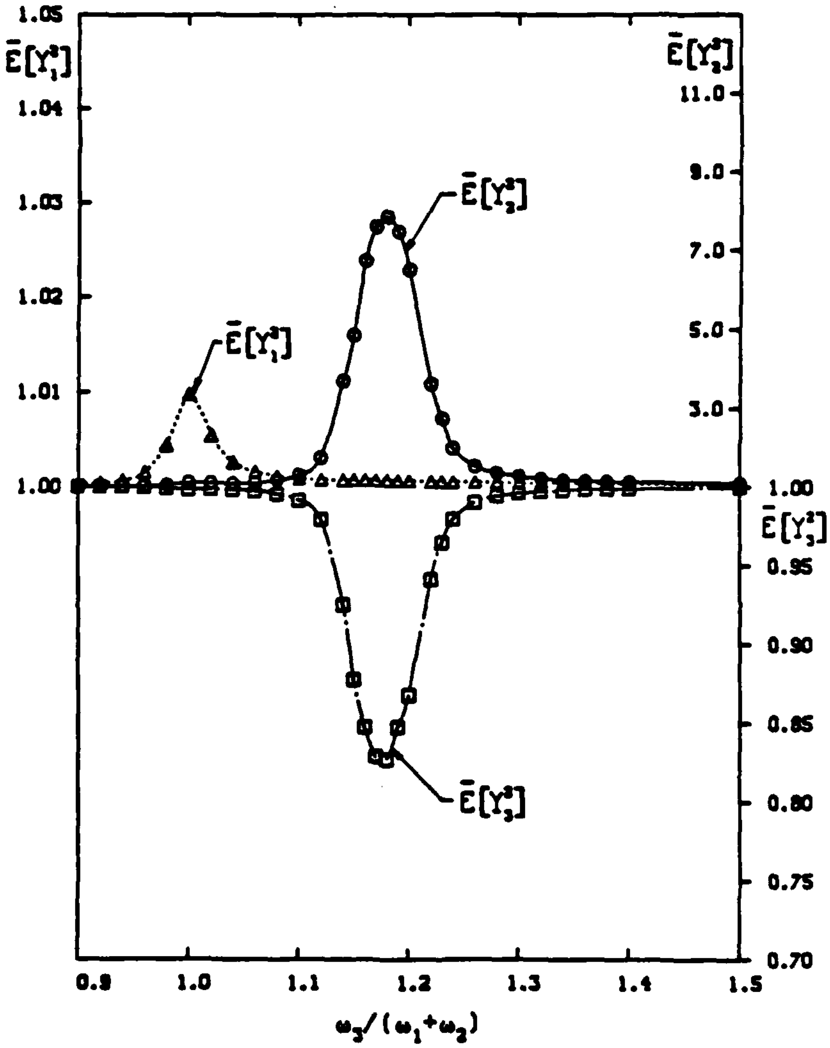

1.05
$\bar{E}[Y_1^2]$
1.04
1.03
1.02
1.01
1.00
$\bar{E}[Y_2^2]$
11.0
9.0
7.0
5.0
3.0
1.00
$\bar{E}[Y_3^2]$
0.95
0.90
0.85
0.80
0.75
0.70
$\bar{E}[Y_2^2]$
$\bar{E}[Y_1^2]$
$\bar{E}[Y_3^2]$
0.9
1.0
1.1
1.2
1.3
1.4
1.5
$\omega_3/(\omega_1+\omega_2)$

Fig. 11

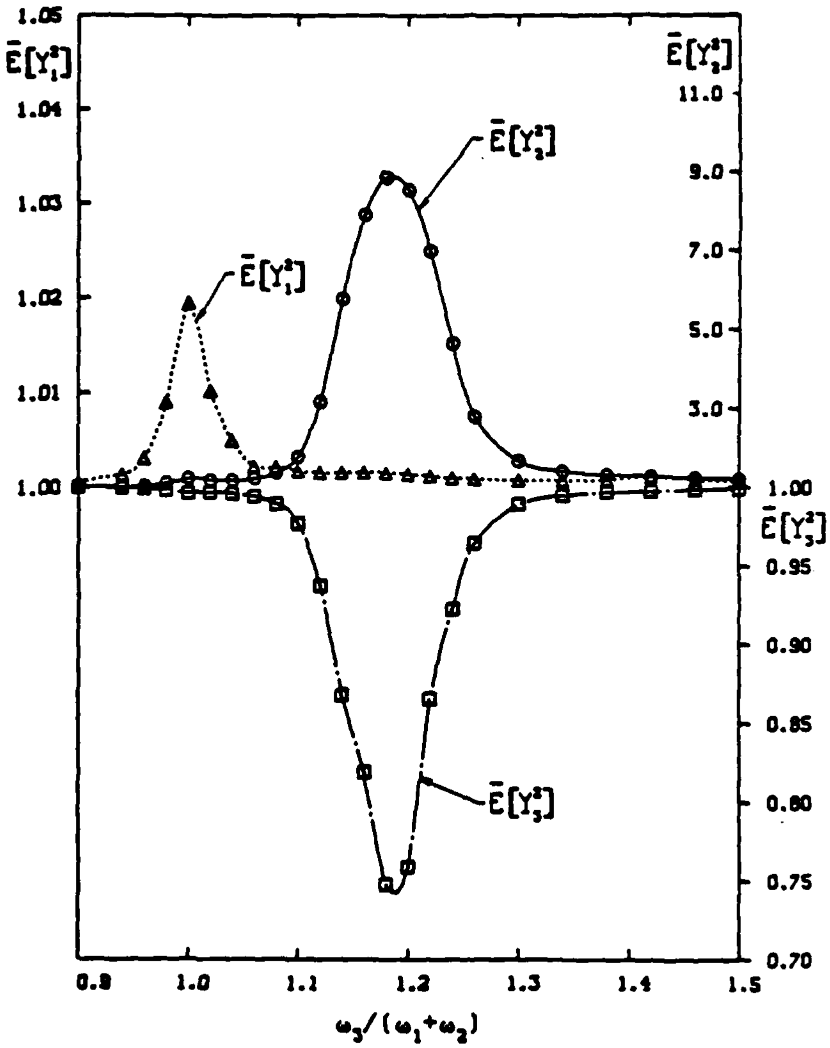
1.05
$\bar{E}[Y_1^2]$
1.04
1.03
1.02
1.01
1.00
$\bar{E}[Y_2^2]$
11.0
9.0
7.0
5.0
3.0
1.00
$\bar{E}[Y_3^2]$
0.95
0.90
0.85
0.80
0.75
0.70
$\bar{E}[Y_1^2]$
$\bar{E}[Y_2^2]$
$\bar{E}[Y_3^2]$
0.9
1.0
1.1
1.2
1.3
1.4
1.5
$\omega_3/(\omega_1+\omega_2)$

Fig. 12

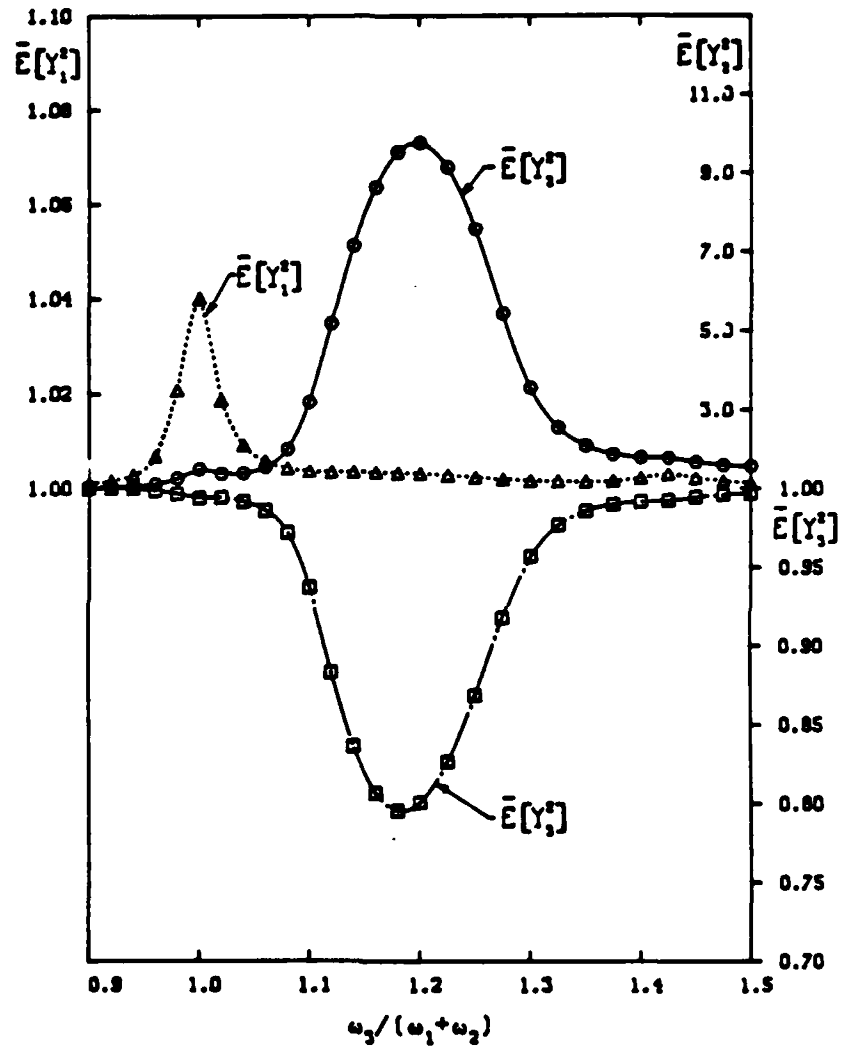

$\bar{E}[Y_1^2]$
$\bar{E}[Y_2^2]$
$\bar{E}[Y_3^2]$
1.10
1.08
1.06
1.04
1.02
1.00
11.0
9.0
7.0
5.0
3.0
1.00
0.95
0.90
0.85
0.80
0.75
0.70
0.9
1.0
1.1
1.2
1.3
1.4
1.5
$\omega_3/(\omega_1+\omega_2)$

Fig. 13

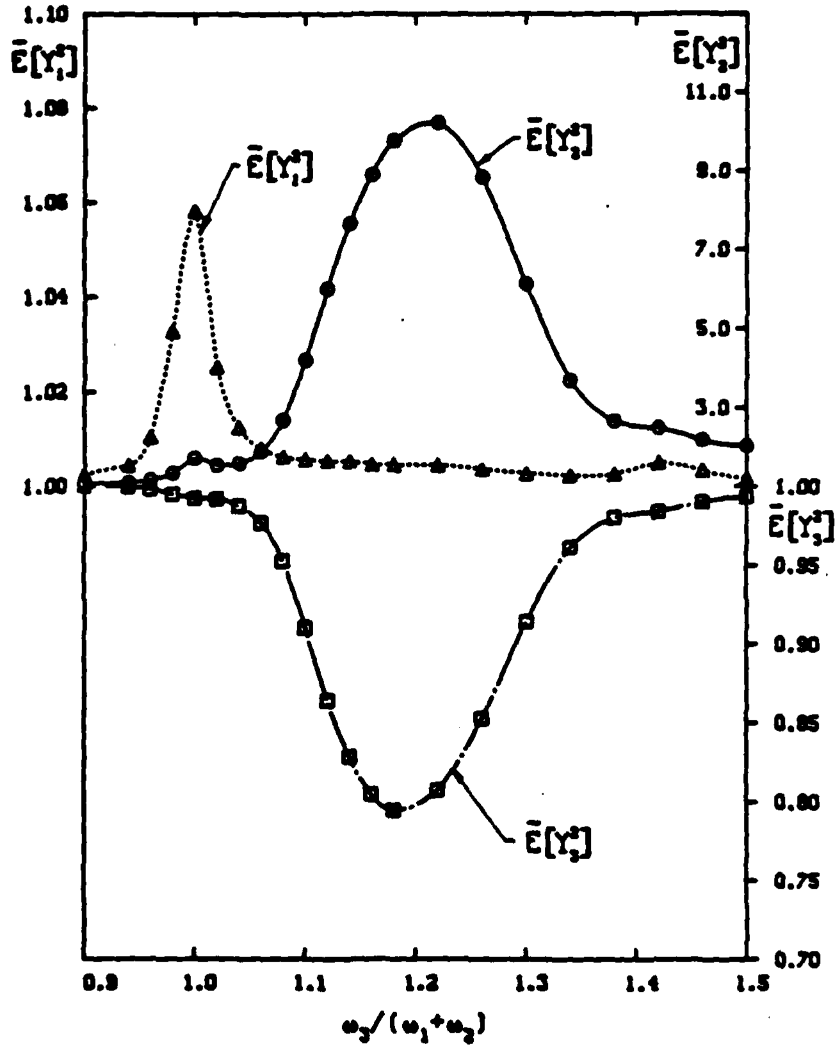

Ē[Y₁*]
Ē[Y₂*]
Ē[Y₃*]
1.10
1.08
1.06
1.04
1.02
1.00
11.0
9.0
7.0
5.0
3.0
1.00
0.95
0.90
0.85
0.80
0.75
0.70
0.9
1.0
1.1
1.2
1.3
1.4
1.5
ω₃/(ω₁+ω₂)

Fig. 14

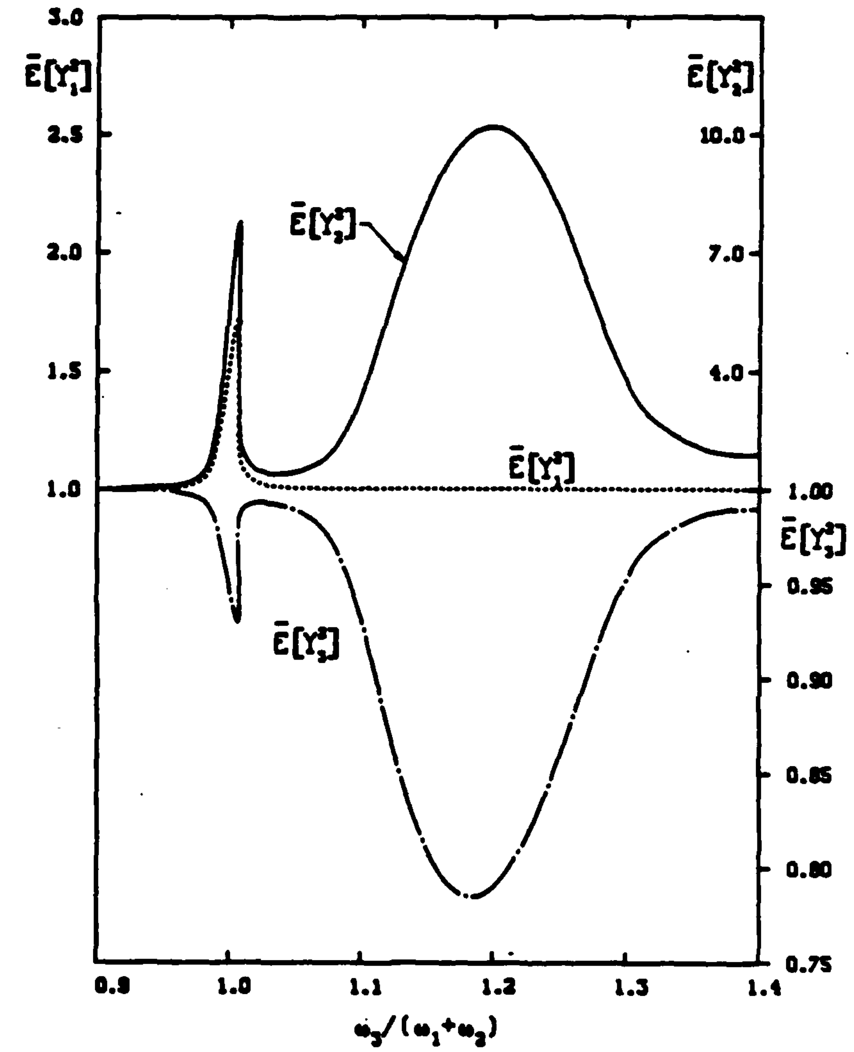
3.0
2.5
2.0
1.5
1.0
$\bar{E}[Y_1^2]$
$\bar{E}[Y_2^2]$
10.0
7.0
4.0
1.00
0.95
0.90
0.85
0.80
0.75
$\bar{E}[Y_3^2]$
0.9
1.0
1.1
1.2
1.3
1.4
$\omega_3/(\omega_1+\omega_2)$

Fig. 15

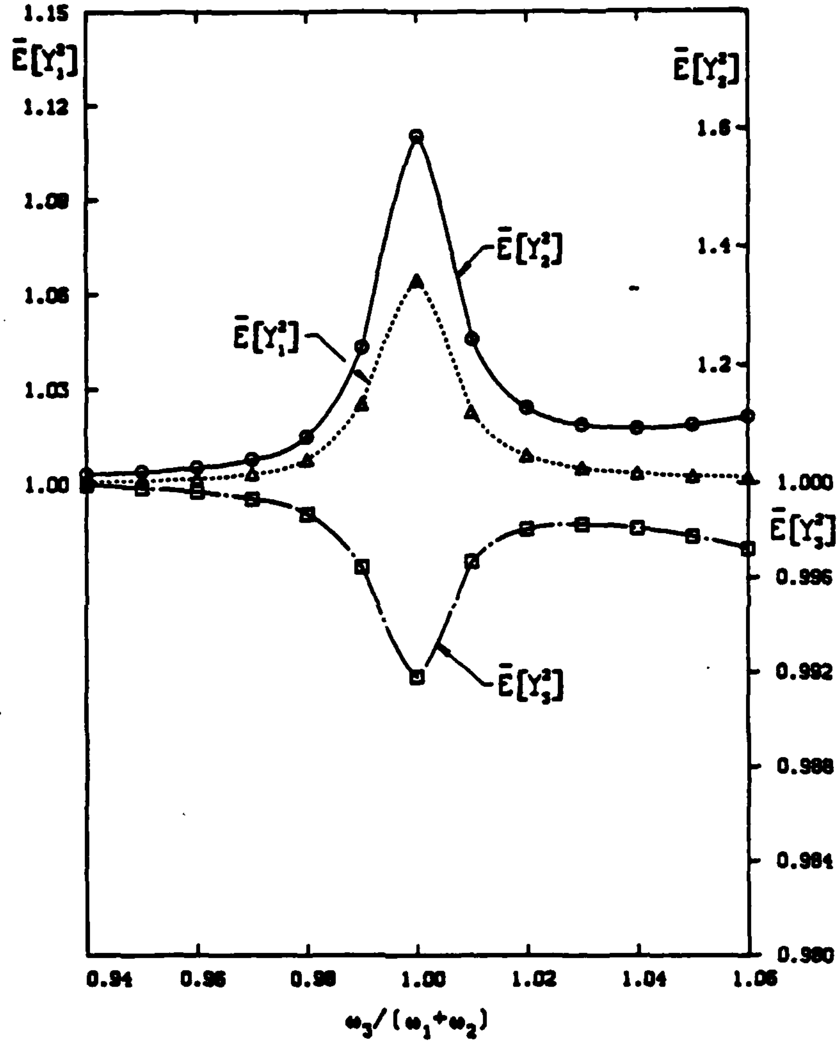
1.15
$\bar{E}[Y_1^2]$
1.12
1.09
1.06
1.03
1.00
$\bar{E}[Y_2^2]$
1.6
1.4
1.2
1.000
$\bar{E}[Y_3^2]$
0.996
0.992
0.988
0.984
0.980
$\bar{E}[Y_2^2]$
$\bar{E}[Y_1^2]$
$\bar{E}[Y_3^2]$
0.94
0.96
0.98
1.00
1.02
1.04
1.06
$\omega_3/(\omega_1+\omega_2)$

Fig. 16

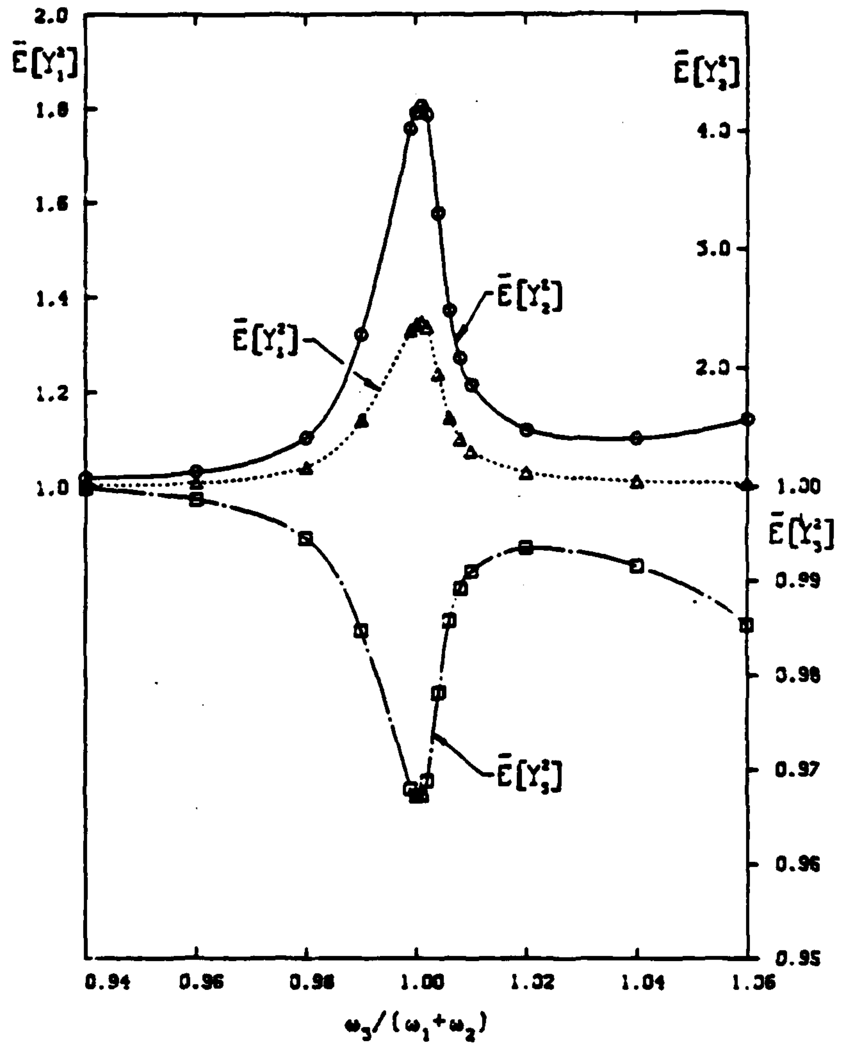
2.0
$\bar{E}[Y_1^2]$
1.8
1.6
1.4
1.2
1.0
$\bar{E}[Y_2^2]$
4.0
3.0
2.0
1.00
$\bar{E}[Y_3^2]$
0.99
0.98
0.97
0.96
0.95
$\bar{E}[Y_1^2]$
$\bar{E}[Y_2^2]$
$\bar{E}[Y_3^2]$
0.94
0.96
0.98
1.00
1.02
1.04
1.06
$\omega_3/(\omega_1+\omega_2)$

Fig. 17

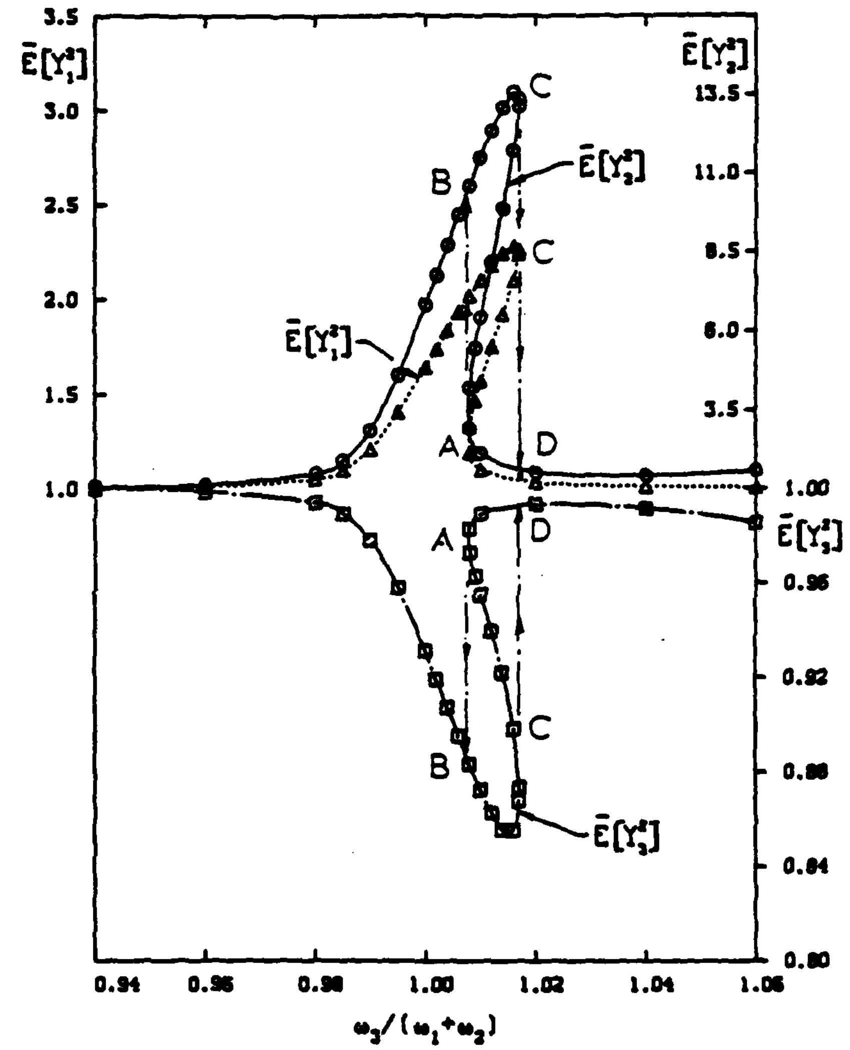

3.5
3.0
2.5
2.0
1.5
1.0
13.5
11.0
8.5
6.0
3.5
1.00
0.96
0.92
0.88
0.84
0.80
0.94
0.96
0.98
1.00
1.02
1.04
1.06
A
B
C
D

Fig. 18

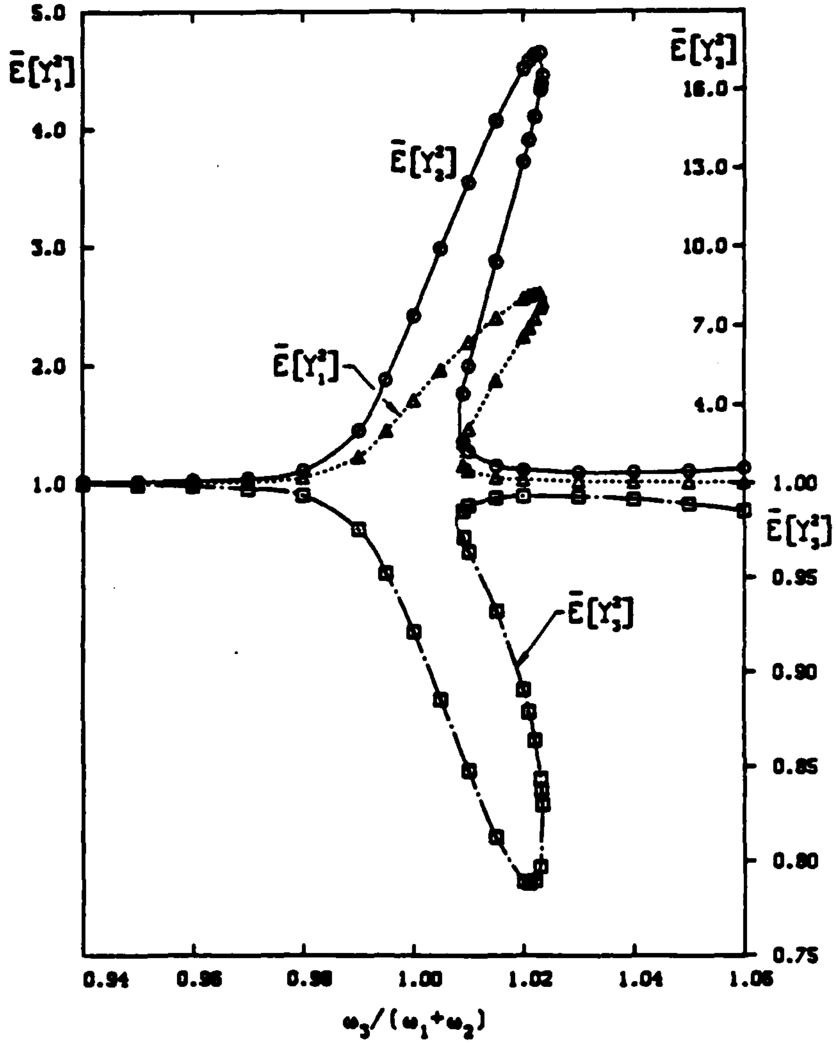
5.0
4.0
3.0
2.0
1.0
16.0
13.0
10.0
7.0
4.0
1.00
0.95
0.90
0.85
0.80
0.75
0.94
0.96
0.98
1.00
1.02
1.04
1.06
$\bar{E}[Y_1^2]$
$\bar{E}[Y_2^2]$
$\bar{E}[Y_3^2]$
$\omega_3/(\omega_1+\omega_2)$

Fig. 19

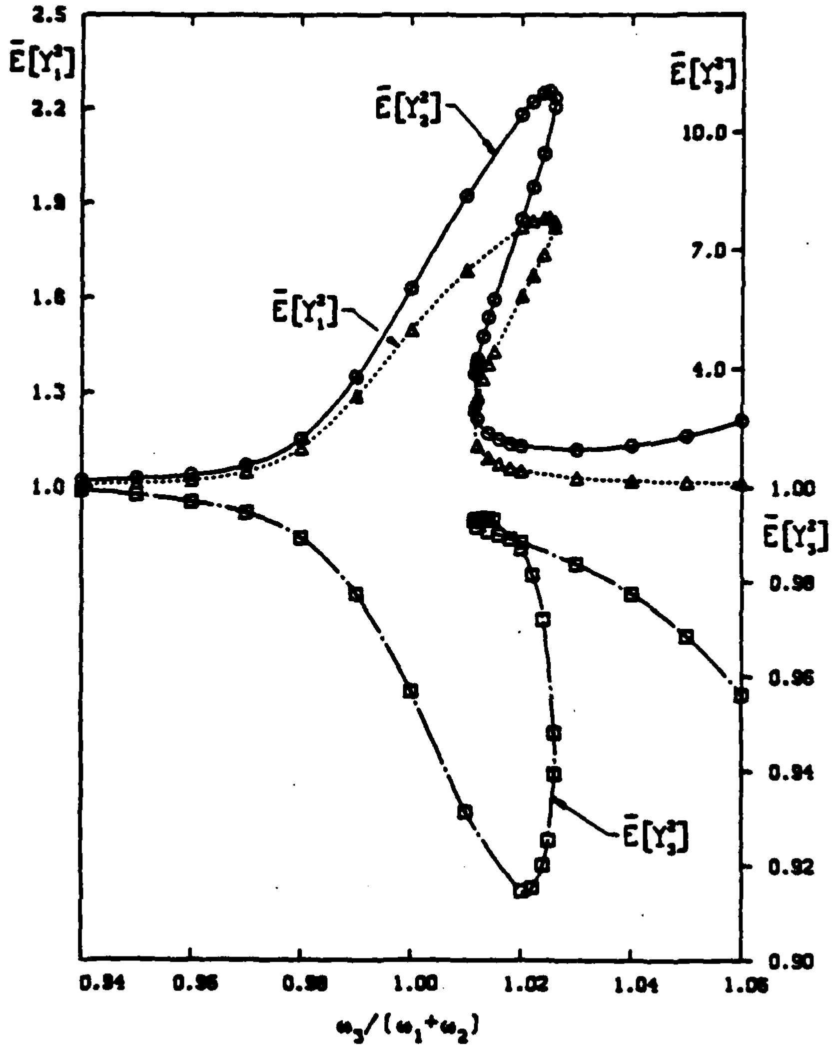

$\bar{E}[Y_1^2]$
2.5
2.2
1.9
1.6
1.3
1.0
$\bar{E}[Y_2^2]$
10.0
7.0
4.0
1.00
$\bar{E}[Y_3^2]$
0.98
0.96
0.94
0.92
0.90
$\bar{E}[Y_2^2]$
$\bar{E}[Y_1^2]$
$\bar{E}[Y_3^2]$
0.94
0.96
0.98
1.00
1.02
1.04
1.06
$\omega_3/(\omega_1+\omega_2)$

Fig. 20

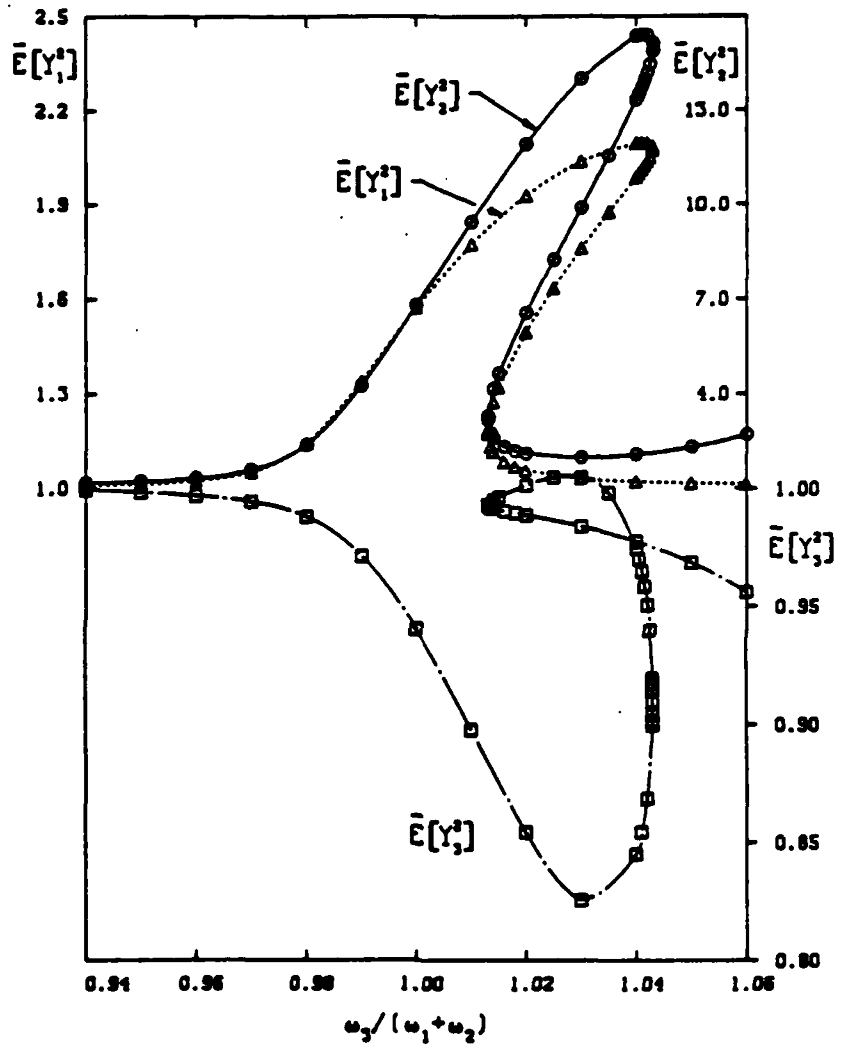

$\bar{E}[Y_1^2]$
$\bar{E}[Y_2^2]$
$\bar{E}[Y_2^2]$
$\bar{E}[Y_1^2]$
$\bar{E}[Y_3^2]$
$\bar{E}[Y_3^2]$
2.5
2.2
1.9
1.6
1.3
1.0
13.0
10.0
7.0
4.0
1.00
0.95
0.90
0.85
0.80
0.94
0.96
0.98
1.00
1.02
1.04
1.06
$\omega_3/(\omega_1+\omega_2)$

Fig. 21

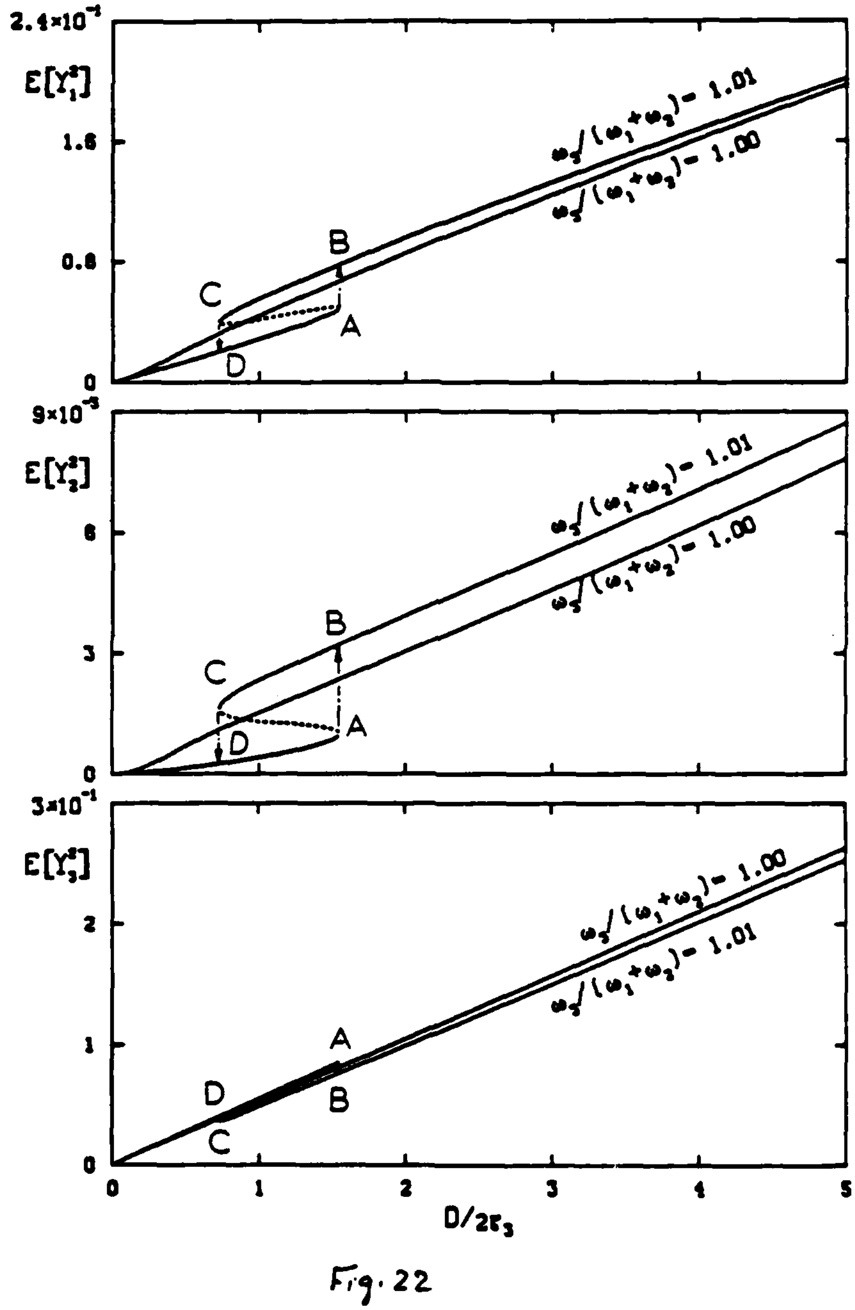

2.4×10⁻¹
E[Y₁²]
1.6
0.8
0
ω₃/(ω₁+ω₂)= 1.01
ω₃/(ω₁+ω₂)= 1.00
A
B
C
D
9×10⁻³
E[Y₂²]
6
3
0
ω₃/(ω₁+ω₂)= 1.01
ω₃/(ω₁+ω₂)= 1.00
A
B
C
D
3×10⁻¹
E[Y₃²]
2
1
0
ω₃/(ω₁+ω₂)= 1.00
ω₃/(ω₁+ω₂)= 1.01
A
B
C
D
0
1
2
3
4
5
D/2ζ₃

Fig. 22

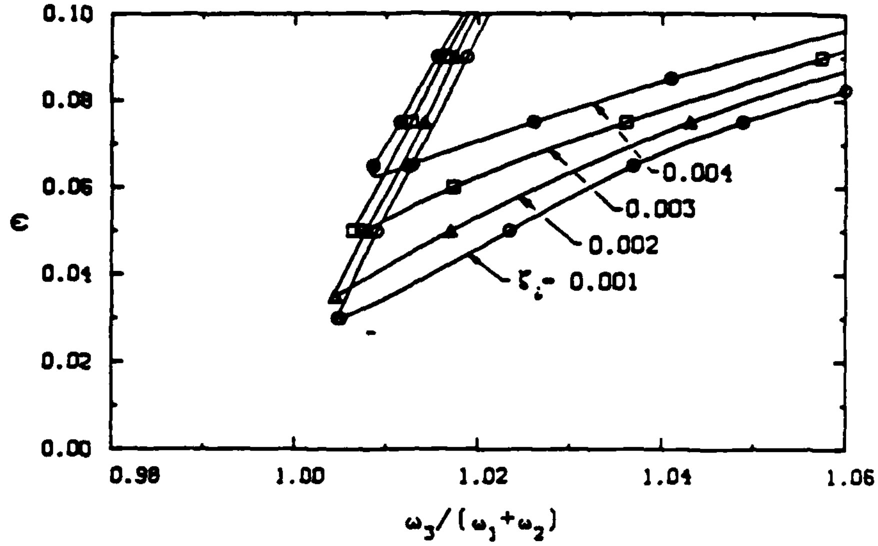
0.10
0.08
0.06
0.04
0.02
0.00
ε
0.98
1.00
1.02
1.04
1.06
ω3/(ω1+ω2)
0.004
0.003
0.002
ζi = 0.001

Fig. 23

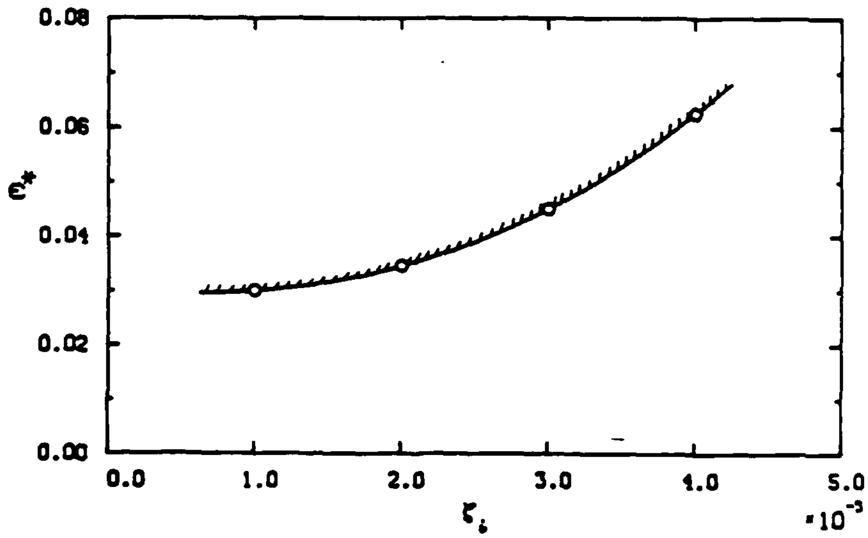
0.08
0.06
0.04
0.02
0.00
ε*
0.0
1.0
2.0
3.0
4.0
5.0
ζi
*10^-3

Fig. 24

ATE

LMED

8